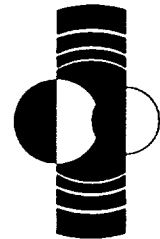
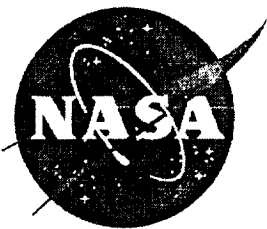


RASCAL

· revolutionary · aerospace · systems · concepts · academic · linkage ·

**November 6-8, 2002
Cocoa Beach, Florida**

2002 ADVANCED CONCEPT DESIGN PRESENTATION



LPI Contribution No. 1152

RASC-AL

(REVOLUTIONARY AEROSPACE SYSTEMS CONCEPTS-ACADEMIC LINKAGE)

2002

ADVANCED CONCEPT DESIGN PRESENTATION

**November 6-8, 2002
Cocoa Beach, Florida**

Sponsored by

Lunar and Planetary Institute

NASA Langley Research Center and the
Revolutionary Aerospace Systems Concepts (RASC) Management Team

ICASE/Universities Space Research Association

RASC-AL Steering Committee

Attrice Hunt-Malone (Lunar and Planetary Institute)
David Akin (University of Maryland)
Jeff Cardenas (Universities Space Research Association)
Ben Clark (Lockheed Martin)
Roger Crouch (NASA Headquarters)
Mike Duke (Lunar and Planetary Institute)
Wally Fowler (University of Texas at Austin)
Laurel Kirkland (Lunar and Planetary Institute)
Josip Loncaric (ICASE)
John Olds (Georgia Institute of Technology)
Lewis Peach (Universities Space Research Association)
Bill Siegfried (Boeing)
Jeff Taylor (University of Hawai'i)
Pat Troutman (NASA Langley Research Center)

Lunar and Planetary Institute 3600 Bay Area Boulevard Houston TX 77058-1113

LPI Contribution No. 1152

ISSN No. 0161-5297

Compiled in 2002 by
LUNAR AND PLANETARY INSTITUTE

The Institute is operated by the Universities Space Research Association under Contract No. NASW-4574 with the National Aeronautics and Space Administration.

Material in this volume may be copied without restraint for library, abstract service, education, or personal research purposes; however, republication of any paper or portion thereof requires the written permission of the authors as well as the appropriate acknowledgment of this publication.

Reports in this volume may be cited as

Names of Students (2002) Title of report. In *RASC-AL (Revolutionary Aerospace Systems Concepts–Academic Linkage): 2002 Advanced Concept Design Presentation*. LPI Contribution No. 1152, Lunar and Planetary Institute, Houston. 146 pp.

This volume is distributed by

ORDER DEPARTMENT
Lunar and Planetary Institute
3600 Bay Area Boulevard
Houston TX 77058-1113
Phone: 281-486-2172
Fax: 281-486-2186
E-mail: order@lpi.usra.edu

Mail order requestors will be invoiced for the cost of shipping and handling.

PREFACE

The Revolutionary Aerospace Systems Concepts–Academic Linkage (RASC–AL) is a program of the Lunar and Planetary Institute (LPI) in collaboration with the Universities Space Research Association’s (USRA) ICASE institute through the NASA Langley Research Center.

The RASC–AL key objectives are to develop relationships between universities and NASA that lead to opportunities for future NASA research and programs, and to develop aerospace systems concepts and technology requirements to enable future NASA missions. The program seeks to look decades into the future to explore new mission capabilities and discover what’s possible. NASA seeks concepts and technologies that can make it possible to go anywhere, at anytime, safely, reliably, and affordably to accomplish strategic goals for science, exploration, and commercialization. University teams were invited to submit research topics from the following themes: Human and Robotic Space Exploration, Orbital Aggregation & Space Infrastructure Systems (OASIS), Zero-Emissions Aircraft, and Remote Sensing.

RASC–AL is an outgrowth of the HEDS–UP (University Partners) Program sponsored by the LPI. HEDS-UP was a program of the Lunar and Planetary Institute designed to link universities with NASA’s Human Exploration and Development of Space (HEDS) enterprise.

The first RASC–AL Forum was held November 5–8, 2002, at the Hilton Cocoa Beach Oceanfront Hotel in Cocoa Beach, Florida. Representatives from 10 university teams presented student research design projects at this year’s Forum. Each team contributed a written report and these reports are included here. The agenda for the Forum included oral presentations by the university teams and representatives from NASA and industry, a poster session, and a field trip to the NASA Kennedy Space Center.

The Forum was organized by the Education and Public Outreach Department at the LPI. This publication was made possible through the collective work of a varied group of individuals. We are grateful to Lewis Peach, Chief Engineer of USRA, for bringing together NASA Langley Research Center and the RASC Team to make RASC–AL a reality. We are also grateful to the students, the university faculty, and teaching assistants for their outstanding student research design projects. We are especially thankful to the RASC–AL Steering Committee for providing their valuable experience and direction to the management of the program. We also thank the LPI’s Publications and Program Services Department and Computer Center for additional logistical support. Finally, we thank Jeff Cardenas of USRA, Ben Hauser of LPI, Pat Troutman of the RASC Team, the Kennedy Space Center’s University Affairs office, and ICASE for special assistance and direction in planning and organizing the Forum.

CONTENTS

Agenda.....	1
The Finalists.....	3
The Teams.....	4
Other Scenes from the Forum.....	6
University Design Studies	
<i>Martian Weather Station</i> Colorado School of Mines	7
<i>P.A.R.T.S.: Plasma Accelerated Reusable Transport System</i> Embry-Riddle Aeronautical University	23
<i>Bifront: A 4th Generation Launch Architecture Concept</i> Georgia Institute of Technology	39
<i>The Hematopoietic Stem Cell Therapy for Exploration of Space</i> Howard University.....	55
<i>Modular Research Rover and Gesture Control System for EVA</i> Pennsylvania State University	67
<i>Integrated Robotic Team for Martian Water Collection</i> Princeton University	78
<i>Exobiology: The Survival Ability of Halophiles Under Martian Conditions</i> University of California, Berkeley.....	94
<i>A Novel Method for Cuttings Removal from Holes During Percussive Drilling on Mars</i> University of California, Berkeley.....	107
<i>Project Endurance: Six 90-Day Missions on the Lunar Surface</i> University of Maryland, College Park.....	122
<i>Self-Sustained Closed Ecological Systems</i> University of Washington	136
List of Participants.....	145

AGENDA

Tuesday, November 5, 2002

6:00 – 8:00 p.m. Registration and Reception

Wednesday, November 6, 2002

7:30 – 9:00 a.m. Steering Committee Breakfast

8:30 – 9:00 a.m. Breakfast
Registration Continued

9:30 – 9:40 a.m. Opening Remarks/Forum Directions/Introductions
Attrice Hunt, Lunar and Planetary Institute

9:40 – 10:00 a.m. Speaker Presentation
Mike Duke, Lunar and Planetary Institute

10:00 – 10:30 a.m. Pat Troutman
NASA Langley Research Center,
Revolutionary Aerospace Systems Concepts (RASC) Management Team

UNIVERSITY PRESENTATIONS

10:30 – 11:20 a.m. University of California at Berkeley — *“Novel Method of Cutting Removal From Holes During Percussive Drilling Mars”*
Faculty Advisor: George Cooper

11:20 a.m. – 12:10 p.m. University of Maryland — *“The Endurance Project: Learning to Live and Work on the Moon”*
Faculty Advisor: Mary Bowden

12:10 – 1:30 p.m. Lunch

1:30 – 2:20 p.m. Pennsylvania State University — *“A Modular Multi-Function Rover and Control System for EVA”*
Faculty Advisor: Michael W. Jacobs

2:20 – 3:10 p.m. Howard University — *“Hematopoietic Stem Cell Therapy for Exploration of Space”*
Faculty Advisor: Seigo Ohi

3:10 – 3:30 p.m. Break

3:30 – 4:20 p.m. Colorado School of Mines — *“Martian Weather Station”*
Faculty Advisor: Barbara McKinney

5:30 – 7:30 p.m. Poster Session

Thursday, November 7, 2002

UNIVERSITY PRESENTATIONS

7:30 – 8:30 a.m.	Breakfast
8:30 – 8:45 a.m.	Forum Directions and Opening Remarks
8:45 – 9:35 a.m.	Princeton University — “ <i>Integrated Robotic Team for Collection of Martian Water Ice</i> ” Faculty Advisor: Daniel M. Nosenchcuk
9:35 – 10:25 a.m.	Georgia Institute of Technology — “ <i>Bifrost: A Large-Scale Solution to Low-Cost Space Access</i> ” Faculty Advisor: John Olds
10:25 – 10:40 a.m.	Break
10:40 – 11:30 a.m.	Embry Riddle Aeronautical University — “ <i>Plasma Accelerated Reusable Transport System (P.A.R.T.S.)</i> ” Faculty Advisor: Mahmut Reyhanoglu
11:30 a.m. – 12:00 p.m.	Josip Loncaric, Universities Space Research Association “ <i>Beowulf Clusters in Aerospace Research</i> ”
12:00 – 1:30 p.m.	Lunch
1:30 – 2:20 p.m.	University of Washington — “ <i>Self Sustained Closed Ecological Systems</i> ” Faculty Advisor: Frieda Taub
2:20 – 3:10 p.m.	University of California, Berkeley — “ <i>Exobiology: The Survival Ability of Halophiles Under Martian Conditions</i> ” Faculty Advisor: David Gan
4:30 – 5:00 p.m.	Speaker Presentation Jeff Cardenas Overview of NASA Institute for Advanced Concepts – NIAC
3:10 – 3:30 p.m.	Break
3:30 – 4:30 p.m.	Panel Discussion, Q & A, RASC-AL Steering Committee
4:30 – 6:00 p.m.	Judges Review

Friday, November 8, 2002

FIELD TRIP

7:30 – 8:00 a.m.	Breakfast
8:00 a.m. – 12:00 p.m.	Field Trip
12:00 – 1:00 p.m.	Lunch and Travel back to Hotel
1:00 – 2:00 p.m.	Awards and Forum Wrap Up

The Finalists

A panel of judges based their awards on both a written report and the oral presentation made at the meeting. And the finalists are . . .



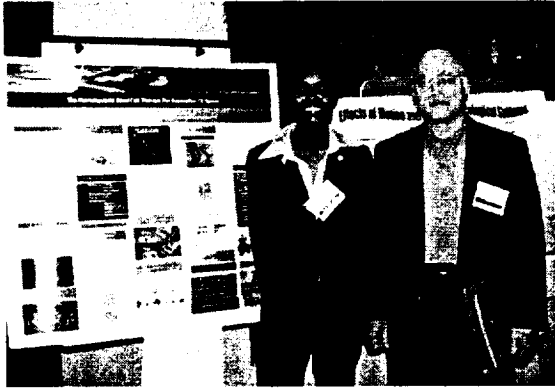
*University of California, Berkeley
"A Novel Method of Cuttings Removal from Holes During Percussive Drilling on Mars"*

*Embry Riddle Aeronautical University —
"P.A.R.T.S.: Plasma Accelerated Reusable Transport System"*



*Princeton University —
"Integrated Robotic Team for Martian Water"*

The Teams



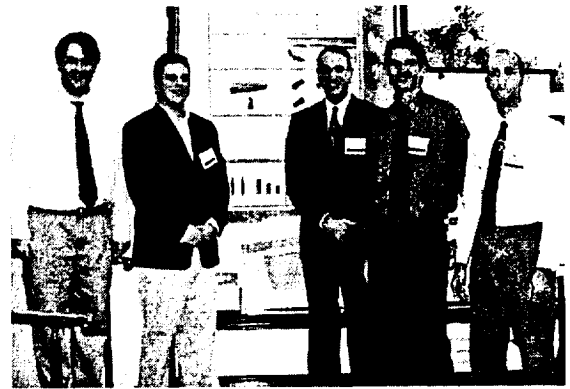
*Howard University
"Hematopoietic Stem Cell Therapy for Exploration
of Space"*

*Pennsylvania State University
"A Modular Multi-Function Rover and Control System
for EVA"*



*Colorado School of Mines
"Martian Weather Station"*

Georgia Institute of Technology
"Bifrost: A Large-Scale Solution to Low-Cost
Space Access"



University of Washington
"Self Sustained Closed Ecological Systems"

University of California, Berkeley
"Exobiology: The Survival Ability of Halophiles Under
Martian Conditions."



University of Maryland
"The Endurance Project: Learning to Live and
Work on the Moon"

Other Scenes from the Forum



Group photo taken at the launch pad at the NASA Kennedy Space Center.

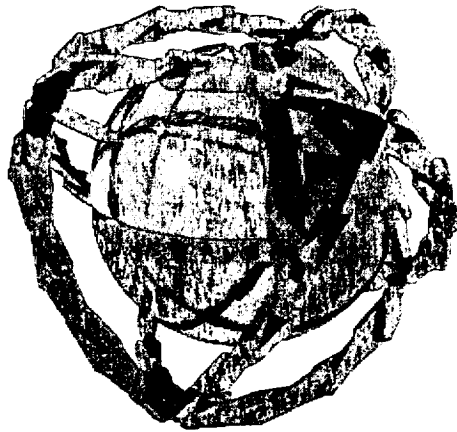
Mike Duke discusses a poster with one of the Forum's student participants.



Audience members listen attentively as one of the student design teams makes their oral presentation.

Martian Weather Station

Colorado School of Mines



Team ARES

William Burnett
J. David Bush
Kendall Harwell
Alan Jones
Joyce Kaneta

Advisors:
Barbara McKinney
Bob Knecht
Chris Duncan

1. ABSTRACT

As the Earth's population continues to grow and resources continue to dwindle, humankind has looked to other planets for possible colonization. With current technology, colonization of Mars is the most viable option. Although general facts about Mars are known, such as its low temperatures, low pressure, and atmospheric density, more specific information is needed. To this end, team ARES from the Colorado School of Mines has designed a module to measure atmospheric conditions. Our module is capable of measuring temperature, pressure, wind speed, and particle concentration.

The module will take measurements every minute and the data will be transmitted twice daily to an orbiting satellite. In order to provide overlap in case of interference during transmission time, because of occurrences such as dust storms, the data will be stored for 24 hours.

Our design is an expanding modular structure, similar to a Hoberman Micro Sphere® by Hoberman Designs, Inc, in which the instruments are protected from the harsh atmospheric conditions yet are still able to take measurements. The interior will consist of eight octants. A rod attached to opposite sides of the frame expands upon landing, opening the frame. A swivel mechanism at the middle of the rod allows the octets to orient themselves. The bottom four octets will house the instruments, computer, and batteries while the top four will be solar panels and have the antennae.

This design is adaptable to various shell designs; also, it is both strong enough to survive and able to orient itself after deployment.

2. INTRODUCTION

This project originated from the Colorado Space Grant Consortium and Ames Research Center. Dr. Knecht, head of the Design (EPICS) Program at CSM, assigned the task of designing a weather station for Mars to the students of the EPICS program. The weather station must be able to measure:

- Temperature
- Atmospheric Pressure
- Wind Speed, and
- Particle Concentration

In the fall of 2001, team ARES designed an expanding module based on the specifications given in Table 1 after considering several possible shapes.

Table 1: Client Specifications

<i>Specification</i>	<i>Value</i>
Volume	2000 to 3000 cm ³
Distance Covered	100 kg ²
Operations	24 hours
Transmission	Twice daily
Data Storage	24 hours to provide overlap
Strength	Must withstand impact with the surface
Shape	Unspecified

The module must be strong enough to withstand impact, but, according to the client, will be housed in some sort of shell that will absorb most of the impact. Team ARES also had to address the issues of power, heat, and transmission. The module must have a transmission system able to send data to an orbiting satellite system; however, no specifications were provided for such a system, our team has stipulated certain requirements for the satellite such that our transmission system will be able to send data to it.

3. APPROACH TO THE PROBLEM

The first thing we did when given the problem was to brainstorm general ideas. Our main concern at this time was the limitations involved. First, we researched general facts about Mars and its climate and atmosphere. In comparison to the Earth's climate, Mars has very low temperatures and pressures, a thin atmosphere, and is subject to severe dust storms. So, one of our problems was to research instruments that would function under these conditions. The values in Table 2 were used in all the calculations.

Table 2: General Mars Data [1,2,3]

<i>Properties</i>	
Maximum Surface Temperature:	25 °C
Minimum Surface Temperature:	-125°C
Surface Pressure:	6 millibars
Composition of the Atmosphere:	95% Carbon
	3% Nitrogen
	1.6% Argon
Diameter:	6792 km
Distance from the Sun:	228,000,000 km
Density:	3940 kg/m ³
Surface Gravity:	3.7 m/s ²

Next, we considered the actual shell and deployment of the module. We felt that it should be able to guarantee an orientation such that the devices could take measurements as well as transmit the data to the satellite. Since the maximum volume was so small, we decided to focus on designing a shell module that would give a maximum amount of space in which we could place the instruments.

3.1 Shell Design

We decided that the best design would be one that expanded upon landing. One possible design would be a cube shaped module that opens up after landing and lies flat on the surface. Another design would be shaped like a pyramid, which would also unfold after landing. A third is just a simple sphere. The main problem with the spherical design was that there was no way to prevent it from rolling after it landed. Although the cube and pyramid design would remain stationary after landing, neither optimized the maximum allowed volume nor guaranteed correct orientation. So now the problem became how to make a spherical module that would remain stationary and guarantee orientation. We decided that the best design would be an expandable sphere that will allow the instrumentation to deploy with the proper orientation (see Table 3).

Table 3: Module Shape Decision Matrix

	<i>Maximize Volume</i>	<i>Ability to easily fit into a Shell</i>	<i>Stationary After Landing</i>	<i>Space for Instruments</i>	<i>Total</i>
Cube	8	7	10	7	32
Pyramid	5	4	10	4	23
Sphere	10	9	3	6	28
Hoberman	10	8	8	10	36

The sphere's geometry is similar to that of the Hoberman Micro Sphere® [4] by Hoberman Designs, Inc. The frame includes an axial, spring-loaded shaft that allows it to expand after deployment and a swivel mechanism that allows it to orient itself. Thus, after deployment and expansion, the module is able to remain stationary. However, should something happen, such as being moved by the dust storm, the swivel mechanism would allow the module to correct its orientation.

The frame has a collapsed radius of 8.95 cm and an approximate expanded radius of 13.35 cm. The swivel mechanism, located at the midpoint of the shaft, provides the instrumentation housing with 360° spherical rotation. The mechanism consists of an axial cylinder for rotation around the axis and mounting pegs for rotation along the axis.

The framework divides the instrument housing into eight separate lobes, each lobe having an approximate working volume of 375 cm³. The upper four lobes will be used for solar power collection, while the bottom lobes will house the instruments, batteries, CPU and Data Storage. This modular design gives us an advantage by allowing us to insulate and heat each lobe to a different temperature, depending on the instrumentation requirements, and separate heating allows us to minimize unnecessary power usage.

As for construction material, we will use an Aluminum-Lithium alloy similar to those used in many current aerospace and cryotank applications. Specifically, McCook Metals Weldalite™ 049 Aluminum-Lithium Plate [5] is ideal because of its high strength, fracture toughness, corrosion resistance, and low density

3.2 Components

After we decided on a module design, the next step was to research instrumentation and components. We discovered, upon research, that there are a limited number of instruments that will function under Mars atmospheric conditions. We narrowed our research to finding types of instruments that would function. Initially, the following are components we felt would work. One year ago, these are the components we felt would be most suitable.

3.2.1 Computer

This component interfaces with the rest of the instruments as well as handling data storage. The best data processor we found was the Sharp LH75410 microcontroller, which was designed for industrial use and can withstand a harsh environment. It is able to handle converting the analog signal from the instruments to a digital signal and contains a timer to control when to take measurements and when to transmit to the satellite. It also contains several serial interfaces to communicate with the transmission device. The storage aspects of the module will be handled by a Sharp LRS1331 chip also designed for use in industrial applications; thus it is highly resilient to extreme surroundings. This chip has enough storage to hold data for about 1300 days of measurements each minute, as well as the functionality program [6].

3.2.2 Thermometer

For a thermometer, we looked at the Thermometrics CTFP10 thermal resistor [7]. Although there are many on the market that meet the requirements for our module, not all of them are guaranteed to function properly under the conditions within the range required for our purposes. A thermal resistor is basically a loop of wire connected to a resisting material that reads temperature by changing its value of resistance as the temperature changes. As the temperature changes, the electrical current is allowed to flow at different rates. However, this simple design is more durable and reliable than other types of thermometers, and it costs far less. Most important though, thermal resistors do not sacrifice accuracy at all. In fact, for the cold temperature range expected on Mars, thermal resistors are among the most accurate devices for temperature measurement.

3.2.3 Barometer

We were unable to find any barometers that both meet the requirements and were also guaranteed to work under Martian conditions. Any available barometer we chose would have to be modified, and thus we decided the Paroscientific model 215A [8] would be easiest to modify to meet our specifications. This pressure sensor applies quartz crystal resonator technology to measure changes in the atmosphere. As the pressure changes a small vibrating crystal inside the barometer changes its oscillating frequency. This barometer is designed to work at low pressures--less than 1500 millibars. Even though this range is relatively low compared to those of other barometers, it will still not be low enough for Martian pressures, which are typically around 10 millibars. If we can modify this barometer to work at lower pressures, possibly by changing the size or shape of the oscillating crystal, it would be accurate enough to provide useful data.

3.2.4 Anemometer

We chose to use a constant temperature type of anemometer, which will operate by running a current through a film or wire to maintain a constant temperature. As wind blows across the film or wire, more current is needed to maintain that temperature and the change in current is converted to wind speed [9]. Wire anemometers tend to be more accurate, but hot film anemometers are more durable. Since our module must gather data for at least one year, we chose to use the hot film type. Since the wind speeds on Mars are not higher than 40 m/s, we do not have to worry about the film overheating [1]. We evaluated Model 1230 from TSI, Incorporated, which has a thin film of platinum on an Alumina substrate and an automated calibrator to attach to the probe. Because the hot film anemometers have no moving parts and can be attached to the frame of the weather station, this type of anemometer significantly reduces the possibility of broken parts. Platinum films have a wide range of operating temperatures, thus reducing the concern over that Mars' low temperatures would affect operation [10]. Constant temperature anemometers were used on the Viking expedition to Mars [9], and in the upcoming 2003 Beagle mission, hot film anemometers will be used [11].

3.2.5 Particle Detector

We chose to use the Microdust Pro™ probe [12] manufactured by BGI, Inc., which is an aerosol photometer. The system emits an infrared beam and uses a near-forward light scattering technique to measure TSP (total suspended particulate matter) in milligrams per cubic meter. The beam passes through the volume of air being sampled where the light is scattered by dust particles. A photo detector picks up the scattered light where the signal can be converted to a mass concentration.

While taking static measurements, the probe must be connected to an air pump to pull a sample volume through the instrument and to keep dust from settling on the lenses [12]. Sensidyne, an air sampling company, manufactures pumps that are ideal for this process [13].

3.2.6 Heat

Logic is written into the central process to determine if any excess power is being generated by the solar panels and also if there is over a 10% excess in expected battery power consumption. Any such excess power, along with an allotted amount of power, will be used to heat the module in order to keep the temperature in the lower octets within the operational temperature of the components they contain. The lower four octets are equipped with insulation and heating elements to accommodate their requirements. Each octet has different requirements and components in each octet radiate variable amounts of heat when in operation, so the central processor takes control of heat management. Finally, space is allotted in both octets for voltage control and management circuitry, as there are two different voltages required for operation of the module and both batteries and solar panels provide widely variable voltages.

3.2.7 Power Consumption

The power consumption for the module ranges is widely based on its mode of operation. The module will take readings every minute. Therefore, the sensors will only need to be operational for a short fraction of each minute. When the module is not taking measurements, the sensors are turned off and the computer is put into nap mode. The module's third cycle is transmission. In order to provide for the power needs of the module, a system of solar panels and batteries has been implemented.

3.2.8 Solar Cell

The top four octets of the module are based around solar panels. While there are four octets, not all will be exposed to the sun at any given time. Modern, commercially available solar panels range from 10% to 14% efficiency and specialty panels made by companies such as Boeing created 26% efficiency panels in 1999, expecting it to rise to 40% by 2002 [14]. To meet the power requirements of our module, any commercially available panels will suffice, assuming they are able to operate in the Martian environment.

3.2.9 Batteries

To accommodate operation when the module is not exposed to the sun, and when the power demand exceeds what the solar power can provide, such as during transmission, a series of batteries will be used. They are located in two bottom octets of the module, opposite each other to balance their weight when the module is orienting itself. The batteries should be able to provide the majority of the power so that if severe dust storms block sunlight or some of the solar cells are damaged, the module can still function. Furthermore, whenever the solar power makes it possible, no load will be placed on the batteries. This will minimize cathode freeze-over, which can dramatically affect battery life over long periods of time [15, 16].

3.2.10 Radio/Transmission

The transmission device we looked at is a dual crystal controlled UHF transmitter made by Radiometrix, part number TXM-418-10. This transmitter will be combined with a low power amplifier and a dish antenna and will be used to transmit the data collected by the instruments. The amp will consume no power when idle. Twenty-four hours of data, at 16-bit accuracy for each measurement, taken once every minute will occupy 11.25kb of space. Thus, the transmitter ideally would be capable of sending data at 45kb/s, yielding an actual data output of about 10kb/s, so that it would be able to transmit all of the data collected, as well as have enough room for protocol overhead and still be able to transmit, even through moderate interference fields [17, 18].

4. RESULTS

However, after considering the overall design and instrumentation of our module and making a computer model, we found several flaws. While all of the instruments are small, we found that when put together in the module with the batteries, the octets were barely large enough to hold all the components. This left little room, literally, for adjustments. Although we liked the concept of how the components functioned, the components were not satisfactory. Thus, we decided to keep the shell design and the type of instruments, but change the instruments themselves wherever possible. We feel that these are the instruments that best meet the requirements.

4.1 Computer

The data processor we are now considering is the S3C44B0X 16/32-bit RISC microprocessor by Samsung, which is based on a 16/32-bit ARM7TDMI RISC CPU core (66MHz) designed by Advanced RISC Machines, Ltd. [19]. This processor is square in shape, with dimensions of approximately 26.0 mm x 26.0 mm. There are four operating modes: Normal, Slow, Idle, and Stop, but the processor will be in either

Normal or Idle for the majority of the time. During Normal mode it will consume up to 235 mW but less than 5 mW when Idle. It handles converting the analog signal from the instruments to a digital signal using its 8 input, 10-bit Analog-to-Digital (A/D) converter. The data processor also contains a timer to control when to take measurements and when to transmit to the satellite. It also contains several serial interfaces to communicate with the transmission device. Finally, it contains Direct Memory Access (DMA) channels to communicate with up to four banks of memory [19].

A memory chip [6] attached to a DMA channel will handle the data storage. It has both volatile and non-volatile memory, so it can handle the operation and storage aspects. The amount of data (collected, stored, etc.) in one-day amounts to approximately 57kbit, assuming data is taken once every minute.

4.2 Instruments

4.2.1 Thermometer

For the thermometer, we will be using Honeywell's model HEL 700 T1A. We are using this model instead of the Thermometrics model because it is smaller and is better able to accurately measure the low Martian temperatures with better accuracy. This is a Thin Film Platinum Resistance Temperature Detector (RTD). These operate by running a current through the film and measuring the resistance, which can then be used to calculate the ambient temperature by the equation

$$R_T = R_0(1 + AT + BT^2 - 100CT^3 + CT^4)$$

where R_T is the resistance (Ω) at the ambient temperature ($^{\circ}\text{C}$), R_0 is the resistance (Ω) at 0°C , T is the ambient temperature ($^{\circ}\text{C}$). The constants A , B , and C are calculated from the equations

$$A = \alpha + \frac{\alpha\delta}{100}$$

$$B = -\frac{\alpha\delta}{100^2}$$

$$C_{T<0} = -\frac{\alpha\beta}{100^4}$$

For the 1000Ω thermometer, these constants are provided in the table below.

Table 4: Constant Values for 1000Ω Thin Film RTD [20]

Alpha (α) ($^{\circ}\text{C}^{-1}$)	0.003850 ± 0.000010
Delta (δ) ($^{\circ}\text{C}$)	1.4999 ± 0.007
Beta (β) ($^{\circ}\text{C}$)	0.10863
A ($^{\circ}\text{C}^{-1}$)	3.908×10^{-3}
B ($^{\circ}\text{C}^{-2}$)	-5.775×10^{-7}
C ($^{\circ}\text{C}^{-4}$)	-4.183×10^{-12}

*For $T > 0^{\circ}\text{C}$, $\beta=0$ and $C=0$

For our thermometer, both the operating and storage temperature range from -200°C to 500°C . The range of temperatures found on Mars is -125°C to 25°C , so this thermometer will easily be capable of operating on the Martian surface. This thermometer also has high accuracy, with a $\pm 0.1\%$ error.

We will use the Honeywell HEL-700, whose dimensions are 1.90 mm by 1.27 mm. There will be one thermometer inside each octet for heating purposes and one on the outside of the module to take measurements. With an operating current of 1 mA (2 mA maximum), this thermometer will require very little power to operate [20].

4.2.2 Anemometer

For the anemometer we will use two Honeywell HEL-705-T-1-5-C3 models, the HEL-705-U-1-5-C3 and HEL-705-T-1-5-C3. These models are similar to the thermometer but will be connected in such a way that allows them to measure wind speed. These models measure wind speed using the hot film anemometer concept we were originally considering. They are Teflon coated with three point NIST calibrators so their accuracy is 0.01%, which allows the detection of much smaller wind variations.

The U1A model has a resistance of 1000Ω and the T1A model has a resistance of 100Ω . These will be connected in a bridge configuration in which current self heats the smaller resistor. We then look at the equation

$$T = T_{amb} + \Delta T$$

where T can be found from the resistance. As T_{amb} changes, the larger resistor compensates so that ΔT does not change. The power required to keep ΔT constant can be related to wind speed.

For these thermistors, both the operating and storage temperature ranges are from -200°C to 500°C . The range of temperatures found on Mars is -125°C to 25°C , so the anemometer easily is capable of operating on the Martian surface. Since the wind speeds on Mars are no higher than 40 m/s and the atmosphere is so thin, we do not have to worry about the films overheating. The operating current for each resistor is 1 mA, with a maximum of 2 mA. Since the current stays the same, and only the resistance varies, the anemometer should not draw more than 4 mA of current. Thus, little power will be consumed during operation [20].

4.2.3 Barometer

For the barometer we will be using the Honeywell 40PC015G1A. It uses Silicon Piezoresistive Technology, which is a silicon pressure sensor. The device consists of thin chemically etched silicon wafer with piezoresistors buried in it. As the pressure changes, it causes the wafer to flex. This results in a strain on the resistors, which produces an electrical output.

The Honeywell 40PC015G1A has a range of 0-15 psi (0-1 bar), with an accuracy of 0.2%. Its operating temperature is -45°C to 125°C and its storage temperature is -55°C to 125°C . All of these specifications are important to our module for several reasons. The average surface pressure of Mars is 0.087 psi. The average pressure on Earth at sea level is 14.696 psi (1 atm), so this barometer will be able to measure the comparatively low pressures on Mars. The temperature for both the storage and operating of the device are low but still not quite low enough to operate on Mars. So in order to accommodate the barometer, it will be inside a heated portion of the module, with only the small port exposed to the atmosphere. The Honeywell 40PC015G1A needs about 5VDC of supply voltage and 10mA max supply current. Thus, the barometer will not drain much of the limited power supply. The barometer is also small in size, which makes it appropriate for the module. The dimensions are 30.9mm x 13.2mm x 19.8mm. Since it is so small it will fit in the module wherever it will take the best measurements [21].

4.2.4 Particle Detector

Since off-the-shelf particle detectors do not meet the criterion for our module, we will be using a particle detector that is based on the concept used in three manufactured models. These models are the Microdust Pro™ by Casella USA, Haz-Dust III™ Particulate Monitor by SKC® Inc., and the DustScan Scout Model 3020 Aerosol Monitor by Rupprecht & Patashnick Co., Inc [22, 23, 24].

These devices use near-forward light scattering technology (N-FLST) to measure TSP (total suspended particulate matter) in milligrams per cubic meter. Our prototype contains a laser diode, which emits a visible beam (630-680nm). As the beam passes through the volume of air being sampled, the light is scattered by dust particles with a barrier to block directly transmitted light. A photo transistor picks up the scattered light where the signal can be converted to a mass concentration. The approximate range of our system, based on the specifications of the three previous models, is 0 to $2500\text{mg}/\text{m}^3$, with a resolution of ~ 0.001 to $0.1\text{ mg}/\text{m}^3$. This instrument will operate at $\sim 2.5\text{ V}$ and draws approximately 60 mW.

4.3 Heat/Insulation

To heat the bottom octets, which house the instruments and batteries, we will use a standard heater. This will be regulated by the computer and thermometers placed inside each octet. The octets will be heated to at least -35°C .

Mars' surface temperature varies from 0°C at noon -120°C at night, which we found from the measurements of a currently orbiting satellite at Mars' equator. Our module must be at 0°C during the day while the batteries are charging and no less than -35°C at night. Each octet will be independently heated in order to conserve power. The heat lost from our module goes through 2 mm of insulation, 3 mm of shell and then encounters the heat convection of the Martian atmosphere directly outside the module. Based on this, we made a simulation using the inside temperature, outside temperature and the equivalent thermal circuit of the three materials to calculate the heat flux. We calculated an average heat loss of 0.876 W. Figure 1 in Appendix A shows the heat loss over a 24-hour period [25].

We are using the CryoCoat™ UltraLight™ made by Composite Technology Development, Inc. This is a modification of their CryoCoat™, a spray on cryogenic insulating element. CryoCoat™ is a 2-part epoxy system that utilizes microspheres as the acting insulating component...noted for its excellent adhesion to almost any substrate, high toughness even at cryogenic temperatures, and a specific gravity of nearly 1 (~ 60 pounds per cubic foot [pcf]). [26]

The UltraLight™ versions of the insulators have an even lower specific gravity of less than 0.2 pcf. They consist of three layers, an adhesive layer, the CryoCoat™ UltraLight™, and a protective coating, which keeps out moisture and is fire-retardant.

This material also has a low thermal conductivity. According to tests performed by Composite Technology Development, Inc. CryoCoat™ is the best insulation in many ways. For instance, a tensile test was conducted with aluminum and carbon composites, each at 77 K and 4 K. While the UltraLight™ insulation had cracking for the carbon composites, it was shown to work very well for the aluminum. At 77 K, the higher temperature, the substrate yielded, while at 4 K, it had no failure. The poor performance on carbon composites should have little to no effect because we will be using an aluminum lithium alloy for our module. This product will be used to insulate all of the instruments, batteries and data storage devices, which is necessary in order to keep all of the devices working in the harsh climate of the Martian planet.

To protect the instruments from radiation, second surface aluminized polyimide tape with acrylic (966) adhesive from Sheldahl will be applied to the interior of the lower octets. The polyimide thickness ranges from 12.5 to 127 μm and the aluminum coating is approximately 1000Å thick. Standard width sizes are from one to four inches, but it may be ordered in any width. The continuous temperature range is from -60°C to 150°C , but the bottom octets will be heated to at least -40°C [27].

4.4 Power Consumption

In order to calculate the power consumption we wrote a computer simulation to model the module as it collects data every minute. The simulation included a list of the equipment in the module and determined whether or not any one would be on at any given time. Both the sleep and alive power consumption of each piece of equipment were taken into account. The number .0398 W was calculated as the average consumption of power due to electronic components. The majority of the power will be consumed during transmission. Since the antenna is a half wave dipole, we approximated the gain to be 3 dB on the satellite and the module. The maximum distance that the module will have to transmit is 1695 km. Using this distance and a frequency of 2.4 GHz, we calculated the loss of free space using the equation

$$\text{Loss of Free Space} = 32.45 + 20 \log(d_{\text{max}}) + 20 \log(f)$$

which gives a loss of 164.6 dB.

We assumed that the receive sensitivity is -95 dBm and the satellite sensitivity is -120 dBm. Then we calculated the power received by the radio with

$$-120 = 10 \log \left(\frac{P_r}{0.001} \right)$$

The satellite needs $1\text{E-}15$ W to receive the transmission. From there we were able to calculate the power the antenna requires during transmission.

$$2 \cdot 3\text{dB} - 164.6\text{dB} = 10 \log \left(\frac{1 \times 10^{-15}}{P_{\text{antenna}}} \right)$$

For a 2.4 GHz system, 7.24 W are needed. Using these same equations, the desired frequency of 1.4 GHz would need 2.51 W, which would significantly reduce overall power consumption [28, 29].

4.5 Solar Cells and Batteries

Our main source of power will be solar cells. The solar panels that we will be using are 26.8% Improved Triple Junction (ITJ) Solar Cells made by Spectrolab Inc. These are “active, radiation-hard solar cell junctions” that are cut to customer specification by the company [30]. We will use quarter-circle shaped cells, which will be attached to the surface of the top four octets of the module. Since the cells cannot be cut to exactly the measurements of the module, we have estimated approximately 90% coverage.

The solar panels have a minimum average efficiency of 26.8% at maximum power [30]. The panels are composed of three layers of Gallium based material to for maximum efficiency. We assumed a Magnesium Fluoride anti-glare coating. As well as providing most of the daylight power, they will also be used to charge the batteries so the module will have power overnight.

We calculated the power from the solar panels by making a program that simulates one complete orbit of Mars around the Sun. The program takes into account such things as the elliptical orbit and the tilt axis. It assumes that the module is located at the equator, and takes into consideration the vectors between the Sun and the module, the reflective coefficient, and the reflection due to the angle.

Assuming that the light is equally polarized and using one of Fresnel’s equations

$$t_{//} = \frac{2n_i \cos \theta_i}{n_i \cos \theta_t + n_t \cos \theta_i}$$

where n_i , the refractive index of magnesium fluoride, is approximately 1.38 and n_t , the refractive index of Mars' atmosphere, is approximately 1.00. Since the pressure and density are very low, we assumed vacuum like conditions. From Fresnel's equation we calculated the coefficient of transmitted energy, $T_{//}$

$$T_{//} = \frac{n_t \cos \theta_t}{n_i \cos \theta_i} \cdot t_{//}^2$$

Using an average solar constant of 622 W/m^2 , we found the power generated by the solar panels

$$P = T_{//} \cdot 622 \text{ W/m}^2 \cdot \cos \theta_i$$

During daylight hours, the solar panels will provide 2.6 W, which averages out to 1.3 W of continuous power over a 24-hour period (see Appendix A) [31].

We will be using Lithium-ion batteries. They come in a variety of sizes and can be specially designed. The best option would be a shape that maximizes the volume of the octets.

4.6 Radio/Transmission/Antennae

For our radio transceiver, we will use the Honeywell HRF-ROC094XC. It is a "half-duplex transceiver" that can be used for digital applications. The chip is used for both control and data transfer using the microprocessor. Data rate of the chip is 128.8 Kb/sec. The Honeywell HRF-ROC094XC has an operating temperature of -40°C to 85°C and a storage temperature of -40°C to 150°C . Since Mars has a low temperature of -125°C and both the operating and storage temperature have a low of -40°C it will be necessary to insulate and heat the chip in order to keep it in operating condition. It operates from a 2.5V power supply, which consumes little of the restricted power that we have available. The optimal frequency to transmit data is 1.4 GHz, but this radio transmits at 2.4 GHz. None of the radios on the market will transmit at 1.4 GHz because it is a licensed frequency. Although 2.4 GHz is feasible, transmitting at 1.4 GHz would significantly reduce power consumption from 7.24 W to 2.51 W.

We will use half wave dipole antennae for our module. It will be folded inside the module and after the shell expands the antennae will unfold. There is a gold reflector attached to one of the top octets, which will rise after the frame expands. Extending vertically from the reflector is a pole that rises to 4.46 cm away from the reflector in order to have maximum transmission pattern. Attached to the end of the pole are two 5.94 cm dipoles at 90° to each other and curved parallel to the sphere. We calculated the height of the pole by using a gain pattern that would give us the maximum transmission time. The gain pattern is elliptical, with a dip in the middle. Although the signal is slightly weaker in the middle, this gain pattern allows the module to communicate during more of the satellite's orbit than a circular gain pattern. According to the gain pattern, we calculated the optimal pole height for 2.4 GHz from the relationship

$$h = \frac{3}{8} \lambda \quad [29, 31]$$

The satellite orbiting Mars will have to be more powerful than our radio in order to properly transmit data. We calculated the amount of time the module will be in contact with the satellite, which is approximately 17 minutes. We calculated this time frame by calculating the satellite's orbit time, assuming it is 400 km above the surface of Mars. We then found the acquisition circle radius of the module. From that, we found the arc length on Mars and the angle of the arc length. By projecting that angle 400 km above Mars' surface we were able to calculate the transmission time. However, these calculations were made assuming a perfectly smooth sphere. For more detailed calculations and equations see the Appendix B [32].

The satellite will be sending out beacons, which will be picked up by the module when the satellite is within contact range. The first beacon the module picks up can then be used as a reference for when transmission can begin. We will use packet-based transmission to send the data to the satellite. This will work by sending little packages of data and waiting for confirmation from the satellite before the next packet is sent. We plan on losing some packets in the transmission but there will be enough time to resend lost packets. Weather disturbances, such as dust storms, will prevent the module from transmitting data but the data storage in the computer will be able to store this information until the next transmission window.

4.7 Shell

The frame is made from an Aluminum-Lithium alloy, with 2.6% Li, which has a high ductility, good damage tolerance, and good corrosion resistance compared to other Aluminum alloys. It also has a lower

density than pure Aluminum. It is commonly used in space applications such as the fuel tanks for space shuttles. Alcoa, Inc. manufactures such an alloy (Alcoa 2090) that meets our requirements [33].

The frame has a collapsed radius of 8.95 cm and an approximate expanded radius of 13.35 cm. To find the dimensions, we wrote a computer model (see Appendix C). The frame expands upon deployment because of a spring-loaded axial shaft. A swivel mechanism guarantees orientation due to gravity. The complete inner mechanism includes small pathways for wiring. There are several possible ways to build it depending upon the strength needed.

4.8 Mass and Cost Analysis

After deciding on which components to use for the module, we made a table of the approximate cost and weight of the complete module as shown below in Table 5. The majority of the mass is from the frame, octet frames, and batteries, which total 2576 g. The solar panels account for the majority of the cost at \$465.37. However, since the panels are available in such small sizes, we can closer approximate the shape of the octets as well as have little waste.

The insulation is also worth noting because, while it is labor-intensive to make, the cost of making enough insulation for 1000 modules would be approximately the same amount as making insulation for one module [25, 34].

Table 5: Approximate Weight and Cost of Module

<i>Component:</i>	<i>Quantity</i>	<i>Cost (\$)</i>	<i>Mass (g)</i>
Thermometers	7	99.40	7*
Barometer	1	44.00	30*
Nephelometer	1	45.00*	20*
Radio	1	6.95	10*
Antenna	1	10.00*	125*
Amplifier Transistor	1	0.30*	5*
Octet Frames	0.576 kg	25.40	576
Frame	1.0 kg	44.10	1000*
Insulation	1	55.63	41.3
Computer	1	20.00*	25*
Memory Chip	1	4.00*	10*
Batteries	1	125.00*	1000*
Solar Cells	672cm	465.37	56.448
	Total:	945.14	2905.748

* indicates estimated values

5. CONCLUSION

Team ARES has designed an efficient, innovative and appropriate weather station. The spring loaded axial shaft and swivel mechanism guarantee the module's orientation upon deployment. The data processing and storage chips are more than capable of withstanding the climate and operating the entire system. They will control when measurements are taken, convert the data from analog to digital, and store and transmit the data. They will also control the heating of the octets so that the instruments are at a proper operating temperature. The instruments chosen will operate in Mars' harsh climate, and return accurate data concerning the changing atmospheric conditions. With a combination of solar panels and batteries, the weather station will have sufficient power to gather, store and transmit data for at least one Martian year. The insulation allows for low heat loss as well as protecting against radiation hardening. The spherical shell design is versatile and small enough to fit in any deployment shell, and the instruments are arranged in the lobe to guarantee the correct orientation.

Overall, our module will have a mass of approximately 2.9 kg, cost less than \$1000, and is versatile enough to be used in many applications.

6. FUTURE STUDIES

At this point, much of the module is purely hypothetical. In order to test the extent of its capabilities, funding is needed to build a working model and expose it to a simulation of the Martian climate. Such

testing would enable experimental observations to be taken into account, such as radiation effects and severe weather effects, particularly those resulting from dust storms. One of the most important aspects that must be considered when testing is the instrumentation exposure to radiation. It is important to look further into radiation hardened components and/or radiation insulation.

Other possible applications for our design include employment to the far side of the moon for research. It could also be dropped in the middle of forest fires to gather information. With these things in mind, we feel that our module is worthy of further development and research.

REFERENCES

- [1] California Institute of Technology, "Mars," <http://pds.jpl.nasa.gov/planets/welcome/mars.htm>, Sept. 5, 2002.
- [2] Lunar and Planetary Institute, "Exploring Mars: Basic Mars Facts," <http://www.lpi.usra.edu/expmars/basicfacts.html>, Sept. 5, 2002.
- [3] "Basic Fact About the Planet Mars." <http://humbabe.arc.nasa.gov/mgcm/faq/marsfacts.html>, Sept. 5, 2002.
- [4] Hoberman Associates/Designs, "Hoberman Micro Sphere®," <http://www.hoberman.com/fold/sphere/microsphere.htm>, Oct. 2, 2001.
- [5] McCook Metals, "Weldalite® 049 Aluminum-Lithium Plate," <http://www.mccookmetals.com/products.htm>, Oct. 25, 2001.
- [6] Sharp Electronics, "LH75410 16/32-bit Microcontroller," http://smaecom1.sharpsoc.com/eprise/main/FldrSharp/Techpub/productfocus/publications/micro/mcu/tec_prodbrief_lh75400.pdf, Feb. 8, 2001.
- [7] Thermal Resistor and Diagram, <http://www.thermometrics.com/assets/images/cryo.pdf>
- [8] Barometer and Diagram:
<http://www.paroscientific.com/Barometers.htm>
- [9] Remote Measurement Systems, "Monitoring the Wind – Speed and Direction," <http://www.measure.com/sensors/sensor-wind.html>, Oct. 28, 2001.
- [10] Honeywell, "Temperature Tutorial," http://content.honeywell.com/building/components/Hycal_Html/temp.asp, Oct. 28, 2001.
- [11] C. Wilson, "Beagle 2 wind sensor," <http://www.atm.ox.ac.uk/user/wilson/B2WS/>, Oct. 28, 2001.
- [12] BGI Incorporated, "Microdust Pro™ - Aerosol Photometer," <http://www.bgiusa.com/iaq/micro.htm>, Oct. 14, 2001.
- [13] Sensidyne, "OEM Micro Air Pumps," <http://www.sensidyne.com/oem/oemproduct.htm>, Oct. 22, 2001.
- [14] Boeing, "Boeing: Spectrolab," <http://www.boeing.com/news/releases/2000/hughes/spectrolab.html>, Jan, 2000.
- [15] Electrochem, "Battery Engineering, Type 26," <http://www.batteryeng.com/type26.htm>, Nov 15, 2001.
- [16] Electrochem. "Function and Performance of Lithium/Thionyl Chloride Cells," http://www.batteryeng.com/func_perf.htm, Nov 15, 2001.
- [17] Quality Kits Technology, "UHF/VHF Preamplifier.," <http://www.qkits.com/serv/qkits/maplin/pages/LT73.asp>, 2001.
- [18] Radiometrix, "UHF Radio Telemetry Transmit Module Data Sheet," <http://www.radiometrix.co.uk/dsheets/txm.pdf>, Jan. 4, 2001.

- [19] Samsung Electronics Co. Ltd., "System LSI Semiconductors," http://www.samsungelectronics.com/semiconductors/System_LSI/32_bit_ARM_based_RISC_MP_U/PDA/S3C44B0X/s3c44b0x.htm, Oct. 10, 2002.
- [20] Honeywell, "Temperature Sensors," http://content.honeywell.com/sensing/prodinfo/temperature/catalog/c15_85.pdf, Oct. 2, 2002.
- [21] Honeywell, "Pressure Sensors," http://content.honeywell.com/sensing/prodinfo/pressure/catalog/c15_31.pdf, Oct. 2, 2002.
- [22] Casella USA, <http://www.casellausa.com/en/>, Oct. 10, 2002.
- [23] SKC Inc., "Haz-Dust III™ Particulate Monitor," <http://www.skcinc.com/prod/haz2.html>, Oct. 10, 2002.
- [24] Rupprecht and Patashnick Co., Inc., "DustScan Scout Model 3020 Aerosol Monitor," <http://www.rpco.com/products/ambprod/amb3020/>, Oct. 6, 2002.
- [25] Personal Interview with Eric Abrahamson, Engineer, CTD, Lafayette, Colo, October 26, 2002.
- [26] Composite Technology Development, Inc., "Insulation, Adhesives, and Coatings Specially Formulated for Space Cryogenic Applications," <https://www.SpaceCryo.pdf>, Sept. 25, 2002.
- [27] Sheldahl, "Second Surface Aluminized Polyimide Tape with Acrylic (966) Adhesive," <http://www.sheldahl.com/Product/bulletins/PBPIVDA966.htm>, Oct. 26, 2002.
- [28] M. Davidoff, *The satellite Experimenter's Handbook*. American Radio Relay League, 1990.
- [29] F. Incropera and D. DeWitt, *Fundamentals of Heat and Mass Transfer: Fourth Edition*. John Wiley & Sons, 1996.
- [30] Spectrolab Photovoltaic Products, "Products-Space-Cells," <http://www.spectrolab.com/prd/space/cell-main.asp>, Sept. 24, 2002.
- [31] E. Hecht and A Zajac, *Optics*. Reading, MA: Addison-Wesley, 1975.
- [32] *The ARRL UHF/Microwave Experimenter's Manual Antennas, Components, and Design*. Newington, CT: The American Radio Relay League Inc, 1990.
- [33] "New Metallic Materials," <http://cheserver.ent.ohiou.edu/ChE620/New%20Metallic%20Materials-Al-Li%20Alloys.ppt>, Sept. 2, 2002.
- [34] R. Pahl (Rob.Pahl@alcoa.com), "Re: Al-Li Quote," October 10, 2002.
- [35] The European Association for Astronomy Education, "Measuring the Solar Constant," <http://www.amtsgym-sdbg.dk/as/solarconstant/>, Sept. 30, 2002.
- [36] "Mars Temperatures: clear atmosphere," <http://www.ucls.uchicago.edu/MartianSunTimes/images/MarsTemp-clear.jpeg>, Oct. 15, 2002.
- [37] Personal Interview with Dr. Tim Ohno, Professor, Colorado School of Mines, Golden, Colo, October 3, 2002.
- [38] Personal Interview with Dr. Orlen Wolf, Professor, Colorado School of Mines, Golden, Colo, September 19, 2002.

APPENDIX A

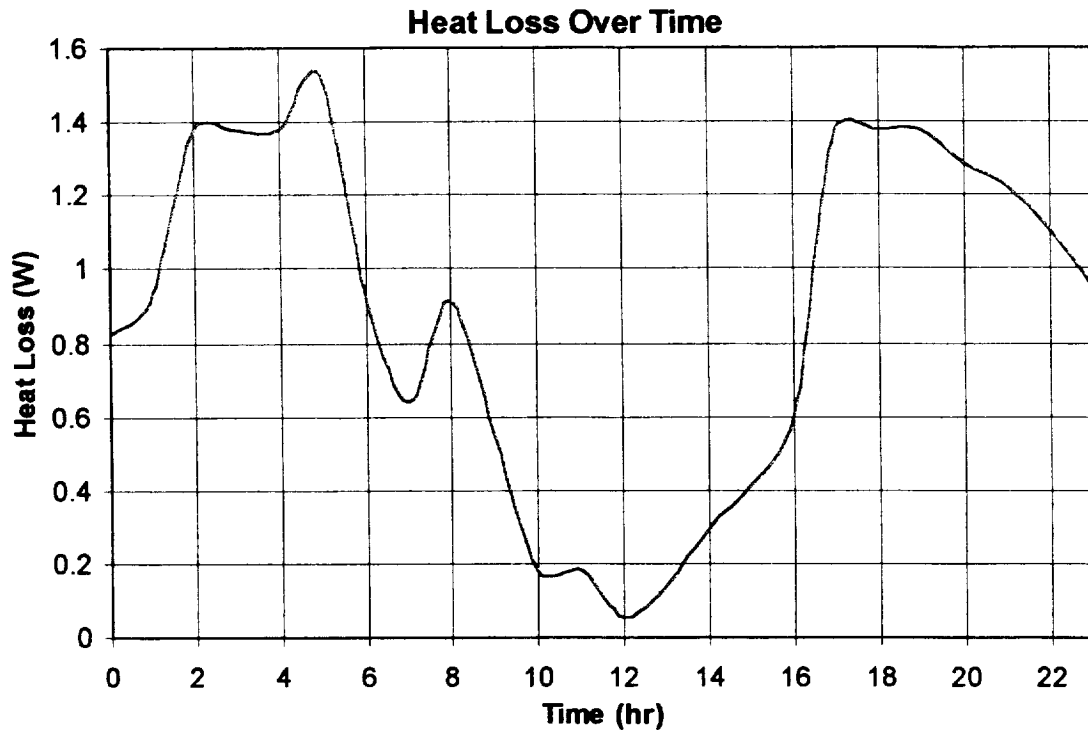


Figure 1: Heat Loss of Module over 24-hour period

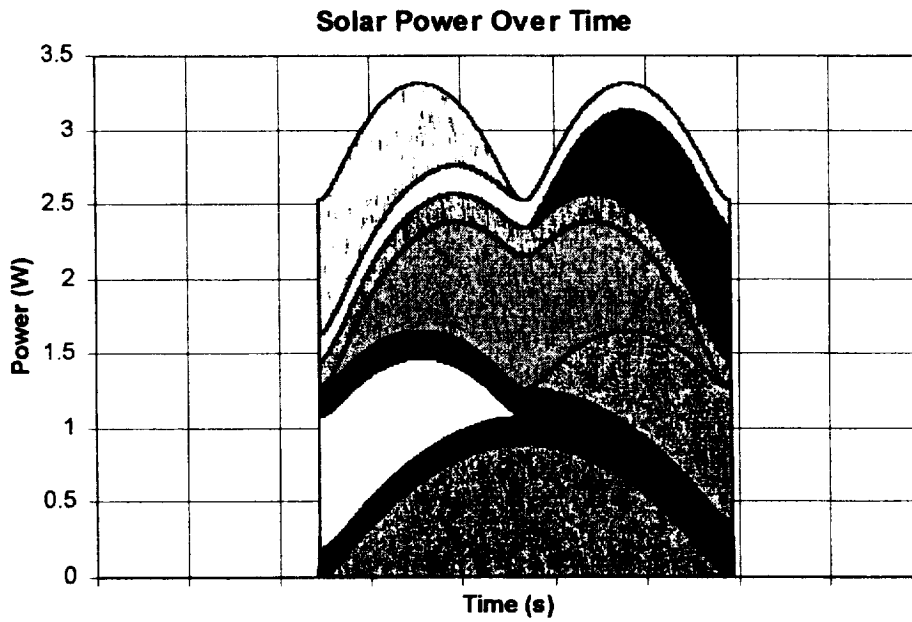
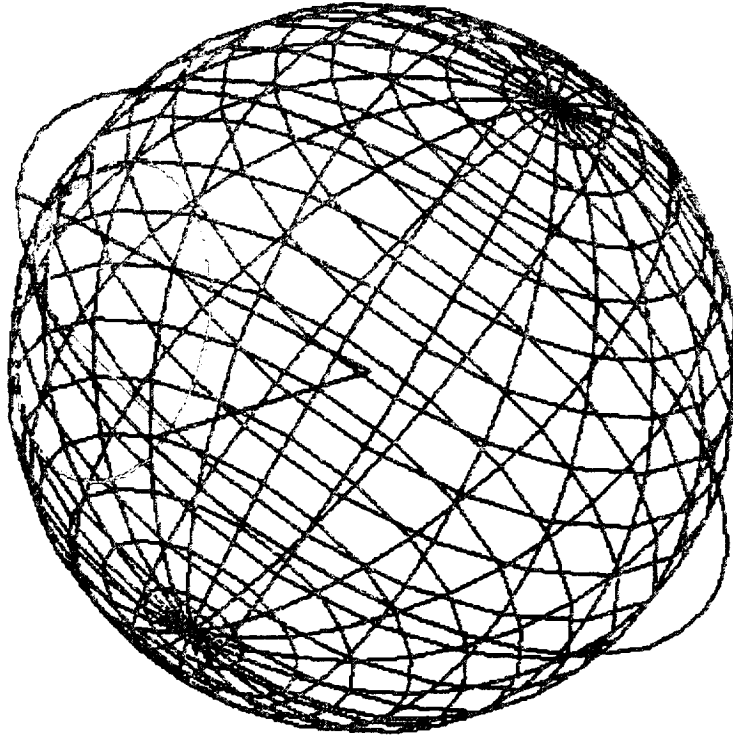


Figure 2: Combined Solar Energy from Solar Panels

APPENDIX B



Acquisition Circle Satellite Orbit

Calculations for Satellite Orbit [32]

Satellite Path=23 860 000 m

Orbital Velocity (v_0)=3.358 km/s

Orbit Time=7105 s

Mars Radius (R)=3397 km

Satellite Height (h)=400 km

Satellite Radius (r) =3797 km

$$s_o = 2R \cos^{-1} \left(\frac{R}{R+h} \right) = 1573 \text{ km}$$

$$Arc_{mars} = 3146 \text{ km}$$

$$R\theta = Arc_{mars}$$

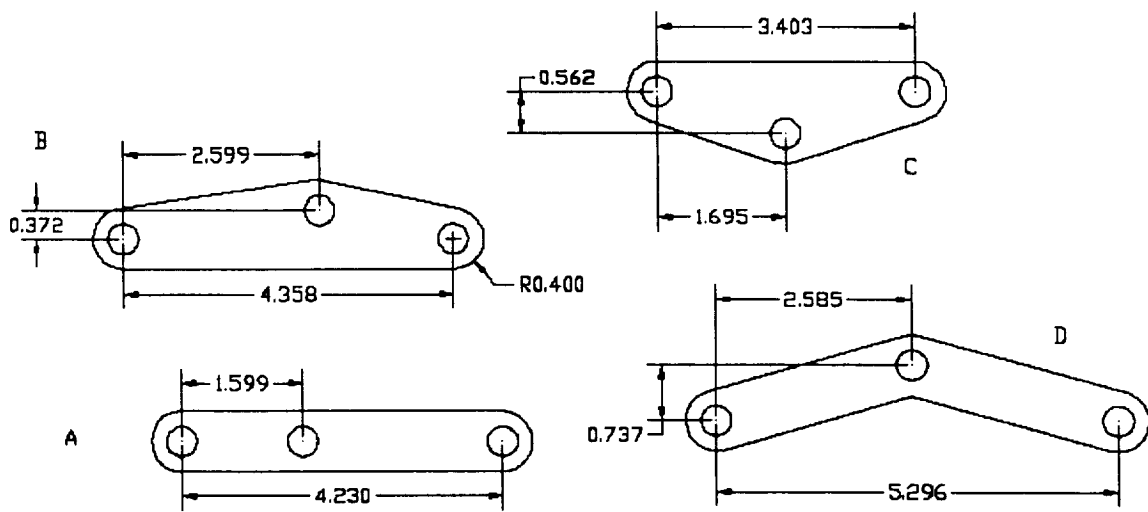
$$\theta = \frac{3146 \text{ km}}{3397 \text{ km}} = 0.926 \text{ rad}$$

$$r\theta = Arc_{satellite}$$

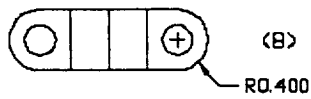
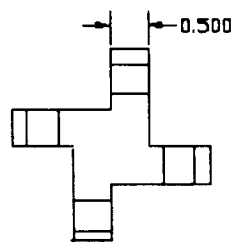
$$Arc_{satellite} = 3797(.926) = 3517 \text{ km}$$

$$time = \frac{Arc_{satellite}}{v_0} = \frac{3517 \text{ km}}{3.358 \text{ km/s}} = 1047 \text{ s} = 17.46 \text{ min}$$

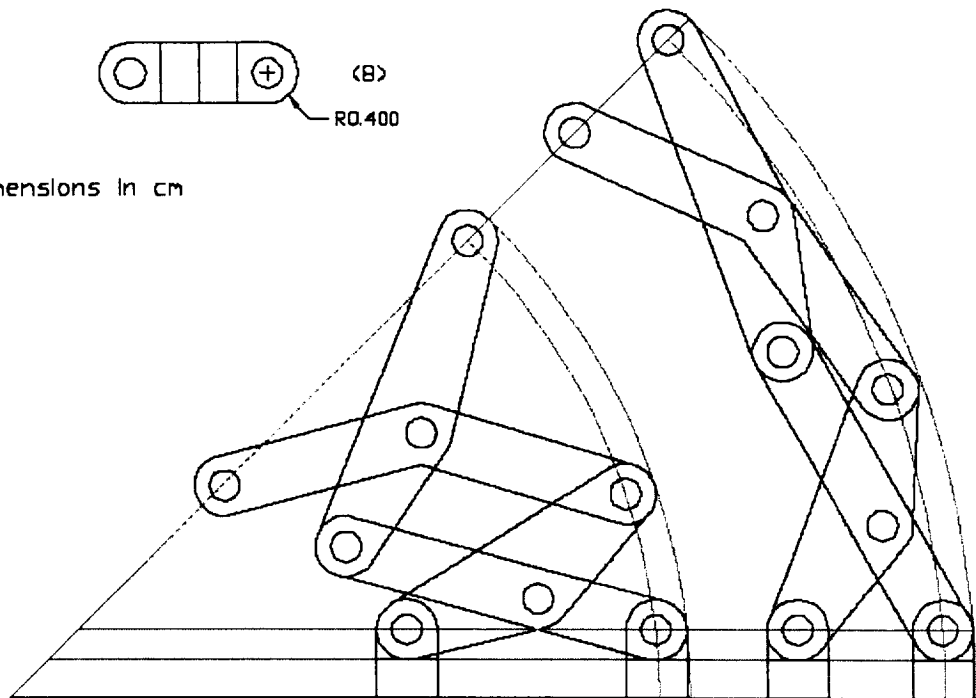
APPENDIX C



A-D: (24) 0.5



All dimensions in cm



P.A.R.T.S.

PLANETARY AERONAUTICAL RESEARCH TRA

S

Submitted by

Michael Ahern - Team Leader

Phil Davis

Van Englund

Jake Gustafsson

Steve Pankov

Chere Sampaio

Phil Savella



Faculty Advisor:

Dr. Mahmut Reyhanoglu

Associate Professor, Engineering Physics

Department of Physical Sciences

Embry-Riddle Aeronautical University

Submitted to:

THE RASC-AL PROGRAM

Lunar and Planetary Institute

Houston, Texas

ABSTRACT

The Plasma Accelerated Reusable Transport System (PARTS) is an unmanned cargo shuttle intended to ferry large payloads to and from Martian orbit using a highly efficient Variable Specific Impulse Magnetoplasma Rocket (VASIMR). The design of PARTS focuses on balancing cost and minimizing transit time for a chosen payload consisting of vehicles, satellites, and other components provided by interested parties.

1 INTRODUCTION

Throughout the last half-century, and especially in the last decade, the exploration of Mars has been a priority of scientific research. From Viking and Mariner performing basic flyby and surface observations, to Pathfinder and Surveyor searching for water and life, this commitment is verified. There is no reason to believe this desire for progress will relent, nor should it. In fact, countless missions are planned for upcoming years that put a permanent scientific presence on and above Mars' surface, not the least of which is establishing a temporary human colony on Martian soil. Building this presence means accelerating missions currently on the drawing boards from ideas into realities. Unfortunately, current methods and technologies in space travel prohibit carrying out even a fraction of the missions we conceive. Sending satellites independently to Mars on chemical rockets is simply cost and time ineffective.

PARTS intends to eliminate this roadblock. Being able to ferry multiple satellites, descent vehicles, and other mission components in one trip immediately improves efficiency, especially by lowering cost to individual participants. Utilizing modern technology, specifically plasma propulsion, makes travel quicker and more fuel-efficient. Transit time will be measured in weeks rather than months, and fuel consumption will be a tiny fraction of what today's rockets require. Once operational in 2015, and having a lifetime of ten years, PARTS will serve as a permanent transportation link between Earth and Mars, and redefine our access to Mars in the way the Shuttle redefined our access to orbit. Establishing this link will greatly accelerate progress for a much wider scientific community.

2 APPROACH TO THE PROBLEM

The vast scope of the problem of establishing this link was immediately apparent. Principally, we would have to:

1. Determine and upscale a plasma-based engine to suit our requirements.
2. Adapt a nuclear reactor and model an associated power system.
3. Design and model a spacecraft and payload bay in accordance with the above.
4. Develop functional docking operations.
5. Maintain weight within a reasonable envelope.
6. Model an appropriate trajectory and mission architecture.
7. Construct a communications link within the constraints of plasma propulsion effects.
8. Decide how such a large-scale spacecraft would be assembled.
9. Ensure the final design was within legal and environmental restrictions.

Initially, these tasks were subdivided among team members based on individual interests and strengths, yet we soon discovered the interdependence between these requirements. Often a solution to one problem meant the creation of a new problem elsewhere. This simple fact of engineering led us to insist on consistent and free communication between group members and transference of ideas among topical segregates. This is chiefly how the PARTS team has operated throughout the course of the last two months and how it will continue to operate until design completion.

The layout of PARTS can be found in Appendix A, which may be used as a reference guide throughout the report. Since PARTS is a cargo shuttle, the launch and payload operations were the first to be defined.

3 PARTS DESIGN

3.1 CARGO BAY

Currently, the largest methods of transporting a satellite from Earth to orbit are the Shuttle and the Delta IV Heavy. Both can lift in the neighborhood of twenty-three metric tons to low earth orbit (LEO). Due to these weight restrictions, the PARTS ship has been separated into two stages. Each will launch separately, one on a Delta IV Heavy and the other on the Shuttle. The first stage of the ship includes everything aft of the nuclear reactor (Figure 1) as well as the power rods for the reactor. The second stage is the inert reactor. Details of both stages are in the following sections. Due to NASA's safety policies regarding launches of nuclear payloads, the reactor will have to be launched second and activated in orbit by a team of astronauts.

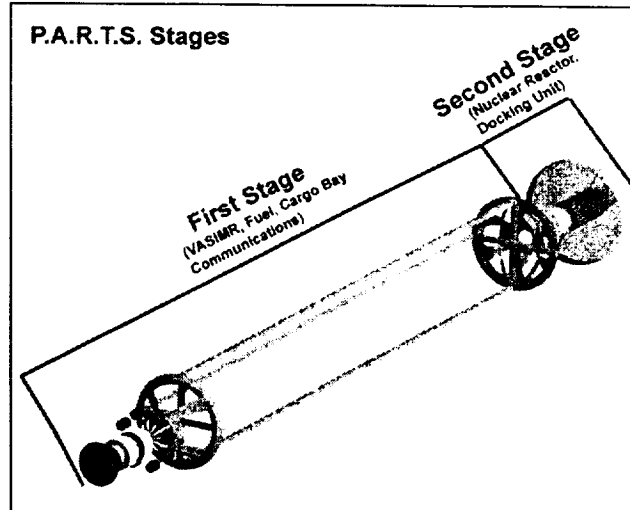


Figure 1 – The Two Stages of PARTS.

The launch of the first stage will begin at the Kennedy Space Center aboard a Delta IV Heavy rocket. The engines will ignite, taking the first stage to LEO. Once free of the Delta IV payload compartment, latches holding the collapsed cargo bay will release. Attitude thrusters attached to the docking unit (Figure 2) will fire continuously for a few seconds, unfolding the bay (Figure 3). Sensors in each member will report the success or failure of the locking mechanisms. Once completely unfolded, depending on sensor output, attitude thrusters on the docking unit and rear connector will fire in opposite directions, pulling the last of the arms into the locked position. If for some reason there is difficulty in deploying the cargo bay, it will be addressed by the astronauts upon arrival of the second stage.

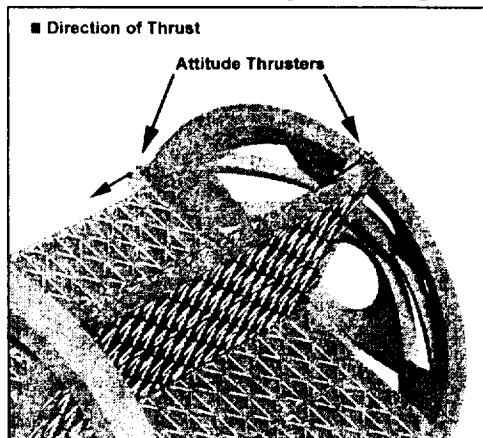


Figure 2 – Attitude Thrusters on the Cargo Bay (two not shown).

At the next available slot after the Delta IV launch, the Shuttle will be sent up with the second stage. Again, the launch will take place from the Kennedy Space Center. Once in orbit, the astronauts will serve a threefold purpose. Firstly, they will

assemble the PARTS spacecraft by docking the two stages. Secondly, they will bring the nuclear reactor online by loading the power rods. Finally, they will serve as a contingency plan should there have been any difficulty in expanding the cargo bay on the first launch.

Once these procedures have been performed, PARTS will be operational. Customer payloads will be sent to LEO aboard Delta IV rockets inside a custom-made payload box, whose details appear in the following section. Payloads will be delivered to a nearby orbit, whereupon PARTS will initiate a sequence of orbital maneuvers to place itself within docking range. At that time it will switch to attitude thrusters and maneuver such that the payload is placed in the cargo bay. Capture Actuators on all three sides of the cargo bay will activate, locking down the cargo. This process will repeat three times, at which point the entire bay will be full. The estimated total mass of the PARTS ship with a full load of three Delta IV payloads is about 90-110 metric tons. At the appropriate time, the ship will engage its engines and depart for Mars.

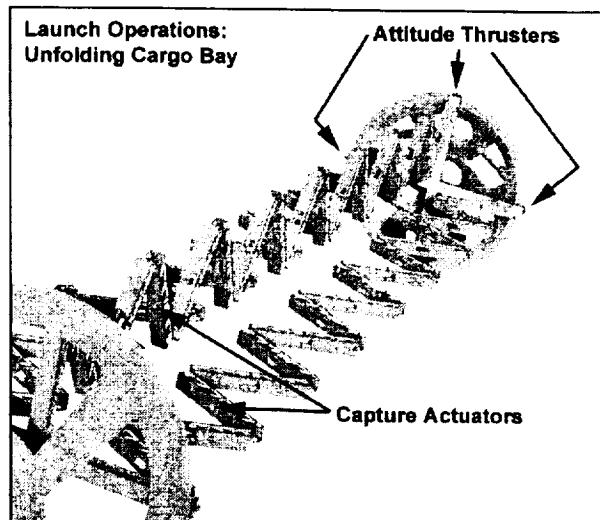


Figure 3 – The Cargo Bay unfolding.

Upon arrival at Mars several weeks later, the ship will begin releasing payloads at their respective orbit altitudes. Starting at the lowest orbit, Capture Actuators will disengage on two of the three sides of the Cargo Bay. The third actuator will give the payload a slight push before disengaging. The payload box will use this push and its internal attitude control system to guide itself slowly from the ship. Once clear of the ship, PARTS will transmit a command to engage explosive bolts placed around the periphery of the box. The bolts will cause the box to separate, releasing the cargo into orbit. After some time the orbit of the box halves will degrade such that the payload box will enter the Martian atmosphere. Finally, after releasing all three payloads into Mars orbits, PARTS will again engage its engines and depart for Earth for refueling and reloading.

3.1.1 TRUSS MEMBERS

The cargo bay will be constructed of aluminum. Aluminum was chosen primarily for its ability to handle large axial loads, which will occur during the unfolding operation.¹⁷ Each member is a truss with hinges on both ends, similar to a door, and a large cavity in the middle (Figure 4). The cavity will house the Capture Actuators, whose details follow. Threaded through each member will be large power cables that will transfer the power from the reactor to the engine.

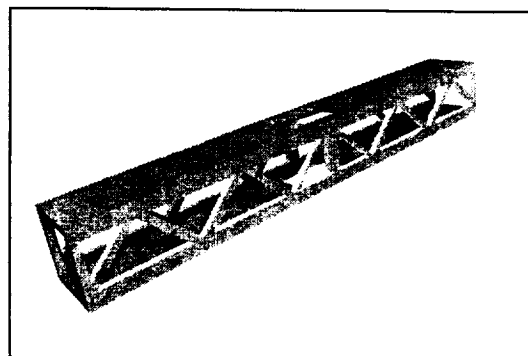


Figure 4 – A Typical Truss Member (hinges not shown).

3.1.2 CAPTURE ACTUATORS

Capture Actuators will be placed in the third, eighth, and fourteenth truss members in each arm of the Cargo Bay. Each actuator is composed of three cylinders that extend out of the base when an electric motor is engaged. The extending arm will be received by the docking mechanisms on the Cargo Shell. Three points of contact will assure that the cargo is maintained rigidly inside the Cargo Bay throughout the duration of the mission.

3.1.3 CARGO SHELL

In order to bring cargo to Mars without having PARTS land on Earth to pick it up, it will be required that cargo be placed in expendable, custom-made shells. These will be filled with cargo while on the ground and then launched into orbit using a Delta IV Heavy rocket. The shells will be about 17 m long and about 4.25 m in diameter. These dimensions come from the payload size restrictions set by the Delta IV Heavy's available cargo space (Figure 5). The shells will be constructed out of aluminum 6061-T6. This material was chosen for three main reasons: it has a high strength to weight ratio; it is easy to machine; and it is, most importantly, not magnetic. In order to properly dock with PARTS, the shells will be equipped with four docking mechanisms

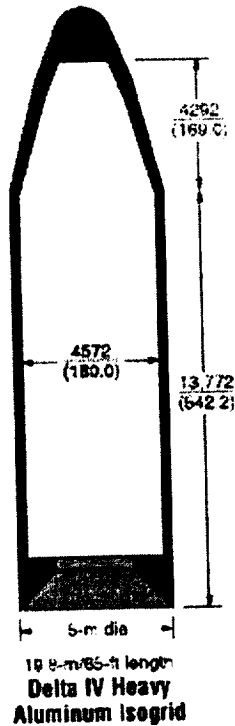


Figure 5 - Delta IV Specifications.

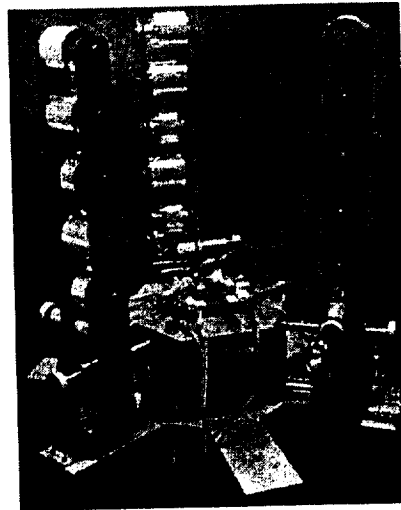


Figure 6 - Docking Mechanism.²⁰

(Figure 6). Four mechanisms were chosen over three so that in any orientation the shell presents an available docking mechanism to dock. These mechanisms will be used to guide in the three capture

Table 1 - Reaction Wheel Specs.²¹

Nominal torque range	+/- 0.20 N-m
Nominal momentum range	+/- 8.6 N-m-sec
Power	40 to 80 W peak
Weight	6.4 kg

actuators located in the cargo truss member. The shells will have a thickness of 0.01 cm. Inside each shell there will be four tiered aluminum rings that will be connected by eight equally spaced bars. These rings will be used to support the aluminum shell. The four docking mechanisms will attach to one of the rings. These mechanisms will be 430 mm in diameter and 420 mm in height. They will each require an average of 12 W of power at 24 V. In order for the cargo shell to properly align for docking it will be equipped with three integrated reaction wheel assemblies (IRWA). The IRWA technology provides a nominal torque range of +/- 0.20 N-m with a nominal momentum range of +/- 8.6 N-m-sec and requires a peak power of 40 to 80 W (Table 1). The reaction wheels are 216x216x102 mm in size. To provide enough power to operate the docking mechanisms and the reaction wheels, lithium thionyl chloride batteries will be used. These batteries provide 175-440 W-hr/kg for about four hours. The batteries will need to provide a maximum of 384 W of power (36 max for each docking mechanism and 80 max for each reaction wheel). Each battery will have a mass of 2.5 kg. There will be a total of two of these batteries, one for earth orbit and one for Martian orbit. The three IRWA's will keep the cargo shell oriented in a parallel position to PARTS. Once the cargo shell gets close to PARTS (about 1 m), the docking mechanisms will start to open at a rate of 20 mm/s. Once the actuators enter the docking mechanisms, they will close at a rate of 20 mm/s. This will allow for a smooth docking operation with PARTS and will not take more than the four hours allowed by the batteries.

Mass considerations had to be taken into effect to construct the cargo shell (Table 2). The outside aluminum casing will have a mass of 154.0 kg, the four rings will have a combined mass of 90.0 kg (22.5 kg each), the eight bars connecting the rings will have a combined mass of 230.0 kg (28.75 kg each), the four docking mechanisms will have a combined mass of 64.0 kg (16.0 kg

each), the two batteries will weigh 5.0 kg (2.5 kg each) and lastly the reaction wheels will have a total mass of 19.2 kg (6.4 kg each). The complete cargo shell will have an approximate mass of 562 kg.

Table 2 - Shell Mass Budget.

Part	Mass (kg)
Aluminum Casing	154.0
Rings	90.0
Bars	230.0
Docking Mechanism	64.0
Battery	5.0
Reaction Wheel	19.2
Total	562.2

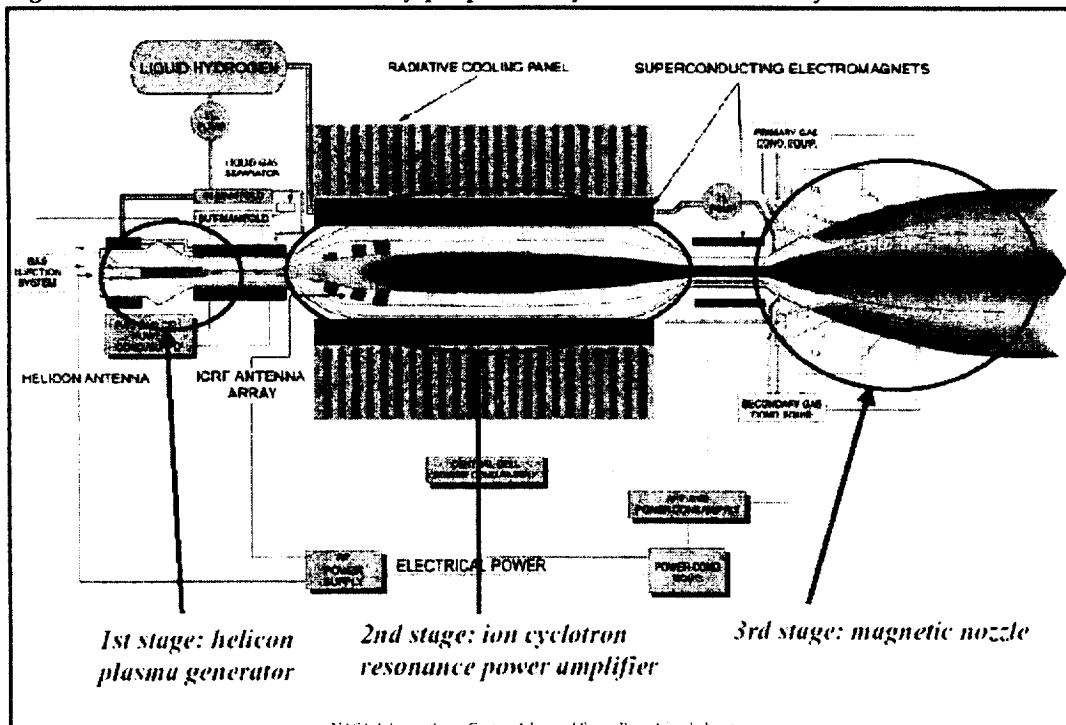
3.1.4 REFUELING

Upon returning to Earth orbit, PARTS will need to refuel its hydrogen tanks. A cargo shell specifically fitted with thermal insulation and cryogenics will launch from the Kennedy Space Center and dock with the ship in the usual fashion. An arm will extend from the rear of the cargo bay to the payload, docking with it. Hydrogen will flow down this arm and into the tanks. The empty box will be ejected from the ship in the normal manner and will burn up on reentry.

For safety reasons, automation of the nuclear power rod refueling is unfeasible. Thus, when supply is used up, a shuttle will have to be sent to dock with PARTS. Astronauts will remove the spent power rods and dispose of them in a manner acceptable to both NASA and the government. New power rods will be inserted, and the PARTS ship will be set for more trips.

3.2 ENGINE

The VASIMR engine, currently under development by NASA, is the leading advancement of a high power, electrothermal plasma rocket.³⁻⁹ Its design incorporates low cost by utilizing hydrogen propellant. The design also provides high and variable specific impulse putting VASIMR at the forefront of any propulsion system available today.⁹



NASA Johnson Space Center, Advanced Space Propulsion Laboratory

Figure 7 - VASIMR Stage Diagram.



Figure 8 – Helicon Antenna.⁴

The first concept involved in the operation of a plasma rocket is the understanding of plasma itself. The gaseous state of a substance is transformed into plasma by heating the substance to extreme temperatures. The electrons are then stripped from the neutral atoms. These electrons, which have a negative charge, and the ionized atoms, which have a positive charge, are combined together making an electrically neutral mix of free charged particles called plasma. Unfortunately, plasma cannot be contained by any known material. Therefore, magnetic fields are needed to control the plasma.

To produce plasma, hydrogen gas will need to be ionized. Hydrogen, in liquid form, will be stored in tanks and flow into a gas separator. From this, neutral hydrogen gas will be injected into the forward-end cell of the engine (Figure 7). In this section, electrically powered radio waves ionize the hydrogen gas in the presence of a magnetic field, which is generated by a series of electromagnetic coils. Dense plasma is formed with a device known as a helicon antenna (Figure 8). The plasma then flows along the magnetic fields into the central cell, where it is further energized by a process known as ion cyclotron resonance heating (Figure 9).

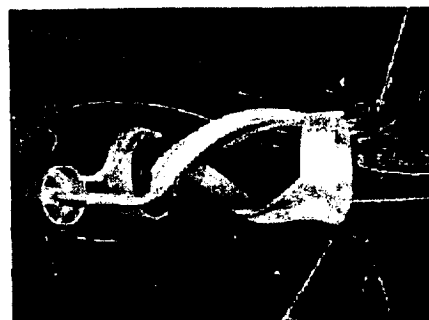


Figure 9 – Ion Cyclotron Resonance Heating.⁴

In this process, additional radio waves resonate with the natural cyclotronic ion motion around the diverging magnetic field lines. This central cell behaves like a power amplifier. The plasma is then channeled into the aft cell, which acts as a hybrid two-stage magnetic nozzle. The nozzle converts the thermal energy of the plasma into a highly directed exhaust stream while efficiently detaching the plasma from the magnetic field.

A critical characteristic of the VASIMR engine is its ability to fluctuate its exhaust parameters with constant power throttling (CPT)⁶, a technique where thrust and specific impulse can be varied while the total power is kept constant. The ability to control power to the helicon antenna and ICRH systems allows the flexibility of the exhaust conditions. For high thrust, radio frequency (RF) waves are mostly fed to the helicon antenna, while more power is diverted to the ICRH system for high specific impulse. The total RF input is kept at a constant maximum for efficient consumption of the electric power source. Since the total power to the engine is kept constant, increasing the exhaust velocity will come at the expense of thrust and vice versa. However, this allows for maintenance of effective thrust at high spacecraft velocities.

Another advantage of the engine is its lack of electrodes, enabling it to operate at higher power densities. The electrodeless design prevents corrosion and contamination that could contribute to premature failure and loss of energy through radiation from the contaminants in the plasma. Another key feature is the engine's use of hydrogen as its propellant. Hydrogen is inexpensive, low weight, and abundant. It acts as radiative cooling for the spacecraft. The ICRH uses high voltage and low current, making mass relatively low and resulting in minimal energy loss. These characteristics incorporate the demands of the mission objectives.

The engineering concepts of the VASIMR design include the specifications of its parameters.

These parameters include the following:

- total input power
- cross-sectional area of the exhaust stream
- density of the exhaust plasma
- thrust produced
- plasma mass flow rate
- plasma exhaust velocity
- initial propellant mass

Current calculations demonstrate that for a given total input power of 15-20 MW, the engine can generate up to 500 N of thrust at 50% efficiency. Once again, varying certain parameters such as plasma density and mass flow rate, thrust and exhaust velocity can be altered. Specific Impulse, comparable to the design requirements, will range from 3,000-30,000 seconds. Computations result in an expected propellant mass to be less than 50% of the total spacecraft mass. Such parameters require technologies that have not been available as of yet. Present limitations will force considerable research and exploration of the engineering aspects of VASIMR. Theoretical studies of VASIMR will eventually be verified with laboratory experiments. In order to achieve a feasible demonstration of the technology required for operation of the engine, an ongoing investigation of design concepts of VASIMR will be necessary.

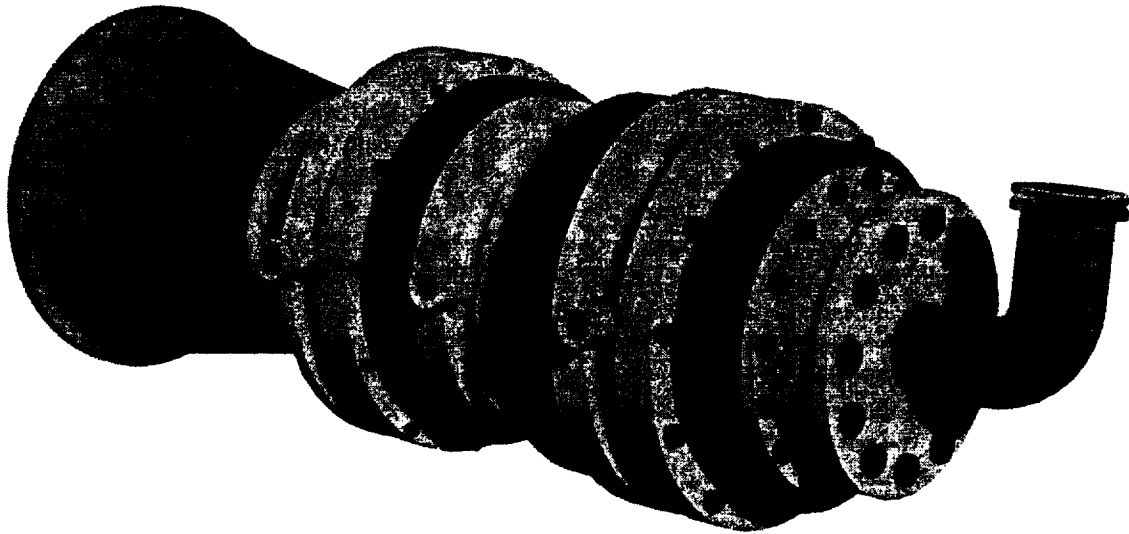


Figure 10 - Solid Model VASIMR.

3.3 TRAJECTORY

Due to the nature of the propulsion system we have chosen, impulsive transfers are out of the question in all regions of the mission: within Earth's sphere of influence (SOI), passing between the planets, and entering Mars' gravitational field. The VASIMR plasma accelerator is simply not of the conventional rocket type. Instead of firing a short-duration pulse to enact an almost immediate step-change in velocity, it will provide a low continuous thrust for an extended period of time.

However, the impulsive situation proves to be undesirable. While relatively fuel efficient as far as chemical propulsion transfers go, the Hohmann transfer takes entirely too long to fulfill our mission objectives. On the other side of the spectrum, high-speed chemical transfers, although requiring little time, are prohibitively expensive in terms of total fuel required, which can easily increase the initial mass of the vessel by several factors. The VASIMR engine provides both the advantage of high-efficiency and high-speed. Our engine requires, and the mission time objective stipulates, that we find a trajectory that allows us to exploit the promise of plasma propulsion.

As a result, the generalized mission architecture follows: the spacecraft starts in low-Earth orbit, where it was originally assembled and presently docks with shipments to be taken to Mars. At the necessary time of deployment, VASIMR will be engaged, imparting a small but continuous acceleration along the velocity vector. This gradually adds energy to the vessel, and will carry PARTS out to larger and larger orbits. Thrusting along the velocity vector results in the most efficient increase in spacecraft energy, illustrated by the relation:

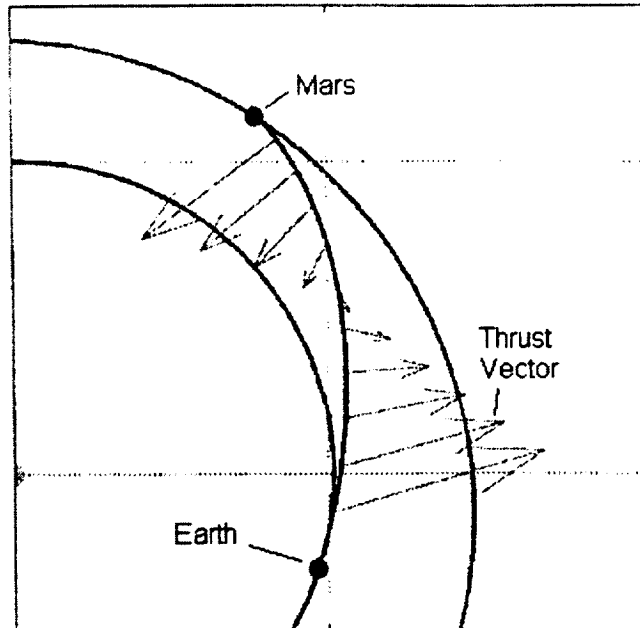


Figure 11 – Optimal Transfer Trajectory.^{2,15}

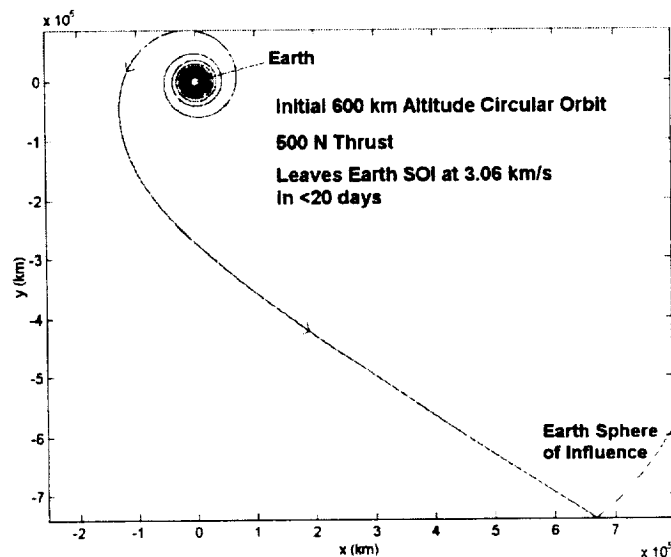


Figure 12 – Opening Spiral Earth Departure.

which is maximum when the acceleration A and the velocity v are parallel. The resultant trajectory is an opening spiral connecting LEO to the edge of Earth's SOI.

$$\frac{d\varepsilon}{dt} = \vec{A} \cdot \vec{v}$$

which is maximum when the acceleration A and the velocity v are parallel. The resultant trajectory is an opening spiral connecting LEO to the edge of Earth's SOI.

At this boundary, the problem shifts to a heliocentric two-body problem. In the first portion of the transfer, PARTS accelerates into a highly elliptical heliocentric orbit that intersects with that of Mars. In the optimal scenario, the acceleration occurs to approximately the halfway point, achieving an extremely high velocity (Figure 11). After this point, retrofiring will slow the craft to a speed acceptable for entering the Martian gravitational field, whereupon a closing spiral trajectory describes the craft's motion toward a desired low orbit around the Martian surface. Of course these three two-body problems are linked by initial and boundary conditions to produce one seamless trajectory profile.

In the example mission created, the spacecraft begins at a low-earth circular orbit of radius 7000 km. Thrusting parallel to the velocity vector at all times, the opening spiral trajectory allows PARTS to leave the gravitational influence of earth in 19.6 days (Figure 12). The spacecraft then continues to accelerate for eight days, after which the engine is shut off. This is a bang-off scenario, and although it is not the shortest possible path, it results in an extremely low-consumption mission. Rendezvous with the Martian sphere of influence occurs 166 days after shut-off. By this time, the ship has been oriented so that thrusting would now occur on the anti-velocity vector. Firing at maximum thrust on this vector results in the settling of PARTS into a circular orbit of 4002 km, 10.2 days after Mars SOI arrival. After all payloads have been released, PARTS will again thrust parallel to velocity resulting in the same type of opening spiral trajectory encountered previously. Only now, with a ship mass approximately half that as before, Mars SOI departure occurs in only six days, and time from earth SOI to parking orbit is only 11 days.

3.4 ATTITUDE CONTROL

Attitude control will be performed by 32 thrusters located in eight positions, four positions immediately forward, and four aft, of the cargo bay. Manufactured by Marquardt, the model R-6C bipropellant thrusters can exert 20 N each, and have a lifespan of more than 16 hours (thrusting time), yet their combined mass is less than 25 kg. In this configuration, they will provide adequate 3-axis control.^{17,18}

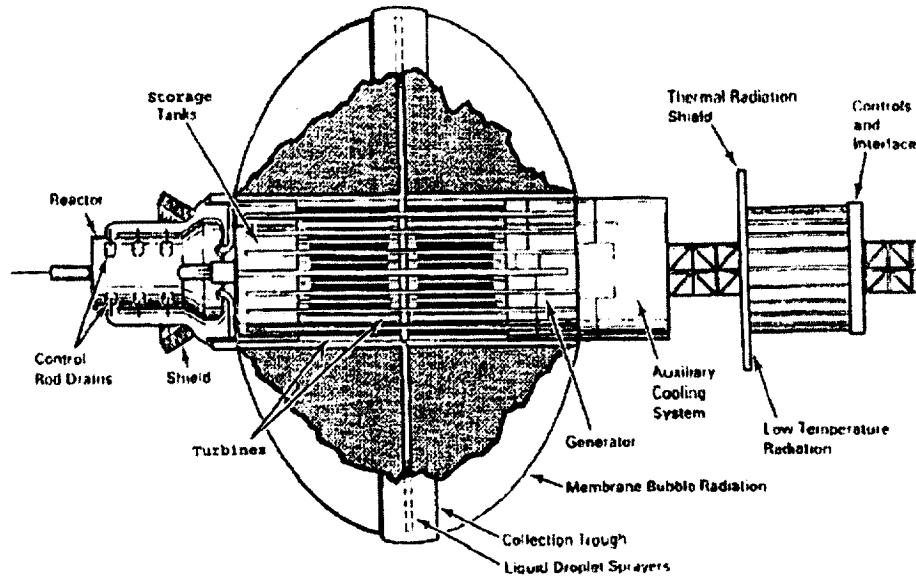
Few orbital corrections will be needed, as we are never remaining in one orbit for very long. However, they will be pulsed extensively while docking with payloads, as precise synchronization in this case is required. Out of parking orbit, pulsing will still be necessary in order to keep the ship aligned with our intended direction of thrust. About halfway to Mars the ship will turn around to begin retrofiring. This significant attitude adjustment must be made expeditiously, thus the steady-state operation of the thrusters will be employed.

Calculations based on a fully loaded ship and worst-case mass distribution have given us expectations for roll, pitch, and yaw rates. We expect pitching or yawing 180° will take no more than 11 minutes, firing four thrusters simultaneously. To roll the spacecraft 360° around its longitudinal axis, firing eight thrusters simultaneously, will take no more than 90 seconds. We feel these high-end estimates are well within reasonable limits.

3.5 NUCLEAR REACTOR

A nuclear reactor capable of producing multi-megawatts of electric power is necessary to allow the VASIMR engine to provide optimal thrust. PARTS will employ a reactor based on Battelle's Rotating Multi-Megawatt Boiling Liquid-Metal Reactor (RMBLR). The RMBLR (Figure 13) uses a bubble membrane radiator to provide up to 20 MW of electrical power at a low specific mass. RMBLR uses Ceramic Metallic Composite (cermet) fuel developed by the Department of Energy for power production and a direct Rankine cycle for converting the power into electrical energy. RMBLR is cooled using boiled liquid potassium and its bubble membrane. Battelle completed its conceptual design, but funding was cut before the reactor could be completed and tested. With the proper funding, the RMBLR concept could be completed with necessary reconfigurations, tested, and implemented on PARTS well within the fifteen year development timeframe.

Rotating Multi-Megawatt Boiling Liquid-Metal Reactor (RMBLR I)

Figure 13 - Rotating Multi-Megawatt Boiling Liquid-Metal Reactor (RMBLR I).¹

3.5.1 REACTOR DOCKING AND POWER TRANSFER

PARTS and RMBLR will be launched separately, necessitating the design of a single use docking system. The docking system must also contain an integrated power transfer system that will transfer the 20 MW of electric power produced by RMBLR to the VASIMR engine. The docking mechanism will be located on the end of the Cargo Bay opposite VASIMR. The mechanism will consist of three parts: the main body, the locking mechanism, and the power outlet (Figure 14). The power outlet consists of 36 sockets each with a surface area of 25 cm² and length of 15 cm. The reactor will be equipped with a "plug." The plug has 36 silver wires that fit perfectly into each of the sockets to transfer power from the reactor to the engine. Silver was chosen because of its low resistivity (1.61 $\mu\text{ohm}\cdot\text{cm}$) and high thermal conductivity (417 W/m \cdot °C). After the reactor plug has completely slid into the ship docking mechanism, the locking mechanism will rotate 45° completely locking RMBLR to PARTS. A manned shuttle mission that will also be responsible for providing the cermet fuel rods for the nuclear reactor will carry out the docking operations.

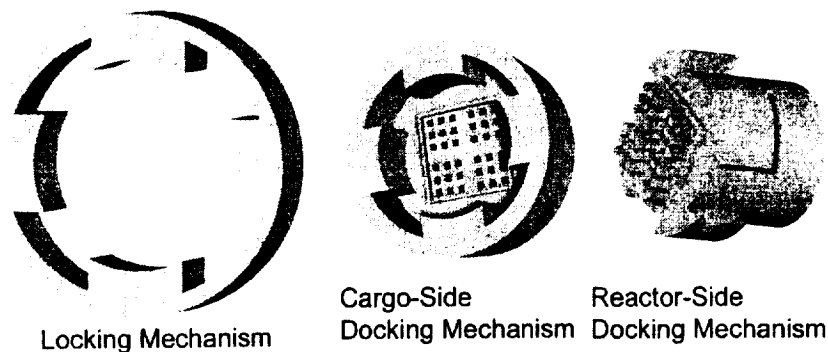


Figure 14 - Docking Mechanism Components

3.6 COMMUNICATIONS

Due to the interference that the plasma imposes on the signals sent directly to earth from the back of the ship (if the signal was sent through the plasma field), communications will be accomplished via a relay satellite in orbit around Mars. The Deep Space Network would be the ideal ground station due to its highly advanced and unsurpassed capabilities for deep space communications. A MARSat from the Mars Network will be used as our Mars-based relay satellite. The Mars Network will consist of a constellation of microsattellites and one or more MARSats in orbit around Mars. The Mars Network will be the communication gateway to future Mars exploration. It is currently being studied at the Jet Propulsion Laboratory (JPL) and the beginnings of the prototype Mars Network are tentatively scheduled to be launched in 2003.

3.6.1 GROUND STATION

The Deep Space Network (DSN)¹⁰ will be used as the ground station for communications to and from PARTS. The network consists of three facilities that are located approximately 120 degrees apart: one at Goldstone, California; one at Canberra, Australia; and one at Madrid, Spain. Each ground station controls one 70 m antenna and several 34 m antennas for communicating with deep space spacecraft. The 70 m dish is the largest and most sensitive DSN antenna, and is capable of tracking spacecraft traveling more than 16 billion km from Earth. Each DSN site has one central Signal Processing Center (SPC) connected to the ground station's antennas. Each SPC is connected in a network, providing hand off capability between stations allowing 24-hour coverage of deep space spacecraft. Also, the three facility locations are located in very dry areas so the communication disturbances due to rain can be neglected. DSN has a designated uplink frequency of 7145-7190 MHz and a downlink frequency of 8400-8500 MHz for X-band telecommunication links.

3.6.2 MARS NETWORK

Mars Network is a proposed constellation of satellites at Mars for providing communication and navigation services to other Mars exploration elements. When it is completed, Mars Network would essentially be an extension of DSN at Mars, enabling substantially more data to be relayed to the Earth than if each Mars exploration element attempted to send back its own data directly.¹³ A MARSat from the Mars Network will be used as a relay satellite for the spacecraft to communicate with Earth. The Mars Network will provide nearly continuous communication possibilities with DSN, however the connection will be lost during times of Mars solar conjunction. There are six superior Mars solar conjunctions that will occur between 2015 and 2026, and during these conjunctions Mars is only in the no communication zone for about 42 hours.¹¹

3.6.3 SPACECRAFT TO MARSAT RELAY

The PARTS ship will have a 3 m, gimbaled, parabola antenna used for communicating with the MARSat relay satellite. Parabolic reflectors will work best with the chosen carrier frequency. Since the signal has to travel five astronomical units (worst case) a large transmitting power will be necessary to carry the signal through space.¹⁶ The PARTS antenna will operate at a transmitting power of 200 W and will use an X-band frequency of 8.4 GHz (wavelength=0.035714 m). PARTS' link budget is shown in Table 3.

Table 3 - Link Budget for PARTS to MARSat

Item	Symbol	Value	Units
Frequency	f	8400-8450	MHz
Transmitter Power	P_t	200	Watts
Transmitter Power	P_t (dB)	23	dBW
Transmitter Line Loss	L_l (dB)	1.5	dB
Transmit Antenna Diameter	D_t	3	m
Transmit Antenna Gain	G_t	45.97	dB
Equiv. Isotropic Radiated Power	EIRP	68.98	dB
Space Loss	L_s	-280	dB
Receive Antenna Diameter	D_r	2.7	m
Receive Antenna Gain	G_r	44.92	dB
Power Received	P_r	-167.75	dB
System Noise Temperature	T_s	75	*K
Signal-to-Noise	S/N	13.80	DB

3.6.4 MARSAT TO EARTH

The MARSat relay satellite consists of a 2.7 m antenna for communications with DSN, using an X-band relay link. It has high power capabilities (>100 W) and is assumed to operate around at least 150 W for relay communications with DSN.¹⁴ The receiving antenna at DSN will be a 70 m antenna cooled to an operating temperature of 28.5 degrees. MARSat's link budget is displayed in Table 4.

Table 4 - Link Budget for MARSat to Earth

Item	Symbol	Value	Units
Frequency	f	8400-8450	MHz
Transmitter Power	P_t	>100	Watts
Transmitter Power	P_t (dB)	>20	dBW
Transmitter Line Loss	L_l (dB)	1.5	dB
Transmit Antenna Diameter	D_t	2.7	m
Transmit Antenna Gain	G_t	44.92	dB
Equiv. Isotropic Radiated Power	EIRP	92.02	dB
Space Loss	L_s	-280	dB
Receive Antenna Diameter	D_r	70	m
Receive Antenna Gain	G_r	72.02	dB
Power Received	P_r	-142.80	dB
System Noise Temperature	T_s	28.5	*K
Signal-to-Noise	S/N	31.25	dB

4 CONCLUSIONS

Although space exploration has been developing at a phenomenal rate, Mars remains the stumbling block. Recent travel to Mars has been tainted by the back-to-back failures of the Mars Polar Lander and the Mars Climate Orbiter. Now, more than ever, time and cost are factors of any planned mission to Mars. By significantly lowering the cost of travel to Mars, PARTS will expedite its development. Satellites, descent vehicles, and supplies - the infrastructure of a manned mission - could all be sent to Mars at a fraction of the cost and a multiple of the speed provided by current technology. In this light, a shuttle link to Mars is necessary. PARTS is this link, and by researching and developing the related technology, the colonization of Mars could arrive years before even the most optimistic chemical-rocket-based prediction.

5 FUTURE STUDIES

In the upcoming months, we will have to expand on our current findings in order to augment our design. We will analyze topics and problems not addressed at this time. Some revisions will include:

1. Continually adapting our use of the VASIMR engine to include significant changes made (and released to the public) by those specifically researching and experimenting with that engine.
2. Revising our application of thrusters for attitude control, and interfacing with a Guidance and Navigation computer yet to be designed.
3. Developing a complete trajectory profile that is seamless in all regions of travel. This will involve solving a multiple-point boundary value optimal control problem. Our goal is to fix thrust state in the problem (so that the engine is always on), yet optimize thrust angle (relative to the flight path) such that trip duration is minimized. Ideally, we can keep this solution general enough that it will apply, after changing initial and boundary conditions, to a mission starting on any date, irrespective of the planets' relative positions.

Additions to the design will include:

1. A full structural analysis of all hardware to ensure loads and torques are within tolerances everywhere.
2. Verification of complete thermal equilibrium of all PARTS components.
3. A comprehensive cost analysis, detailing all research, development, and production costs.
4. A balanced determination of risk, considering both the risks of preventable system failure and environmental catastrophe.

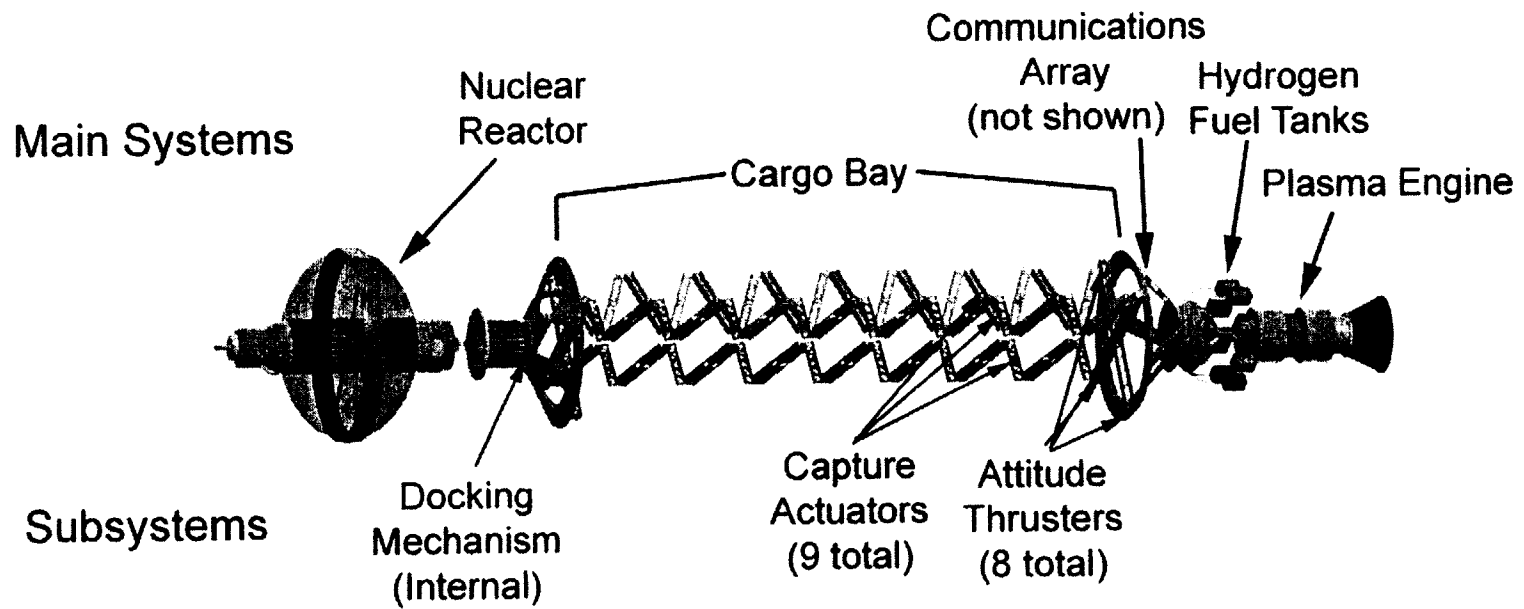
6 OUTREACH

Interacting with the community is an important part of any project. Team PARTS will be presenting its design in front of Embry-Riddle Aeronautical University (ERAU) faculty, graduate students, and family members of the design team later this year. Several projects are planned to do miniature presentations in front of local elementary and middle school students. This will encourage younger students to get involved in the engineering and space fields. Also, articles on PARTS will be printed in the local Daytona Beach newspaper, *The News Journal*, the ERAU school newspaper, the *Avion*, and the *Engineering Physics Newsletter* to garnish exposure to the design project.

7 REFERENCES

1. Barnett, John. "Nuclear Electric Propulsion Technologies: A Summary of Concepts Submitted to the NASA/DoE/DoD Nuclear Electric Propulsion Workshop". Pasadena, CA, 1990 pgs. 23-26.
2. Bertrand, Regis and Jacques Bernussou and Isabelle Barthes. "Optimal Low-Thrust Interplanetary Direct Transfers". IAF-99-A.6.01.
3. Chang Diaz, Dr. Franklin R. and et al. "A Flight Demonstration of Plasma Rocket Propulsion". AIAA-2000-3751.
4. Chang Diaz, Dr. Franklin R. and et al. "Helicon Plasma Injector and Ion Cyclotron Acceleration Development in the VASIMR Experiment". AIAA-2000-3752.
5. Chang Diaz, Dr. Franklin R. and et al. "Particle Simulations of Plasma Heating in VASIMR". AIAA-2000-3753.
6. Chang Diaz, Dr. Franklin R. and et al. "The Physics and Engineering of the VASIMR Engine". AIAA-2000-3756.
7. Chang Diaz, Dr. Franklin R. and et al. "Simulations of Plasma Detachment in VASIMR". AIAA-2002-0346.
8. Chang Diaz, Dr. Franklin R. and et al. "The Development of the VASIMR Engine". Available: <http://spaceflight.nasa.gov/mars/reference/aspl/develop.pdf> (October 13, 2002).
9. Chang Diaz, Dr. Franklin R. "Variable-Specific-Impulse Magnetoplasma Rocket". Lyndon B. Johnson Space Center, Houston, TX. Available: <http://www.nasatech.com/Briefs/Sep01/MS23041.html> (October 13, 2002).
10. Deep Space Network. Available: <http://deepspace.jpl.nasa.gov/dsn/> (November 2, 2002).
11. Hastrup, R. and D. Marabito. Communications with Mars During Periods of Solar Conjunction: Initial Study Results. Available: http://ipnpr.jpl.nasa.gov/tmo/progress_report/42-147/147C.pdf (November 2, 2002).
12. Lewis, Frank L. and Vassilis L. Syrmos. Optimal Control (2nd Edition). John Wiley & Sons, Inc. : New York. 1995.
13. Mars Network. Available: <http://marsnet.jpl.nasa.gov/index.html> (November 2, 2002).
14. Microsats for Mars. Available: http://www.beyond200.com/news/story_454.html (November 2, 2002).
15. Petro, Andrew. "VASIMR Plasma Rocket Technology". Advanced Space Propulsion Laboratory: NASA JSC Houston, Texas. May 2002.
16. Satellite Link Between Earth and Mars. Available: <http://arnaud.labouebe.free.fr/Satellite.html> (October 30, 2002).
17. Wertz, J.R. and W. J. Larson. Space Mission Analysis and Design (3rd Edition). Kluwer Academic Publishers: California. 1999.
18. Zandbergen, B.T.C. "Performance and Operating Data for Typical Rocket Engines". Available: http://dutlsisa.lr.tudelft.nl/Propulsion/Data/Rocket_motor_data.htm (November 2, 2002)
19. <http://www.boeing.com/defense-space/space/delta/deltaPayload.htm>
20. <http://horse.mes.titech.ac.jp/research/docking/docking.html>
21. <http://www.rti.org>

PARTS Configuration



***Bifrost*: A 4th Generation Launch Architecture Concept**

Rohrschneider, R.R., Young, D., St.Germain, B., Brown, N., Crowley, J., Maatsch, J., Olds, J.R. (Advisor)

Space Systems Design Lab
School of Aerospace Engineering
Georgia Institute of Technology
Atlanta GA 30332-0150

Abstract

A 4th generation launch architecture is studied for the purpose of drastically reducing launch costs and hence enabling new large mass missions such as space solar power and human exploration of other planets. The architecture consists of a magnetic levitation launch tube placed on the equator with the exit end elevated to approximately 20 km. Several modules exist for sending manned and unmanned payloads into Earth orbit. Analysis of the launch tube operations, launch trajectories, module aerodynamics, propulsion modules, and system costs are presented. Using the hybrid logistics module, it is possible to place payloads into low Earth orbit for just over \$100 per lb.

Introduction

Humanity has dreamed of expanding their realm to include space and other planetary bodies and to use space to improve our own planet. Most of these goals require a large mass in Earth orbit. However, before this becomes practical the cost of access to space must be reduced drastically. *Bifrost* is one of many 4th generation launch concepts designed to reduce the cost of access to space, and hence enable projects such as space solar power and human exploration of other planets. The overall architecture is based on a concept developed by Powell et al [1].

Bifrost consists of a magnetic levitation launch tube with the exit end elevated to approximately 20 km. A common hybrid logistics module (HLM) is designed to attach to an array of propulsion modules that accommodate different missions. This paper focuses on the trajectory analysis for placing the HLM into LEO, and the solar electric propulsion module for circularizing payloads in Geosynchronous Earth orbit (GEO). A brief description of the remaining components is also provided for completeness.

Concept Overview

The architecture consists of an evacuated magnetic levitation launch tube, with one end elevated to 20 km located on the equator, which sends a vehicle into an elliptic Earth orbit. The apogee of the orbit depends on the desired destination. The launch tube is capable of launching either a HLM and associated hardware, or the deep space space shuttle (DSSS). The HLM is a payload canister with a common interface for the propulsion module. It can contain several different internal configurations for launching different types of payload. Three propulsion modules exist for three different in-space purposes. For circularizing in low Earth orbit (LEO) there is a solid apogee kick motor. For unmanned operations in near Earth space there is a module with a liquid rocket engine. For circularizing payloads in Geostationary Earth orbit (GEO) there is a low thrust electric propulsion module. The DSSS has a passenger cabin and uses a propulsion system based on the liquid rocket engine module. It can be used for manned missions to the moon, and beyond with its refueling capability. Each component of the architecture is described in the following sections in more detail. Appendix A shows a summary of each component in the architecture.

Launch Tube

The launch tube uses magnetic levitation technology to accelerate a vehicle through an evacuated tube to orbital speeds. Each vehicle is loaded into the 5 meter diameter launch tube through an airlock to maintain the vacuum. Due to acceleration limits on human cargo, the tube must be about 1400 km long. Track acceleration can be varied to change the departure velocity for different missions and to accommodate human payloads. The tube is elevated using large magnets to repel the tube from the ground, and it is held down using adjustable length cables to vary the exit angle.

The launch tube is located on the equator to take advantage of the Earth's rotation, and the exit end is elevated to about 20 km to reduce drag on the vehicle being launched. The launch tube concept is based on the Startram concept developed by Powell et al [1]. Figure 1 shows an artist's rendering of a vehicle being launched using the *Bifrost* launch tube. The cables that hold the tube down and make adjustment of the departure angle possible are clearly visible in the sketch.

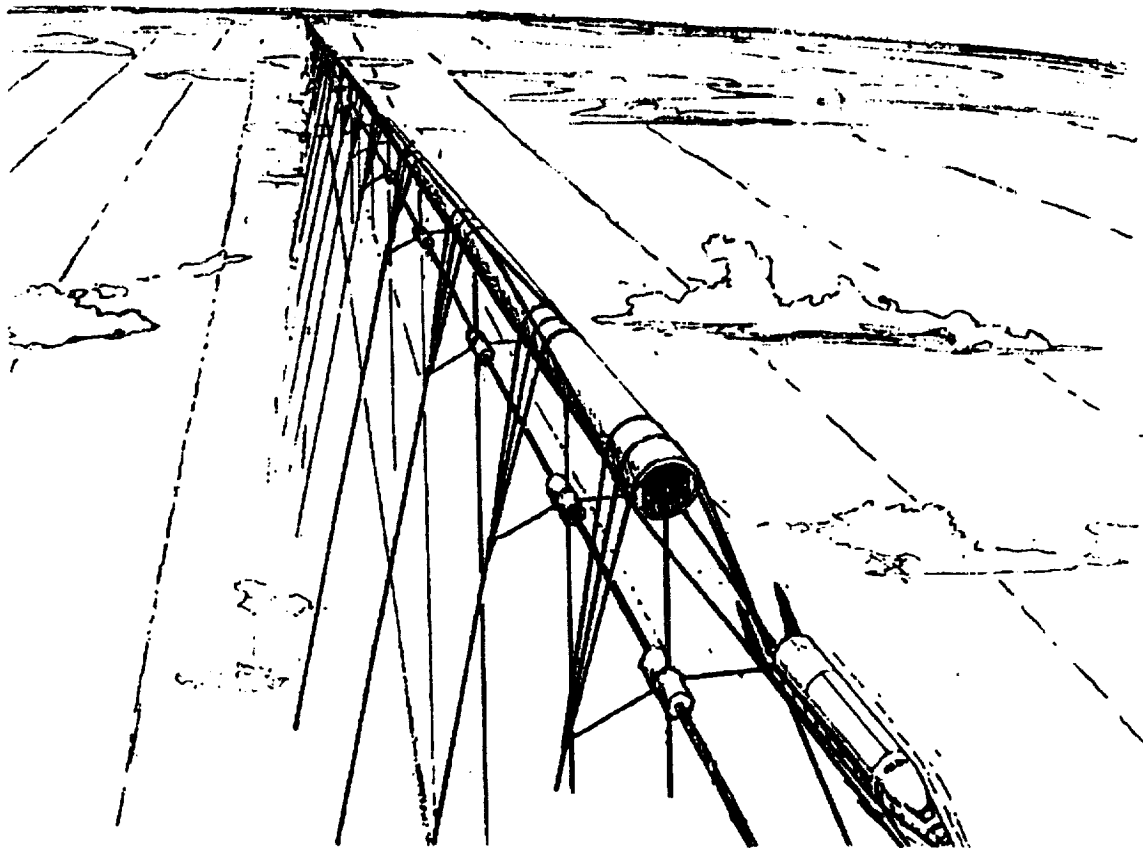


Figure 1: Artist's rendering of a vehicle being launched using the *Bifrost* launch tube. [1]

DSSS

The deep space space shuttle is designed to be a refuel-able spacecraft which will be used for a variety of manned missions to both earth based as well as interplanetary space. Two different DSSS configurations will be analyzed and sized. Both variants of the DSSS will consist of large expansion ratio liquid rocket engines to impart 6,000 m/s of velocity to the spacecraft. The differences in the

configurations will be in the fuels analyzed (LH2 and CH4). These different propulsion types are summarized in Table 1. Figure 2 shows a possible configuration for the DSSS which is capable of carrying 8 passengers and 250 kg of payload.

Table 1: Propulsion Characteristics For DSSS

Type	Liquid	Liquid
Propellants	LOX-LH2	LOX-CH4
Cycle	Expander	Expander
Mixture Ratio	5.5	3.5
Expansion Ratio	175	175
Isp _{vac} (sec)	463	368

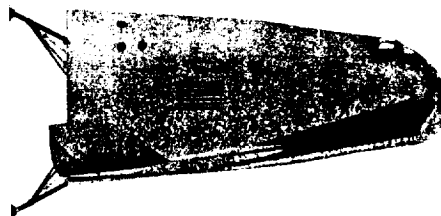


Figure 2: DSSS configuration.

DSSS Missions

As aforementioned the DSSS module was sized to accomplish a ΔV maneuver of 6,000 m/s. This sizing allows the DSSS module to complete many different missions. An analysis was conducted to find the required ΔV to accomplish different missions including space tourism, Lunar Landing missions, L1 missions, as well as different Mars trajectories. A summary of the missions is included in Table 2.

Table 2: Trajectory Analysis for the DSSS.

	Space Tourism	Lunar Lander*	Mars Hohmann	Mars 120 day [†]	Mars Lander*
Circularization	300 m/s				
Leaving LEO		3106 m/s	3590 m/s	5139 m/s	3590 m/s
Arrival		1445 m/s	2093 m/s	4847 m/s	2093 m/s
DeOrbit	275 m/s	2070 m/s			160 m/s
Ascent		2070 m/s			2280 m/s
Total Delta V	575 m/s	8691 m/s	5683 m/s	9986 m/s	8123 m/s

Table 2 (Continued): Trajectory Analysis for the DSSS.

	L1 Hohmann	L1/Mars Transfer*
Circularization		
Leaving LEO	3089 m/s	3089 m/s
Arrival L1	224 m/s	224 m/s
Depart L1		224 m/s
TMI		501 m/s
Mars Insertion		2093 m/s
Total Delta V	3312 m/s	6130 m/s

* Refueling Required

[†] Not Possible with current configuration

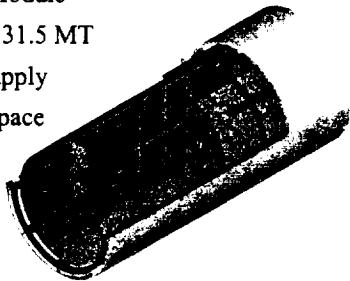
As this table depicts, the DSSS will be able to accomplish space tourism, Mars Hohmann, and L1 Hohmann missions without refueling. It should be noted that the Mars Hohmann mission is very slow and would not be feasible with this size manned spacecraft. The other missions such as Lunar Lander, L1/Mars Transfer and Mars Lander are possible if the infrastructure exists to facilitate refueling of the DSSS. Currently missions to Mars in 120 days are not possible with the propellant available on the 6,000 m/s sized DSSS. Additional propellant volume and therefore ΔV can be added to the DSSS, but it would result in a larger more costly spacecraft.

HLM

The hybrid logistics module is designed to have a common interface for attaching to various propulsion modules, aero-shells, and the launch tube. Four HLM internal configurations were analyzed for this project. They include a logistics configuration, a water transport configuration, a space solar power configuration, and a communications satellite configuration. Packaging for each module is shown in Figure 3. The HLM measures 5 meters in diameter, 12 meters long, and has an empty mass of 11.1 metric tons. For simplicity of the propulsion modules, the RCS system is located on the HLM.

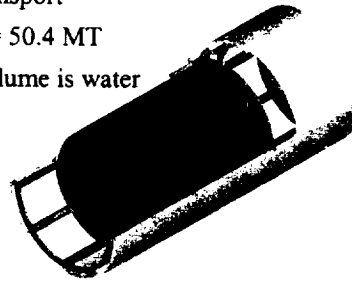
Logistics Module

- GLOW = 31.5 MT
- ISS Re-supply
- Storage Space



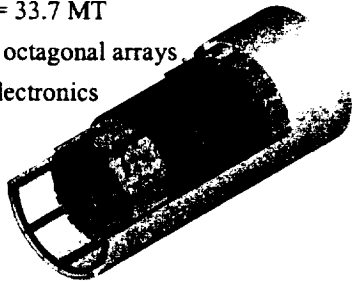
Water Transport

- GLOW = 50.4 MT
- 1/6 of volume is water



Space Solar Power

- GLOW = 33.7 MT
- Fwd/Aft octagonal arrays
- Center electronics



Comm. Satellites

- GLOW = 19.3 MT
- 1-2 comm. sats.

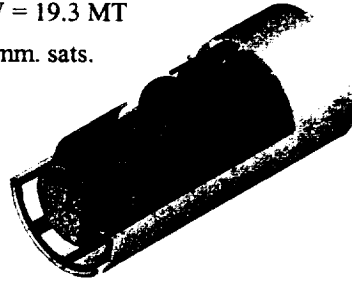


Figure 3: Four configurations for the HLM showing packaging and total mass.

Propulsion Modules

Three different propulsion modules were designed to integrate with the HLM. They include a solid apogee kick motor for circularizing in LEO, a liquid rocket engine for near Earth operations and further with refueling, and a solar electric propulsion module for circularizing in GEO.

Solid Module

For circularizing in LEO, a solid propellant motor was chosen due to the low velocity change required, and the low cost of solid rocket motors. About 300 m/s is required to circularize in a 400 km circular orbit assuming the launch trajectory has its apogee at the same altitude. Parameters for the solid motor are shown in Table 3. Figure 4 shows an artist's conception of the solid propulsion module.

Table 3: Parameters for the solid rocket propulsion module.

Type	Solid
Propellants	AP, Al, HMX, HTPB Binder
Expansion Ratio	85
Ispvac (sec)	297

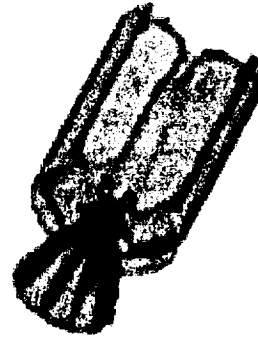


Figure 4: Schematic of the solid propulsion module.

Liquid Module

The liquid propulsion module is designed to carry payload to accompany manned missions using the DSSS and to deliver payload to Mars. The 120 day Mars mission is the highest delta V of the possible missions for the liquid propulsion module at 10 km/s. A payload of the most massive HLM, the 50.4 ton water transport module is assumed. Rocket engine performance was calculated using SCORES [2], an in-house liquid rocket engine analysis code, using the parameters shown in Table 4. A schematic of the liquid propulsion module configuration is shown in Figure 5.

Table 4: Parameters for the liquid rocket engine.

Type	Liquid
Propellants	LOX-LH2
Cycle	Expander
Mixture Ratio	5.5
Expansion Ratio	175
Ispvac (sec)	463

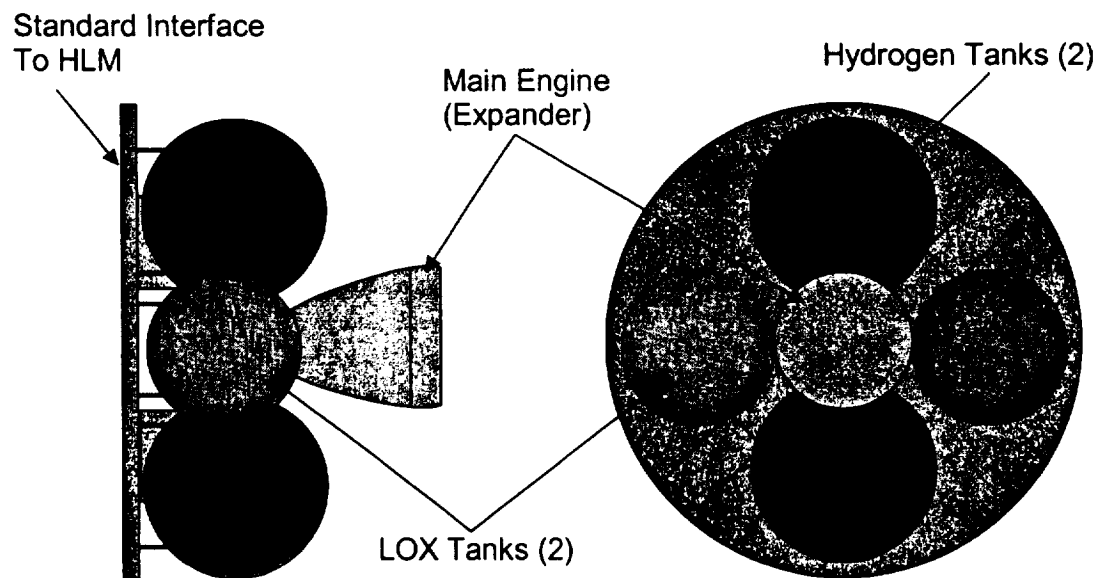


Figure 5: Schematic of liquid propulsion module configuration.

SEP Module

The SEP module makes use of the high efficiency of electric propulsion to circularize a payload in GEO from a highly elliptic transfer orbit. The module first circularizes by thrusting for approximately 60° centered around apogee, and then thrusting continuously to slowly spiral out to GEO. Due to the low thrust of the propulsion, a solid apogee kick motor is fired on the first orbit to raise the perigee to 100 km altitude. Figure 6 shows a schematic of the trajectory.

The vehicle makes use of inflatable technology to increase the specific power of the solar collection system. Two inflatable

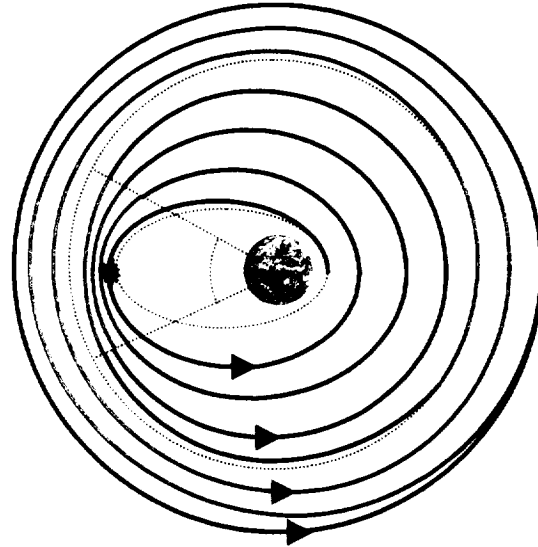


Figure 6: Notional spiral trajectory showing circularization, and the orbit rising to GEO.

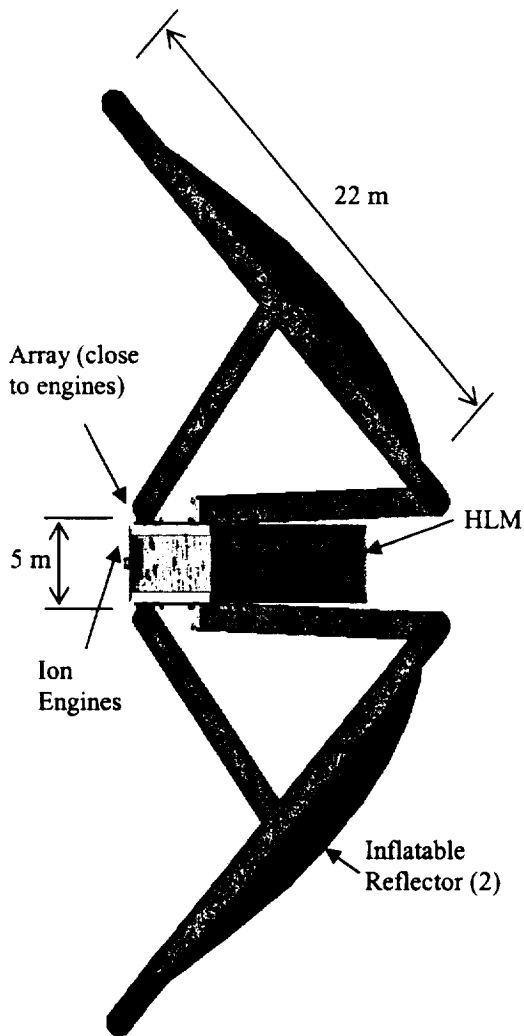


Figure 7: Configuration of the SEP module. HLM attaches on the right.

concentrating reflectors are attached to opposite sides of the vehicle, and are supported by inflatable struts. Light is reflected from the inflatable reflectors through a lens, off a mirror, and onto a solar array. This complicated light path allows for two key features: only light passes through the rotating joint of the reflectors, and the solar arrays are close to the electric propulsion. The complexity and weight of the system is minimized by only passing light (and not electricity) through the rotating joint of the reflectors. Proximity of the power source to the load reduces the line losses by about 4%, and reduces the mass of wiring. Due to the size of the inflatable reflectors, a deployment system is necessary for the rotating mechanism and the lens. The configuration of the vehicle is shown in Figure 7.

The power generation system uses the inflatable reflectors to concentrate sun onto a solar array. The array is composed of triple junction GaInP₂/GaAs/Ge solar cells operating at 30% efficiency. To prevent the cell efficiency from dropping due to heat, a thermal control system is necessary. Mass per area of the inflatable structure was assumed to be similar to hardware produced by L'Gard [3]. Total mass of the power system comes to 900 kg to produce 86.8 kW of electric power.

The propulsion system consists of a Xenon ion engine. The analysis was based on propellant type, exhaust velocity and available power. Using the available power, the Isp is calculated. A curve fit of thruster efficiency as a function of Isp from [4] is used to get the thrust after reducing the input power to account for the power processing unit. Engine mass was also calculated using curve fits from [4], and accounts for the engine and the power processing unit.

Trajectory analysis was performed using an in-house numerical integration code based on Cowell's method. Two steps were required for the trajectory from the launch tube to GEO. The first step used eccentricity as the stopping condition and commanded thrust for about 60° of true anomaly centered on apogee. The next phase used continuous thrust to increase the orbital radius until GEO was reached. Both phases maintained the thrust parallel to the velocity vector. The Earth shades the vehicle for only 4.8% of the orbital period, and so was not accounted for. Since the SEP module only thrusts for 60° of the orbit, launch timing can be used to determine the argument of periapsis to keep the thrust segment out of the shadows during circularization.

Use of a computational framework enabled system-level numerical optimization. Each of the disciplinary analyses were wrapped and added to the model. In addition to the disciplinary analysis, several built in optimization methods are available. The design was converged using a script component that performs fixed point iteration.

After several trial runs, sequential quadratic programming was chosen as the most effective optimization scheme of those available in ModelCenter®. The optimization process used the normalized initial mass for the objective function, with the goal to minimize this quantity. Table 5 lists the constraints and the design variables with their upper and lower bounds. θ , the angle of the rear reflector support strut is limited to prevent shading from the strut. The rear strut length, D_r , and the overall reflector length, L_{refl} , are limited in size to keep the structural dynamics problems to a minimum. Side constraints were placed on the parabola constant, X_{refl} , exhaust velocity, and magnification to keep them within physically reasonable bounds. The design variables are the parabola constant, the position of the lower edge of the reflector, X_{refl} , the exhaust velocity, and the magnification. All other quantities were fixed due to the *Bifrost* launch architecture.

To aid the optimizer, the objective function, the constraints, and the design variables were all normalized. The default settings were used for finite difference gradients and convergence.

Table 5: Constraints and design variables with their bounds.

Variable	Lower Bound	Upper Bound
θ (deg.)	3	None
D_r (m)	None	60
L_{refl} (m)	None	45
Parabola Const.	0.001	0.1
X_{refl} (m)	0.01	1.0
Exhaust Vel. (m/s)	14,000	40,000
Magnification	40	800

Results

This project focused on analysis of the launch trajectory, and the design of the SEP module. Results from the analysis and optimization from those two activities are presented below. Additional work was done on the DSSS and solid propulsion module and the cost of launch using the DSSS and HLM.

LEO Launch Trajectory

Trajectory analysis of the HLM was performed using the Program to Optimize Simulated Trajectories (POST) [5]. Due to the preliminary stage of the study, a parametric representation of the data was desired. Launch tube release velocity, exit angle, altitude, and aero-shell geometry were varied, and the required spacecraft velocity increment to reach LEO (400 km circular orbit) was recorded. Dynamic pressure, heat rate, and acceleration were also recorded for use as constraints.

Aerodynamic analysis was performed using the Aerodynamic Preliminary Analysis System II (APAS) tool [6]. Three different aero-shells were analyzed for the HLM, to determine the sensitivity of the trajectory to the aerodynamic performance of the HLM. The three shapes analyzed are shown in Figure 8 along with their respective drag numbers. Figure 9 shows the variation in drag coefficient as a function of Mach number for each length of aero-shell. The reference area is the cross-section area of the vehicle.

The aerodynamic data from above was then used in POST to create velocity increment charts. Figure 10 shows a representative plot of the results of the trajectory trade study using the lowest drag aero-shell with the acceleration, heat rate, and dynamic pressure constraints marked on each curve. Values of all constraints increase as the release velocity increases.

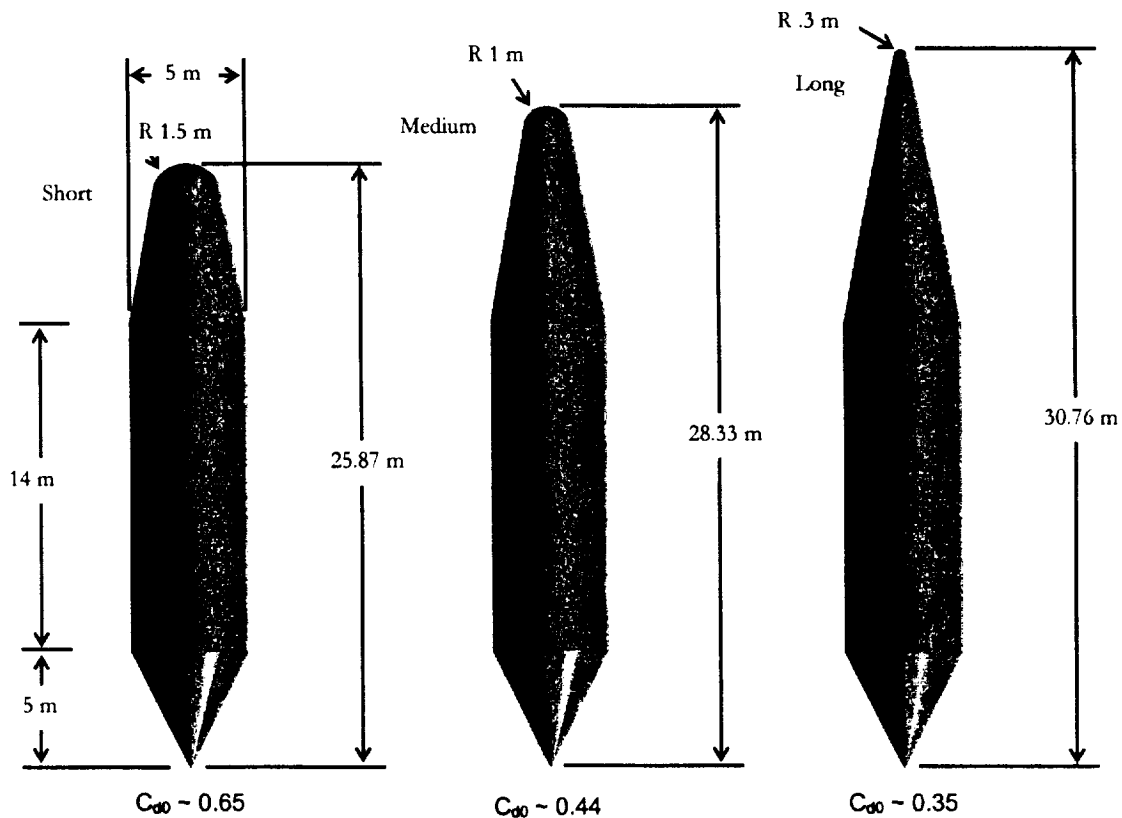


Figure 8: Geometry for the three different aero-shells studied.

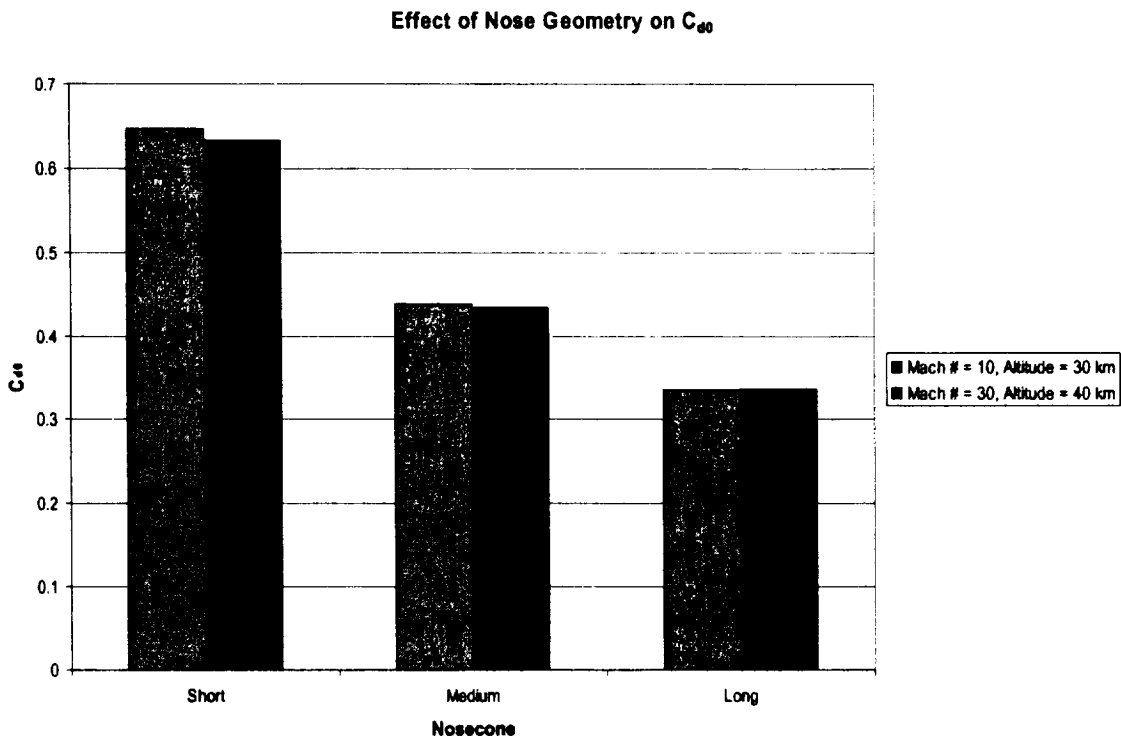


Figure 9: Comparison of drag at Mach 10 and Mach 30 for the three different aero-shell lengths.

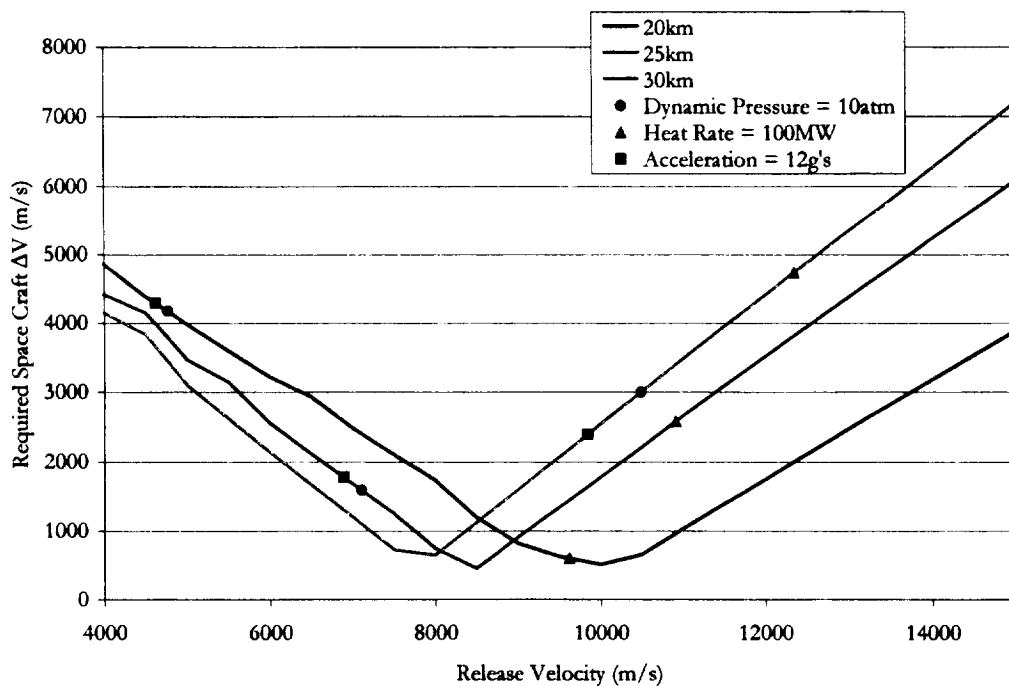


Figure 10: Trade study of release velocity and spacecraft supplied velocity increment to enter LEO using the lowest drag aero-shell at a 6° release angle. Dynamic pressure, heat rate, and acceleration increase as release velocity increases.

DSSS

As described in the preceding sections two fuels were analyzed for the DSSS, CH₄ and LH₂. Both variants of the DSSS use LOX as an oxidizer and are sized for the ΔV requirements of 6,000 m/s. Since the launch tube inner diameter is set at 5 meters only the length of the overall shuttle was changed to meet the propellant requirements. A set cargo (manned and cargo) volume of 80 m³ was used for both variants of the DSSS to accommodate the eight passengers and 250 kg of cargo. Table 6 is a sizing summary of the DSSS.

From the sizing analysis it is shown that the hydrogen configuration, although having a higher Isp, results in approximately a 45% increase in volume and length. This of course does not include any technology enhancements such as slushed hydrogen, which may be technologically viable when *Bifrost* becomes operational. Table 6 shows a sizing summary of the DSSS.

Table 6: Sizing summary of the DSSS.

Propulsion:	LH2/LOX	CH4/LOX
Landing Isp (sea level)	440 sec	350 sec
In-space Isp	462 sec	368 sec
Installed Eng. T _{sl} /We	55	75
Overall T/W at Exit	0.8	0.8
O/F Ratio (weight)	5.5	3.5
Geometry:		
Total Propellant Mass	64,185 kg	96,857 kg
Oxidizer Volume	51 m ³	65 m ³
Fuel Volume	148 m ³	50 m ³
Non-Cabin Volume	56 m ³	39 m ³
Total Est. Volume	335 m ³	234 m ³
Est. Length	17.0 m	11.9 m
Sizing:		
Mass Ratio	3.76	5.27
Initial Mass	87,459 kg	119,541 kg

Solid Module

Using the above trajectory analysis and a simple sizing routine, a mass was determined for the solid propulsion module for each of the four HLM configurations. In order to produce only four different solid rocket motors it will be necessary to ballast the HLM to one of the masses listed in Figure 3 above. Table 7 shows the mass of the solid propulsion module for each HLM configuration.

Table 7: Solid propulsion module mass for each HLM configuration.

HLM Configuration	HLM Mass (metric tons)	Solid Propulsion Module Mass (kg)
Water Transport	50.4	6,150
Space Solar Power	33.7	4,120
Logistics Module	31.5	3,850
Communications Satellites	19.3	2,357

SEP Module

On completion of the optimization, the vehicle had lost significant mass from the initial guesses for the design variables. The final values of the design variables and select outputs are shown in Table 8. All variables are up against constraints except for the parabola constant, and the reflector dimensions L_{refl} and D_1 . Since no time constraint was specified the exhaust velocity is at the maximum allowed for ion engines to maximize the engine Isp, and hence reduce mass. The reflector dimensions are primarily derived from the exhaust velocity since this determines the power required and the reflector size. Trip time came to 575 days due to the lack of a time constraint. Depending on the cargo, this trip time may not be acceptable. Earlier in the design process optimization was performed with a minimum thrust constraint of 13 Newtons, resulting in a trip time of 190 days, but a much higher initial mass of 49,530 kg. The full 12 point mass breakdown structure is shown in Table 9.

Operations and Cost

Operations analysis was also performed as a contributing analysis to determine the cost of the launch architecture. The Architecture Assessment Tool – enhanced (AATe) written at Kennedy Space Center was used in the development of the operational model for *Bifrost*. The analysis is based on data taken from Space Shuttle operations but uses aggressive assumptions in terms of automation and required maintenance. Figure 11 shows the results of the site layout and analysis.

The operational model and costs were added to a weight based costing model to determine overall system costs. The DSSS is designed to last for 500 flights with a unit cost of \$2.5B, while the HLM is expendable with a unit cost of \$6M including a propulsion module. The ground facility was assumed to be paid for by a government, but the operational and maintenance costs are covered by the launch operator. All non-recurring costs were distributed evenly over the 40 year program life. Table 10 shows the remaining assumptions for each vehicle, the life cycle cost for each vehicle, and the total cost per unit mass to orbit using the HLM. This architecture shows drastic improvement over current launch technology, and enables launch for just over \$100/lb.

Table 8: Design variables and selected outputs after optimization.

Variable	Value
Parabola Constant	0.03476
X_{refl} (m)	0.9779
Magnification	40.0
Exhaust Velocity (m/s)	40,000
θ (deg.)	3.0
D_1 (m)	18.7
L_{refl} (m)	22
A_{refl} (m ²)	305
Mass Ratio	1.04622
M_{init} (kg)	40,610
Propellant Mass (kg)	1,790
Engine Thrust (N)	4.22
Engine Isp (sec)	4,077
Engine Propellant	Xenon

Table 9: Mass breakdown statement for the optimized SEP module.

Component	Mass (kg)
Structure	1,450
Power Generation	830
Power Distribution	50
Thermal Control	190
Propulsion	480
Control and Avionics	110
Margin (20%)	620
Dry Mass	3,730
Reserves and Residuals	90
Pressurant	1
Payload	35,000
GEO Mass	38,820
Boost Propellant Mass	1,790
M_{init}	40,610
AKM Mass	170
Initial On Orbit Mass	40,780

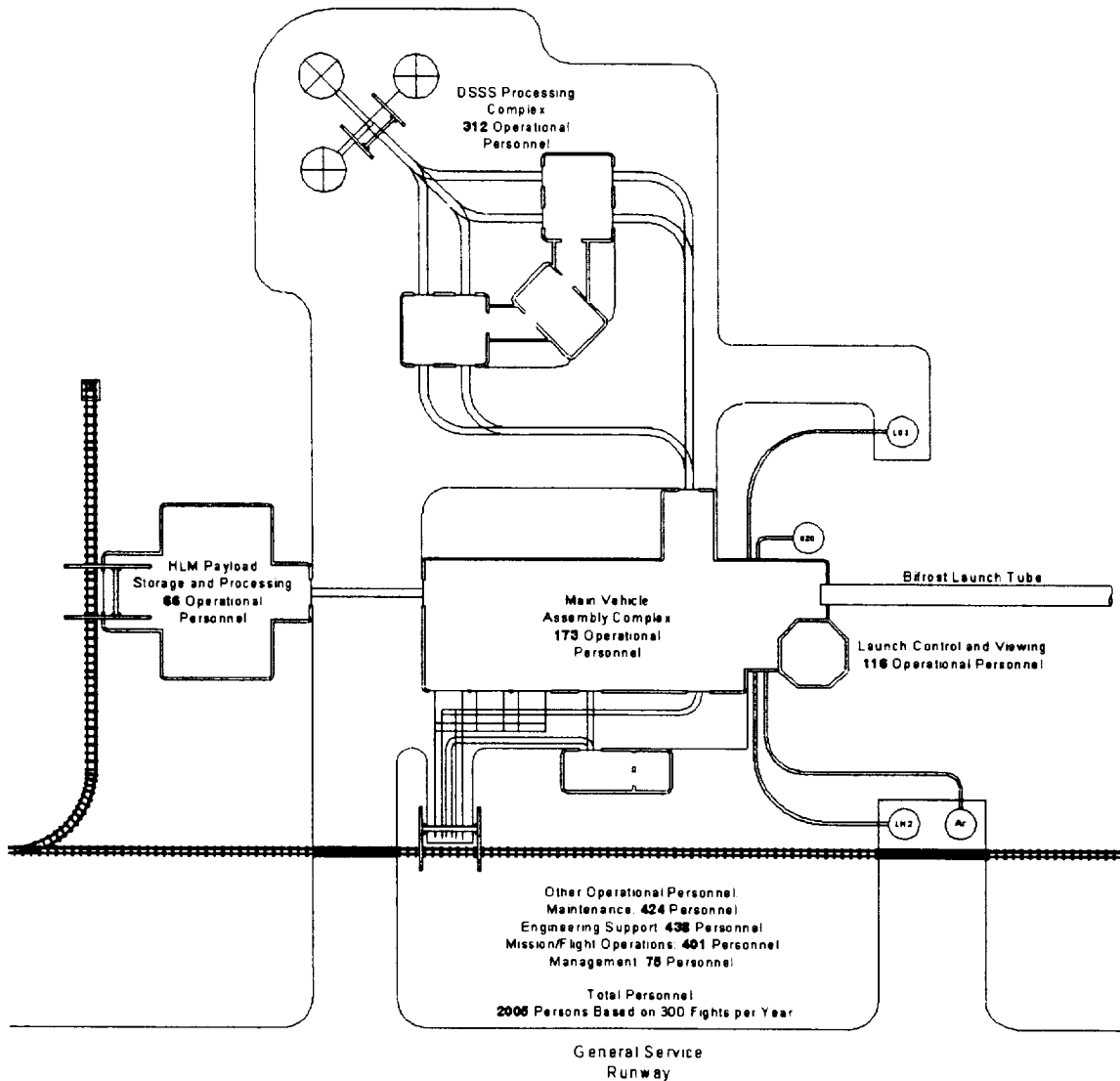


Figure 11: Operational layout showing number of required personnel to operate *Bifrost*.

Table 10: Cost of *Bifrost* architecture in FY02\$.

DSSS			HLM		
Flights Per Year	50	flights	Flights Per Year	250	flights
DDT&E	10,000	M	DDT&E	1,000	M
Fixed Cost per Year	519	M	Fixed Cost per Year	1,145	M
Variable Cost per Flight	9.73	M	Variable Cost per Flight	6.63	M
Total Cost per Flight	20.10	M	Total Cost per Flight	11.21	M
Total Life Cycle Cost	40,207.41	M	Total Life Cycle Cost	112,087.08	M
			Total Cost Per Payload kg	224.17	\$/kg
			Total Cost Per Payload lb	101.67	\$/lb

Conclusions

Detailed analysis was performed for the launch trajectory to LEO, and for the SEP module. The launch trajectory to LEO was explored and a parametric model is now available for use in overall architecture optimization. Input parameters include aero-shell, release velocity, and exit angle. Heat rate, acceleration, and dynamic pressure were also recorded for use as constraints. Optimization was performed on the SEP module which resulted in an initial mass of 40,780 kg and a trip time of 575 days to GEO carrying a 35,000 kg payload. By increasing the thrust to 13 N a more reasonable trip time of 190 days to GEO was achieved, but at the much higher mass of 49,530 kg.

Preliminary analysis of the DSSS and solid propulsion modules was also performed. Two fuels were explored for the DSSS, CH₄ and LH₂. As expected the hydrogen fueled vehicle had a lower initial mass of 87,460 kg but was bulkier, measuring 17m long. The methane fueled vehicle had an initial mass of 119,540 kg at a length of only 12m. The solid propulsion module required different mass modules for each different HLM configuration. Module mass varied from 6,150 kg to 2,360 kg for payloads ranging from 50.4 mt to 19.3 mt.

The *Bifrost* architecture is designed to reduce the cost of access to space and to enable a large number of missions. The analysis presented in this paper shows that the *Bifrost* architecture is successful in reducing the cost of launch. If the government pays for the facility, the cost of placing one pound of payload into orbit using the HLM is just over \$100.

Future Work

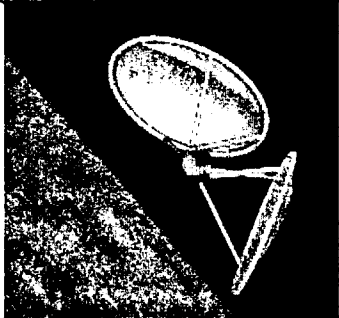
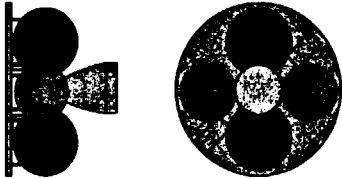
Though much analysis has been performed on the *Bifrost* architecture, there is still room for improvement. There are several components that could benefit from more detailed analysis including the liquid and solid propulsion modules and the DSSS. Generation of a complete mass breakdown structure for these modules would result in better cost and maintenance analyses. The launch trajectory to GEO also requires further analyses and could validate some of the assumptions made in the design of the SEP module.

Once a complete model of each component of the architecture is complete, optimization of the overall system based on the predicted launch market could be performed. This analysis could show the correct number of each module to manufacture in order to minimize the cost of payload, manned or unmanned, to orbit. Care would need to be taken in the choice of market model since the *Bifrost* concept has the potential, itself, to change the market model.

References

1. Powell, J.R., Maise, G., Paniagua, J., Rather, J.D.G., "StarTram: A New Approach for Low-Cost Earth-to-Orbit Transport," IEEE 0-7803-6599-2/01, 2001.
2. Way, D. W., Olds, J. R., "SCORES: Web-Based Rocket Propulsion Analysis Tool for Space Transportation System Design," AIAA 99-2353, 35th AIAA/ASME/SAE/ASEE Joint Propulsion Conference, Los Angeles, CA, June 20-24, 1999.
3. Cassapakis C., Lichodziejewski D., "Inflatable Power Antenna Technology," AIAA paper 99-1074, January 1999.
4. Henry, Humble, Larson, Space Propulsion Analysis and Design, New York: McGraw Hill, 1995.
5. Brauer, G.L., Cornick, D.E., Stevenson, R., "Capabilities and Applications of the Program to Optimize Simulated Trajectories," NASA CR-2770, February, 1977.
6. Sova, G., Divan, P., "Aerodynamic Preliminary Analysis System II, PartII – User's Manual," NASA CR-182077, April, 1991.

Appendix A
Summary of *Bifrost* architecture components.

Component Name	Picture	Initial mass (kg)	Cost per Flight (FY02\$ Millions)	Payload (type, kg)	DV (m/s)
DSSS		87,460 (LH2) 119,540 (CH4)	20.1	8 passengers 250 kg payload	6,000
HLM		50,400 (water trans.) 33,700 (space solar power) 31,500 (logistics module) 19,300 (Comm. Sats.)	11.21 Including propulsion module	Water Space solar power Equipment & Inst. Communication Sat.	
SEP Module		40,780		HLM Assumed to weight 35,000 kg to GEO	1,805
Liquid Propulsion Module				HLM	10,000

Component Name	Picture	Initial mass (kg)	Cost per Flight (FY02\$ Millions)	Payload (type, kg)	DV (m/s)
Solid Propulsion Module		6,150 (water trans.) 4,120 (space solar power) 3,850 (logistics module) 2,360 (Comm. Sats.)		Water Space solar power Equipment & Inst. Communication Sat.	300
Launch Tube				HLM + Propulsion Module + Aero-shell or DSSS	>4,000

THE HEMATOPOIETIC STEM CELL THERAPY FOR EXPLORATION OF SPACE

Howard University

Students: Allana Nicole Roach, Jelena Brezo

Research Associate: Bak C. Kim

Faculty Advisor: Seigo Ohi

ABSTRACT

Astronauts experience severe/invasive disorders caused by space environments. These include hematological/ cardiac abnormalities, bone and muscle losses, immunodeficiency, neurological disorders and cancer. While the cause of these symptoms are not yet fully delineated, one possible explanation could be the inhibition of hematopoietic stem cell (HSC) growth and hematopoiesis in space. HSCs differentiate into all types of blood cells, and growing evidence indicates that the HSCs also have the ability to transdifferentiate to various tissues, including muscle, skin, liver, neuronal cells and possibly bone. Therefore, a hypothesis was advanced in this laboratory that the hematopoietic stem cell-based therapy, herein called the hematopoietic stem cell therapy (HSCT), could mitigate some of the disorders described above. Due to the magnitude of this project our laboratory has subdivided it into 3 sections: a) HSCT for space anemia; b) HSCT for muscle and bone losses; and c) HSCT for immunodeficiency. Toward developing the HSCT protocol for space anemia, the HSC transplantation procedure was established using a mouse model of β -thalassemia. In addition, the NASA Rotating Wall Vessel (RWV) culture system was used to grow HSCs in space condition. To investigate the HSCT for muscle loss and bone loss, donor HSCs were genetically marked either by transfecting the β -galactosidase-containing plasmid, pCMV.SPORT- β -gal or by preparing from β -galactosidase transgenic mice. The transdifferentiation of HSCs to muscle is traced by the reporter gene expression in the hindlimb suspended mice with some positive outcome, as studied by the X-gal staining procedure. The possible structural contribution of HSCs against muscle loss is being investigated histochemically. Since there are reports that hindlimb suspended mice show decreased immunity, an ability to eliminate bacterial infection by the host immune system may

be compromised in these mice. To prove this, we have transformed *Escherichia coli* with the plasmid, pCMV.SPORT- β -gal, which were then used as the gene-marked bacteria to infect control and the hindlimb suspended mice. Preliminary results by the X-gal wholemount staining procedure indicate that the hindlimb suspension unloading indeed cause the immunodeficiency and the HSCT could help eliminate the reporter gene-marked *E. coli*.

DESIGN POBLEM

To maintain astronauts' homeostasis in space using hematopoietic stem cell therapy, so as to enable them to "go anywhere at any time".

INTRODUCTION

Several reports indicate that astronauts develop hematological abnormalities, including space flight anemia, abnormal red cell morphology and structure, thrombocytopenia, 5-20% reduction in red blood cell mass, decreased hemoglobin concentration and hematocrit, and lowered serum erythropoietin levels (1-5). It is likely that stem cell self-renewal is also inhibited in space, reducing the total number of totipotent stem cells in bone marrow. These abnormal hematopoiesis in 0/ μ G could adversely affect the astronauts' homeostasis. One avenue to overcome the abnormal hematopoiesis might be to supply normal hematopoietic stem cells (HSCs) periodically, e.g. once in two weeks, to astronauts. As the abnormal blood cells will be destroyed in time, the newly supplied HSCs could differentiate to normal blood cells, thus, maintaining the healthy hematological status of the astronaut for some duration. This process could be repeated and made as routine throughout the long-duration space mission so as to maintain this equilibrium state. This is the essence of our proposed hematopoietic stem cell therapy (HSCT) in space; namely, the objective is to

prevent disorders to take place, rather than to repair already damaged tissues: the Preventive Medicine over the Reparative Medicine. And thus, the HSCT could be applied to various disorders in space, including space anemia, immunodeficiency and muscle and bone losses, as discussed below. It must be emphasized that the HSCs should be prepared on the ground from individual astronaut's blood preflight and kept frozen. The HSCs should be designated to each astronaut and should not be intermixed. During the flight the HSCs would be thawed and grown and expanded. Following the culture, a half of the HSCs would be used for transplantation and the other half frozen for the next culture. In this way, the individual HSCs would be maintained as a normal stock during the long-term space flight. A robotic culture system and stem cell injection machine would ease the astronaut's operation, which project we have recently initiated. The transplanted HSCs should be astronaut's own, i.e. autologous transplantation, avoiding the danger of graft-versus-host disease (GVHD). Hence, no myeloablation by toxic chemicals, such as cyclophosphamide and busulfan, would be necessary.

Growth of Hematopoietic Stem Cells in Space

The HSCT in space will necessitate establishing an optimal condition for growing normal HSCs in $0/\mu$ gravity from the frozen state. The growth and expansion of HSCs in space could be achieved by the use of NASA Rotating Wall Vessel (RWV) system. Thus, in this paper we describe a part of our efforts to culture HSCs in the RWV system with some positive outcome. The RWV, aside from the low gravity simulating effect, seems to have a beneficial effect on the growth of HSCs, since according to our experience these cells require constant mixing in a low shear force environment and spatial colocation of participating cell populations or growth factors. We believe that such a condition may reflect *in vivo* status of HSCs, since the body is a constantly moving environment to them. In consideration of these facts, we have been collaborating with the NASA-NIH Center for Three-Dimensional Tissue Culture (J. Zimmerberg, Director), conducting several experiments to establish the HSC culture in RWV system (6,7). While the initial study indicated severe inhibition of the HSC growth in the RWV system, by changing the conditions we recently succeeded to grow and expand the HSCs (see Fig. 4, below). Other laboratories have also reported the use of RWV culture system for

mouse HSCs (8) and erythroleukemia cell line (5), with apparent inhibitory effect of the RWV on the cell growth and differentiation. As the methods of isolation and culture of HSCs are different in each laboratory, it is necessary to delineate the optimal condition of growth for the individual preparation. In addition, since multiple steps are involved in HSCT, and gene therapy in future, it is necessary to develop conditions, which suit individual needs, so that one controlled flow system is available in the laboratory.

HSCT for Space Anemia

Space anemia may manifest in two forms. One is the anemia experienced by astronauts when they return to earth from μ gravity conditions (4). The other occurs in long duration flight in μ gravity, since studies on hematopoiesis in space indicated that both proliferation and differentiation of blood cells were severely inhibited. Erythropoiesis was more affected than myelopoiesis (2). In our lab, studies on HSCT for space anemia are coupled with studies on the transplantability of HSCs, since the ability of the recipient to express donor hemoglobin is indicative of successful transplantation and differentiation of HSCs. In addition, successful expression of donor hemoglobin indicates that HSCT is successful in mitigating anemic conditions. Transplantability of cultured HSCs can be analyzed by using β -thalassemic mice (9). The β -thalassemic mice, which colony we have established in this institution, have been quite useful for us to establish the transplantation procedure and also to evaluate the quality of HSCs for transplantation. Since the hemoglobin molecule of the animal clearly differs from those of wild type mouse and heterozygotes, as analyzed by the cellulose-acetate electrophoresis, the transplantation can be assessed by characterizing hemoglobin species in the transplanted recipients. Thus, transplantability of HSCs grown in RWV system can be analyzed by the β -thalassemic mouse transplantation system. Regarding the β -thalassemic mouse, it is noteworthy that despite the difference in basic mechanisms between the β -thalassemia and spaceflight, there are uncanny similarities in their phenotypes. Namely, the β -thalassemic mouse shows abnormal red cell morphology, reduced hemoglobin concentration and hematocrit, decreased body weight and size, and brittle bones. It may be that the common underlining cause is a hypoxic condition in the body due to reduced hemoglobin concentration, which both disorders display. Thus,

this mouse offers a good test model for HSCT, and the protocol derived thereof could well be relevant to space-caused disorders.

HSCT for Muscle and Bone Loss

Emerging reports indicate an extraordinary plasticity of HSCs; namely the HSCs, the so-called adult stem cells, can differentiate not only to all types of blood cells but also to muscle, skin, liver, neuronal cells, and possibly bone (10-18). According to Blau et al., as much as 15% of muscle cells could be derived from the transplanted HSCs in normal mouse (17). With regard to bone repair, Cobbs' group showed that not only a fractured bone but also completely disconnected bone gap was repaired by bone marrow derived mesenchymal stem cells (12,18). If this holds true in space, the HSCs could be useful to countermeasure various space-caused symptoms, especially muscle and bone losses (19). Since one of the aims of our HSCT is to maintain the homeostasis of muscles and bones, as in hematopoiesis above, during long-duration space missions such as Mars exploration, our working hypothesis is that combined with exercise, periodic autologous HSC transplantation might prevent muscle and bone losses of the astronauts during the long-term exposure to 0/ μ G, the differentiating HSCs contributing to the repair of these atrophying tissues. We are investigating these possibilities, using a mouse hindlimb suspension unloading model (20). Since this model is frequently used to simulate astronauts' bone and muscle losses in space, as well as bed-rest patients on earth, information obtained from this investigation may shed light for the countermeasures. Our experimental design involves the use of transgenic (tg) mice which harbor ubiquitously expressing β -galactosidase (LacZ) gene (21) or green fluorescent protein (GFP) gene (22). The HSCs are prepared from these mice and being transplanted to isologous wild type mice that are hindlimb suspended. If the LacZ-HSCs differentiated to muscles and bones, then examination of these tissues for β -galactosidase expression, which can be detected by X-gal (23), blue-color staining, would signify the possibility. Similarly, GFP-HSC can be monitored by the fluorescence emission. While these are the initial studies, more refined anatomical/histological examinations would be necessary to ensure the actual integration of grafted cells to existing tissues. In space situation, our hope is that the earth-programmed HSCs would either form new muscle cells of ground type or fuse to the existing cells to

make ground type fibers. As to the frequency of HSC transplantation, the interval could be determined by the rate of muscle fiber transition from slow to fast type (19, 24, 25). The incoming HSCs should prevent this remodeling and thus, this myosin heavy chain (MHC) isoform change can be the determining factor for frequency.

While it is premature to speculate the contribution of HSCs for repair of bone loss and muscle loss in space, the participation of HSCs for needed repair is apparent from the above reports. In addition, the localization of HSCs to bones and muscles might in the future make it possible to perform HSC-mediated ex vivo gene therapy in space (6,7,27), using insuline-like growth factor 1 (IGF-1) gene which would promote growth of bones and muscles (26) in an autocrine/ paracrine fashion. A few words need to be added on the muscle derived stem cells (MDSC), which subject is currently actively pursued by several investigators (28-30). Although we are also working on the MDSC in a mouse system, reproducing pre-plating methods of Huard's laboratory (29), there may be a potential difficulty of this approach to space program because of the invasive operations needed to prepare MDSC: namely, muscle specimens from the astronauts have to be obtained before the flight. Unrelated individual's MDSC would result in graft-vs-host-disease. Thus, the MDSC approach may not be applicable to the space-based stem cell therapy, at least at the current level of technology. Compared with this situation, hematopoietic stem cells can be prepared from the astronauts' blood samples, as is commonly done.

HSCT for Immunodeficiency

Studies on hematopoiesis in space using human HSCs (CD 34+ cells) indicated a decrease in both erythropoiesis and myelopoiesis (2). This decrease in myelopoiesis can then lead to decrease in immunity at μ gravity conditions. Other studies have indicated alterations of several immunological parameters, including leukocyte blastogenesis, cytokine production and leukocyte subset distribution (32-33). Since HSCs have the potential to differentiate into all types of blood cells, including leukocytes, HSCT should be able to mitigate these abnormalities. Since one of the aims of our HSCT is to maintain the homeostasis of immunity during long-duration space missions such as Mars exploration, our working hypothesis is that periodic autologous HSC transplantation might prevent immunodeficiency of

the astronauts during the long-term exposure to 0/ μ gravity, the differentiating HSCs contributing to the maintenance of the immune parameters. We are investigating these possibilities, using a mouse hindlimb suspension unloading model (20). Since this model is frequently used to simulate effects of spaceflight on physiological changes of the body, information obtained from this investigation may shed light for the countermeasures. Our experimental design involves the use of wild type (C57BL) mice which are then intraperitoneally infected with *E. coli* harboring the plasmid, pCMV.SPORT- β -gal. Examination of the tissues for β -galactosidase expression, which can be detected by X-gal (23), blue-color staining, would signify the level of immunity of host system: with blue-color staining being inversely proportional to the ability of mice to eliminate the bacteria: the more intense blue-color staining indicative of a decrease in immunity. The second stage would then be to mitigate this immunodeficiency *via* HSCT. The HSCs are prepared and transplanted to isologous hindlimb suspended mice. If the HSCs mitigated the immunodeficiency, then examination of these tissues for β -galactosidase staining, would signify the possibility of HSCT.

MATERIALS AND APPROACH

Experimental animals:

β -thalassemic mouse, C57BL/6Hbbth/Hbbth: the breeding pairs were purchased from the Jackson Laboratory, ME and thereafter bred in this institution to establish a colony. Breeder pairs for LacZ-mouse, B6;129S-Gtosa26 and GFP-mouse, C57BL/6-TgN (ACTbEGFP)1Obs were also purchased from the Jackson Laboratory and bred in this institution. The latter two mice express the respective reporter genes ubiquitously, except for erythrocytes and hair in the GFP-mouse. The animals were handled and experimented according to the protocols of the Howard University IACUC and IBC.

Purification of mouse HSCs:

The HSCs were prepared as described previously (31). Briefly, the mice were sacrificed and the tibiae and femora harvested; no treatment with 5-fluorouracil (FU) was done, unless otherwise noted. The marrow cells were obtained by flushing the bones with Hank's Balanced Salt Solution (HBSS) with 2% FBS. The bone marrow (BM) HSCs were enriched/purified by Histopaque 1077 (Sigma

Chemical Co.; $\rho = 1.077$ g/mL) density gradient centrifugation, followed by negative and positive immunomagnetic purging. Primary antibodies used for this purpose were rat anti-mouse L3T4 and anti-mouse Lyt2 antibodies (Becton Dickinson) for negative selection, and rat anti-mouse Thy 1.2 antibody (*ibid.*) for positive selection. Magnetic goat anti-rat IgG Ab (BioMag; Advanced Magnetics, Inc.) was used as the secondary antibody in both cases, and the immuno-positive cells were selected by a magnet (BioMag Separator). In our hand, the purified Thy-1.2⁺ Lin⁻ stem/progenitor cells account for 0.1 to 0.4% of initial bone marrow cells. In some instances, the Sca-1 selection was also applied to further purify the stem cell population, yielding Thy-1^{lo}Lin⁻Sca-1⁺ (34).

Long-term liquid suspension culture of mHSCs in static culture:

The static culture serves as the control to the RWV culture on the ground-based experiments. The condition of static culture is as follows: purified HSCs was seeded in a membrane-vented culture flask in IMDM + 20% FBS, supplemented with 10 ng/ml of recombinant stem cell factor (SCF), Epo (2 U/ml), IL-3 (50 U/ml), IL-6 (2 U/ml), GM-CSF (2 U/ml), Penicillin, Streptomycin, and 0.1% starch. The cells were incubated at 37°C with 7% CO₂ in a 100% humidified chamber. Cell growth kinetics was monitored by counting Vital Red-stained cells every three days for more than one month. Medium is replenished once a week. The HSCs sustained vigorous growth in this culture system for more than 12 months.

Culture of mHSCs in the Rotating Wall Vessel:

The RWV culture is conducted in collaboration with L. B. Margolis and W. Fitzgerald in the NASA-NIH Center for Three-Dimensional Tissue Culture, who operates the NASA RWV culture system. The RWV culture was conducted with 12 rpm and the medium described as for the static culture. Expansion of HSC was determined by cell counting as well as by measuring the Thy-1^{lo}Kit⁺ population by flow cytometer (with FITC- anti-Thy-1.2 antibody (Ab) and Rhodamin-anti-cKit Ab).

Engraftment assay for the cultured HSCs using β -thalassemic mice:

To eradicate recipient's marrow cells in preparation for HSCTP, Cyclophosphamide (CP) and Busulfan (BS) were used, rather than γ -irradiation. The drug-treatment is chosen over the whole body irradiation,

because the latter method is not commonly used for bone marrow transplantation (BMT) in humans with hemoglobinopathies. CP (200mg/kg, i.p.) and BS (80 mg/kg, p.o.) in Hank's Balanced Salt Solution (HBSS) were administered to mice on two consecutive days. Twenty-four hours later, 10 day-precultured HSCs (apx. 1×10^6 cells) in HBSS were injected into ocular veins. Contrary to our concern, the β -thalassemic mice (C57BL/6-Hbbth/Hbbth) could tolerate the drug regimen quite well, even better than the wild type. Both static cultured and the RWV-cultured HSCs, usually after 7-10 days of the culture, were harvested, resuspended in HBSS, and injected into eye vein of the marrow ablated β -thalassemic mice. As the nil control, another group of β -thal mice were injected with HBSS alone. The three groups of mice were maintained in isolation cages for an extended period for testing blood samples.

HSC transplantation (HSCTP):

The transplantation was carried out according to the procedure described (7,35). For LacZ-mouse, strain 129S was used as the recipient to prevent GVHD. While our routine method of HSC injection is through ocular vein, intramuscular injection to thigh is also being tried, aiming to deliver HSCs directly to leg muscles and bones.

Hemoglobin typing by cystamine-cellulose acetate electrophoresis:

Approximately 0.1 mL of peripheral blood was collected from the retroorbital sinus of mice using a 2 mg/mL Na-heparin as an anticoagulant. Blood cells were lysed with 2 vol. of 'Hb Elution Solution' (ISOLAB; 0.05% KCN, 1% Triton X-100, Na-azide) and the sample reacted with an equal volume of cystamine solution [66.7 mM cystamine, 1.33 mM dithioerythritol, 0.1 M (NH₄)OH]. The samples were run on a cellulose acetate electrophoresis (7,36).

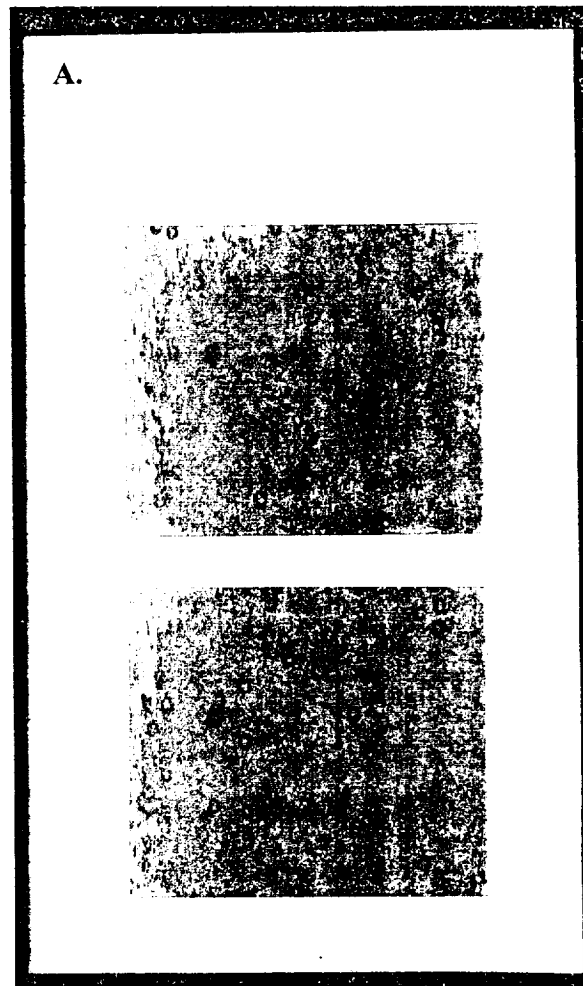
Lac Z staining Procedure:

The HSCs in culture were harvested by centrifugation, fixed with formalin/glutaraldehyde and stained with X-gal-Fe cyanide solution (23). The differentiation of HSCs to muscles was assessed by the Lac Z marker. Harvested tissues were stained according to the procedure of Schmidt et al. (21).

RESULTS

Purification and the liquid suspension culture of mouse hematopoietic stem cells (mHSCs)

Fig. 1A shows mHSCs prepared in this laboratory. These cells are uniformly rounded cells and account for approximately 0.3% of initial bone marrow cells. Upon culturing in our liquid suspension culture system, the cells grew in clusters, the shape resembling hanging grapes (1B). These clusters of cells appear to represent colonies that developed in the liquid suspension culture. Mixing the culture by several repeated pipetting dissociated the clusters, forming free single cells.



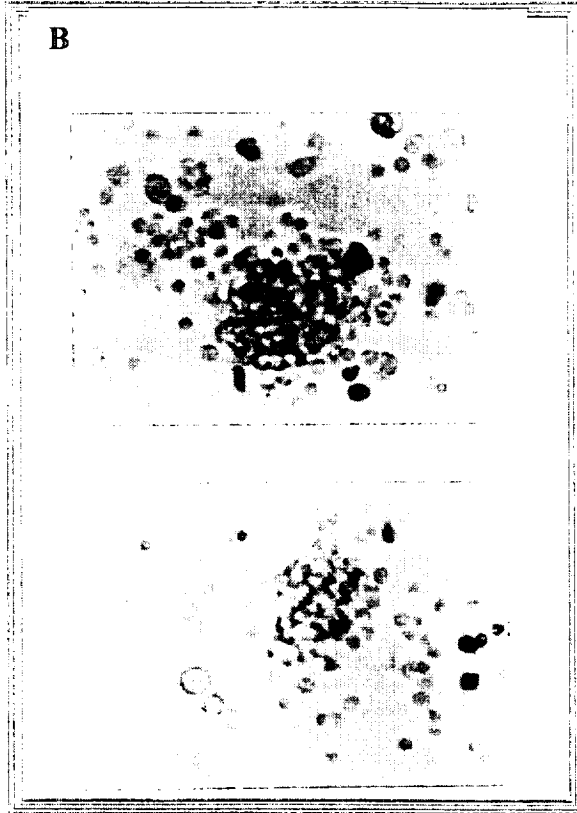


Fig. 1. Characteristics of mouse hematopoietic stem cells. A: The purified mouse hematopoietic stem cells. Mouse HSCs were purified/enriched by immunomagnetic selection and suspended in the MEM/20% fetal bovine serum. The picture was taken under the Leitz inverted phase microscope. Magnification: 250x. B: Liquid suspension culture of hematopoietic stem cells. The purified HSCs were incubated in a liquid suspension culture medium in a vented 25 cm² flask for 10 days at 37 °C, 7% CO₂ in a humidified chamber and observed under the microscope as in A.

Differentiation of mHSCs to various blood cell lineages

Basic characteristics of hematopoietic stem cells is an ability to differentiate to various blood cells. In the methylcellulose clonogenic assay system in the presence of erythropoietin (Epo) and IL-3, our HSCs did differentiate to Burst forming unit-erythroid (BFU-E), Colony forming unit-granulocyte, erythroid, megakaryocyte (CFU-GEM) and Colony forming unit-monocytes (CFU-M) (Fig. 2), thus satisfying pluripotential nature of stem cells. BFU-E colony was reddish colored due to hemoglobin production in the cells; CFU-GEM also contained some hemoglobinized cells.

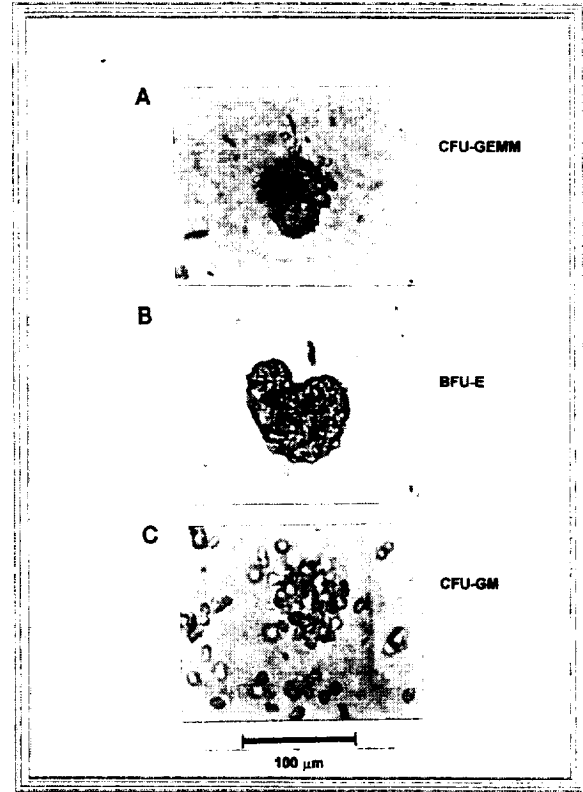


Fig. 2. Clonal cell culture of purified/enriched mouse HSCs. The purified cells were seeded in the medium containing methylcellulose and cytokines on the first day of culture. Following 14 days culture, colonies were observed under Leitz inverted phase microscope and the picture was taken. Three kinds of colonies were apparent and these were classified as, (A) Colony-forming unit granulocyte/erythroid/monocyte/megakaryocyte (CFU-GEMM) which had a "fried egg" appearance with a compact hemoglobinized area at the center of the colony. The peripheral flat lawn consists of non-hemoglobinized translucent cells that may be either large or small; (B) Burst-forming unit erythroid (BFU-E): a densely packed group of orange- to dark-red hemoglobinized cells without contamination of translucent cells; and (C) Colony-forming unit granulocyte/macrophage (CFU-GM): a flat, non-hemoglobinized colony consisting of translucent cells. Magnification: x 250.

Kinetics of HSC growth in liquid suspension culture

1) Static culture: When cultured in our liquid suspension culture system, which does not contain stromal cells, the HSC numbers in the static culture oscillated, having growth phase and apoptic phase (Fig. 3). Arrows in the figure indicate medium changes during the culture; however, this oscillating pattern appears to be independent of the medium change. Thus, the self-regulating growth pattern is quite unique to the stem cell culture. Flow

cytometric analysis for Thy-1.2⁺ cells increased from 4.5% to 70% and c-Kit⁺ cells increased from 25% to 90%, indicating the expansion of stem cells. During the growth phase, it is possible to subculture and expand the stem cells. In one attempt, we have kept the liquid culture for 18 months.

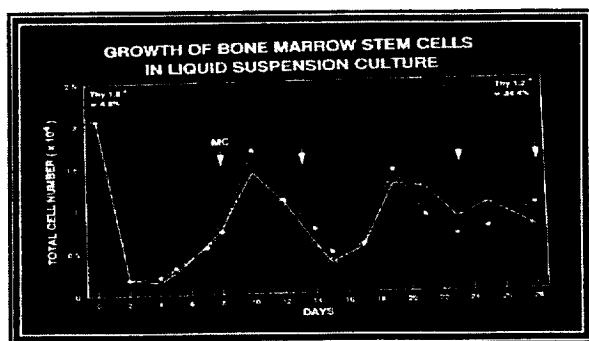
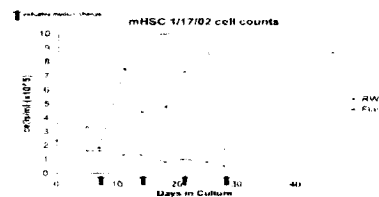


Fig. 3. Growth kinetics of hematopoietic stem cells in liquid suspension culture. The purified mHSCs were grown in the liquid suspension culture as in Fig. 1 B and the cell numbers were counted as indicated in the graph. The cell numbers were determined by using hemocytometer after staining cells with Vital Red. Medium change (MC) is indicated by arrows. Duplicate cultures are shown.

2) RWV culture: Fig. 4 shows the growth pattern of mHSCs in the RWV culture. As reported by others, the HSC growth was severely inhibited in the Bioreactor system (Fig. 4A), compared with the static culture. However, the inhibition could be overcome by two independent mechanisms: the use of High aspect ratio vessel (HARV) system, as well as by the "1 G exposure" regimen (Fig. 4B). The latter operation is to periodically stop the rotation of RWV culture. Flow cytometric analysis during the culture indicated 98% Kit⁺ cells and about 4% Thy 1.2⁺ cells. The detailed study will be published elsewhere.

GROWTH OF MOUSE HEMATOPOIETIC STEM CELLS IN THE NASA-RWV CULTURE

A) Growth of mHSCs was severely inhibited in the RWV culture



B) But, modification of the culture condition has led to the growth of HSCs.

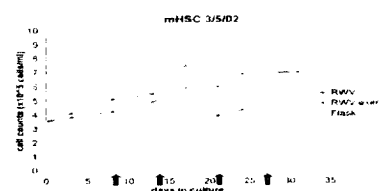


Fig. 4. Growth kinetics of mouse hematopoietic stem cells in the NASA RWV culture. A: The purified mHSCs were grown either in a static flask culture or the RWV system. Note the inhibitory effect of the RWV system on the HSC growth. However, modification of the culture condition has led to the growth of HSCs, B.

HSC transplantation to β -thalassemic mice

1) β -thal hemoglobin (Hb) types: When hemoglobin is treated with cystamine, the chemical undergoes disulfide interchange reaction with hemoglobin, adding extra positive charges (as cysteamine) to Hbs (36). Since the mouse β^{minor} -globin has an additional cysteine residue in relation to β^{single} , the Hb^{d-minor} is clearly separated from Hb^{single} by cellulose acetate electrophoresis after the reaction with cystamine. The Fig. 5A shows the pattern of Hb species of our β -thal mice by this method: the wild type C57BL/6J gives one band (hemoglobin single, Hb^s), while the heterozygote (C57BL/6Hbb^s/Hbbth) has two bands, Hb^{single} and Hb^{d-minor}. The β -thalassemic mice showed only one band: Hb^{d-minor}.

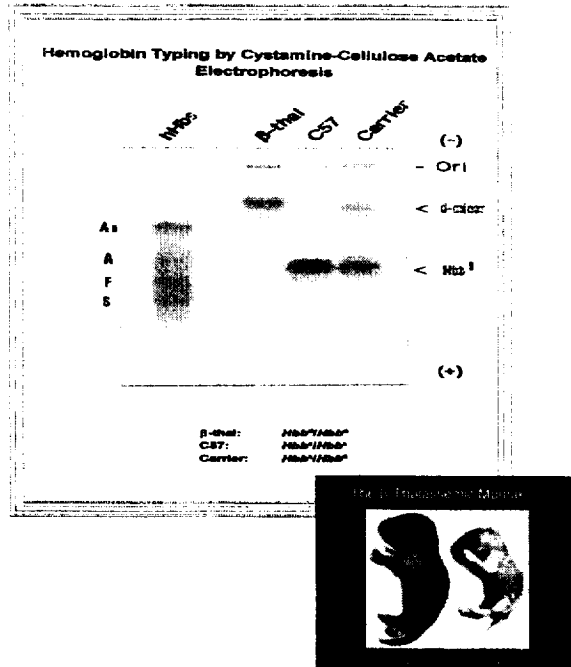


Fig. 5. A: Hemoglobin typing by cystamine-cellulose acetate electrophoresis. Blood samples from the wild type (C57BL/6J), heterozygote, and β -thalassemic mice are treated with cystamine and electrophoresed in the cellulose acetate strip and stained by Ponceau Red. Human hemoglobin markers are shown in the extreme left lane. Ori: origin of sample application; d-minor: Hemoglobin diffuse minor; Hbb^s: hemoglobin single. B: HSC transplantation in the β -thalassemic mice. HSCs prepared from heterozygotes were culture for 10 days in the liquid suspension culture and injected to β -thalassemic mouse (5×10^5 cells/mouse). Following either 3 weeks or 5 weeks post operation, the mouse blood were taken and analyzed by cellulose were sacrificed and analyzed by cellulose acetate electrophoresis. Note the appearance of Hb^s in the transplanted β -thalassemic mice, with more time elapsing the band getting stronger.

2) Correction of β -thalassemia by HSC transplantation: The successful bone marrow transplantation (BMT) of β -thalassemic mice with HSCs from C57BL/6J will result in conversion of hemoglobin type in the recipient blood from Hb^{d-minor} to Hb^s. Since this combination often killed the β -thal recipients, probably due to the GVHD, we opted to transplant HSCs from heterozygote to β -thal mice (Fig. 5B). The figure shows the chimerism of hemoglobin species in the recipients. The longer period of post-transplantation results stronger donor hemoglobin bands (compare 3 weeks vs. 5 weeks).

Genetic marking of HSCs

In order to trace the transplanted HSCs in the hindlimb suspended mice, HSCs were designed to be genetically marked, using reporter genes. We have attempted two methods: one is to transfect HSCs with a plasmid harboring β -galactosidase (β -gal) reporter gene, and the other is to isolate HSCs from β -gal transgenic mice. Fig. 6A shows the β -gal plasmid-transfected HSCs, which were subsequently stained by X-gal staining procedure, while Fig. 6B shows the HSCs isolated from the transgenic mice, similarly stained with X-gal. The transfection resulted in more than 50% of HSCs to be marked with β -gal, while 100% of HSCs from the transgenic mice were positive in X-gal staining.

Transplantation of the marked HSCs for HSCT for muscle loss

To initiate the HSC therapy for bone and muscle losses, we set up the mouse hindlimb suspension unloading system in this laboratory. Currently, β -galactosidase-marked HSCs are being transplanted to the isologous hind limb suspended mouse and differentiation of the HSCs to muscles are investigated by X-gal staining procedure. GFP-marked HSCs will be also used in the future. Effect of exercise on the HSC engraftment and differentiation is being investigated. If the engraftment/differentiation were proven, further studies, such as integration/participation of HSCs to existing muscle structure, will be conducted. Effect of HSCT and exercise on the prevention of slow- to fast-type muscle fiber is under investigation utilizing myosin heavy chain (MHC) isoform analysis (24,25,37).

Transplantation of HSCs for HSCT for immunodeficiency

To initiate the HSC therapy for immunodeficiency, we set up the mouse hindlimb suspension unloading system. Examination of hindlimb suspended mouse, following *E. coli* /p β -gal injection indicated an increase in the intensity of blue-color compared to control mice, when the tissues are stained with X-gal. This indicates a decrease in the ability of hindlimb suspended mice to eliminate *E. coli* and therefore a decrease in immunity. Observation of hindlimb suspended mice injected with isologous HSCs indicated an increase in agility and alertness of mouse. When these mice were injected with *E. coli*/p β -gal and the tissues subsequently stained with X-gal, less stain was detected compared to hindlimb

suspended mice that are not treated with HSCs, indicating regaining of immunity by HSCT. This area of research is currently subject to further investigation and more detailed testing.

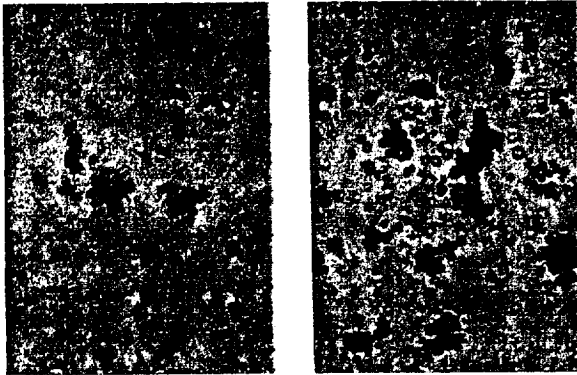


Fig. 6. Lac Z marking of HSCs. HSCs were purified either from A. wild type C57 BL/6J or B. β -galactosidase-transgenic mouse and cultured in a liquid suspension culture system. The wild type HSCs were then transfected with pCMV.SPORT. β -gal (LifeTechnology, Inc.) by Lipofectamine method and stained by X-gal. With regard to the HSCs from the β -gal transgenic mice, the culture was expanded for 3 weeks and an aliquot of the liquid suspension culture was stained with X-gal. The pictures were taken under the Leitz inverted phase microscope. Magnification: x 250.

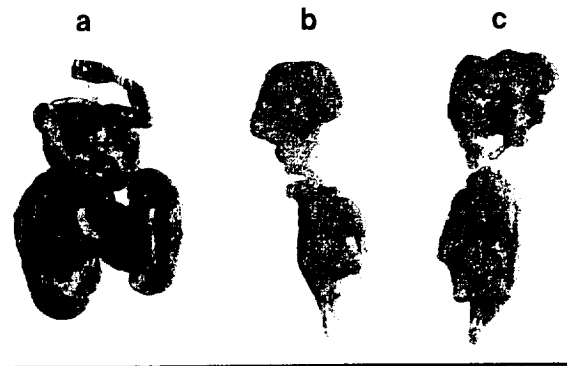


Fig. 7. Transplantation of β -gal-HSCs to a hindlimb suspended mouse. HSCs from a β -gal transgenic mouse were isolated and expanded, and thereafter about 2×10^5 cells in 0.25 ml of HBSS was injected to thigh and gastrocnemius regions of the right leg of a hindlimb suspended mouse. Two days later, the mouse was sacrificed and various tissues harvested and stained by X-gal stain. Note that segments of the large and small intestine (a) were strongly stained, while the portions of left leg (b) and right leg (c) were positive by the stain. Pictures were taken by Nikon Coolpix 5000.

DISCUSSION

We have hypothesized that the hematopoietic stem cell-based countermeasures, hematopoietic stem cell therapy (HSCT), might be effective in maintaining health condition of astronauts during long-duration space missions, such as Mars exploration. While there are several known symptoms which astronauts experience in $0/\mu$ G, we are focusing three areas at this time, namely hematological disorders, immunodeficiency and muscle loss. To formulate the relevant techniques and protocols, two animal models are being used in the ground-based experiments: β -thalassemic mouse and mouse hindlimb suspension system. The goal is to countermeasure/cure hematological abnormalities of β -thalassemic mouse as well as muscle loss and immunodeficiency of the unloaded mouse. In this paper, some of the success of correcting β -thalassemic mouse as studied by the hemoglobin change is presented (Fig. 5B). Successful cure of β -thalassemia by HSCT may normalize various hematological parameters. These would include white blood cell counts, lymphocyte counts, hematocrit, reticulocytes counts, RBC volume (MCV), and hemoglobin content (MCHC) (38). Therefore, these parameters are being measured in the marrow transplanted β -thalassemic mice in comparison to mock treated mice. This transplantation system has been quite useful in this laboratory to establish transplantation procedures as well as to evaluate transplantability of HSCs. Therefore, it is in our plan to test the quality of HSCs grown in the NASA Rotating Wall Vessel (RWV) culture by the β -thal transplantation system. Thus, the HSCT protocols derived from this animal model would be highly relevant to the HSCT for space-caused hematological abnormalities.

With regard to the study on efficacy of HSCT for muscle loss, the current goal is to delineate participation of HSCs in repair/prevention of muscle and bone losses in the hindlimb suspended mouse. The reporter gene marked HSCs are useful to trace transdifferentiation in the transplant recipient. We have successfully marked the HSCs with β -galactosidase expression by two methods, transfection and transgenic mouse, which are presented in Fig. 6A,B. The transfection method will be useful for marking human HSCs in the future clinical trials. Further physicochemical analyses for the actual countermeasure will be performed. These will include: 1) Measurement of muscle weight; 2) Study of prevention of MHC transition by HSCT; 3)

Measurement of muscle strength; 4) Other biochemical marker studies (19). Insulin-like growth factor (IGF)-1 treatment of HSCs is being considered to stimulate the muscle growth (19,26). In addition, using the hindlimb suspension model, effect of exercise on the HSCT for muscle loss can be investigated. Combined with proper exercise regimen, periodic HSC transplantation might prevent bone and muscle losses. These studies are under way in this laboratory.

Thus far, our preliminary results have successfully indicated that not only do hindlimb suspended mice suffer immunodeficiency, but also that the HSCT has the capability of mitigating these symptoms. Our current goals are now to quantify the degree of immunodeficiency exhibited in the hindlimb suspended mouse and then to possibly establish the process of HSCT for immunodeficiency. Since astronauts suffer a decreased immunity similar to that of hindlimb suspended mice, the HSCT protocols derived from this animal model would be highly relevant to the HSCT for immunodeficiency in astronauts.

FUTURE PLANS

One major spin-off of the HSCT could be an opportunity to develop stem cell-mediated *ex vivo* gene therapy in the future (6,7). As our expertise lies on adeno-associated virus (AAV)-mediated gene therapy, the vector containing IGF-1 could be constructed and used for muscle gene therapy in space. The adeno-associated virus, serotype 2 (AAV-2), is a human parvovirus, which contains a linear single-stranded DNA of 4,675 nucleotides (nt), having broad host-range and tissue-specificity (39,40). Because the virus is a **non-pathogen**, the virus promises to be a safer vector for gene therapy than other pathogenic viruses, such as, adenovirus, retrovirus and herpes virus. This non-pathogenicity of AAV, compared with other vectors, is particularly important for the space program, because of the enclosed environment in a spaceship. Exploiting these advantages of AAV-2, starting in 1985, we have constructed recombinant AAVs (rAAVs) that harbor human globin genes as well as an anti-HIV-1 *gag* ribozyme (anti-*gag* Rz) for eventual use in gene therapies of the hemoglobin disorders, the β -thalassemia and sickle cell disease, and AIDS, respectively (31,35,41,42). Putting all the techniques together, we are currently trying to cure mouse model of human β -thalassemia (35). Once these mice are

cured by gene therapy, we will then move to possible clinical trials for human patients. Many laboratories worldwide are now using the rAAV system for various gene therapy projects with promising results (43-45). With regard to the space program, this system promises to be a good model system for developing space-based gene therapy, and our long-term plan is to conduct the model experiment on International Space Station.

ACKNOWLEDGEMENT

This work was in part supported by the NASA Institute for Advanced Concepts (NIAC)-Universities Space Research Association (USRA).

REFERENCES

1. Nicogossian A, Huntoon C, Pool S Eds (1994). *Space Physiology and Medicine*, 3rd ed.; Lea & Febiger: Philadelphia, PA
2. Davis TA, Wiesman W, Kidwell W, Cannon T, Kerns L, Serke C, Delaplaine T, Pranger A, Lee KP (1996). Effect of spaceflight on human stem cell hematopoiesis: suppression of erythropoiesis and myelopoiesis. *J Leukoc Biol* 60: 69-76.
3. Tavassoli M (1982). Anemia of spaceflight. *Blood* 60, 1059-1067.
4. Alfrey CP, Rice L, Udden MM, Driscoli TB (1997). Neocytolysis: physiological down-regulator of red-cell mass. *Lancet* 349, 1389-1390.
5. Sytkowski AJ, Davis KL (1998). Reduced erythropoiesis in microgravity: A cellular basis for the anemia of space flight. *Blood Abstract* #2845.
6. Ohi S (1999). Developing protocols for recombinant adeno-associated virus-mediated *ex vivo* gene therapy. *Proc. 2nd NASA Kennedy Space Center Conference*, pp. 34-36.
7. Ohi S (2000). Developing protocols for recombinant adeno-associated virus-mediated gene therapy in space. *J Grav Physiol* 7, 67-68.
8. Quesenberry PJ, Grimdi CI, Rao S, Stewart FM (1997). Hematopoietic stem cells cultured in rotating bioreactors show a defect in engrafting capability. *Blood Abstract* #3392.
9. Skow LC, Burkhart BA, Johnson FM, Popp RA, Popp DM, Golberb SZ, Anderson WF, Barnett LB, Lewis SE (1983). A mouse model of β -thalassemia. *Cell* 34:1043-1052.
10. Vogel G (2000). Stem cells: New excitement, persistent questions. *Science* 290: 1672-1674.
11. Krause DS, Theise ND, Collector MI, Henegariu

- O, Hwang S, Gardner I, Neutzel S, Sharkis SJ (2001). Multi-organ, multi-lineage engraftment by a single bone marrow derived stem cell. *Cell* **105**: 369-377.
12. Jaiswal RK, Jaiswal N, Bruder SP, Mbalaviele G, Marshak DR, Pittenger MF (2000). Adult human mesenchymal stem cell differentiation to the osteogenic or adipogenic lineage is regulated by mitogen-activated protein kinase. *JBC* **275**:9645-9652.
13. Brazelton TR, Rossi FMV, Keshet GI, Blau HM (2000). From marrow to brain: Expression of neuronal phenotypes in adult mice. *Science* **290**:1775-1779.
14. Mezey E, Chandross KJ, Harta, G, Maki RA, McKercher SR (2000). Turning blood into brain: Cells bearing neuronal antigens generated in vivo from bone marrow. *Science* **290**:1779-1782.
15. Corti S, Strazzer S, Del Bo R, Salani S et al. (2002). A subpopulation of murine bone marrow cells fully differentiates along the myogenic pathway and participates in muscle repair in the *mdx* dystrophic mouse. *Exp Cell Res* **277**:74-85.
16. Blau HM, Brazelton TR, Weimann JM (2001). The evolving concept of a stem cell: Entity or function? *Cell* **105**:829-841.
17. Blau HM, Weimann JM, Brazelton TR (2001). The evolving concept of stem cell: Entity or function? *Mol Biol Cell* **12**:134a.
18. Cobbs CS, Jennings MJ, Pittenger MF (2001). Molecular and cellular evidence of adult stem cell plasticity. *Mol Biol Cell* **12**:134a.
19. Muscle Research in Space: International Workshop (1997). *Internl J of Sports Med* **18**, Supp 4, S257-331.
20. Morcy ER (1979). Spaceflight and bone turnover: correlation with a new rat model of weightlessness. *BioScience* **29**: 168-172.
21. Schmidt A, Tief K, Foletti A, Hunziker A, Penna D, Hummler E, Beermann F (1998). *LacZ* transgenic mice to monitor gene expression in embryo and adult. *Brain Res Protocols* **3**:54-60.
22. Okabe M, Ikawa M, Kominami K, Nakanishi T, Mishimune Y (1997). 'Green mice' as a source of ubiquitous green cells. *FEBS Lett* **407**:313-319.
23. Beckwith JR (1980). *Lac*: The genetic system. In *The Operon* (ed. Miller JH and Reznikoff WS). Cold Spring Harbor Laboratory, Cold Spring Harbor, NY.
24. Ohira Y, Jiang B, Roy RR, Oganov V, Ilyina-Kakueva E, Marini JF, Edgerton VR (1992). Rat soleus muscle fiber responses to 14 days of spaceflight and hindlimb suspension. *J Appl Physiol* **73**: 51S-57S.
25. Adams GR, Haddad F, McCue SA, Bodell PW, Zeng M, Qin L, Qin AX, Baldwin KM (2000). Effects of space flight and thyroid deficiency on rat hindlimb development. II. Expression of MHC isoforms. *J Appl Physiol* **88**:904-916.
26. Adams GR, McCue SA, Bodell PW, Zeng M, Baldwin KM (2000). Effects of space flight and thyroid deficiency on rat hindlimb development. I. Muscle mass and IGF-1 expression. *J Appl Physiol* **88**: 894-903.
27. Ohi S, Aguilar A, Kim BC (2000). Recombinant adeno-associated virus-mediated gene therapy in space. *Grav Space Biol Bull* **14**: 43.
28. O'Brien K, Muskiewicz K, Gussoni E (2002). Recent advances in and therapeutic potential of muscle-derived stem cells. *J Cell Biochem Supp* **38**: 80-87.
29. Qu-Petersen Z, Deasy B, Jankowski R, et al (Huard J) (2002). Identification of a novel population of muscle stem cells in mice: potential for muscle regeneration. *J Cell Biol* **157**: 851-864.
30. Seale P, Sabourin LA, Girgis-Gabardo A, et al (Rudnicki MA) (2000). Pax7 is required for the specification of myogenic satellite cells. *Cell* **102**: 777-786.
31. Ohi S, Kim BC (1996). Synthesis of human globin polypeptides mediated by recombinant adeno-associated virus vectors. *J Pharm Sci* **85**: 274-281.
32. Sonnenfeld G (1998). Immune responses in space flight. *Int J Sports Med* **19**:S 195-204
33. Cogoli A (1993). The effect of hypogravity and hypergravity on cells of the immune system. *J Leukoc Biol* **54**: 259-68.
34. Spangrude GJ, Heimfeld S, Weissman IL (1988). Purification and characterization of mouse hematopoietic stem cells. *Science* **241**: 6862.
35. Ohi S, Kim BC, Goldson A, Dinndorf P (1999). Hematopoietic stem cell therapy of the β -thalassemic mice: Toward recombinant adeno-associated virus-mediated gene therapy for hemoglobinopathies. *Mol Biol Cell* **10**, 268a.
36. Whitney JB III (1978). Simplified typing of mouse hemoglobin (*Hbb*) phenotypes using cystamine. *Biochem Genet* **16**: 667-672.
37. Talmadge RJ, Roy RR (1993). Electrophoretic separation of rat skeletal muscle myosin heavy-chain isoforms. *J Appl Physiol* **75**:2337-2340.
38. Bethel CA, Muruges D, Harrison MR, Mohandas N, Rubin EM (1993). Selective

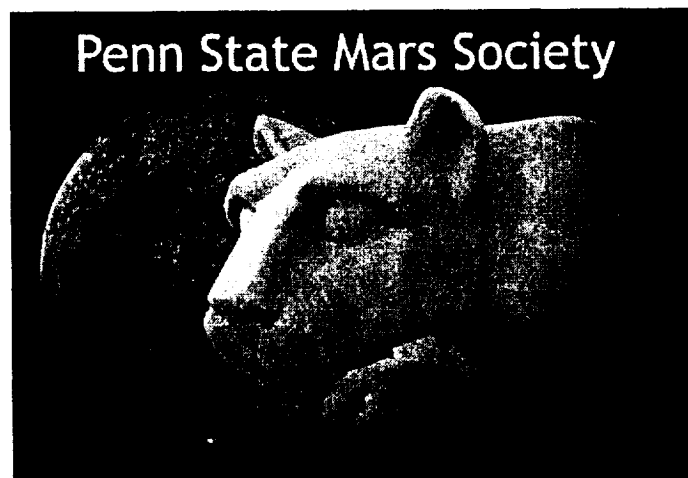
- erythroid replacement in murine β -thalassemia using fetal hematopoietic stem cells. *Proc Natl Acad Sci USA* **90**: 10120-10124.
39. Rose JA (1974). Parvovirus reproduction. In *Comprehensive Virology*; Fraenkel-Conrat H, Wagner T Eds., Plenum Press: New York; vol. 3, pp. 1-61.
 40. Berns KI (1984). *The Parvoviruses*; Plenum Publishing Corp.: New York.
 41. Ohi S, Dixit M, Tillery MK, Plonk SG (1990). Construction and replication of an adeno-associated virus expression vector that contains human β -globin cDNA. *Gene* **89**: 279- 292.
 42. Dixit M, Webb MS, Smart WC, Ohi S (1991). Construction and expression of a recombinant adeno-associated virus that harbors human β -globin-encoding cDNA. *Gene* **104**: 253-257.
 43. Flannery JG, Zolotukhin S, Vaquero MI, LaVail MM, Muzyczka N, Hauswirth WW (1997). Efficient photoreceptor-targeted gene expression *in vivo* by recombinant adeno-associated virus. *Proc Natl Acad Sci USA* **94**, 6916-6921.
 44. Kay MA, Manno CS, Ragni MV, Larson PJ, Couto LB, McClelland A, Glader B, Chew AJ, Tai SJ, Herzog RW, Arruda V, Johnson F, Scallan C, Skarsgard F, Flake AW, High KA (2000). Evidence for gene transfer and expression of factor IX in haemophilia B patients treated with an AAV vector. *Nat Genet* **24**:257-261.
 45. Wang B, Li J, Xiao X (2000). Adeno-associated virus vector carrying human minidystrophin effectively ameliorates muscular dystrophy in *mdx* mouse model. *Proc Natl Acad Sci USA* **97**:13714-13719.

PENNSSTATE



Modular Research Rover and Gesture Control System for EVA

**Submitted by the Penn State Mars Society pursuant to the
NASA 2002 RASC-AL Forum**



Student Team Co-Leaders

Joel Richter (jdr212@psu.edu) & Kevin Sloan (kfs113@psu.edu)

Student Team

Elizabeth Barnwell, Adrienne Benski, Amy Blank, Kevin Clark,
Lisa Legget, Steve McGuire, Nima Moshtagh, Paul Smidansky,
Ryan Swanson, Andy Summerville, Sandy Toh, Jeff Weiss

Student Team Faculty Advisor

Mike Jacobs

1. Abstract

As technology and computing power increases at extraordinary rates, our ability to effectively explore our solar system increases to new levels. The immediate future will see the continual development of robotic exploration as our primary means of exploring other planets. Once the time does arise for mankind to again push his frontiers to new limits, our definition of space exploration will be completely redefined. However, human exploration of our solar system cannot happen without the assistance of our robotic counterparts which helped blaze the trail into space. This transition to human exploration will see astronauts beyond the immediate communication reaches of Earth being forced to work with equipment that was at one time controlled by large teams of scientists and engineers with immediate access to significant computing resources.

In order to deal with these problems, the Penn State Mars Society is developing a new method of robotic control that allows an astronaut in the field on the surface of Mars to be able to directly control any robotic equipment that he could potentially be working with. By integrating virtual reality (VR) gloves into an astronaut's space suit gloves, his hands now become an accurately measurable and rather versatile input device. Gloves of this nature are rather small and unobtrusive, and as such, can very easily be incorporated into the gloves that an astronaut would be wearing. The gloves as an input system will remain passive until activated by a command from the user. At this point, they begin to actively monitor the hand's motion. They would relay this information to a computer on-board the rover, which would in turn convert this complex hand model into a command to execute. When the user is ready to free himself from the input state, another unique gesture can be used to deactivate the control system.

This method of interfacing with a computer will require refinement and testing, and for that purpose a rover is being built. As well as providing a test subject for the control system, the rover highlights another unique feature of our project. One issue that mission planners will surely face with a manned mission (as well as they do for all missions, human or robotic) is the trade-off of reducing overall cost and weight, while still sending ample equipment. Most rovers and other robotic equipment sent will be optimized for one specific portion of the mission, and will consequently lay idle for lengthy periods of time. To solve this issue, we are designing a modular research rover, which will maximize the versatility of the available equipment. The idea behind this rover is a standard rover base which will provide all of the

major systems, including power, computing, locomotion, navigation, and communications. Separate modules will be able to be attached both mechanically and electrically to the base, allowing vast expansion of the base rover. The base will accept a few modules at a time; however these units will be able to be interchanged with great ease throughout the course of the mission. Since individual modules will be significantly smaller and cheaper than entire rovers, they will clearly be a better option from a mission logistics standpoint.

2. Introduction

When the first manned missions are sent to Mars, the teams will require an extremely high level of self sufficiency. With communication delays to Earth as long as forty minutes, they will be virtually isolated. Despite their circumstances, they will still be expected to perform as though in an ideal setting. In order for these explorers to be able to maximize their time, and produce large quantities of data, new methods for planetary exploration must be developed.

One scenario that needs improvement is a small team of astronauts (or possibly even a single astronaut) conducting field work far away from their base. This seemingly commonplace scenario will find team members out facing the elements and conducting research. It seems only natural for research rovers to accompany the team into the field. However, having to deal with robotic equipment while in a pressure suit presents several issues, the main one being control. By incorporating virtual reality glove technology into the astronaut's gloves, his hands become a quick, easy and effective input device. A simple hand command can activate the gloves, and the rover begins to respond to hand gestures, which are interpreted as commands. Our stranded astronaut now has complete flexibility in the control over all of the different robotic equipment and machines that will be in the field with him.

All plausible mission outlines for the first manned missions to Mars entail the crew collecting extraordinary amounts of data in many different areas. Most of the field work would be conducted with research rovers such as those described above, each specializing in a different task. The amount of rovers to be sent will quickly add up. A much smaller fleet of modular rovers allows for mission flexibility while significantly cutting back on overall mission cost and weight. These modular rover bases, which will accept a wide variety of scientific units, will operate on a very standard platform. Because all of the equipment will have interchangeable components, the astronauts will be able to effectively

Penn State Mars Society – RASC-AL 2002, “Modular Research Rover and Gesture Control System for EVA”

handle most basic problems that could arise in the field. This modularity, coupled with the simplicity of the glove input, tackles many of the difficulties that an astronaut would face in the field that would otherwise severely restrict his productivity.

3. Approach

Members of the Penn State Mars Society participated in the two previous HEDS-UP competitions sponsored by LPI (Lunar and Planetary Institute) and NASA. From the experience that we were able to gain during those two years a plan for the future started to mature. The first goal was to work on a project that was more than a paper concept; it had to be something that could be developed, built and tested. By keeping a design simply on paper, there is no room for refinement, nor any validation of the design. There was much more to be learned by taking a design past the concept phase to a final product.

A second objective was to steer away from the one year projects of the past. One of the inherent difficulties that was faced each year was sitting down and finding a new problem to solve. Furthermore, this narrow time frame never allowed us to do more than an initial investigation into a solution, much less work on an actual product. This also will give incentive for people to stay in the project for multiple years, because there has been a very high turnover rate each year for the three years since this group was formed.

Another aim was to work on something unique; yet be within the scope on an undergraduate student group. Selecting such a topic was difficult because NASA and the space industry has been around for a rather long time, and most interesting projects that are not extremely advanced have been thoroughly studied.

With those as the motivating factors behind the search for a project, options were discussed. The reason the astronaut/computer interface was chosen was because it was an area that appeared to be totally unexplored. The reason it has been unexamined so far is that as long as real-time communication with Earth is possible, it is not necessary. Mission control can assist an astronaut through every step of every mission. Once humans venture out of the Earth-Moon system and communication delays emerge due to the extremely long distances traveled, a computer interface for astronauts will become necessary.

The decision to pick gesture recognition as the method of control to be tested was made after many other options were considered. No other option provided the same flexibility and seamless integration that VR gloves did. Once this decision

was made, it became clear that the project would fit the other two objectives. The gesture control system needed a test subject, leading to the second part of this project. A rover fit that requirement perfectly as it was something that could be expected to be controlled by an astronaut in a space suit on Mars. It also provided a great opportunity learn about design and construction of a sophisticated combination of machinery and electronics. This forced the project to be multidisciplinary, and has led to the formation of a balanced team consisting of aerospace, mechanical, electrical and computer engineers.

The large scope of the project, building a rover and defining and implementing a gesture recognition and control system, lends itself to drawing out the project over multiple years. Both parts can be greatly improved even once they are fully functional. Because the rover is being designed with modularity in mind, much work can be devoted to adding capability and features to the rover after the chassis is completed. Additionally, the gloves can be improved by modifying them to add more degrees of freedom and possibly implementing some sort of force feedback. This project has excellent possibilities for future work, and the future course will be determined by evaluating the past progress to address shortcomings and improve on strengths.

4. Results

4.1 Prototype

Initial investigations into the different systems of our design showed that our team would be best served by beginning work on a scaled down prototype. In our case scaled down refers not to the size of our prototype, rather its complexity. Our work was divided up into two separate areas: the glove and gesture recognition software, and the rover.

Glove and Gesture Recognition Software

Fundamentally, the system developed to interpret gestures has three major components: input filtering, gesture recognition, and device-specific output. Each of these components runs in a separate thread of execution, exchanging data through buffer queues. By multithreading the processing jobs, the overall program can process data without depending on the complexity of individual components.

Compared to other commercially available input devices, we feel that a virtual reality glove is the best candidate to be adapted to use while wearing a pressure suit. In order to use a keyboard, the individual keys would need to be large enough to be reached without trouble from bulky gloves. If the key size were to be scaled appropriately, the overall size of the keyboard would be ungainly. A traditional

Penn State Mars Society – RASC-AL 2002, “Modular Research Rover and Gesture Control System for EVA”

joystick is limited by the number of input dimensions; generally, only two degrees of freedom are present through the manipulation of the stalk, with additional degrees provided by trigger buttons or other small actuators. Even if the additional buttons were to be scaled to be usable from a pressure glove, there simply are insufficient degrees of freedom available for general-purpose tasks. Although we do not describe alternative input devices, designed for the impaired or for fully immersive environments, we are looking at novel user interfaces that might be adaptable to an outer space or planetary environment.

We begin with a description of the input devices available for our use. For this project, we have obtained two 5DT Technologies, Inc. virtual reality gloves, each with a serial interface to the host machine. These gloves have five finger sensors, and then an auxiliary roll and pitch sensor. Each finger sensor consists of an optical fiber that wraps around the length of the digit, such that the flexion of a finger bends the fiber. In an electronics package attached to the body of the glove, a light source emits light, and photosensors observe the transmission through the fiber. The glove is calibrated based on the principle that as an optical fiber flexes, the intensity of a transmitted light will vary as a linear function of the flexion. This flexion is represented as a single 8-bit byte value to the host. The roll and pitch sensors also produce 8-bit accurate results. After opening each device, we are ready to sample data.

In order to submit a sample to the processing pipeline, we must first read the data stream coming from the glove(s), and then assign the sample to the processing pipeline. To interpret the raw glove data, we utilize a vendor-supplied library function that returns the actual value measured by the glove hardware. Since our project was designed to have the option of using multiple gloves, we keep track of the mapping between samples and gloves. From the input module's point of view, there is no more work to be done, and so the next sample is obtained.

Once a sample has been provided to the processing pipeline, the next stage is a simple exponential filter that serves to regulate noisy input data from the gloves. This stage was added after initial testing indicated that users have slightly shaky hands; after filtering, the data is much smoother and appropriate to use in a decision process.

After data filtering, logical gestures may be interpreted out of the physical data. We define a gesture to be a region of flexion for each digit. In practice, we have found that the output of the gloves can be divided into only three or four “zones”, due to the fact that a human cannot repeat gestures with exact precision. Assuming that each finger was

capable of producing each position independently, there are a maximum of 1024 gestures; this number is entirely too optimistic. For example, as a limitation of the design of the individual gloves that we are using, the thumb measurement only has two zones; we have also found that users are not as comfortable with intermediate positions of the thumb as with positions of the fingers. Secondly, most people cannot move their pinky finger without incurring some movement in the ring finger; in the same vein, the ring finger generally implies a movement in the middle finger. Truly independent movement is only possible for the index and middle fingers. We divide the limitations into two categories: extrinsic for those limitations such as the thumb movement that are a result of the manufacture of the glove, and intrinsic for those limitations such as the non-independent movement of the pinky finger. Extrinsic constraints may be mitigated by investing in higher-quality gear; for our purposes, however, the performance of our gloves is adequate.

Since the virtual reality gloves are measuring one of the user's primary world interaction mechanisms, there may be situations where a user does not want his gestures to be interpreted. Similarly, a user may direct his gestures toward different targets. To accommodate these requirements, we represent the gesture recognition engine as a Mealy finite state machine, with glove data driving both transitions and outputs. Glove data is monitored for transition events, and then transformed into an output value appropriate for the device. We envision a future system in which there exists a hierarchy of states such that an initial gesture selects a device to control, and then subsequent gestures navigate the state space for a given device. In our testbed, we have only one controllable device with one interpretation of glove data; thus, we have the two states illustrated in Figure 1. This single interpretation is a “direct-drive” state; the user's hand movements are directly interpreted into motion of the target. In more advanced control layouts, this direct drive state would be a child state of a general device selection state. For our purposes, this representation is appropriate for our prototype.

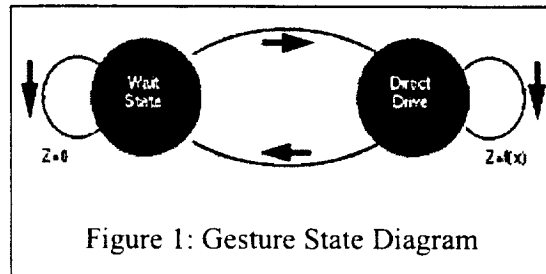


Figure 1: Gesture State Diagram

Penn State Mars Society – RASC-AL 2002, “Modular Research Rover and Gesture Control System for EVA”

If any device output is necessary, the gesture engine passes a request off to an appropriate output processing thread for the device at hand. Since both of our devices are locomotion devices, we have only one output thread. Depending on the capabilities of the controlled devices, different formats are supported. For our prototype device, we chose a basic serial format that can accommodate translational and rotational movement commands.

To facilitate the independent development of software from the underlying hardware, we opted to use a network robot hardware simulator. Called “Player/Stage”, this simulator is designed to allow a controller to be developed under simulation, and then use the same binary code on the real hardware. One of our group members is employed at a mobile robotics laboratory on campus, and his managers have graciously allowed us to test the gesture control system on real robots. These robots are ActivMedia Pioneer 2-AT class devices; one under glove control is pictured in Figure 2. This image is a clip from a movie that shows the range of motion of the glove control system; the rover is put through a series of maneuvers combining forward and reverse rotational and translational movement.

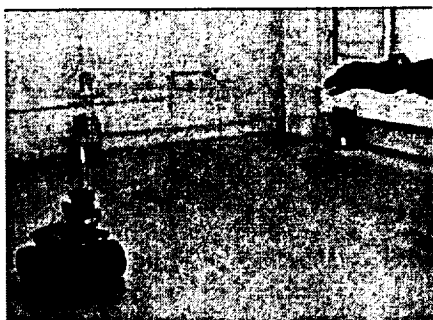


Figure 2: Pioneer Robot and Glove

For obvious reasons it is desirable to have a functional platform on which to display the glove input technology, especially one small and portable. With this desire in mind, we have interfaced the glove control with a standard rc car. These simple toys are not only effective visual tools, but at the same time are very easy to interface with. For simplicity we connected a microcontroller directly to the remote unit, allowing us to use the already existing wireless components. The four output pins used by the microcontroller are connected to the four different contacts in the remote; forward, reverse, left and right. In addition to providing us with a valuable demonstration tool, it also served as a solid instruction tool for newer members in dealing with

microcontrollers and interfacing with different inputs and outputs.

Rover Prototype

During the spring of 2002, the Penn State Mars Society built a rover prototype in order to become familiar with basic construction techniques and learn likely issues that would be encountered when building the actual rover. The other benefit from the prototype construction was to gain experience in group design work and also learn what parts were available for purchase, which turned out to be a substantial limiting factor on the design. Many problems arose during the prototype construction that were not anticipated in the design stages; thus construction of a prototype proved valuable in bringing these problems to the forefront and allowed for design modifications to the next rover in order to eliminate these problems, which are outlined in Table 1.

Problem	Action
Bolted construction - joints of very poor quality, rover lacked sufficient stiffness, joints were not square, and poor craftsmanship	Welded construction will be used on future designs
Wheel struts were extremely weak	Struts will be eliminated, dramatically increasing strength
Wheels did not allow for traversing major obstacles	Treads will be used on future designs
Round axles were difficult to epoxy to wheels	Axles will be welded to wheels

Table 1, Lessons Learned

The basic design of the rover was chosen to meet short time deadlines and to be cost effective. The design consisted of a box constructed out of aluminum square stock. Because no member of the team was proficient in welding at that time, the box had to be bolted together using aluminum angles to fasten each corner. Aluminum struts were bent into an upside-down U shape then bolted on the base of the rover to serve as the holders for the wheels and motors. Wheels were used because they are cheap and simple to attach, as opposed to treads which the next design will eventually employ. A box style frame was chosen because of the ease of construction and to mimic the storage capacity of the future rover. Constructing the rover prototype proved to be a very valuable experience and will allow future rovers to be

Penn State Mars Society – RASC-AL 2002, “Modular Research Rover and Gesture Control System for EVA”

better designed as well as significantly easier to build.

4.2 Product Design for Future Work Gloves and Gesture Control System Gloves Overview

As described above, we are currently using five sensor Data Gloves developed by 5DT (Fifth Dimension Technologies), on loan from the Computer Science and Engineering Department at Pennsylvania State University which measures finger flexure (one sensor per finger) and the orientation (pitch and roll) of the user’s hand. However, gloves that contain additional sensors can allow for greater customization in regard to commands that may be created for instructing the rover. 5DT’s fourteen sensor gloves not only measure finger flexure with two sensors per finger, and hand orientation; they can also measure the degree of abduction between the fingers, allowing for even greater expandability of the command processes, accounting for an analysis of finger-finger interactions. Furthermore, the gloves that 5DT develops are also offered in wireless models. This becomes very convenient for the astronaut. For example, it would decrease the need to lug a laptop on his/her back. The commands can be sent directly to the rover, from the gloves, where all the processing of those commands can be performed on the rover’s onboard computer.

Immersion, another major producer, offers a very impressive line of gloves. Branded “CyberGlove,” they are offered in eighteen and twenty-two sensor models, and they can perform every function that 5DT’s Data Gloves can, and can measure additional movements, such as thumb crossover, palm arch, wrist flexion, and wrist abduction. The only difference between the eighteen and twenty-two sensor gloves is that the twenty-two sensor gloves contain three sensors to measure finger flexion instead of two, one sensor per each joint on the finger. Unfortunately, they do not offer wireless transmission of the commands. This leaves virtually no possibility of free movement without an accompanying backpack computer. All data transfer is done through a single cable that can be bought in ten foot or twenty-five foot lengths. However, to the degree that these gloves can measure hand movement, the number of commands that can be programmed is virtually limitless, thus offering optimal convenience in that regard.

With all of the impressive gloves on the market, there become natural trade-offs with the level of accuracy in modeling desires versus cost. As alluded to previously, there is a natural point at which

accuracy in hand modeling becomes irrelevant as it surpasses the ability of a human to control his own hand. The gloves above which measure different types of hand movements, as opposed to adding accuracy, are probably the most desirable.

At this point it would seem prudent to discuss the field practicality of our glove control system. As noted previously, the gloves are hard wired to the serial input on a computer. This limitation is one that we are facing due to the model of gloves that we have been provided. Although wireless gloves are commercially available; they are naturally more expensive. Despite the need for the gloves to be physically connected to a computer, this does not limit their application to a laboratory setting. Our implementation of this control system will eventually entail a small, lightweight laptop that can be worn in a backpack. The glove-end laptop will communicate to the rover via wireless Ethernet. By connecting through the laptop, the range of the gloves would be drastically improved, due to the nature of the two different styles of communications systems. This modification will allow us to effectively simulate a wireless glove control system.

Gesture Recognition Control Expansion

In our current prototype, there are many more degrees of freedom in the controller than the device. Since one of the future goals of the project is to have glove control over several devices, we expect to take advantage of the excess freedom. However, a complicated control system will lead to human confusion and error. To make the gesture language easier to learn and apply, we will be adding a second glove to the system. In this extension, a gesture state transition can use one or both gloves for data input.

The use of two hands will make a system easier to interact with, but also raises the concern that a user will not be able to carry or hold anything while performing a two-handed gesture. In response to this issue, a complete backup gesture system could be implemented such that no command is impossible to perform without two fully functional gloves. The two-handed state transition could serve merely as a convenient shortcut to the same destination state as a series of single-handed transitions.

To experiment with two-handed control, a rudimentary case in which the second glove controls an independent device has been implemented. This independent device is the gripper/lift combination on the front of the Pioneer robots; this device is only used to test out the capabilities of the gesture recognition system while our final project is under construction.

In the discussion regarding the hardware system of the virtual reality glove hardware, it was noted that

Penn State Mars Society – RASC-AL 2002, “Modular Research Rover and Gesture Control System for EVA”

each glove requires a serial port for communications. With our available computer resources, we were unable to run both gloves using the same host; the solution to this problem came through the previously mentioned Player robot server. Since both glove-host machines were on the same network as the robot, each could control its device independently. The point of this extension was to show that the same binary code could interpret gestures independently, as opposed to having a left-hand controller and a right-hand controller.

Although this scheme works as a proof of concept, we expect to use a host that is capable of driving both gloves simultaneously. The use of a robot server does point out a possible source of redundancy; if the gesture-based primary control system were to fail in the field, less efficient but functional alternatives could be engaged to complete the mission.

Our approach is extensible in terms of the gesture control hierarchy; one need only define an entrance transition, an optional output as a function of the current state and current inputs, and an optional exit transition. We have chosen a simple initial model to serve as a proof of concept for a more complex control system; since the device to be controlled is a simple model, a simple controller will suffice. As we expand the function of our rover device, states may be added to the controller to control these additional hardware capabilities.

We expect that new devices to be added will conform to one of a few standard controllable classes of devices. Dividing the devices into such categories as actuators, locomotion, or sensors will allow a generic implementation of both computer code and gesture language. The upshot is that any locomotor base can be controlled by the same gestures, assuming that an appropriate hardware interface has been developed to the standard specifications. In this fashion, a gesture control system is not limited to a single robotic platform; such a limitation would be very inconvenient from a user's perspective in terms of training, storage and maintenance. By abstracting out device specifics, we can integrate a wide variety of peripheral devices without having to change the standard gesture engine. We refer to this prospect as a “universal language”, since the user need not be concerned with the physical characteristics of the device.

Every device that is to be controlled by the gesture recognition system may have one or more operating modes. For example, a sensor will have two modes: data output and configuration input. To accommodate these different operations, one can simply add states into the device hierarchy for each possible mode of operation, defining the same three

characteristics: entrance transition, output, and exit transition. This construction is evident in our very simple state diagram referred to earlier in the paper; there are two operating points for the rover: direct control and off. We envision a third point: autonomous operations.

To add an autonomous controller to the gesture engine, we must augment the state hierarchy. First, we must add a state where the position device is selected, but no outputs are modified. The purpose of this state is to allow a user to choose a device with which to interact. The second additional state is a configuration state that permits a user to select an autonomous action, to be activated on exit. In setting up the transitions, we note that a direct control state should override the autonomous action; this contention should be addressed in the output routines. The fundamental idea is that the gesture engine could allow a manual intervention, resuming autonomy when the user has moved on to another task. This addition is straightforward when considered in the context of our described framework.

Previously, it was mentioned that a group member works at a mobile robotics laboratory. This laboratory is the Applied Research Laboratory at Penn State; the laboratory performs contract research within the areas of interest of its research fellows. In the process of developing the gesture control system, our member's manager has taken an interest in further developing some of the control strategies described within as applicable to Discrete Event Control systems and robotic autonomy. In addition to rover robots, there is shared interest in six degree of freedom controllers for robotic vehicles such as submarines and dirigibles. We look forward to developing our system in conjunction with the Applied Research Lab's support.

Rover Design Size

The first design decision that had to be made once the purpose of the rover was defined was its size. The key considerations were payload size, usefulness in the field, cost, and ease of construction. Some of these considerations pointed to different sizes, so compromise was necessary. A small rover is most useful when accompanying a person because it can navigate small crevasse and caves which would not permit human investigation. If the rover is operating away from humans, a large size would be more useful because that would allow it to collect more samples and travel faster and farther. Obstacles would also prove less difficult to avoid with a larger rover.

The largest factor in determining the size of the rover being constructed is the payload it is going to

Penn State Mars Society – RASC-AL 2002, “Modular Research Rover and Gesture Control System for EVA”

carry. In order to have reasonable usefulness, it must carry an on-board computer. This became the largest size constraint because a laptop was chosen based on low cost and easy availability. The rover also had to carry motors and a battery, which occupy a large portion of the volume of the vehicle. There are many additional components which take up a small amount of space, but did not dictate the design of the rover. In order to accommodate a laptop and have sufficiently powerful motors to travel at a desired speed, a minimum size became apparent.

The rover under construction is 24" long, 16" wide and the main compartment is 10" high. This compartment will sit about 8" off the ground suspended by shock absorbers on a bottom plate containing the motors and axles. The wheels chosen will be 10" in diameter. See figure 3 for an overview of the rover design.

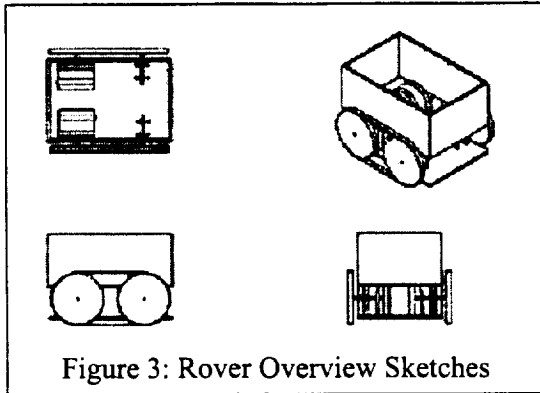


Figure 3: Rover Overview Sketches

While choosing a laptop as the computing payload determined the size, there were several other reasons this size was the best choice. Constructing a much smaller rover would have been very difficult because parts would have to be machined to more stringent tolerances and assembly would have required more precision. In addition, the electronic components small enough to fit on a smaller rover are very expensive. If the rover was much larger, components such as the frame, battery and motors would become very expensive as the design approached the size of an ATV.

Locomotion

Perhaps one of the most crucial aspects of the rover, selection of motors and design of the drive system has proven to be a challenge. Design problems in these areas include matching motor power consumption ratings with available batteries, selecting motors with enough torque and appropriate revolution rates, and weighing the respective merits of treads versus wheels.

For the rover under construction, the electric motor must have sufficient power to propel an 80 lb (with $g=32.2\text{ft/s}^2$) rover, which is the proposed weight. We have preliminarily estimated the necessity of a 1/8 horsepower minimum output to obtain the speed desired. Additionally, the need for a gearbox to reduce the shaft revolutions and boost torque is obvious. Given the time and resource constraints of our project, a motor with a combined, pre-built gearbox would be highly desirable. However, most 1/8 horsepower motors with attached gearboxes operate on 90V, in contrast to our desired 12V based on typical battery output.

The question of wheels versus treads has been quite difficult to solve. The advantage to treads is improved operation on rugged terrain, but it comes at a cost of reduced motor efficiency and greater difficulty in construction. Because tracks would be more useful in the field, the decision was made to include tracks in the final design. However, anticipated difficulties in construction have led us to decide to build the rover which wheels which could be converted to tracks at a future time. This will keep the track option available while allowing the rover to be constructed to a working state more quickly.

Suspension

Suspension is an important aspect of any mechanical vehicle or rover because of vibrations and obstacles that will be encountered. The amount of external interference depends a great deal on the type of terrain the rover is designed to scale. Obstacles must be anticipated for the rover, along with normal vibrations from small irregularities in the ground. The suspension on the rover is also necessary because of internal vibrations from the motor. These vibrations and other obstacles make suspension necessary because of their effect on the solid structure of the rover as well as the equipment on it. Vibrations affect the structure of the rover because they can loosen bolts and other connections. The primary concern is weakening of welded joints, although this is less of a concern that the loosening of bolts as occurred in the prototype. Vibrations have a negative affect on the equipment on board, such as computers, modules, and electrical wiring, as well. Any wiring has a chance of coming loose while undergoing vibrations and electronics can be damaged if shaken too hard.

For these reasons the decision was made to develop a suspensions system for our rover. The motors and wheels will be mounted to a separate base level, which will be attached to the main frame of the rover by shock absorbers. This base level is the only part of the rover directly exposed to the main causes

Penn State Mars Society – RASC-AL 2002, “Modular Research Rover and Gesture Control System for EVA”

of vibration: that caused by the ground upon the wheels and that caused by the motors. By this design, the vibration will not directly affect the rest of the rover. Two shock absorbers, each measuring approximately four inches long, will connect each corner of the base level to the equipment bay. The pin joints attaching them to the frame will be offset so that the each one of a corner pair will allow for small movement in the direction perpendicular to the other, as shown in figure 4. This will account for motion other than that which is directed up and down. To provide additional stiffness in the forward/backward, left/right directions, tubes will be attached to the base level that fit into holes drilled in the equipment bay, allowing for unrestrained up/down motion, but restrict motion in the other four directions.

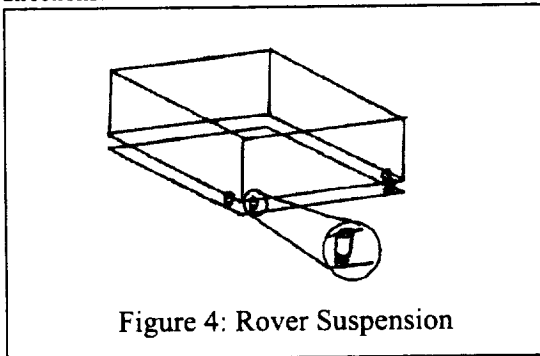


Figure 4: Rover Suspension

On Board Computing/Electronics

When looking into the on board computing requirements, there are two main directions to take. The first follows along with most commercial rovers, and involves single board computers, also referred to as PC104. PC 104 is highly powerful, versatile and expandable, which is why it is preferred in most applications of this nature. However, all of its benefits result in it having a very large price tag. For that reason, we have elected to utilize our second option, a laptop computer. Despite being bulky in comparison to PC104 they are much more readily attainable, and consequently much more cost effective. Having an on board laptop provides the rover with an extreme amount of flexibility, not only due to the computing power, but because of the peripheral support as well.

When considering the rover as a fully functional mobile laboratory for an astronaut working in the field, the laptop's display will also be a valuable tool. While the primary operation of the rover will not necessitate an interactive display, more advanced options will. For example, any data analysis, or complex operation of the rover will be able to be controlled through menus and other similar visual working environments.

Microcontrollers will need to be used to interface the laptop to a large majority of the on board hardware, including motors and sensors. During initial construction stages we will be using the Parallax Basic Stamp 2. This microcontroller is very simple compared to most devices of its kind. The Stamp 2 itself has 16 I/O pins plus 2 additional serial pins with which to communicate to the main rover processor. The stamp can store approximately 500-600 instructions within its on chip EEPROM, and can process these instructions at about 4,000 instructions per second. The stamp is programmed in PBasic, which is a slight variation of Basic programming language. This will be used in the prototype because of its simplicity. It is capable of handling all of the processes which will be used on the prototype and debugging any errors will be much easier to do. For the final design, the Stamp 2 will be replaced with a Motorola HC711E9 microcontroller, henceforth referred to as the HC11. This device is a much more robust controller than the Stamp 2. It is programmed in assembly language, allowing for much more user defined programming. The chip has 512 bytes of on-chip ram and EEPROM, as well as 12Kbytes of EPROM. It is also capable of running at higher speeds, which can be set by the user, than the Stamp 2, and has more than twice the I/O pin count due to having several ports. An additional component included is an 8-bit A/D converter. This microcontroller will be used on the final design because of its robustness and superiority to the Basic Stamp 2.

The on board computing resources will also allow us to do work with stereo vision. Two firewire cameras will be connected to the laptop, and can be used for a variety of autonomous navigation tasks. More basic tasks will allow the rover to keep track of where its operator is in the immediate region. Further work with this area can also be used for hazard detection and avoidance. This will be used directly in fully autonomous operation, as well as in direct drive state. The rover will have the ability to override a user's input if the operation (i.e. drive off of a cliff that the user cannot see) is deemed inadvisable.

Modularity

An issue being addressed in this rover design is long term usefulness and flexibility. Extremely specialized rovers are the most logical solution when sending single unmanned missions that will only last a period of weeks or months. When humans travel to Mars, they will most likely take numerous rovers with them, as well as spare parts to keep them running for a long time. With this being the case, it makes sense to get as much usefulness out of each

Penn State Mars Society – RASC-AL 2002, “Modular Research Rover and Gesture Control System for EVA”

rover as possible. The balance between specialization for a specific goal and long term usefulness leads to one conclusion.

Rovers that are sent to Mars on a human expedition will almost certainly be modular. This will allow the rovers to serve several purposes through the duration of the mission. The idea is that a rover chassis can be built to accept payloads with standardized connectors and control implementations, as shown in figure 5. The modular system will consist of a bay in the top of the rover into which scientific instruments will dock. There will be a connection for power, data transfer to the rover computer, and mechanical connections to latch it in place. Simply by plugging in the module and connecting the latches, the new module will be ready to use. The rover chassis will provide every module with locomotion, communication back to the astronaut and habitat, and a computer to process the data collected by the module.

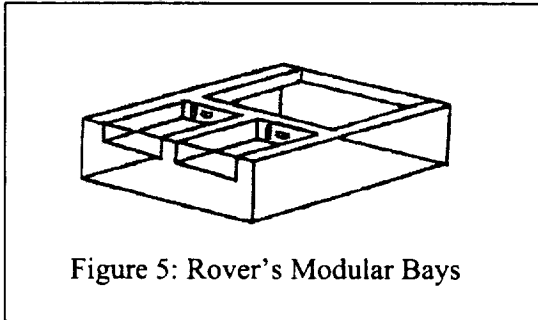


Figure 5: Rover's Modular Bays

This modularity allows for more types of science packages than there are rovers, increasing the mission capability at a lower cost than specialized rovers. Redundancy is also increased, because a failure will most likely take place on the rover chassis and not the module, due to the complexity of the drive system and the harsh Martian environment. If the chassis fails, the module can be placed in another rover with no loss of functionality.

The key to modularity is a set of standards which all electronic equipment will operate on. While this is not a new idea, it has not been widely put into practice. The need to adopt a standard is clear considering the time required to rewrite drivers and software to transfer hardware from one rover to another. One member of the Penn State Mars Society experienced this hassle while working at NASA Ames when he saw many hours spent transferring a camera designed for one rover to another. While this leads to wasted time on Earth, astronauts will not necessarily have the luxury of time to reprogram equipment. This could lead to equipment lying dormant if there is a problem on the rover carrying it. When everything costs tens of thousands of dollars per pound to deliver it to the Martian surface, this

will not be tolerable. The benefits will naturally carry over to Earth, reducing the time it takes to make hardware for one rover work with another.

Implementing modularity first requires a rover, so construction of modules is on hold until the rover is at a sufficient state of completion to allow for the use of modules. The eventual goal of this implementation of modularity is to demonstrate the simplicity of the changing modules with such a system as well as providing further features for the gesture recognition system control. The exact modules have not been decided on yet, but will likely include advanced video equipment and rangefinders. The actual modules used on Mars would naturally include packages used to study meteorological conditions, take samples of soil and rocks, and perform basic field analysis of them. Other possibilities include construction equipment such as a bulldozer blade or a crane.

5. Future Studies & Testing

Project Timeframe & Possible Extensions

By the end of 2002 designs will be finalized for the rover base, as well as plans for extensions of the glove control system. Construction will begin early in 2003 and will focus primarily on the rover base. A fully functioning mobile base, complete with on-board computing systems will be running by May of that year. In addition, this stage will see basic stereo vision applications implemented. This includes simple tasks such as locating, and driving to, an astronaut in the field. Glove control will also be expanded to a two-glove input system that will begin to allow us increased flexibility in the control of the rover. Over the course of the 2003-2004 academic year the rover base will be completely finalized and fine-tuned, and we will begin to develop different modules that can be used in field tests.

Field Testing

Once the mobile rover base has been completed, we will begin with very basic field tests. By analyzing its response to different situations and testing environments we may gain added insight that can be applied towards latter systems on the rover, including the individual modules. As we develop the rover and glove control system into a fully mature state field testing will obviously become a very logical step in this project. Because the focus of this project isn't so much the actual technology as it is the implementation of that technology, most of the knowledge to be gained will come from these experiments. An ideal testing situation would be at The Mars Society's Mars Desert Research Station

Penn State Mars Society – RASC-AL 2002, “Modular Research Rover and Gesture Control System for EVA”

(MDRS) in southern Utah. At MDRS, Mars Society members conduct studies in manned Mars missions from an operations standpoint. More specifically, they look at many of the human factors of a manned Mars mission, including how work will be performed. The Mars Society has expressed a strong interest in local chapters testing their work at the station, and we feel that this would be an ideal situation and a beneficial partnership.

6. Conclusion

Because this project has been built with modularity in mind, there are inevitably countless extensions which could easily be explored and implemented. The stereo vision system can be expanded to perform more advanced autonomous navigation tasks. This includes hazard detection and obstacle avoidance, two very crucial abilities. Beyond even the rover we will have built, we can begin to explore team robotics to tackle even more varied situations. One such example would be a separate module which serves simply to deploy a microrover. Microrovers would be designed for the sole purpose of going where a larger rover simply cannot access. Since the glove control system is designed as a universal language, controlling an entire team of rovers would be a natural extension of the basic command language. While a plethora of possibilities exist, this outlines just a few of the possible extensions for this project.

7. References

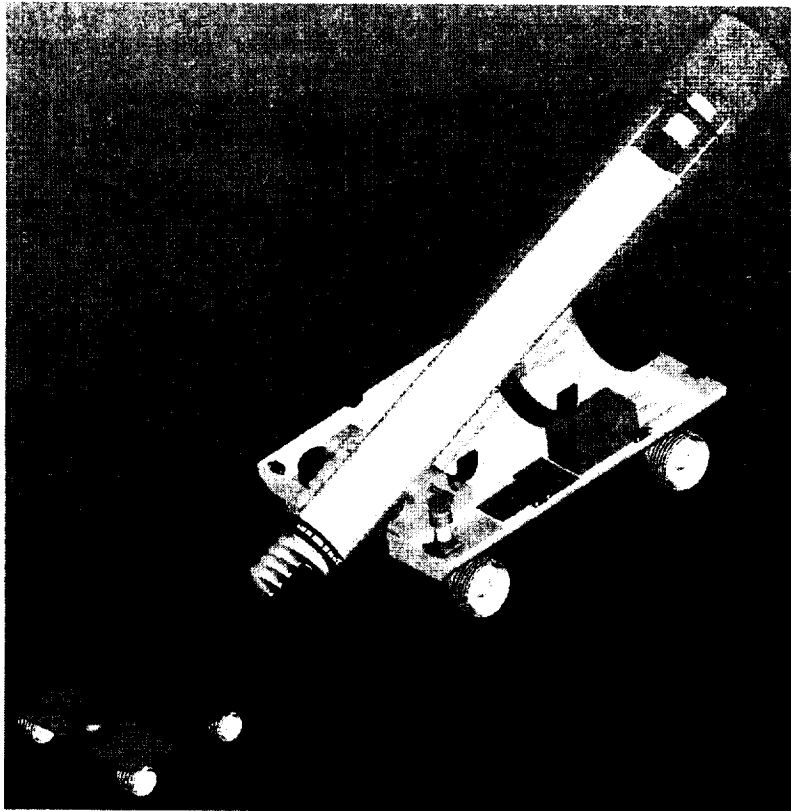
- [1] Brian P. Gerkey, Richard T. Vaughan, Kasper Støy, Andrew Howard, Gaurav S. Sukhatme, and Maja J. Mataric; "Most Valuable Player: A Robot Device Server for Distributed Control;" *Proceedings of the IEEE/RSJ International Conference on Intelligent Robots and Systems (IROS 2001)*, pages 1226-1231, Wailea, Hawaii, October 29 - November 3, 2001.
- [2] The Mars Society; "The Mars Society: Mars Desert Research Station;" <http://www.marsociety.org/mdrs/index.asp>
- [3] Stephen McGuire, Joel Richter, Kevin Sloan; "A Modular Multi-Function Rover and Control System for EVA;" October 2000.
- [4] Fifth Dimension Technologies; "Welcome to the Fifth Dimension;" <http://www.5dt.com>
- [5] Immersion Corporation; "Immersion Corporation – Welcome to the Immersion Web Site;" <http://www.immersion.com>
- [6] Parallax Inc.; "Parallax Inc. : BASIC Stamp Microcontrollers;" <http://www.parallaxinc.com>
- [7] Motorola Semiconductors Products Sector; "68HC11E9 Product Summary Page;" http://e-www.motorola.com/webapp/sps/site/prod_summary.jsp?code=68HC11E9&nodeId=01M98635
- [8] McMaster-Carr; "McMaster-Carr Supply Company;" <http://www.mcmaster.com>

8. Acknowledgements

We would like to thank our sponsors and supporting groups:

- The Pennsylvania Space Grant Consortium
- The Pennsylvania State University College of Engineering
- The Schreyer Honors College at the Pennsylvania State University
- The Department of Computer Science and Engineering at the Pennsylvania State University
- The Applied Research Laboratory at the Pennsylvania State University

Integrated Robotic Team for Martian Water Collection



Kristina Alemany¹, Kristen Bethke¹, Niraj Bhatt², Brent Bollman², and Jonathan Viventi²

Advisors: Professors Daniel Nosenchuck¹, Stephen Lyon², and Michael Littman¹

¹Department of Mechanical and Aerospace Engineering, Princeton University, Princeton NJ 08544

²Department of Electrical Engineering, Princeton University, Princeton NJ 08544

*2002 RASC-AL Student Design Competition
November 6-8, 2002
Cocoa Beach, FL*

Abstract

This paper is in response to a request for papers from the Lunar and Planetary Institute for the annual conference of its Revolutionary Aerospace Systems Concepts-Academic Linkage program. An integrated robotic team for the collection of subsurface Martian water ice was designed, based on the 2001 Mars Odyssey discovery of the signatures of a significant amount of water ice on Mars. Gamma-ray spectrometer readings indicate that in large regions near the Martian poles, the soil between 60 and 100 cm beneath the surface contains 40% to 73% water ice by volume. The extraction and transport of this water would enable human habitation and exploration on Mars because water can be consumed by humans and chemically transformed into hydrogen and oxygen fuel. This study adopted the philosophy that a team of small robots can perform this collection task more efficiently and more reliably than one large, multi-task robot.

A concept was designed for a team of small autonomous robots that traverse the Martian soil to detect, extract, and transport ice to a central holding and processing location. The team consists of drilling rovers that penetrate the Martian surface, collect frozen water and soil, and deliver this ice/soil mixture to quicker, less massive transporting rovers.

A top-level design of the entire robotic team was produced. For the drilling rover, initial specifications were determined for the structure, drive train, command and data handling, navigation, communication, and power subsystems. The water detection subsystem of the transporting rover was also given initial specifications. The robotic team's water collection method was then designed in more detail. The system consists of a 10 cm auger followed by a 100 cm collecting tube that drills to a depth of 100 cm and to collect all of the encountered dry and ice-rich soil. The system then transfers only the ice-rich mixture to a transporting robot, which delivers it to the processing plant. Engineering drawings were created for this water collection design and for the design of the drilling rover.

This preliminary design for Martian water collection calls for a team of 30 drilling robots and 10 transporting robots. The team has a total system mass of 700 kg and the capability of collecting 65000 kg of water in a 180-day water collection mission.

1. Introduction

1.1 Mars Odyssey Finds Water

Gamma-ray spectrometer readings from the 2001 Mars Odyssey spacecraft indicate that the top 1 meter of Martian soil is rich in hydrogen poleward of 60° south latitude and in areas poleward of 60° north latitude. This identification of hydrogen suggests the presence of large amounts of water ice in the top 1 meter of soil. The discovery that this hydrogen-rich layer corresponds to areas of predicted ice stability based on atmospheric and soil conditions strengthens the argument for the presence of ice. The ice is more highly concentrated in the lower portion of this top meter of soil, with a starting point that decreases in depth with increasing latitude, beginning at approximately 60 cm near 60° north and south latitudes. By weight, the ice constitutes $35 \pm 15\%$ of the subsurface material, which corresponds to a range of 40 to 73% ice by volume¹.

1.2 Implications of Water Discovery

These findings have a direct impact upon the possibility of human exploration of Mars. In 1997, the Mars Reference Mission was created by NASA to lay out a preliminary plan for the first human missions to Mars, as well as to outline the necessary technologies that must be developed to carry out such missions. Two of the main objectives of the Mars Exploration Program are to conduct: (1) "Human missions to Mars and verify a way that people can ultimately inhabit Mars" and (2) "Applied science research to use Mars resources to augment life-sustaining systems," also referred to as in situ resource utilization (ISRU). Additionally, there is a focus on relying on automation, especially with regards to ISRU systems, which must be operational even before humans leave Earth. NASA plans on using Mars' in situ resources mainly to produce propellant, which will fuel the astronaut's ascent vehicle used to return to orbit at the culmination of their mission. These resources will also be used to provide "fuel for surface transportation, reactants for fuel cells, and as backup caches of consumables for the life support systems." As of 1997, the plan was to use the Martian atmosphere for the production of these necessary elements, and to import hydrogen from Earth. However, "should sources of indigenous and readily available water be found, this system could be simplified." The presence of water ice is thus a significant discovery that will eliminate much of the need for transporting resources from Earth, thereby reducing launch mass and mission costs².

1.3 Concept for Integrated Robotic Team for Collection of Water

The Mars Reference Mission has also identified extraterrestrial mining techniques and resource extraction processes as two of the technology developments required to make human exploration feasible². This paper will address these technology needs by designing a system that will detect, extract, and transport the subsurface ice to a central holding location where it can be processed to create propellant and compounds for crew life support. This system will consist of an autonomous team of small robots that will traverse the Martian soil, extracting, collecting, and transporting the ice.

1.4 System Strategy

The unique aspects of this concept are its method for water collection and its focus on teamwork and distribution of tasks. A team of small robots is preferred to one large robot for several reasons. First, utilizing a team of small robots will enable mission costs to be reduced. Second, it will provide a more robust system by significantly reducing the impact of single-point failures. If multiple robots operate in parallel, then the failure of one individual robot will not cause the mission to fail. Furthermore, contingency can be factored into the system so that the water collection quota will be reached even if several robots fail. Third, a team of small robots has the advantage of being able to cover more surface area at one time than one large system. The area that one large robot can cover is limited to its rate of water extraction and movement. For a team of robots, however, this rate is multiplied by the number of robots, allowing for more water collection at the same time. The gamma-ray spectroscopy of Mars penetrated only 1 meter into the Martian soil, so the existence of water ice has only been confirmed down to 1 meter in depth. Because the depth of the extraction is limited, a team of robots that covers a large horizontal area will extract more water than a single system that can reach high vertical depths.

1.5 Design Focus

The focus of this design will be on the water collection system, since this is the new technology that makes the robot unique from other Mars rovers. The paper focuses on the requirements for the system as a whole, and the design iterations and final results for the water collection device. Because the other subsystems are driven by the design of the water collection system, they are currently in a preliminary design phase, and are briefly outlined in this paper.

2. Approach

To address the problem of subsurface frozen water collection via a team of small robots, it is necessary to follow a systems engineering approach. With this method, the objectives of the mission are established, and from these, the top-level requirements of the system are derived. Using the top-level requirements as guides, the actual design process begins. Iterations are carried out for each subsystem; possible methods for achieving the mission objectives are suggested, studied, and eliminated if requirements are not met. In the end, the design is based on the method that best meets the objectives and follows the requirements. Currently, the concept for the integrated robotic team is in the design iteration phase. The water collection subsystem has been through several iterations, but for each of the less revolutionary subsystems, only one or two designs have been studied.

2.1 Top-Level Requirements

According to this systems engineering approach, the first task is to define the objectives and top-level requirements of the robotic system. The essential functions of the system are mobility, water detection, water extraction, water transfer, and water transport. The ultimate goal is a system that improves upon the Mars Reference Mission while performing these functions to achieve the objectives of the Mars Exploration Program. Improvement on the Mars Reference Mission includes an increase in fault tolerance and lower mass, volume, and power consumption levels.

A review of NASA's most recent plans for Martian ISRU establishes a basis for comparison. The 1997 Reference Mission document outlines an ISRU plant concept that consists of two ISRU plants, together producing 23200 kg of water for crew members and 20200 kg of oxygen and 11600 kg of methane fuel for each Mars Ascent Vehicle (MAV). These ISRU plants are designed to produce enough fuel for two missions. Using gases from the Martian atmosphere and hydrogen transported from Earth, the plants combine the Sabatier, CO₂ electrolysis, and H₂O electrolysis processes to produce the methane and oxygen and water by-product. The combined mass of the plants is approximately 7100 kg, their total volume can be assumed to be on the order of 100m³, and their total required power is on the order of 100 kW². While it provides some detail about utilization of the resources of the Martian atmosphere, the Reference Mission document does not address any sort of transport of Martian regolith. NASA's 90-Day Lunar/Mars Study does, however, provide specifications for a mining excavator/loader vehicle, a hauler vehicle, and their power system. The combined mass of these vehicles exceeds 4500 kg, and their total volume is at least 36 cubic meters³. Considering together the atmospheric ISRU plants of the Reference Mission and the regolith movers of the 90-Day Study, NASA's current plans for Martian resource utilization involve a mass, m_{current} , of more than 11600 kg ($m_{\text{current}} \approx 7100 \text{ kg} + 4500 \text{ kg}$) and a volume of more than 100 m³.

Decreasing the mass and volume by a factor of eight would comprise a significant improvement on the current NASA Martian ISRU concept. A mass decrease would reduce the payload mass of the vehicle that transports the robotic system to Mars and would therefore reduce the fuel requirements and launch costs. According to this eight-fold decrease goal, the first system requirements are that the water collection team's total mass, m_{max} , remains under 1500 kg ($m_{\text{max}} \approx m_{\text{current}} / 8$) and its volume remains below 12 m³.

Based on the amount of methane and oxygen fuel required by the Reference Mission, it is reasonable to assume that 5000 kg of liquid hydrogen will be needed to ascend to Martian orbit. To produce 5000 kg liquid hydrogen, 45000 kg of water are needed. The 23200 kg of water required by the Reference Mission for crew life support system caches also still must be collected. Accordingly, the next requirement is that the robotic team delivers 68200 kg during the mission's timeframe, which was set at 180 days. Such a delivery requirement dictates a delivery rate of approximately 15 kg of water per hour, based on a continuously operating system.

Table 2.1 Mission Objectives for Integrated Robotic Team for Martian Subsurface Water Collection

Essential Functions	Other Objectives
<ul style="list-style-type: none"> - Mobility - Water detection - Water extraction - Water transfer - Water transport 	<ul style="list-style-type: none"> - Achieve objectives of Mars Exploration Program - Improve on Mars Design Reference Mission

Table 2.2 Top-Level Requirements for Integrated Robotic Team for Martian Subsurface Water Collection

Metric	Requirement
Mass	< 1500 kg total
Volume	< 12.5 m ³ total
Water Delivery	(68200 kg in 180 days) + 100% Contingency \approx 30 kg/hour

2.2 Mission and Environmental Assumptions

In addition to the top-level system requirements that have been defined, there are certain mission and environmental assumptions that must be made in order to begin the design of the robotic system. These assumptions are listed in Table 2.3.

Table 2.3 Assumptions for Martian Environment for Martian Water Collection Mission

Issue	Assumption
Landing Site	60°N, 240°E ($\pm 5^\circ$)
Elevation	3000 m below sea level ⁴
Composition of Ice Layer	40% to 73% ice by volume
Depth of Ice Layer	60 cm to 100 cm
Water Collection Area	85 m x 85 m
Temperature	-75° C to 0° C
Air Pressure	6.55 mb to 6.85 mb
Wind	Less than 10 m/s with frequent afternoon dust storms
Gravity	3.7 m/s ²
Dry Soil Grain Size	0.1 μ m to 1500 μ m
Dry Soil Density	1.2 \pm 0.2 g/cm ³ to 1.6 \pm 0.4 g/cm ³

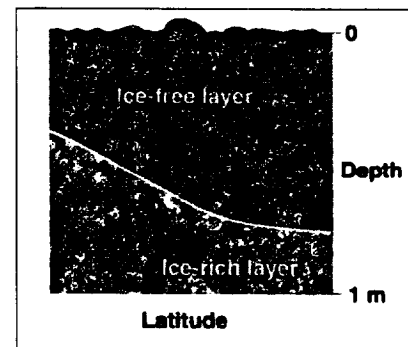


Figure 2.1: Martian Subsurface Model Resulting from Mars Odyssey Findings⁵

The landing site was chosen in the Northern hemisphere because of the less rocky and mountainous terrain that it affords, facilitating landing and mobility for the robotic team. The latitude value of 60° N was selected because at higher latitudes, the presence of a seasonal carbon dioxide cap would hinder water detection and collection, and at lower latitudes, the concentration of ice decreases⁶. The longitude value of 240° E was chosen because it lies in the region that is closest in elevation to the landing sites of Viking (1976) and Pathfinder (1997). At these landing sites, the air pressure was above the triple-point of water, which is necessary for liquid water to be sustained without artificial pressurization. Additionally, this landing site corresponds to one of the areas where Mars Odyssey findings predict the presence of subsurface ice¹. From these findings, it can be assumed that at the chosen landing site, frozen water comprises 40 to 73% of the soil, by volume, at depths between 60 and 100 cm. At this depth, the soil temperature does not exceed -73° C⁶. The composition of the subsurface regolith is not homogeneous; therefore, the robotic system will seek out areas to extract water that are greater than 50% ice by volume, in order to maximize the efficiency of the system. In order to extract 65000 kg of water, an extraction area of 85 m by 85 m is needed. This calculation assumes a 50% efficiency in extracting ice from the subsurface, and it assumes that only 10% of this area is tapped for water. This 10% value was chosen because the percentage of the subsurface that exceeds 50% ice by volume is unknown and because mobility would be hindered if the entire collection area were littered with craters.

The environmental conditions that the robotic system will experience are based upon measurements taken by previous robotic missions. The air pressure and temperature ranges are based upon those experienced by Pathfinder⁷, which landed at 19.13° N latitude and 326.78° E longitude. Although temperatures above 0° C are relatively common during summer afternoons, they only last for a few hours. Winds are generally less than 10 m/s, but afternoon dust storms are fairly common. The surface soil conditions were analyzed by Pathfinder and the Viking landers, and because they were similar, it has been assumed that the soil in the Northern hemisphere is uniform in all locations¹. The near-surface regolith contains a mixture of soil that is relatively coarse-grained and mostly igneous in origin and soil that is mostly fine-grained and dominated by some mixture of palagonite and

clays⁶. Based on JSC Mars-1 (Mars simulated soil)⁸, the grain size ranges from 0.1 to 1500 μm , and its density ranges from $1.2 \pm 0.2 \text{ g/cm}^3$ to $1.6 \pm 0.4 \text{ g/cm}^3$. The water collection area has a top layer of dry dust strewn with boulders. The near surface soil is generally dry, but may have from a few tenths to a few percent of chemically bound water⁶. Because no rover has analyzed the composition or nature of the soil below the surface, it is assumed that the soil is uniform in the top 60 cm, and the soil that is mixed with the ice layer is also similar in composition to the surface layer.

An additional assumption was made concerning the existing space system architecture at Mars. It is assumed that by 2025, the projected time frame of this mission, a constellation of global positioning system (GPS) satellites will be in orbit around Mars⁹. Thus, any GPS-equipped vehicle on the surface of Mars can receive signals from these satellites to ascertain its position on the Martian surface.

3. Results

With all of the requirements determined, designs for the robotic team can be considered. Because the water collection system is the unique function of the robot, its design is studied first and used to drive the design of the remainder of the robot. The design that resulted from this study consists of a team of drilling rovers that penetrates the Martian surface, collects frozen water and soil, and delivers this ice/soil mixture to quicker, less massive transporting rovers. Upon choosing this water collection system, the rest of the robots' structure and functionalities can be designed. In the following sections are the specifications for each subsystem of the robotic team. The general strategy of the robotic team is outlined first. The physical subsystems are then described, beginning with the water collection system. The rationale behind the design of the water collection system is given in detail.

3.1 Teamwork and Strategy Subsystem

The chosen method for water collection requires a team of drilling rovers that is capable of extracting 30 kg of ice every hour (see Table 2.2). To obtain 30 kg of ice, the team must collect 65000 cm^3 of ice/soil mixture. This required volume, V , of ice/soil is calculated with ρ , the density of ice; C , the composition of the mixture; and m , the required mass of ice:

$$V = \frac{m}{\rho C} = \frac{30000 \text{ g}}{(0.931 \frac{\text{g}}{\text{cm}^3})(50\%)} = 64445 \text{ cm}^3 \approx 65000 \text{ cm}^3. \quad (3.1)$$

This design assumes that the driller rover can efficiently collect ice/soil from 30 cm of the 40 cm-deep ice-rich layer. With an auger diameter of 10 cm and a collection height of 30 cm, 30 driller rovers are needed to collect 65000 cm^3 of ice/soil mixture, assuming that each robot performs one cycle per hour. The number of drills, N , is calculated with V ; d , the auger diameter; and h , the height of the ice/soil mixture:

$$N_{\text{drill}} = \frac{4V}{\pi d^2 h} = 27 \approx 30. \quad (3.2)$$

Transport rovers complete the job that these 30 driller rovers begin. The transport rovers simply receive the ice/soil mixture from the bottom section of the driller's collection tube and deliver it to the central processing station. Figure 3.1 illustrates this cooperation between the driller and transport rovers. It is reasonable to assume that the transporter's delivery of material will occur at a rate 3 times faster than the driller's extraction; consequently, 3 times fewer transport rovers than driller rovers are needed. Assuming this 3-fold relation between operating rates, 3 driller rovers are serviced by every 1 transport rover. The required volume of the transporter's holding tank, $V_{\text{transport}}$ is then:

$$V_{\text{transport}} = 3 \times \frac{V}{N_{\text{drill}}} = 3 \times \frac{65000 \text{ cm}^3}{30} = 6500 \text{ cm}^3. \quad (3.3)$$

The linear dimensions of the transporter robot can then be on the order of $(6500 \text{ cm}^3)^{1/3}$, or 19 cm x 19 cm x 19 cm.

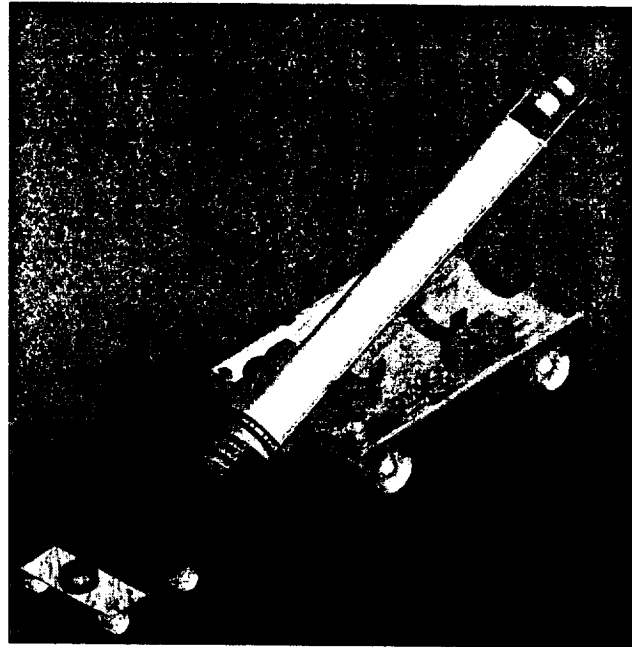


Figure 3.1 Cooperation of Driller and Transport Rovers for Martian Subsurface Water Collection

3.2 Water Collection Subsystem

As water collection is the team's unique function, design efforts were concentrated on the water collection system. An extensive iterative process was followed, and several possible designs emerged as the key design issues were explored. This section explains the design options that were considered and presents the final specifications that resulted from the iterative design process.

3.2.1 Water Collection Design Iterations

Figure 3.2 outlines the design iteration process that was followed for the water collection system. The figure shows each design problem that arose, the possible solutions to each problem, and the methods considered for implementing each system. The chosen solution for each problem is shaded, and arrows point to the subsequent decision.

3.2.2 Explanation of Water Collection Decisions

The final design was chosen to minimize both the complexity of the system and the amount of power required by the system. Complexity can be reduced by limiting the number of moving parts and mechanical systems, which is critical in a system that must function autonomously and without the ability to make repairs. Additionally, low complexity decreases the chances of fatigue failure, which is an important consideration for a system that is required to run continuously for 180 days.

3.2.2.1 Removal of Dry Soil Layer

To access the ice beneath the top layer of dry soil, two solutions were considered: (1) exposing an entire region of the ice layer by clearing away large portions of the top layer of soil or (2) penetrating through the top layer of dry soil each time a section of ice is extracted. The latter option was chosen because of the difficulty of clearing away large areas of dry soil. The main difficulty arises from the soil's lack of stability. The frequent dust storms on the Martian surface also pose the danger of filling in the quarries with dust and burying the robots. As a result, the optimal design consists of each robot independently drilling through the top layer of dry soil each time it removes a section of ice.

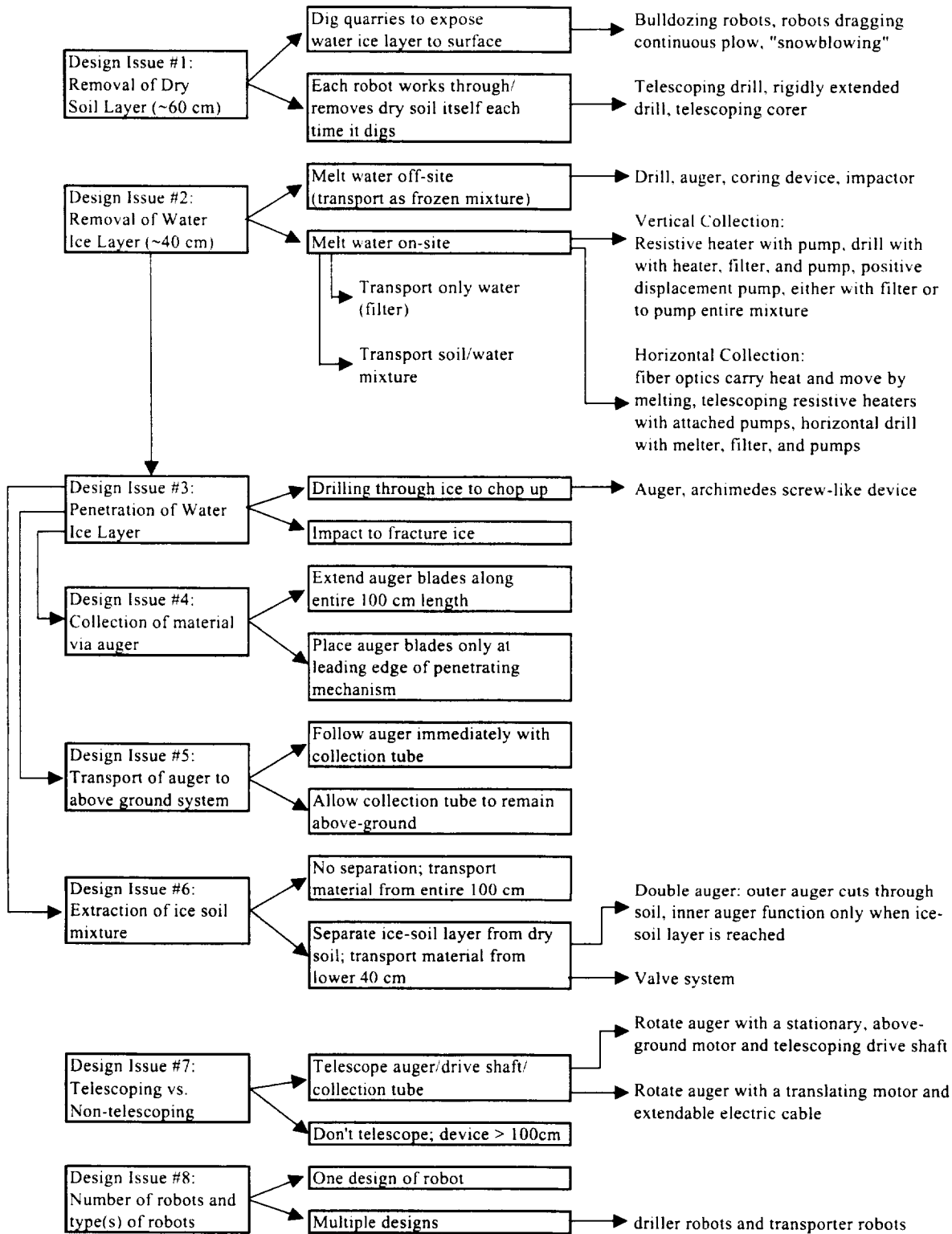


Figure 3.2 Design Issues, Solutions, Implementations, and Decisions in Determining a Method for Martian Water Collection

3.2.2.2 Removal of Water Ice Layer

To extract the ice, there were also two general solutions: (1) melting the ice on-site or (2) melting the ice off-site. The advantages to having each robot melt its own water included carrying less material back to the central location and reducing using only heating elements rather than moving parts. Several problems arose from this design, however. First, a heating element alone would not be sufficient; a drill-like device would still be necessary because the composition of the ice-rich layer is up to 50% soil by volume. Next, separation of the water from the soil would require a filter, which would have a high likelihood of clogging because of the small particle size of the soil, as small as 0.1 microns. Such small particles tend to settle very slowly, and typically have Reynolds numbers less than one. These flows are generally dominated by viscous effects, and Stokes showed that the velocity of a one micron particle is approximately equal to:

$$V_p = \frac{2\rho g R^2}{p\mu} \approx 0.15 \text{ mm/s} \quad (3.4)$$

Due to Stokes drag, the smallest particles encountered by the filter would travel much slower than the rest of the flow, causing the filter to clog. Because of this problem, it would have been necessary to carry back at least some of the soil. Third, the containment of liquid water would require a regulated environment because at the Martian atmospheric pressure, liquid water only exists between approximately 0 and 10°C. Finally, simple energy calculations reveal that providing the heat of fusion to melt the ice requires significantly more energy than fracturing and lifting the frozen ice and soil mixture. To melt 300 g of water at 0 C, 100200 J are required, while energy only on the order of 100 J is required to fracture and lift the 800 g of frozen soil that contains 300 g of water. The following calculations show how these values are derived.

$$E_{melt} = m_{ice} \Delta h_{fusion,ice} = (300 \text{ g})(334 \frac{\text{J}}{\text{g}}) = 100200 \text{ J} \quad (3.5)$$

$$\begin{aligned} E_{mechanical} &= E_{fracture} + E_{lift} = w_{frozen \text{ soil fracture}} V_{soil} + m_{soil} a_{Mars} d_{lift} \\ &= (165 \frac{\text{kPa}}{\text{m}})(644.5 \text{ cm}^3) + (300 \text{ g})(3.69 \frac{\text{m}}{\text{s}^2})(1.25 \text{ m}) \\ &= 106 \text{ J} + 1.4 \text{ J} = 107 \text{ J} \end{aligned} \quad (3.6)^{10}$$

Melting the ice off-site by carrying the frozen ice/soil mixture back to the central holding location is the preferred option. Although this option requires carrying the entire ice/soil mixture, this transportation would be necessary even if the ice is melted on site. Because the robot must get through the dry soil layer in either case, an attractive method is to use the same tool to extract both the dry soil and ice/soil layers. An auger is an ideal tool for accomplishing this task, since it serves both to drill through the soil and to displace it upwards simultaneously. An auger will granulate the ice/soil mixture as it drills, making it easier to transport and store. The torque required to push a 10 cm-diameter drill through soil is significant. Typical small cordless drills deliver a torque of 8 N-m for a 1cm drill bit. This corresponds to 80 N-m for the rover's 10 cm auger. At high rotational speeds, achieving a torque of 80 N-m would require more power than is available ($P = T\omega = 1780 \text{ W}$ for ω of just 200 rpm). However, high rotational speeds are not necessary. If the auger can descend 0.5 cm in one revolution, then a speed of 20 revolutions per minute would enable the auger to penetrate 100 cm in just 10 minutes. A 10-minute drilling time fits into the requirements of the mission, and a speed of 20 rpm requires 178 W of power, which achieves the design goal of minimizing the required power.

3.2.2.3 Design of Auger

The first consideration when designing the auger device was whether or not to extend the auger the entire 100 cm length of the hole being drilled or to place a shorter auger at the end of a drive shaft. The initial incentive for creating a 100 cm auger was to ensure that all of the material would be transported upwards to the surface. However, the 6 kg mass required by an auger of that length would cause the robot to exceed its mass constraints. Additionally, a full-length auger is not required for the soil to be transported upwards.

The auger will displace soil upwards toward the surface as it drills. A collection tube or tank will then collect the material being displaced. While a tube or tank that remains above the surface is the simplest option, a support structure would be necessary to maintain the structure of the hole created by the auger. Because the drive shaft will have a smaller diameter than the hole created by the auger, the hole will collapse behind the auger as it travels

downward through the dry soil layer. Therefore, a collection tube that follows the auger into the soil is the preferred option.

3.2.2.4 Separation of Ice/Soil Layer

It would be ideal to separate the top 60 cm of dry soil from the bottom 30 cm of ice/soil mixture. This separation would require fewer trips to the central holding tank or decrease the size of the storage tank on each robot. Two possible design iterations were rejected based upon the complexity of the systems. The first involved two augers, one inside the other. The inner auger would be covered while the outer auger drilled through, collected and disposed of the dry soil. Upon reaching the ice-rich layer, the outer auger would be covered, and the inner auger would drill through and collect the ice-rich soil. The second design required only one auger, and would use a valve to direct the dry soil out of the robot and the ice-rich soil into a holding tank on the robot. Both designs would add mechanical complexity. The alternative design that was chosen consists of a non-telescoping auger that expels the desired bottom 30 cm into a transporting rover and the unwanted top 60 cm back to the Martian surface.

3.2.2.5 Telescoping of Auger versus Non-telescoping System

Another design issue involves the choice between a telescoping and a rigid non-telescoping drive shaft/collection tube. Telescoping allows for a more compact robot design with the ability to drill to the required depth. However, telescoping adds complexity and multiple moving parts. Additionally, a telescoping drive shaft and collection tube would have to be covered with a shroud to prevent mechanism-locking from fine soil particles. The trade-off is between a compact telescoping design and a larger non-telescoping design. The final design consists of a tube with a length of 125 cm, which contains the non-telescoping collection tube and drive shaft connected to a 10 cm auger.

3.2.2.6 Single Robot Type versus Multiple Robot Types

The design of the water collection robot lends itself to a system that consists of two types of robots: a drilling water collection robot and a water detecting and transporting robot. Because the driller robots' sole purpose is to drill and extract the ice, their mobility becomes less important. These robots can be built with the primary focus on drilling. A second robot will serve as a water detecting and transporting robot. This focus of these robots will be on mobility, and they will be more agile, smaller and lighter.

3.2.3 Preliminary Design of Water Collection System

The chosen water collection method consists of drilling to a depth of 100 cm and collecting all of the dry soil and ice-rich soil encountered in the resulting 100 cm column. This method is implemented with a 10 cm auger followed by a 100 cm collection tube. The tube and auger are stowed horizontally within an outer protective cylinder on the driller rover. When the rover reaches a drilling location, a shoulder motor on the rover drives the cylinder to rotate about an axis normal to its length. When the cylinder is oriented vertically, the rotation ends and the auger becomes operational.

A translating motor drives the rotation of the rigid auger and drive shaft assembly, and parallel lead screws drive the insertion of the collection tube into the subsurface. A roller bearing interface between the drive shaft and the collection tube allows the collection tube to transfer the downward force from the lead screws into vertical thrust for the auger. This bearing is embedded in a disk that is rigidly connected to the collection tube. Cut-outs in the disk allow soil to travel up the collection tube. Because the bearing is fully constrained to the drive shaft in the vertical direction, and the disk is fully constrained to the collection tube in the vertical direction, the drive shaft (and auger) matches the vertical translation of the collection tube. As the auger and collection tube descend into the subsurface, the rotation of the auger directs soil from the top 60 cm and ice-rich soil from the lower 40 cm upwards into the tube. Once the entire column of soil is inside the tube, the lead screws reverse their rotation, and the tube, drive shaft, and auger ascend back into the outer protective cylinder above the surface. The bottom 10 cm of ice/soil mixture remains in the auger blades; this material is allowed to escape back to the surface as the auger retracts upwards. Consequently, a cylindrical volume of ice/soil mixture that measures 30 cm in depth by 10 cm in diameter contains all of the desired water. Once the auger and collection tube have been fully retracted, the rover's shoulder motor pivots the water collection cylinder 45 degrees away from vertical, the transporter robot positions itself below the cylinder opening, and the auger rotates in reverse until the ice/soil layer has been released. Finally the transporter rover drives away, and the auger rotates until the collected dry soil layer is expelled onto the Martian surface.

Princeton University: Integrated Robotic Team for Martian Water Ice Collection

A ledge that is embedded into the outer cylinder supports both the spool that contains the extendable cable of the auger motor and the motor that drives the rotation of the lead screws. At the bottom end of the outer cylinder, a tightly-fitting guide keeps the drive shaft and collection tube in alignment as they enter the subsurface. Figures 3.3 and 3.4 highlight the main components and dimensions of the water collection device.

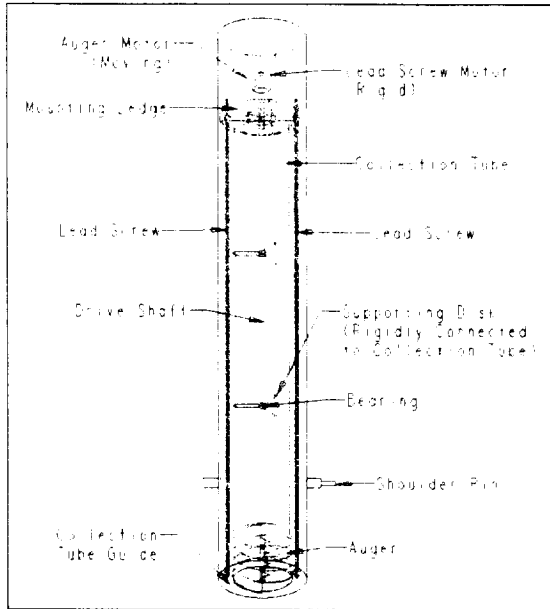


Figure 3.3 Components of Martian Water Collection Device

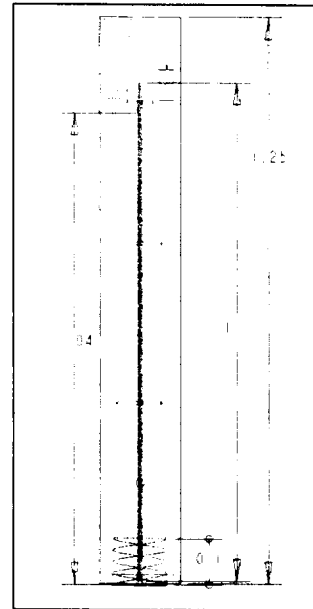


Figure 3.4 Dimensions (in meters) of Martian Water Collection Device

To illustrate better the functionality of the water collection device, Figure 3.5 provides a shaded view, with the outer cylinder transparent. Figure 3.6 shows an exploded view of the outer cylinder, collection tube, and auger. Figure 3.7 details the guide that stabilizes the auger and collection tube as they enter the subsurface.

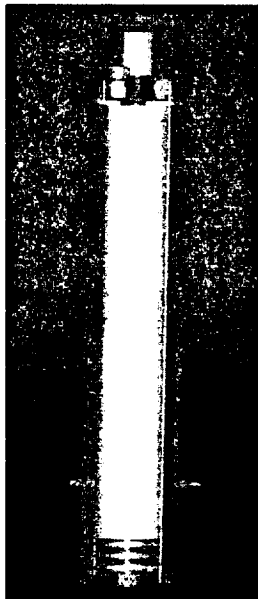


Figure 3.5 Shaded View of Martian Water Collection Device

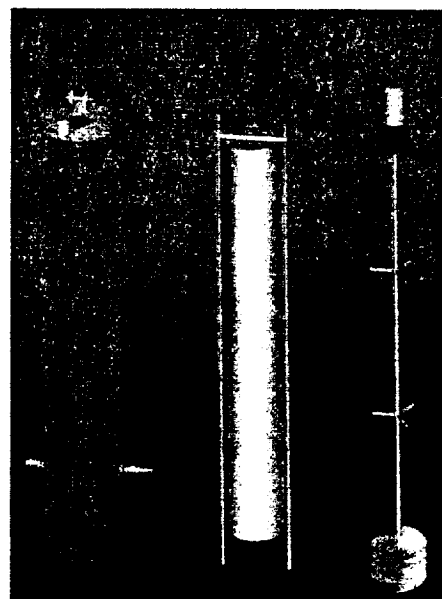


Figure 3.6 Exploded View of Martian Water Collection Device

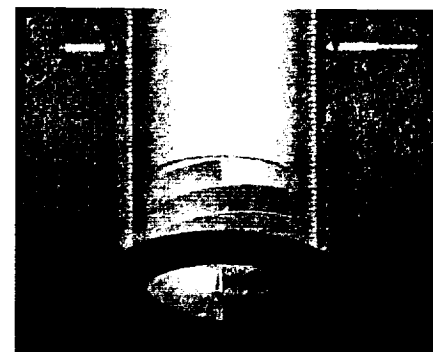


Figure 3.7 Detailed View of Auger Guide on Martian Water Collection Device

3.3 Structure Subsystem

The structure of the drilling rover exists to support, actuate, and transport the water collection device. Its supporting members are comprised of cold temperature resistant metal. The total mass of the rover is 18 kg, and it measures 125 cm, 31 cm, and 50 cm at its longest, tallest, and widest points. In addition to the water collection device, the main components supported by the structure of the rover are the wheels and their motors, the shoulder bearing for the water collection cylinder, the shoulder motor, the Mars GPS device, the feedback and control microcontroller, the high-level microprocessor, and communications transmitter, and 2 125-watt radioisotope thermoelectric generators (RTGs). All of these components will be explained in the subsystem sections that follow. Figure 3.8 displays the rover's general structure and all of its main components, and Table 3.1 lists these components. Figures 3.9 and 3.10 illustrate the basic dimensions of the drilling rover.

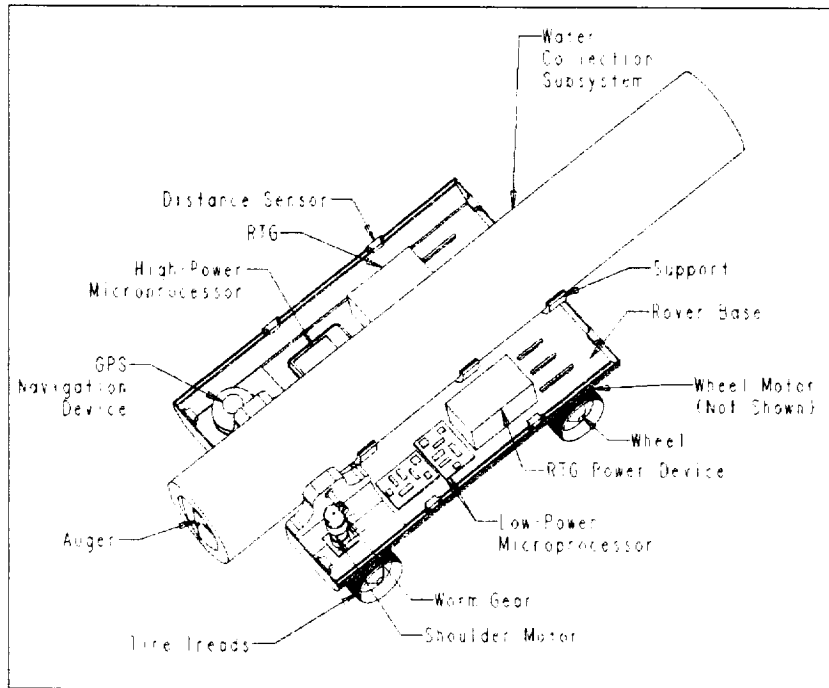


Table 3.1 Main Components of Driller Rover and their Masses

Component	Mass (kg)
Drive Shaft (98cm)	0.6
Auger (10cm)	0.4
Auger Motor	1
RTG 1	5
RTG 2	5
Tilt Motor	1
Lead Screw Motor	0.5
GPS	0.2
High-power Processor	0.2
Low-power Processor	0.2
Wheel & Motor	0.5
Supporting Structure	2
TOTAL	18.1

Figure 3.8 Layout and Components of Driller Rover for Martian Water Collection

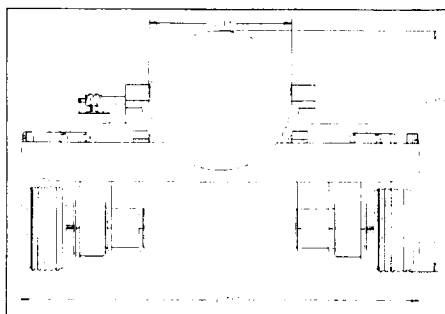


Figure 3.9 Front View of Driller Rover for Martian Water Collection

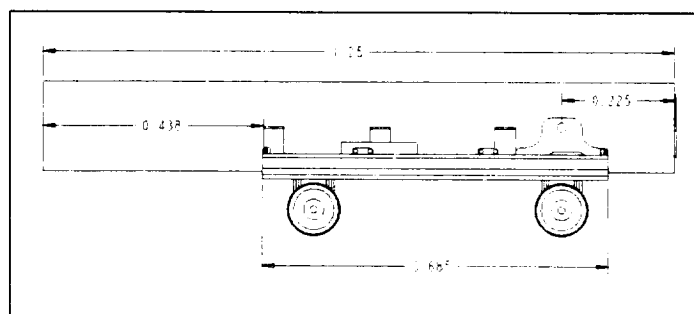


Figure 3.10 Side View of Driller Rover for Martian Water Collection

Figure 3.11 depicts the rover with the water collection device in its operational, vertical position. Figure 3.12 shows a view of the rover with the water collection device stowed horizontally, ready for rover movement. The rover is shown with the non-drilling end in the foreground.

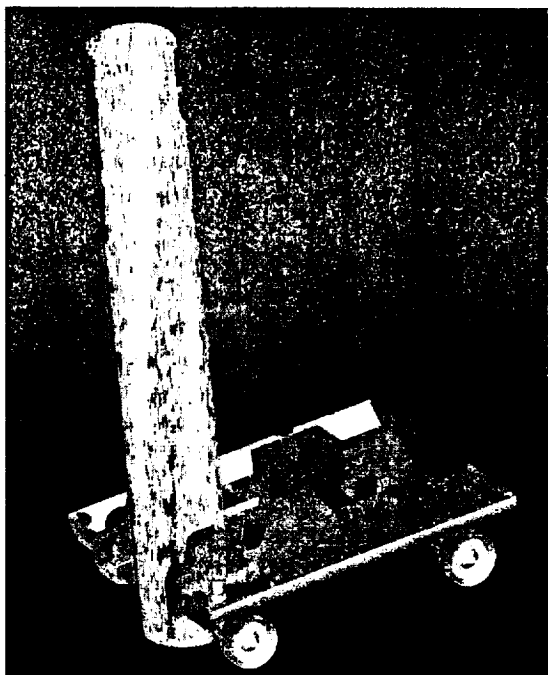


Figure 3.11 Martian Water Collection Rover with Operational Drill

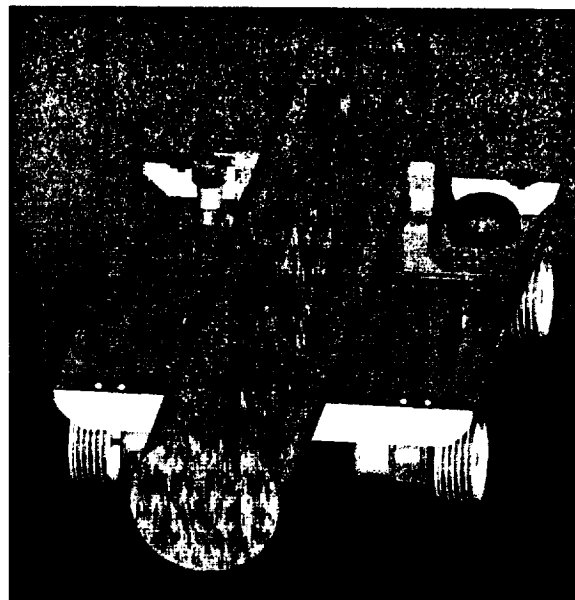


Figure 3.12 Martian Water Collection Rover with Stowed Drill

3.4 Drive Train Subsystem

The drive train of the driller rover will consist of four wheels each driven by an individual motor. They are covered with treads for traction on the Martian soil. To enable the rover to clear any surface obstacle that is 5 cm or less in height, the wheels are 10 cm in diameter. Each wheel motor draws power from the RTGs based on the signal it receives from the rover's microprocessor. Figures 3.11 and 3.12 depict each wheel motor directly shafted to its respective motor. In further work, the design may place the motors on the rover base, directly above wheels, with right-angle gears providing the connection between the motors and the wheels. Because the rover is only required to travel distances less than 85 m and can take several minutes to travel those distances, it needs only to achieve velocities on the order of 0.5 m/sec. For wheels that are 10 cm in diameter, the motors need to operate at the low speed of 100 rpm.

3.5 Command and Data Handling Subsystem

The feedback and control system of both the drilling rover and the transporting rover are run by an embedded microcontroller, which handles a limited set of time-critical tasks. This feedback and control processor controls the speed and movement of the robot, drilling mechanisms, water detection, object avoidance, and docking. For such processes, latency is a prime consideration.

Computationally intensive tasks such as data storage and processing, navigation, drilling site selection optimization and communication require a processor with greater computational power than the microcontroller for hardware control. Consequently, on each type of rover, a second processor handles these tasks. This extra complexity incurs greater power usage, but power consumption of this higher level system can be minimized by powering down components or scaling the clock speed of the processor when full capabilities are not required.

Designing the system with two separate microprocessors is an attractive option because it increases the fault tolerance of the system. Traditionally, each robot would be simplified and much of this processing would be done

by a central computer. A simplified robot and central computer would also simplify coordination between teams of working robots. However, a central control station giving out orders to all robots introduces a single point of failure in the system. If each robot can instead make its own decisions, that responsibility is distributed evenly among the robots. A second disadvantage of a central control station is the higher power that it would require. If it is considered how microprocessor cycles per mW have increased linearly over the past 20 years, a significant power savings can be seen since RF uses a virtually constant amount of power per amount of data passed.

3.6 Communications Subsystem

The water collection team uses wireless communications to allow a team of robots to work on shared tasks. Both types of robots broadcast messages to the entire collective through an ad hoc peer-to-peer 2.4 GHz network. The communication module has enough RF power output to be broadcast over the entire water extraction area. This model allows the rovers to share and aggregate vital information, such as water concentration and obstacle avoidance data. This method has been chosen because of the availability of hardware and software modules to handle the physical and logical layers with reliable performance and low power usage.

3.7 Navigation Subsystem

The navigation system works under the assumption mentioned above that GPS satellites are in orbit around Mars. Each driller rover and each transport rover contain a GPS receiver that is supplied with differential correction factors over the wireless network from a central computer and GPS receiver. The motivation for differential GPS is to increase the accuracy of the mobile GPS stations. The design assumes that the base station is located at a fixed location so error correction factors can be calculated by comparing the known position to the position obtained by the GPS receiver. These correction factors are subsequently applied to all the robots to achieve the resolution needed to reliably locate other robots on the Martian surface. While the base station could represent a single point of failure, it is assumed that sufficient redundancy has been built into the Martian GPS system, as it will be critical to many other mission objectives.

3.8 Power Subsystem

Each driller rover is powered by radioisotope thermoelectric generators (RTG). RTGs are lightweight, compact power systems that are highly reliable. RTGs are not nuclear reactors and have no moving parts. They use neither fission nor fusion processes to produce energy. Instead, they provide power through the natural radioactive decay of plutonium-238, a non-weapons grade isotope. The heat generated by this natural process is changed into electricity by solid-state thermoelectric converters. RTGs enable rovers to operate at significant distances from the sun or in other areas where solar power systems would not be feasible.

Radioisotope power sources are the enabling technology for space applications requiring proven, reliable, and maintenance-free power supplies capable of producing up to several kilowatts of power and operating under severe environmental conditions for many years. Previous space missions that have used radioisotope power sources include the Apollo lunar surface scientific packages and Pioneer, Viking, Voyager, Galileo, and Ulysses spacecrafts. The Mars Reference Mission alludes to plans for a "Dynamic Isotope Power System" that delivers power at a specific power of $9 \text{ W}_e/\text{kg}^2$. Assuming a two-fold increase in technology every ten years, it can be estimated that radioisotope power systems will have specific powers of approximately $35 \text{ W}_e/\text{kg}$ by the year 2025. Consequently, the driller rover is powered by two 5-kg RTGs, each delivering 125 W_e of power. They deliver a more conservative specific power of $25 \text{ W}_e/\text{kg}$. The 250 W_e of power that they deliver is sufficient for all of the rover's electrical systems.

RTG power sources are superior to other power system options. Solar power is an frequently used option, but to produce 250 W_e of power with 30%-efficient photovoltaic cells, a cell surface area of more than 1 m^2 is required. This surface area A_s is given by:

$$A_s = \frac{P_{\text{required}}}{I_{\text{Mars}} \eta} = \frac{250W}{(600 \frac{W}{m^2})(0.3)} = 1.39 \text{ m}^2, \quad (3.7)$$

where I_{Mars} is the solar flux at Mars and η is the efficiency of the photovoltaic cells. Adding almost 1.5 m^2 surface area to each rover would cause the robotic team to exceed its size limitation. Another drawback of solar cells is that they cannot operate continuously or completely independently. They must cycle through charging and discharging cycles that depend on the length of solar exposure, and they work in conjunction with batteries that store and deliver power when the cells are not exposed to sunlight. These batteries increase the mass of the power system, and the

Princeton University: Integrated Robotic Team for Martian Water Ice Collection

dependence of the photovoltaic power system on sunlight means that continuous operation of the robotic water collection team could not be ensured. Compact, continuously functioning RTGs are desirable over solar cells.

3.9 Water Detection Subsystem

The robotic team depends on the transport rovers to detect water in the near subsurface. The transport rovers be equipped with water detection systems that can determine the regions where the 60 to 100cm-deep portion of the soil contains more than 50% ice by volume. The transport rovers direct the driller rovers to these water-rich locations. The water detection system uses a lightweight, low-power, ground-penetrating radar (GPR) system to probe the Martian subsurface for aqueous slayers in solid state. Advantages of radar include relatively low mass and power, high signal controllability, and high resolution imaging of subsurface cross sections. A GPR operating in two frequency bands centered around 10 MHz and 500-1000 MHz or sweeping through the 10-1000 MHz region, can provide information about the subsurface with high resolution at shallow depths, which is the region of interest. This technique is considered essential for targeting a mobile drill and for providing 3-dimensional geologic context for drill results. GPR can also be used for subsurface hazard avoidance during long rover traverses¹¹. The penetration depth of a GPR on Mars is highly dependent on the stratigraphy and lithology of the subsurface layers. The radar responses from geophysical models of surface characterization, soil properties at microwave frequencies, and three-dimensional stratigraphy mapping based on what could be expected on Mars have been simulated by Leuschen et al¹².

In choosing this method, it was first determined that any water detection system must avoid surface contact to minimize the number of mechanical parts and to maximize the area covered. The non-contacting systems that were considered included infrared, neutron, nuclear magnetic resonance (NMR), and electromagnetic radiation such as ground-penetrating radar. Infrared was discounted because the depth of penetration was only a few microns. NMR was not feasible because of the lack of a magnetic field on Mars. The electromagnetic method was chosen because it was simple to implement and the most reliable.

4. Conclusion

The systems design approach to the problem of Martian subsurface water collection attempted to lay out a set of critical mission requirements and then to best meet these through several phases of design iterations and optimizations. The water collection system chosen meets and exceeds every requirement set out at the beginning of the design process. The team of robots has a total mass and volume of 700 kg and 6 m³ and possess the capability to collect the required mass of water with 100% contingency. These characteristics are marked improvements over the 90-Day Study's plan for a Martian mining excavator/loader vehicle, hauler vehicle, and their power system. Therefore, the team of small robots more efficiently and more reliably meets the task of Martian ISRU by taking advantage of the recent Mars Odyssey discovery. The concept of using a team of small robots proposes a revolutionary approach, improving upon the customary notion that a large robot is required to accomplish such a full-scale task as mining for frozen water on Mars. The integrated robotic team presented in this paper is a concept that should be taken into consideration for future Mars mission that desire a more efficient and reliable approach to autonomous in situ resource utilization.

5. Further Work

As mentioned above, this paper is the result of the preliminary design phase for Martian subsurface water collection. The conceptual design for the robotic team and the preliminary design of the water collection system have already been laid out, and the next phase is to complete the iteration process for the remaining individual subsystems. This includes designing the interface between the various subsystems to ensure that they will function together. Once all of the subsystems have been designed, the final detailed design must be completed, including the selection of appropriate materials and hardware for robust operation in the Martian environment. Particular attention must be paid to thermoregulation, radiation shielding, and protection from dust prevalent in the atmosphere.

Princeton University: Integrated Robotic Team for Martian Water Ice Collection

While the details are being completed on all of the subsystems, prototyping and experimentation will begin on the water collection system to optimize its design and to ensure its proper functioning. This will include creating a simulated Martian soil and replicating Martian environmental conditions as much as possible. Once the water collection system is built and its interface with the rest of the subsystems has been designed, it will be incorporated into a fully operational robotic system. The final step is to build the transport robot and to demonstrate the ability of the pair of robots to work as a team to detect, collect, transfer, and transport the water.

6. References

1. Boynton, W. V., W. C. Feldman, et al. (2002). "Distribution of Hydrogen in the Near Surface of Mars: Evidence for Subsurface Ice Deposits." *Science* **297**: 81-85.
2. "Human Exploration of Mars: The Reference Mission of the NASA Mars Exploration Study Team." Hoffman, S.J. and Kaplan, D.I., eds. NASA Special Publication 6107. July 1997.
3. NASA, "Report of the 90-Day Study on Human Exploration of the Moon and Mars", November, 1989.
4. *Labeled MOLA Map of Mars* [Image]. MOLA Science Team [cited 4 November 2002]. Available from http://ftpwww.gsfc.nasa.gov/tharsis/map_lab.html.
5. *PIA03803: Cross-Section of Icy Soil* 2002. [Image]. NASA, 28 May 2002 2002 [cited 23 September 2002]. Available from <http://photojournal.jpl.nasa.gov/catalog/PIA03803>.
6. Feldman, W. C., W.V. Boynton, et al. (2002). "Global Distribution of Neutrons from Mars: Results from Mars Odyssey." *Science* **297**: 75-78.
7. *Mars Pathfinder - Science Results - Atmospheric and Meteorological Properties* 2002. NASA [cited 24 September 2002]. Available from <http://mars.jpl.nasa.gov/MPF/science/atmospheric.html>.
8. Allen, C. C., R. V. Morris, et al. (1997). JSC Mars-1: Martian Regolith Simulant. Houston, TX, Lunar and Planetary Institute.
9. Personal Communication with NASA Revolutionary Aerospace Systems Concepts Human Outer Planet Exploration Study Team. NASA Langley Research Center. July 2002.
10. Andersland, Orlando B., and Branko Ladanyi. Introduction to Frozen Ground Engineering. New York : Chapman & Hall, 1994.
11. Farr, T. G., D. Beaty, et al. (2001). Electromagnetic sounding of Mars from a Lander or rover: Results of an instrument study for 2007. Conference on the Geophysical Detection of Subsurface Water on Mars, Houston, TX, Lunar and Planetary Institute, NASA.
12. Leuschen, C. J., S. P. Gogineni, et al. (2001). Simulation and Design of Ground-Penetrating Radar for Mars Exploration. Conference on the Geophysical Detection of Subsurface Water on Mars, Houston, TX, Lunar and Planetary Institute, NASA.

EXO BIOLOGY: THE SURVIVAL ABILITY OF HALOPHILES UNDER MARTIAN CONDITIONS

University of California at Berkeley, Earth and Planetary Science Dept.
Berkeley, CA 94720

Students: Huitung Chu and, William Sheng
 Advisors: David C. Gan and Lawrence Kuznetz

Abstract

The recently developed Odyssey gamma-ray spectrometer (GRS) has detected high concentrations of hydrogen, which strongly indicates there is permafrost and water ice in the upper meter of soil in the South Pole region of Mars. This finding presents the possibility that halophilic (salt loving) Archea might be present in its ice. It is possible that there may be areas of saline ice on Mars, since saline is found in Arctic ice. Halophiles are known to survive well under adverse conditions and have possibly lain dormant since the Upper Permian (250 million years) in salt deposits (2, 3, 7, 9).

Consequently, two halophiles isolated from San Francisco Bay salt ponds were selected to determine if they could survive the severe Martian conditions. To date, they have survived at least 8 months under experimental conditions. Future experiments will include dormant halophilic isolates from Lake Searles red salt crystals and Upper Permian Berchtesgaden rock salt.

Introduction

Martian surface conditions are not favorable for living organisms. The low pressures of 6 to 10 millibars of 95% carbon dioxide, a mean temperature of -80°C and the presence of superoxides formed by intense ultra-violet (UV) light irradiation, destroy organic compounds. However, some adverse terrestrial conditions did not deter organisms known as Extremophiles from surviving. In fact, the Martian conditions are very similar to the lyophilization process (freeze/dry by vacuum) used for preserving microbial cultures in the laboratory. Water is considered an essential element and appears to be lacking on the Martian surface. However, the presence of liquid water appears feasible and its presence has been demonstrated by experimentation under certain conditions. (12, 13, 14). It most likely exists as surface liquid water for a short time and as subsurface water or permafrost, which may support life forms.

A brief survey of Extremophiles: Among them are the Archea group which include: thermophiles from thermal hot springs and sub oceanic thermal "smokers"; barophiles, bacteria surviving in deep oceans under extremely high pressures; methane bacteria found in swamps, and sulfur hot springs; and psychrophiles (cold loving) found in the Lake Vostok Ice Shelf. Highly radioactive environments such as the Oakridge Atomic and Three Mile Reactors, showed the presence of Deinococcus radiodurans, whose ability to survive extremely radioactive environments is accomplished by constantly repairing damaged DNA with numerous copies of DNA. Another Extremophile is the arthropod-like tardigrades (21). They are so unique that a separate phylum, known as Tardigrada, was created for them. Commonly known as "water bears" they can survive desiccation for a hundred years, in vacuum, while subjected to extreme temperatures and high radiation.

Other Extremophiles include Bacillus infernus, a strict anaerobe isolated from a Virginia mine basalt at depth of 2.8 km. Cryptoendoliths were found to form a unique biological niche in an Antarctica Dry Valley in porous sandstones despite the harsh conditions of low moisture, near freezing temperatures, high winds and high UV flux (16,17). Halophilic (salt loving) archea are found universally in salt ponds and lakes and even as dormant cells or as biopolymers in rock, salt crystals (figures 1, 2 3,4)) and in evaporates and desert varnish. There are also recent findings of evaporates on Mars (21).

Halobacteria are facultative anaerobes, which use rhodopsin that produces ATP from ADP; they survive lysis in a high NaCl environment by maintaining a high concentration of cellular potassium ions. Another halophile uses halorhodopsin as a chloride pump (22). In addition to its role in metabolism, the pigments serve as a shield

flux (16,17). Halophilic (salt loving) archea are found universally in salt ponds and lakes and even as dormant cells or as biopolymers in rock, salt crystals (figures 1, 2 3,4)) and in evaporates and desert varnish. There are also recent findings of evaporates on Mars (21).

Halobacteria are facultative anaerobes, which use rhodopsin that produces ATP from ADP; they survive lysis in a high NaCl environment by maintaining a high concentration of cellular potassium ions. Another halophile uses halorhodopsin as a chloride pump (22). In addition to its role in metabolism, the pigments serve as a shield against UV light and help to raise the temperature by absorbing sunlight. Sodium chloride also protects the cells from UV light. Other survival mechanisms include cellular potassium and sodium, which are also essential for enzyme function and for using glycine-betaine (18,19).

In our laboratory experiment, dormant Archea halophiles were recovered from Searles Lake red salt crystals and Upper Permian (250 million years) rock salt from the Berchtesgaden salt mines in Germany. There have been others instances of recovered halophiles from the Berchtesgaden and English salt mines in addition to New Mexico caves and even 650 million year old salt deposits (1, 2, 3, 4, 5). The claims for some of these recoveries are under debate. Some reasons for this skepticism include possible contamination and intrusion of more recent halophiles in water into the permeable salt crystals (23). It is common knowledge that recent age salt crystals harbor viable halophiles and their recovery is not difficult (1,16). We subsequently selected halophiles because of their ability to survive long periods under adverse conditions, and their dormancy period. Culturing them in a high salt concentration media excludes most contaminants. They are also readily available. For these reasons, they are a good candidate for this exobiology experiment (5,21). Moreover, since the Mars subsurface may have salt deposits and saline, the likelihood of finding halophiles is promising (6).

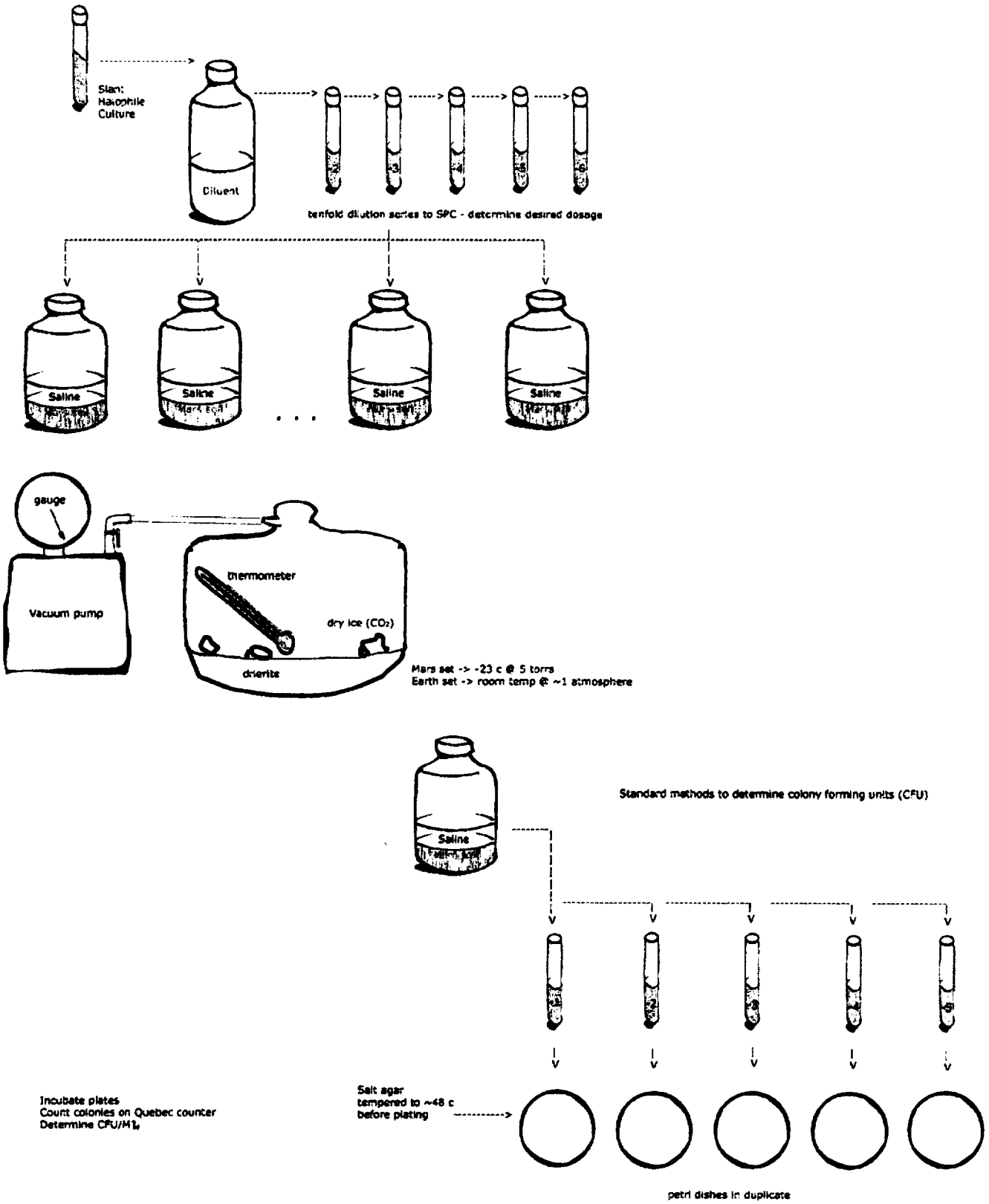
For the first experiment, we tested two fresh halophilic isolates from the San Francisco Bay to determine if they were able to survive under Martian conditions: Halobacterium (Haloferax) volcani (24), originally isolated from the Dead Sea, is mainly gram positive, nonmotile, disk shaped; with colonial morphology – smooth, round edges and displays orange pigment. The second isolate, designated as Halophile 1W is gram variable, non-motile, having short rods, with colonial morphology - smooth, round edges, and displays a yellow pigment (25). Both can tolerate 30% and 20% NaCl concentrations, respectively.

Method

Two halophiles, Haloferax volcani, and one designated as Halophile 1W, were isolated from the San Francisco Bay salt ponds. They were cultured in ATCC 1270 medium: NaCl-194 g, MgCl₂ 16 g, MgSO₄ 24 g, CaCl₂ 1.0 g, NaHCO₃ 0.2 g, KCl 5 g, NaBr 0.5 g, Yeast Extract 5.0 g, 1 L water, PH 7.3.

Plating was done with Salt Tryptose Glucose Yeast Extract Agar (STGYA): Tryptone-5.0 g, Yeast Extract-2.5 g, Glucose-1.0 g, NaCl –10g, Distilled Water- 1 L, pH 7.2. High Salt Concentration Agar was used to determine the degree of salt tolerance in cultures, a series of 30, 60, 120 and 150g NaCl g/ L was added to the STGYA medium. It was found to be impractical to culture halophiles on 25% NaCl agar because the salt crystallizes on the agar surface before the slow growing halophiles show growth of colonies.

Titered suspensions of each species in 1% saline, were added to Mars Soil Simulant JSC-1 Mars (10), cultured in 200 mL medicine bottles, and then placed into a bell jar containing dry ice to create a CO₂ atmosphere, using Drierite to remove water vapor. The internal pressure was adjusted to 5 torrs pressure and the assembly was frozen to -23° C in a freezer for the test (fig 7). A duplicate set was also run to serve as the Control set using ambient temperatures and atmosphere conditions in a bell jar that was exposed to light. A non-halophilic spore former, Bacillus mycooides, was selected for comparison. Periodic determinations of survival ability were performed by the heterotrophic plate count (HPC) method found in Standard Methods (7). Ten fold dilution series were made with 1% saline for plating. Plating for each dilution was done in duplicate. After incubation at 37°C for 72 hours, enumeration of colonies was done visually with a Quebec Colony Counter; Colony Forming Units (CFU) were then determined using Standard Methods (7). See Flow Chart.



Results

Survival Ability of Halophiles under Martian Conditions

Experiment Duration: Nov 2001 to October 2002

		<u>Nov 30 '01</u>	<u>Jan 4 '02</u>	<u>Jul 17 '02</u>
<u>Colony Forming Units (CFU) per milliliter</u>				
<u>Mars Set</u> <u>-23°C</u> <u>5 torrs CO₂</u>	<u>Haloferax</u> <u>volcanii</u>	2,200,000	1,200,000	420,000
	<u>Halophile</u> <u>1W</u>	2,900,000	1,800,000	270,000
	<u>Bacillus</u> <u>Mycooides</u>	1,800,000	not done	240,000
<hr/>				
<u>Earth Set</u> <u>Room Temperature</u> <u>Ambient pressure</u>	<u>Haloferax</u> <u>volcanii</u>	3,500,000	2,200,000	2,100,000
	<u>Halophile</u> <u>1W</u>	2,500,000	1,800,000	2,400,000
	<u>Bacillus</u> <u>Mycooides</u>	3,500,000	not done	290,000

Discussion

The Mars Set showed a decrease in numbers of Colony Forming Units (CFU) for both halophiles and Bacillus mycooides, a non-halophilic spore former. In the Earth Control set, halophiles showed less decrease in CFU than the Mars Set. Bacillus mycooides showed a similar decrease in numbers; this decrease may be possibly attributed to freeze/thaw damage of cells incurred by periodic removal from the bell jar for testing. The Earth Control colonies were orange while the Mars Set colonies were white (fig 8). This difference may be attributed to the pigments of the rhodopsin family, which are photosynthetic (5); subsequently, future experiments will be conducted to determine the role of light on colonial color.

Concerning the recovery of dormant halophiles from salt, the findings are under debate because of permeation of more recent halophiles in water by a temperature gradient (15). However, the molecular biological signatures showed that the ancient halophiles are significantly different from the modern species (2).

Future Experiments

1. To determine if the decrease in numbers of the Mars Test Set was due to freeze/thaw effect, aliquots of halophile/soil will be distributed to multiple containers to avoid freeze/thawing. Only one container from each set will be removed periodically for testing, thus ensuring the integrity of the remaining containers.
2. Dormant halophilic isolates recovered from Searles Lake and Upper Permian Berchtesgaden rock salt will be tested by the previously described method, except that the Mars Set will be subjected to -80° Celsius (average

Martian temperature) with CO₂. These isolates were cultured from sterilized salt crystals or rock salt. Sterilization was achieved by flaming and exposure to a UV germicidal lamp in a Sterilgardhood (Baker Co) for one to two hours, with frequent rotation of the crystals to assure complete surface sterilization. The weighed crystals were then dissolved in 1% saline to a final concentration of ~10 to 15% NaCl (1.5 to 2.5 molar) and then cultured in the ATCC Medium 1270 for several weeks at room temperature. A control UV sterilization run was done to determine the efficacy of our UV surface sterilization technique. A Control UV sterilization run was completed to determine the efficacy of the sterilization technique by testing < 2m diameter crystal. No growth of halophiles were observed with this run.

3. Koch Postulates Experiment: To prove that an etiological agent causes a disease, a pure isolate culture of the suspect agent will be tested in a susceptible host. Recovery of the agent in question demonstrates that the agent is responsible for the disease. This procedure is known as Koch's Postulates. In this future experiment, a pure culture of halophile will be allowed to crystallize in a sterile saturated salt solution for dormancy. Successful recovery of the dormant halophile will satisfy Koch's Postulates requirements.

Description of isolates to be used for future experiments:

<u>Source</u>	<u>Colonial Morphology</u>	<u>Gram Stain</u>	<u>Growth in % NaCl Medium</u>				<u>ATCC 1270</u>
			<u>6</u>	<u>9</u>	<u>12</u>	<u>15</u>	
Searles Lake	yellow, smooth, regular	var. cocci ~1 µm	+	+	+	+	+
Searles Lake	white, smooth, regular	var cocci~1 µm	+	+	+	+	+
Searles Lake	yeast, white, smooth	pos. ~ 5 um	+				
Berchtesgaden	yellow-orange, smooth	var. cocci	+	+	+		+

Conclusion

The halophiles, Haloferax volcani and Halophile 1W, were able to survive under Martian conditions; however their decrease in numbers may be attributed to the freeze/thaw effect. The Martian halophilic archaea species, better adapted to their harsher environment, may survive in greater numbers than the terrestrial strains used in this experiment.

Outreach Activities

Cal Day Open House UCB Mars Missions Projects Booth and Posters 2001 and 2002

City of Oakley School District Science Fair Booth Display and Posters

Acknowledgements

University of California at Berkeley:

Professors William Dietrich, Jillian Banfield and Michael Zach of the Earth and Planetary Science Dept.
Professor Antje Hofmeister, Plant and Microbial Biology Dept., Professor Frank Morrison, Material Science Dept. and UCB students: Grace Lee and Eric Lin.

NASA

Dr. Michael Hecht, Jet Propulsion Laboratory, Pasadena, Drs. Richard Quinn and Robert Haberle, Chris McKay and Marc Cohen of Ames Research Center

California State Department of Health Services

Dr. Daniel Mills, Microbial Diseases Laboratory (now with USDA Western Regional Laboratories)

Biovir Laboratories

Dr. Richard Danielsen and Professor Robert Cooper

Ms. Monica Gan for manuscript review

References

1. Armstrong, W.P. 1981 "The Pink Playas of Owens Valley", *Fremontia* 93-10
<http://waynesword.Palomar.edu/plsept98.htm>
2. Vreeland, R, Rosenzweig, W, Powers, D., 2000 "Isolation of a 250 Million-year old Halotolerant Bacterium from a Primary Salt Crystal" *Nature* 407: p897-900
3. Stan-Lotter, H., McGenity, T. J., Legat, A., Denner, E., Glaser, K, Stetter, K. O., Wanner, G 1999 "Very Similar Strains of Halococcus salifodinae are found in geographically separated Permo-Triassic salt deposits" *Microbiology* 145: p3565-3374
4. Dyall-Smith, M., Danson, M 2001 "Life of Brine: Halophiles in 2001" *Biology* 2(12) Reports 4033.1-4033.3
5. Landis, G. 2001 "Martian Water: Are There Extant Halobacteria on Mars?" *Astrobiology* 1(2): p161-164
6. Spears, J, Levy, R. "Life Within Rock Salt: A Surprising Diverse Neighborhood" 102nd Meeting of American Society for Microbiology paper N 145. May 19-23, 2002 Salt Lake City UT
7. <http://www.uib.no/ums/magazine/updates/Halophile/halophile.htm>: "Life at the Extreme"
8. "Standard Methods for the Examination of Water and Wastewater" APHA, AWWA and WEF 20th edition, 1999
9. Grant, W. D. "Halobacteria: the Evidence for Longevity" *Extremophiles*, v, 270-287, 1998
10. Allen, CC, Jager, K.M., Morris, R V, Lindstrom, D. J., Lindstrom, M.M. and Lockwood, J.P. "JSC Mars-1: A Martian Soil Simulant, Space 98, American Society of Civil Engineers: April 1998
11. Boone, D.R., Lin, Z., Zahn, D.L, Ballowill, Drake, G R., Stevens, O.T., Aldrich, H.C. "Bacillus infernus sp. nov, an Fe (III)- and Mn (IV)-reducing Anaerobe From the Deep Terrestrial Subsurface" *Int. Journal Systematic Bacteriology*, 45: 441-448
12. Kuznetz, L and Gan, D "On the Existence and Stability of Liquid Water on Mars Today", *Astrobiology*, 2: 183-195, 2002
13. Haberle, R.M., McKay, C.P., Schaeffer, J, Joshi, M., Cabrol, N.A. and Grin, E.A. Meteorology Control on the Formation of Paleolakes on Mars (Abstract 509) Proceedings of the Lunar and Planetary Science Conference. Available at: <http://www.lpi.usra.edu/meetings/lkpsc2000/pdf/1509.pdf>. 2002
14. Hecht, M. "Metastability of Liquid Water on Mars" *Icarus*, 156, 373-387 2002

15. Parkes, J. Microbiology: "A Case for Bacterial Immortality" *Nature*, 407, 844-848, 2000
16. National Academy of Space Bulletin. "Limits of Life on Earth" chap. 4 and Web Page:
www.nas.edu/ssb/bcmarsch4.htm
17. Vestal, J.R. "Cryptoendolithic Microbiota from the Antarctic Cold Desert" *Applied Environmental Microbiology*, 54, 960-965 1991
18. Litchfield, C. "Survival Strategies for Microorganisms in Hypersaline Environment and the Case for Life on Mars", *Meteoritics and Planetary Science*, 33, 813-819 1998
19. Landis, G.A. "Searching for Life: The Case for Halobacteria on Mars" STAIF Conference on Space Exploration Technology, AIP Conference Proceedings, 552, 393-396 2001
20. Landis, G.A. "Water, Pink Salt and Cold Dry Gullies: Halobacteria and the Case for Life on Mars" *Analog* (April) 2001
21. Rothchild, L. "Life in Extreme Environments" *Ad Astra* Jan/Feb 32-41, 2002
22. Mukohata Y, Matsuno-Yag, A, Kaji, Y. "Light Induces Proton Uptake and ATP Synthesis by Bacteriorhodopsin depleted Halobacterium" in Morishita, H. and Masui, M. (eds) *Saline Environment*, *Bus. Ctr. Acad. Sci Japan*, 31-37
23. McKay, C. (personal communication, Aug 2002)
24. *Bergey's Manual of Systematic Bacteriology*, Williams and Wilkins. 1989

Table 1. Chemical Compositions

Oxide	VL-1	VL-2	Pathfinder	JSC Mars-1	
	Wt%*	Wt%*	Wt%**	Wt%***	Wt%****
SiO ₂	43	43	44.0	34.5	43.5
Al ₂ O ₃	7.3	7	7.5	18.5	23.3
TiO ₂	0.66	0.56	1.1	3.0	3.8
Fe ₂ O ₃	18.5	17.8	16.5	12.4	15.6
MnO	n.a.	n.a.	n.a.	0.2	0.3
CaO	5.9	5.7	5.6	4.9	6.2
MgO	6	6	7.0	2.7	3.4
K ₂ O	<0.15	<0.15	0.3	0.5	0.6
Na ₂ O	n.a.	n.a.	2.1	1.9	2.4
P ₂ O ₅	n.a.	n.a.	n.a.	0.7	0.9
SO ₃	6.6	8.1	4.9	n.a.	n.a.
Cl	0.7	0.5	0.5	n.a.	n.a.
LOI	n.a.	n.a.	n.a.	21.8	n.a.
Total	89	89	89.5	101.1	100.0

n.a. not analyzed; all iron calculated as Fe₂O₃

LOI (loss on ignition) weight loss after 2 hrs at 900°C; includes H₂O and SO₂

* Viking landers 1 and 2 XRF (mean of 3; Banin et al, 1992)

** Pathfinder APXS (mean of 5, norm. to 44 wt% SiO₂; Rieder et al, 1997)

*** XRF (Hooper et al, 1993)

**** XRF (volatile-free, normalized; Hooper et al, 1993)

Volatile Content Martian soil simulant JSC Mars-1 contains considerable water. Heating experiments in flowing argon demonstrate weight losses after one hour ranging from 7.8 wt% at 100°C to 21.1 wt% at 600°C. These numbers represent total volatile loss, which is probably dominated by H₂O but would also include SO₂ if sulfates are present.

The Martian surface soil, by contrast, is extremely dry. Viking experiments released 0.1 to 1.0 wt% water from soil samples heated to 500°C (Biemann et al 1977).

Halobacterium media (ATCC medium 1270)

NaCl	194 grams
MgCl ₂	16 grams
MgSO ₄	24 grams
CaCl ₂	1 gram
KCl	5 grams
NaHCO ₃	0.2 grams
NaBr	0.5 grams
Yeast extract	5 grams
distilled water	up to 1 liter

adjust pH to 7.3

(add 15g agar for solid media)

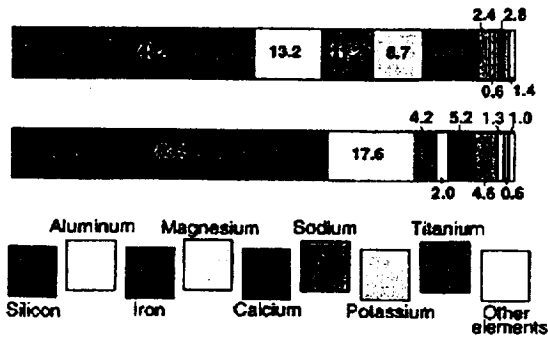
Mars Pathfinder

Analysis of Martian Samples by the Alpha Proton X-Ray Spectrometer: Preliminary Results Comparison with SNCs and the Earth

	Mars			Earth		
	A-3, Rock "Barnacle Bill"	A-5, Soil	SNCs (Mars Meteorites)	Continental Crust		Oceanic Crust
	weight %	weight %	weight %	Average	Sediments	weight %
				weight %	weight %	
MgO	3.1	8.6	9.3 - 31.6	3.1	3.1	7.7
Al ₂ O ₃	12.4	10.1	0.7 - 12.0	15.2	13.0	15.6
SiO ₂	55.0	43.8	38.2 - 52.7	60.2	50.0	50.7
K ₂ O*	1.4	0.7	0.022 - 0.19	2.9	2.0	0.17
CaO	4.6	5.3	0.6 - 15.8	5.5	8.4	11.4
TiO ₂	0.7	0.7	0.1 - 1.8	0.7	0.7	1.5
MnO*	0.9	0.6	0.44 - 0.55	0.1	0.1	0.16
FeO	12.7	17.5	17.6 - 27.1	6.05	5.5	9.9
FeO/MnO	14.1	29.2	37.0 - 51.5	-	-	-

*Values for potassium (K) and manganese (Mn) are probably too high and subject to revision after further analysis.

What is the composition of the lava?



Chemical composition of lavas erupted by Hawaiian volcanoes and Mount St. Helens. Numbers are weight percent oxide.
Courtesy of U.S. Geological Survey.

The lava is basalt. Hawaiian basalts contain about 50% silica, 10% each of iron, magnesium, calcium, about 15% aluminum, 2% titanium and 2% sodium.



Figure 1. Photomicrograph (100x oil immersion) of six bacteria-shaped particles in primary fluid inclusion from 97 kyr old salt in Badwater salt core (85 meter depth).



Figure 2. Time sequence photomicrograph (40x) of rod-shaped particle that is moving with a fluid inclusion from a 9 kyr salt in Badwater salt core (8 meter depth).

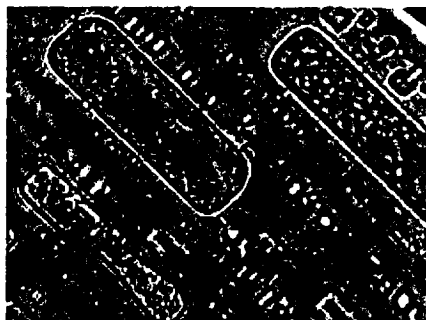


Figure 3. Halophiles trapped within salt crystal grown in laboratory media. Photomicrograph (40x) taken one week after crystal formed. The halophiles are mobile and tend not to be fixed to crystal wall.

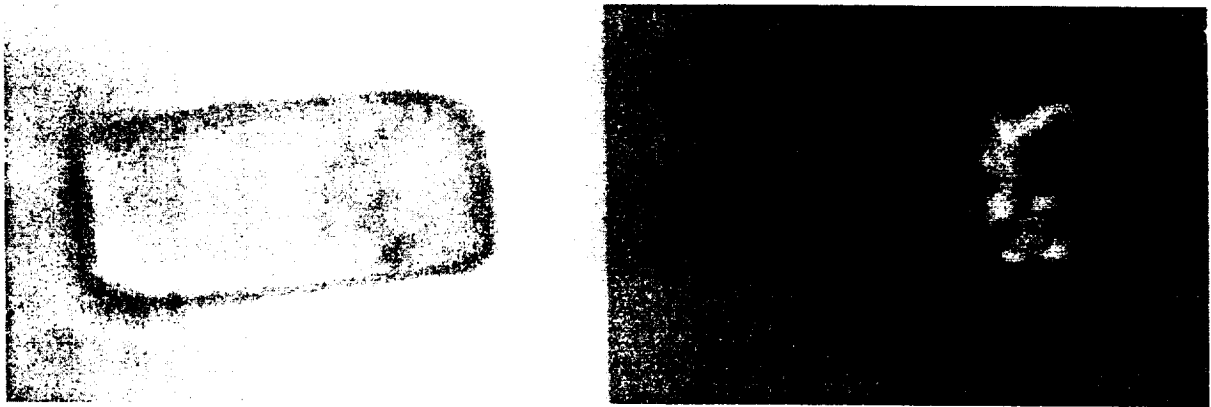


Figure 4. Fluid inclusion in a 20-million-year-old salt crystal, in visible (left) and ultraviolet light. Fluorescence under ultraviolet is consistent with the presence of organic matter. But it is not conclusive evidence, nor does it provide information about the type of material — which might be the remains of entombed bacteria or, conceivably, the intact biopolymers of ancient but viable bacteria. The crystal is about 65 micrometers in length. (Image courtesy of W. D. Grant.)



Figure 5. The vivid red brine (teeming with halophilic archaebacteria) of Owens Lake contrasts sharply with the gleaming white deposits of soda ash (sodium carbonate). The picturesque Inyo Range can be seen in the distance.



Figure 6. Sea-ice diatoms can reach such densities that their photosynthetic pigments color the underside of ice floes brown. The sea-ice organisms grow throughout the ice in brine channels, the brown vertical lines in the image on the right, as well as in porous ice which can be seen as dark brown horizontal layers.
(Photograph by D. N. Thomas.)



Figure 7. Halophile survival test using bell jars.

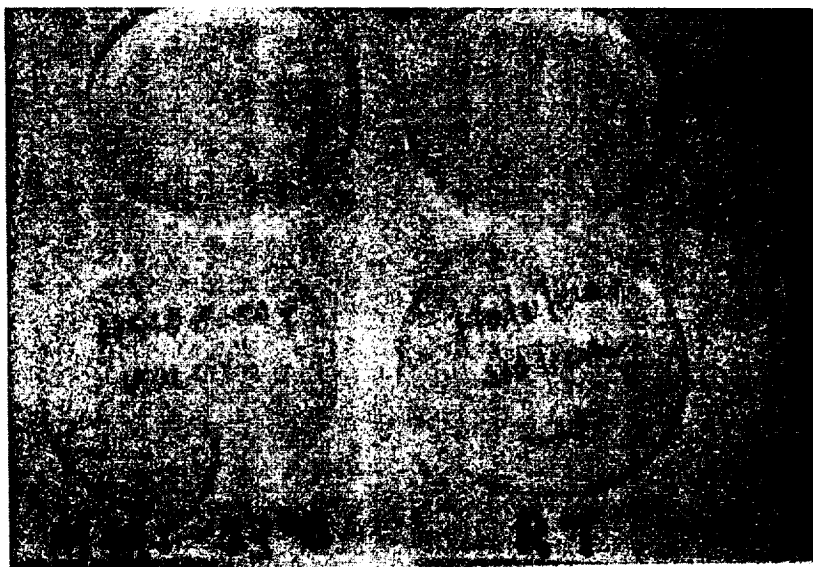


Figure 8. Mars Set and Earth Control Set – Haloferax volcani colonial color differences.

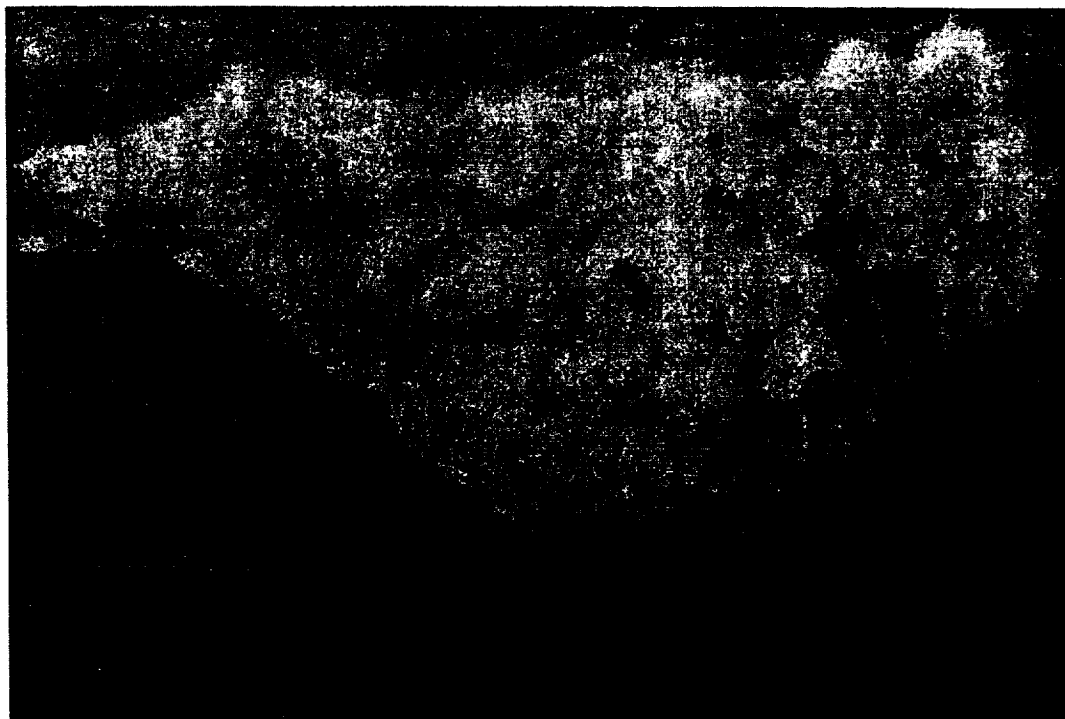


Figure 9. Searles Lake red salt crystals containing dormant halophiles.

Revolutionary Aerospace Systems Concepts-
Academic Linkage (RASC-AL)
Cocoa Beach, Florida, USA.
November 6-8, 2002

A NOVEL METHOD FOR CUTTINGS REMOVAL FROM HOLES DURING PERCUSSIVE DRILLING ON MARS*

Kris Zacny[†], Michael Quayle, Mara McFadden,
Adam Neugebauer, Kenji Huang and
George Cooper (Faculty Advisor)

University of California, Berkeley.

Acquiring samples from the subsurface of Mars poses many challenges. The scientific return increases with the depth from which the samples are obtained, but so does the risk. Thus, it is important to develop a fully autonomous drilling platform that will be capable of accessing the required depth and retrieving cores for scientific analysis. The method of drilling most likely to succeed will be a conventional mechanical core drill, either rotary or percussive, with a mechanical system for removing the cuttings and rock core from the hole. Instead of fluid flushing systems for removing cuttings, which would be very difficult to provide and in addition may contaminate the sample, an auger system is the best solution for rotary drilling. However, no such solution has been identified for the percussive drilling method. To solve this problem, a novel means of conveying cuttings out of the hole during percussive drilling has been developed and is presented in this paper. It relies on the reciprocating action between a pair of surfaces covered with bristles. Experimental results show that there is an optimum ratio of particle diameter to bristle length that gives the highest speed of particle conveyance. This new method also stabilizes the hole so that the drill string may be removed to recover a rock core sample.

1 Introduction

Pictures of Mars seem to reveal telltale signs of the presence of liquid water in the past: ice caps, dry riverbeds, and familiar erosion patterns. But where is the water now? The history of Mars' water is of the highest concern because in all experience on Earth, where there is water, there is life. Consequently, the natural first step in answering the question of life on Mars is finding water on Mars, and prior to that, developing the technology and instrumentation to do so. In order to gain the information necessary to develop techniques for searching for water on Mars, NASA has launched a comprehensive information gathering effort. NASA's series of Mariner and Viking missions has been returning pictures, atmospheric data and soil analysis since 1965. Currently the remote sensing

*Invention Disclosure, UC Case No.:B02-109, 'Method of Cutting Removal From Drilled Hole'

[†]Contact person, Department of Civil and Environmental Engineering; email: kzacny@uclink.berkeley.edu

missions, namely the Mars Global Surveyor and Mars Odyssey orbiters, are gathering photos and data while orbiting Mars. These photos indicate that if water is present on Mars, it is not visible on the surface. This, in addition to the inconclusive results of the Viking tests for life, suggests that if Martian water is going to be found, we are going to have to look below the surface. Thus in-situ sampling and analysis for water or bio-signatures must be the next step after remote sensing. Subsurface sampling methods have been explored in detail by numerous researchers including Blacic et al.² from Los Alamos National Laboratory. His work has led to the realization that drilling is the most likely means of recovering samples. As technology advances, an automated drilling and sample return mission to Mars becomes possible, but still poses daunting problems.

2 Problem Statement

In general, planetary exploration missions aim to carry out in-situ analysis and possibly return samples to Earth for more thorough examination. In particular, missions to Mars need such capabilities in the near future. Thus there is a strong interest in obtaining samples from below the surface.

The extreme conditions on Mars' surface and its great distance from Earth are the two largest obstacles to a drilling mission. Mars' atmospheric pressure is only one percent of Earth's atmospheric pressure. This has severe consequences because most drilling processes utilize compressed air or liquid to flush holes of the particles, or cuttings, that have been drilled. On Mars, the power necessary to compress the atmosphere to a useful pressure is more than it is reasonably possible to provide. Fluid, on the other hand, can not be used because it would freeze or evaporate and may contaminate the sample. The second obstacle on Mars, its great distance from Earth, requires any lander to be mostly autonomous. When Mars is in conjunction with Earth, the one-way communication delay is approximately twenty minutes. This delay would make attempting to operate a lander by remote control a virtual impossibility. In the following pages a plan for a simple, autonomous and efficient solution to these drilling problems is outlined. Major emphasis is given to the novel method of cuttings removal, which was invented specifically for a Mars-like environment that prohibits flushing fluids or air. First we examine the common methods of rock excavation.

3 Methods of Rock Excavation

The rock excavation process consists of two stages which can occur either simultaneously or separately. The first stage is breaking the rock and the second stage is the extraction of cuttings from the hole. Failure to remove the cuttings in time results in their being pulverized into progressively finer particle sizes without extending the hole, making drilling very inefficient. Similarly, the drilling process should be engineered to produce the largest particle sizes that may be conveniently removed. This is because in general, the most efficient drilling process produces the coarsest particles.

3.1 Mechanism of Rock Drilling

Rock drilling devices remove rock by one of four basic mechanisms, as shown in Figure 1: melting and vaporization, thermal fracturing, mechanical breaking, and chemical reaction.

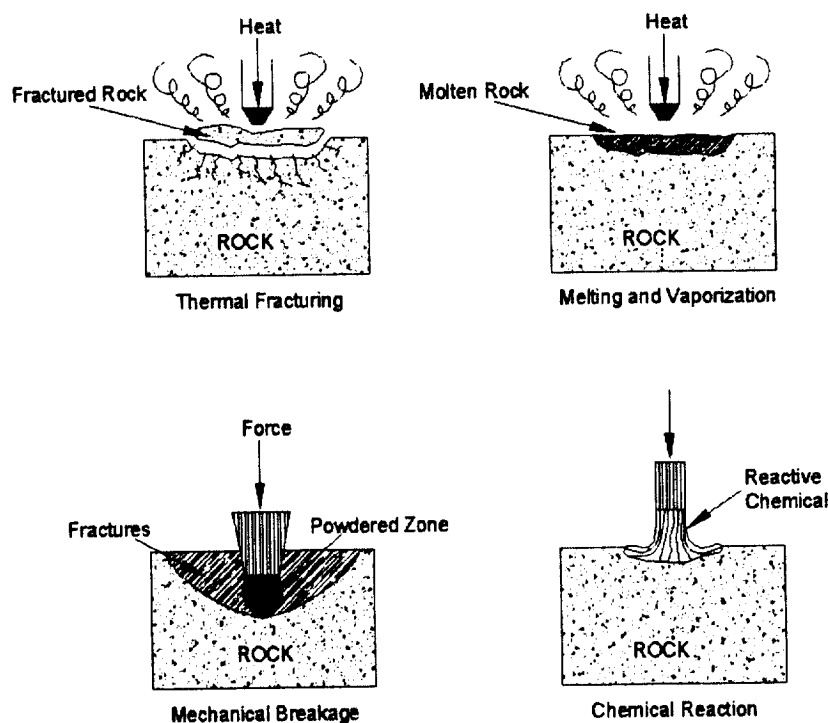


Figure 1: Basic methods of rock excavation.

Drills that melt and vaporize the rock such as laser and electron beams can not be used because they produce a change in the properties of the material being drilled. This same reason prohibits the use of thermally fracturing drills, because they might produce localized melting. Finally, chemical drilling can not be considered because it utilizes highly reactive chemicals to dissolve the rock. In addition, rock heating drills that thermally fracture the rock, can not be used because they produce localized heating and in turn change the properties of the rock. This leaves mechanical drills that drill the rock by impact, abrasion or erosion as the only reasonable method of acquiring samples. These mechanisms induce tensile or shear stresses, which exceed the rock strength and produce plastic yielding or brittle fracture. However, some of the mechanical drills such as jet drills, explosive charges, and pellet impact drills are not suitable, because they would contaminate the samples. Thus the drilling equipment most likely to succeed would be a conventional rotary or percussive core drill, with diamond cutting elements or tungsten carbide inserts, and a mechanical system for removing the cuttings and rock core from the hole.

3.1.1 Rotary Drilling

The clear benefit of using rotary drilling is that cutting removal can be accomplished using an auger; however this method has several drawbacks. First, rotary drilling requires both significant weight to push the bit against the rock surface and torque to turn the bit⁶. Both the weight on bit and rotational speed of the drill need to be carefully designed for specific rocks. On Mars, where the

gravity is only forty percent as strong as Earth's, the problem of adequate weight on bit becomes even more serious.

Drilling in Arctic^{7,9} has uncovered a more subtle drawbacks of drilling in extreme environments. Arctic drilling provides surface data, showing how rotary drilling performs in frozen rock and soils, specifically noting that rocks tend to get stronger as temperature decreases⁵. However, no experiments have been conducted in near vacuums, low temperatures, and carbon dioxide atmospheres. These parameters are important because diamonds, which will probably be used on the drill bits, tend to turn into graphite at temperatures above 870 Kelvin in carbon dioxide atmosphere due to their reaction with the oxygen in carbon dioxide¹. High temperatures like these can occur during dry cutting if the rotational speed or weight on the bit are large.

Furthermore, although an auger, which can be used with rotary drilling, has been used for centuries, little is known about how various parameters affect the drilling and cuttings removal processes. Terrestrial experience with augers shows that close 'hands-on' control by the driller is often necessary to ensure success. Thus it is not certain how well an auger will work on Mars under automatic or remote control conditions.

3.1.2 Percussive Drilling

During percussive drilling, the drill bit vibrates up and down. Rotation, if it occurs, is not essential to the rock breaking process. The impact of the bit onto the rock performs the drilling. Considering the limitations of rotary drilling, percussive drilling has several benefits that may prove it to be the superior drilling mechanism for use on Mars. Percussive drilling does not require any rotation or weight on bit because it uses high frequency impacts to fracture the rock. In addition, the drill bit may not require sharpening, can be made to operate at cryogenic and high temperatures, and can be used to probe unconsolidated formations like sand as well as very hard rocks like a basalt. Bar-Cohen et al.⁴ from JPL did extensive work with an ultrasonic drill, which very much resembles a percussive drill, and suggested that this form of drilling will be the most successful on Mars due its low power requirements. However, the major drawback with percussive drilling is that augers cannot be used for conveying cuttings from the hole bottom to the surface, unless the drilling device is made to rotate as well as reciprocate.

3.2 Methods of Cuttings Removal

Extracting cuttings from the hole is as important as breaking the rock itself. Failure to remove the newly crushed or cut rock results in them being pulverized into smaller particles. This makes drilling very inefficient. On Earth, liquid or gas is the most common method of cuttings removal. In addition to lifting the rock cuttings, the drilling fluid or gas also cools and lubricates the drilling bit; lack of lubrication would result in higher friction between the drill bit and the rock and thus larger heat production which can damage the drilling bit.

However, cuttings removal on Mars poses several special problems. Among these are the very low temperature (down to -150 degrees Celsius) and low atmospheric pressure (approximately 6 mbar). The low temperature precludes the use of liquids to remove cuttings from the hole as they might freeze. However, even if a drilling fluid was found with a very low freezing point, the use of it would be obviated by considerations of mass and sample contamination. Low pressure makes it unlikely that one will be able to use a gas flow for that purpose, since the energy requirement to compress a sufficient amount of the Martian atmosphere to blow the cuttings out of the hole is

prohibitive⁸. A closed cycle system could be developed to reuse the gas, but it should be ensured that the gas would not permeate the Martian rock. This could only be guaranteed if the rock was impermeable, and no such assumption should be made. A remaining possibility is to use mechanical means to lift the cuttings. Of the various methods that can be considered, Blacic et al.² of LANL have suggested that the auger may be the only candidate for rotary drilling. For percussive drilling however, there is no obvious solution.

4 Approach to the Cuttings Removal Problem

The most effective ways to lift cuttings out of a hole include circulation of fluid or air. However, if for any reason air or fluid cannot be used, an auger can do the job provided the drilling motion is rotary. In dry percussive drilling, however, the motion is up and down and there is no mechanism to lift the cuttings out of the hole. For this reason we have developed a novel means for conveying the drilled cuttings of a rock or soil-like material, characterized by having two opposed surfaces covered by angled hairs or bristles. Both sets of bristles point approximately in the direction in which it is desired to convey the cuttings, usually upwards. The two sets of bristles are placed close enough to overlap or just barely touch, depending on the diameter of particles being transported. The process is illustrated in Figure 2. As well as cleaning the hole, the new method also stabilizes the hole so that a drill string may be removed to recover a core sample, and then placed back in the hole. Such a system should be successful on Mars as it requires minimal supervision.

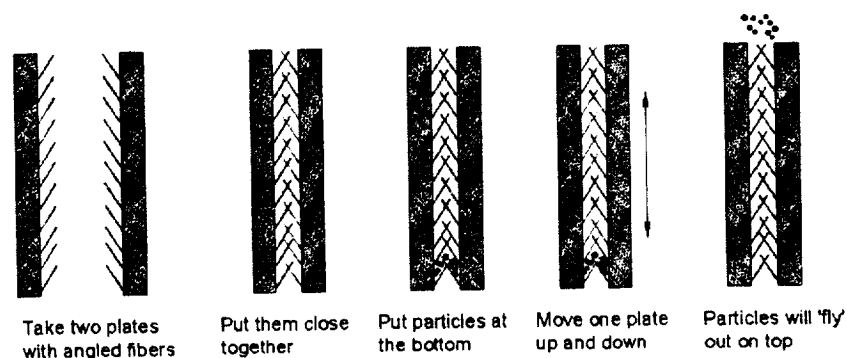


Figure 2: New method of lifting cuttings out of a hole.

The principle of the invention lies in the oscillatory motion of the two plates with angled bristles attached to them as indicated in the Figure 3. One plate can be stationary (but it doesn't have to be) and other one moves up and down with a low amplitude and high frequency. If a particle is trapped in one of the plates, the bristles of the other plate will scoop it out and transfer it to the other plate. This process lifts the cuttings out of the drilled hole.

4.1 Experimental Setup to test Cutting Removal Method

In order to test this theory of cuttings removal, we conducted a series of trials with an experimental apparatus simulating a casing and percussive core barrel. The experimental apparatus

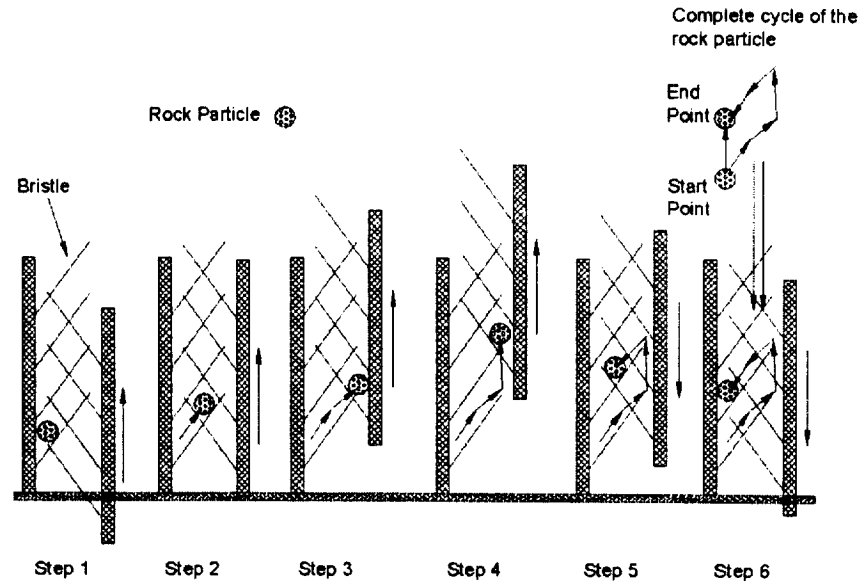


Figure 3: Principle of transferring of cuttings between the plates with the bristles.

Ski skin	Description	Length (mm)
Purple	Nylon plush laminated to cotton backing material	4.1
Blue Cow	Nylon plush laminated to synthetic backing material	4.3
Black	Mohair laminated to cotton backing material	3.2

Table 1: Length of bristles for given ski skins type

consisted of three main parts: a motor, an offset linkage, and two plates covered with bristles (Figure 4). The variable speed, electric motor was used to create a motion that simulates the vibrations of a percussion drill. The motor was connected to an offset linkage, which converted the rotation into a purely vertical movement of specified amplitude. The offset linkage was in turn connected to one of the bristled plates, while the other was held stationary. The two plates illustrated in Figure 5 correspond to the oscillating coring bit and casing of the drill mechanism. For the initial data, both the speed of the motor and the placement of the offset linkage were held constant, yielding a constant frequency and amplitude of vibration in the plates. However, in further research the amplitude could be varied. Rather than attempt to create plates of angled bristles, ski skins of various fiber types and lengths were used to cover the plates. The names of the ski skins together with the length of each fiber and type of the material is given in Table 1. Black Diamond Equipment, Ltd³ provided the ski skins, along with the data for the skins' material composition and hair length.

To gather the data, a standard procedure was followed for several fiber and cutting sample types. First, the apparatus was loaded with a small amount of simulated soil cuttings. The samples of river sand and glass beads of various diameters as shown in Table 2. The loading was done by laying one plate on its side and placing the cuttings below a specified start line. The second plate was then closed against the first, holding the sample in place, and the apparatus turned upright. At

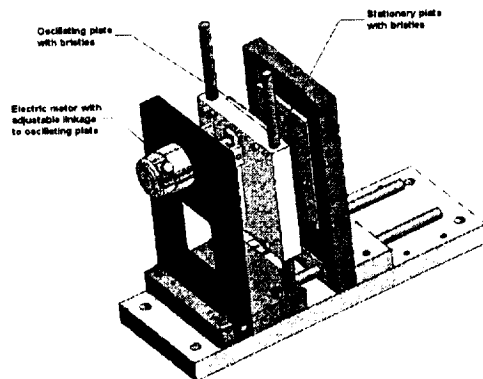


Figure 4: Cad drawing of Experimental Setup.

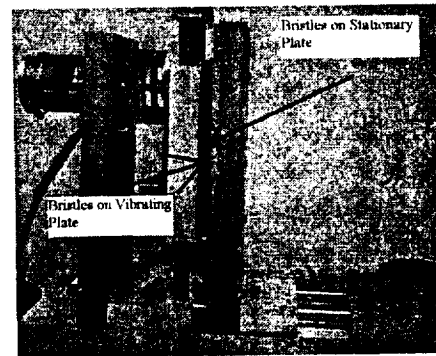


Figure 5: Photograph of Experimental Setup.

Particle type	Diameter (microns)
River Sand	< 75
River Sand	75-105
River Sand	75-105
River Sand	105-149
River Sand	149-177
River Sand	177-250
River Sand	250-295
River Sand	295-420
River Sand	420-590
River Sand	840-1190
Glass Beads	2000

Table 2: Particles used in the experiments.

a signal, the motor was turned on and a timing system started. When the first particle was ejected from the top of the plate, the time was marked. From this time and the known distance the particle had travelled, the velocity of each sample was determined; this was our independent variable. The velocity was then plotted against particle diameter for a constant fiber type, and a curve showing an optimal diameter-to-fiber length ratio was expected to be found. This procedure was performed for three different types of ski skin. For each set of variables a total of ten experiments was performed and the final results were averaged.

4.2 Experimental Results

We expected that the results of our experiment would show an optimum ratio between particle diameter and bristle length. Thus, we expect the graph of our results, velocity of particles vs. diameter of the particles, to take the form of a downward-pointing inverted curve shown in Figure 6. Given the length of the bristles, if the particles are too large or too small, they would move up slowly or not at all. Our task then was to determine this optimum ratio between particle diameter and bristle length. By extrapolating the results we also intended to be able to determine the best bristle length to use when given the size of particles that will be generated during percussive drilling.

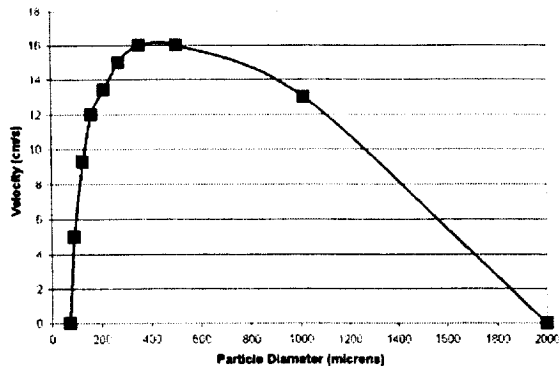


Figure 6: Anticipated shape of the curve.

The results of our initial experiments met our expectations as they showed a definite correlation between particle velocity and bristle length, given a particle size. Raw data for the experiment, using three different bristle lengths and a multitude of particle sizes, are plotted in Figure 7. Plotted in Figure 8 are the same data normalized against bristle length. Note that data points corresponding to zero vertical velocity were obtained when no particles appeared on top after an extended period of time.

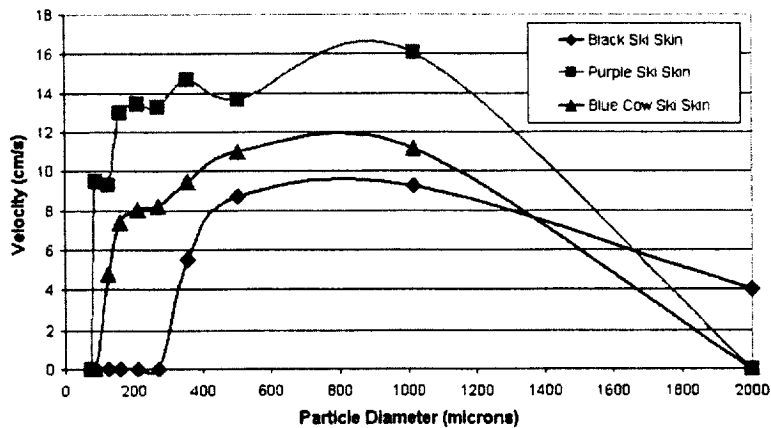


Figure 7: Cuttings removal results.

The results show that the purple ski skin proved best at handling most sizes of particles, from small (90 microns), to large (1015 microns). However, the purple ski skin failed to convey the large 2000-micron glass beads. The 'Blue Cow' ski skin transported all particles except 75, 90, and 2000 microns, the extreme ends of the range. However, across the range, it always had slower speeds than the purple ski skin. The black ski skin worked well for particles between 295 and 2000 microns, but failed to convey any particles smaller than 295 microns. Thus, each ski skin seemed to perform best with different sizes of particles. This is what we expect given the different bristle length of each ski skin. However, after normalizing the diameter of the particles against the length of the bristles we

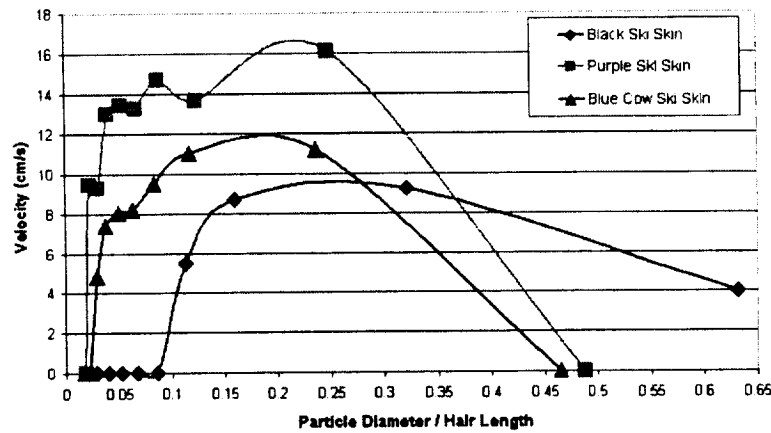


Figure 8: Cuttings removal results normalized against bristle length.

expected the peaks of the three curves to coincide. By comparing graphs with the raw data (Figure 7) and with the normalized particles diameter (Figure 8) it is clear that not only these peaks do not coincide but in fact they are shifted further away from each other. This leads to the conclusion that bristle length is not the only factor that needs to be considered. In order to explain these varying results we had to look at other physical characteristics of the ski skins such as areal density (number of bristles per unit area), angle between the bristle and the surfaces and material properties of the bristle, such as stiffness.

4.3 Discussion of Results

We believe that the angle between the bristles and the backing of the ski skin is the second most important factor after the bristle length. However, a close analysis of the results shows that this angle can also be influenced by the areal density and stiffness of the bristles. Thus when analyzing the effects of the angle, the stiffness and areal density of the bristles should also be taken into account.

If the bristles are very stiff, the angle with the vertical is maintained, whereas if they are very flexible the angle can be much larger as the bristles deflect under load. The amount of deflection could be due to two factors. Firstly, heavier particles would cause larger deflection than lighter particles. The second factor is the density of the bristles per unit area. If the density is too large, the bristles will tend to rub against each other and get stuck between each other. If this happens, bristles which are on the plate that momentarily moves down, can pull and deflect the bristles on the opposite plate down with them.

According to Black Diamond, the supplier of the ski skins, the skins are manufactured identically until the lamination process colors and coats the individual bristles on the skin. This lamination process definitely alters the stiffness of the bristles as well as their thickness. The larger thickness of the bristles in turn will alter the angle the bristles make with the vertical. We can assume that the initial density of bristles per given area before lamination and coloring was the same. Yet, because of the difference in thickness of the bristles, the resultant density of the bristles on different ski

skins could vary. We were only able to measure the lengths of the individual bristles, but could not determine the exact angles, stiffness and density of the bristles on the ski skins. However, we managed to evaluate the stiffness of each skin qualitatively. The black ski skin was found to be the stiffest of all, while the purple ski skin was the least stiff. The 'Blue Cow' ski skin was moderately stiff.

In ideal conditions, to determine the effect of ski skins length we could obtain ski skins that would only differ in bristles length, and all remaining factors like density, stiffness and angle of bristles would remain the same. Similarly, we could evaluate the effect of the bristles density, by keeping bristles length, stiffness and angle the same and varying only bristles density.

In addition, two experimental parameters need to be considered. The first parameter is the amplitude of vibrations, which together with bristle stiffness and areal density can alter the angle of the bristles. If the amplitude is larger than two bristle lengths and the frictional forces are large, the bristles can deflect 180 degrees until they are pointing down. Thus, by changing the amplitude we can alter the angle bristles make with vertical to the one that is desired. The second experimental parameter is the distance between the two plates. If the angle of the bristles is small and the distance between the plates is large, only large particles will be conveyed, while small ones will be stuck between the plate and the root of the bristles. If the distance is decreased or the angle increased, then these small particles could be scooped out and conveyed upwards as indicated in Figure 9.

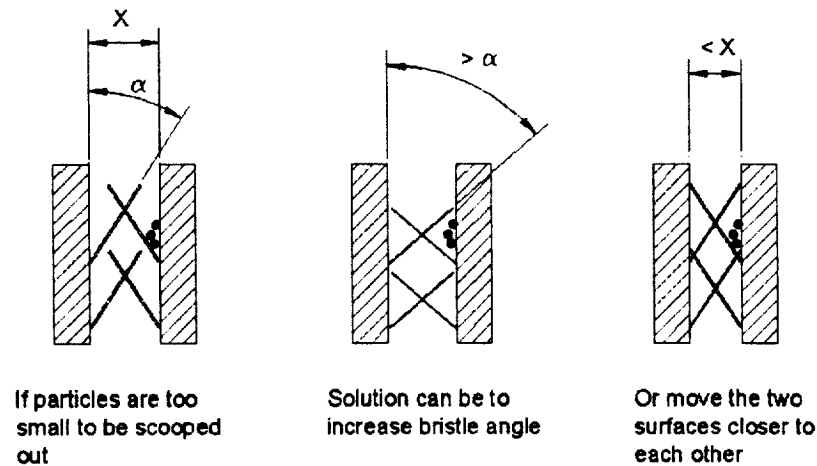


Figure 9: Effect of distance between the two surfaces covered with bristles.

Thus, we cannot assess with great accuracy the effect that bristle's angle, areal density or stiffness had on the performance on each ski skin. However, it is quite clear that these parameters together with the operational parameters like distance between the bristles and amplitude of vibrations affect the performance of the ski skins as well. Thus the main result is that bristle length can be viewed as the primary parameter affecting performance of the ski skins while secondary parameters are areal density, angle and stiffness of bristles.

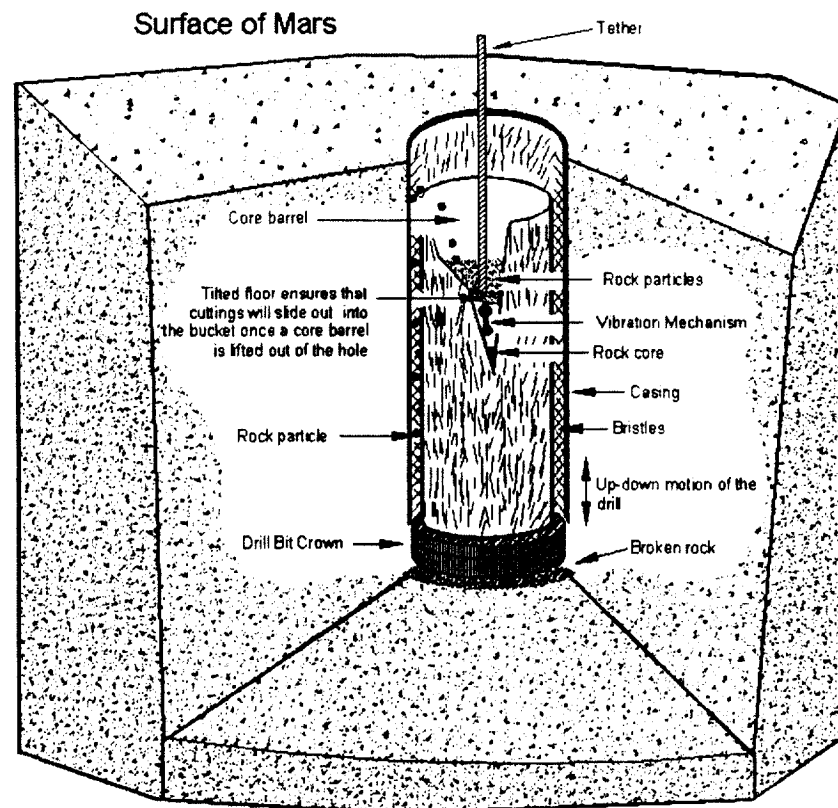


Figure 10: In-situ drill set up including casing.

5 Complete Percussive Drill Setup

Although the heart of our design is the novel way of conveying cuttings out of the hole, we decided to design a complete drilling apparatus. This set up includes a coring bit for crushing the rock, and a casing that aids in cuttings removal and stabilizing the hole. The bristles are placed on the inner side of the casing and the outer side of the drill or core barrel as indicated in Figure 10. The top of the core barrel/drill is open allowing the cuttings to fall inside and accumulate on top of the angled plate. Once the core barrel/drill is pulled out of the hole, cuttings will slide out into the surface container by gravity.

If a drilling setup is different from the one we described in this paper and it happens that the drilling string is continuous, each section of the drill string can have such a chamber. Thus if the lower one fills up, cuttings will be automatically transferred to the next level. It is also possible for the cuttings to be lifted all the way to the surface and entirely out of the hole.

The coring bit and casing are more closely described in the following sections.

5.1 Coring Bit

The coring bit consists of three main chambers and a tether cord, as illustrated in Figure 11. The purpose of the very top chamber is to collect fine cuttings that are conveyed from the hole bottom. The floor is slanted to aid in cuttings removal. Upon lifting the coring bit to the surface, the cuttings would slide out due to gravity into a bucket. These cuttings would be further conveyed into a pulverizer and examined by different instruments. The middle chamber houses the vibration inducing apparatus. This apparatus is part of a closed loop system where the frequency and amplitude are closely monitored and adjusted if necessary. The bottom chamber houses the rock core. Once the rock core fills up the chamber, its top surface would push against a latching system connected to the bottom of the coring bit, separating the core at the bottom and securing it so it does not slide out. The coring bit would have its outer wall covered with bristles. This would form a second surface required for conveying of cuttings out of the hole. The tether from which the coring bit would be suspended consists of a power cord that would provide electricity to the vibrating apparatus, a signal cord for control signals (this would be a part of closed loop feedback system), and a tensile cord for pulling the core drill out of the hole.

5.2 Casing

The casing, illustrated in Figure 12, serves three purposes. The first purpose is to aid in cuttings removal by having the inner surface covered with bristles. The second purpose is hole stabilization which is especially important when the coring bit is lifted out of the hole. The third purpose is to keep the coring bit vertically aligned and in turn keep the hole vertical. This would be required only initially, as once the core drill starts cutting the rock, the drilled rock core inside the core drill would keep the drill vertical. Sometimes, however, the rock core that is supposed to keep the drill vertical might shear. Then the casing would be employed once again to guide the coring bit vertically. As an added benefit, the casing can have small slots cut out in its surface at different places. These slots can be very useful if at the end of coring process, a hole is to be used for in hole measurements. Many instruments can be lowered into such holes and in-situ measurements of the rock strata can be obtained.

6 Conclusions

A novel means for conveying the drilled cuttings during percussive drilling, characterized by having two opposed surfaces covered by angled hairs or bristles is described. Both sets of bristles point in the direction in which it is desired to convey the cuttings. As well as cleaning the hole, the new method also stabilizes the hole so that a drill string may be removed to recover a core sample, and then placed back in the hole. This method of cuttings removal was developed for drilling on Mars where conditions preclude the use of air or a flushing fluid for this purpose. The paper also describes a complete percussive drilling set up that could be used in the sample retrieval mission on Mars.

Experimental data showed that there is a relationship between particle size and bristle length for optimum cuttings removal. For different sets of surfaces we found an optimum diameter of particles that resulted in the fastest rate of particle removal. This optimum ratio differed between different types of surfaces pointing to the fact that length of bristle is not the sole factor that determines the rate of particles removal. Other parameters such as areal density of bristles, stiffness of bristles and

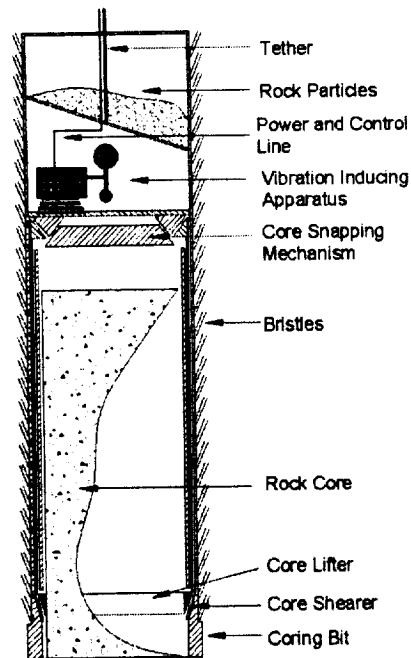


Figure 11: Percussive Coring Bit

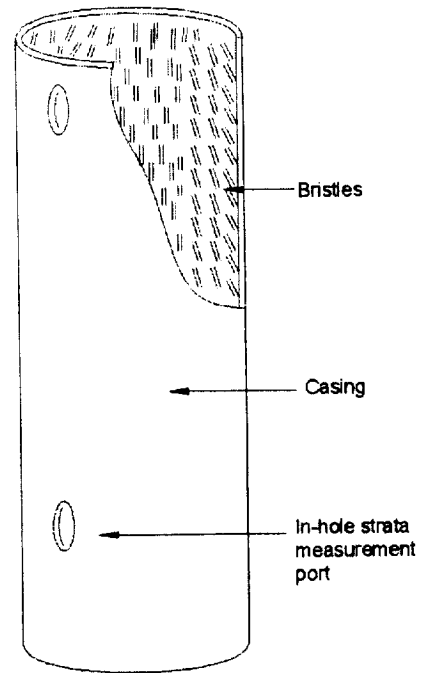


Figure 12: Casing.

the angle that the bristles make with the vertical must also be considered.

The operational parameters of the percussive drill, namely the distance between the two surfaces covered with bristles and the amplitude of the percussive drilling action can also alter the performance of the drilling system.

The problem with heat build up due to lack of circulating drilling liquid or gas can be overcome by stopping the drill periodically to let it cool.

7 Future Studies

We plan to improve and expand upon our research in two primary areas: first, by refining our data collection methods, and second, by broadening our data analysis. To complete our first goal of refining our data, we plan to normalize the velocity measurement by precisely measuring the frequency of the plate, and accurately gauge the particle speed by analyzing a digital video of each trial. The frequency of the plate can be easily measured by shining a laser just above the top of the oscillating plate, and placing a photo sensor behind it. The signal of the photo sensor can then be converted into the frequency of the plate. Digital video will yield a more precise measure of velocity because each trial can be viewed at a greatly reduced speed, and compared to the time between each digital frame. This will eliminate the inevitable human error involved in timing. For our second goal, broadening the data analysis, the parameters identified as the most prominent, i.e. angle, density, and stiffness of bristles can be measured precisely along with bristle length. This will allow us to determine which of the above parameters might be optimized for maximum performance,

and will yield a more thorough analysis of the data recorded.

In addition to improving our experimental methods, the plans for the future of this research include new applications for this idea. Any field that requires the transportation, primarily lifting, of fine particles could benefit from this new method. For example, the agricultural industry often moves large amounts of grain from silos. Using this method, a closed tube of concentric cylinders could convey the particles with no losses to the environment, and take up considerably less space. We are continuing to develop further ideas for applications and modifications to this simple and efficient conveyance system.

8 Outreach

The Mars Drilling Group has participated in various ways to reach out to the community. Prior to becoming a specialized entity at Berkeley, the Mars Drilling group was part of a broader research class named *Mars 2012*. Every year the class adds its own unique flair to Cal Day, a celebration of UC Berkeley's vast and varying extracurricular activities. We created interactive presentations to give visitors to Berkeley a hands-on experience of our research (Figure 13). In 2001 the class took home the 'Most Interesting Display Award' from the facilitators of Cal Day.

To reach out to the community beyond Berkeley, the Mars Drilling group participated in a science fair organized by Oakley Junior High School in Oakley, California. The fair was an exciting effort to combine the imagination of local students of all grades with the experience of area businesses and colleges. At the fair we showcased our research activities and presented interesting facts about Mars, explaining and demonstrating research items to adults and children alike. We also were able to volunteer as judges for the projects of local students.

We have also reached out to the greater scientific community for their feedback and experience. We held videoconferences (Figure 14) with both Johnson Space Center and NASA Ames Research Center, where we presented our projects to NASA scientists for input and review. These links between current and future scientists have provided a wealth of knowledge and experience not available from research alone.

Presently, our group aims to involve local high school students in our research. In an effort to give them a taste of things to come, we plan to have a few interested students from Berkeley High School come to our lab to learn and participate in our research activities. So far, we have one enthusiastic student that comes for every meeting, but we anticipate more soon. Who said that beginnings are easy?

9 Acknowledgements

We would like to extend our thanks to Professor Frank Morrison for his financial assistance and Mr. Liang Yu for the drilling animation. Last but not least, we would like to extend our gratitude to the Black Diamond Equipment Company for supplying ski skins.



Figure 13: Outreach during Cal Day

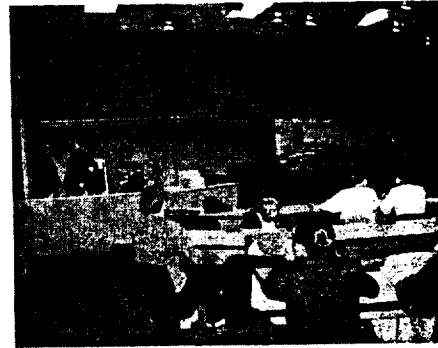


Figure 14: Videoconference with NASA scientists.

References

- [1] A. Bakon and A. Szymanski. *Practical Uses of Diamond*. Ellis Horwood, 1993.
- [2] J. Blacic, D. Dressen, and T. Mockler. Report on conceptual system analysis of drilling systems for 200m depth penetration and sampling of the martian subsurface. Technical Report LAUR00-4742, 2000. GeoEngineering Group, Los Alamos National Laboratory.
- [3] Ltd. Black Diamond Equipment. <http://www.bdel.com>.
- [4] Y. Bar-Cohen et al. Ultrasonic, sonic drilling, coring (usdc) for planetary applications. In *Proceedings of SPIE's 8th Annual International Symposium on Smart Structures and Materials*, Newport, CA, March 2001. 4327-55.
- [5] R. Heins and T. Friz. The effect of low temperature on some physical properties of rock. *American Insitute of Mining, Metallurgical and Petroleum Engineers*, (SPE 1714):189-196, 1967.
- [6] Rao Karanam and B. Misra. *Principles of Rock Drilling*. A.A. Balkema Publishers, 1998.
- [7] John McCoy. Performance of a williams auger in permafrost. *US Army Snow Ice And Permafrost Research Establishment, Corps of Engineers*, Special Report 38, January 1960. Wilmette, Illinois.
- [8] R. Schoepfel and A. Sapre. Volume requirements in air drilling. *American Insitute of Mining, Metallurgical and Petroleum Engineers*, (SPE 1700):49-56, 1967.
- [9] P. Sellmann and M. Mellor. Drill bits for frozen fine-grained soils. *Cold Regions Research and Engineering Laboratory, US Army Corps of Engineers*, Special Report 86-27, August 1986.

Project Endurance: Six 90-day Missions on the Lunar Surface

University of Maryland, College Park
Department of Aerospace Engineering, Undergraduate Program

Theresa Battaglia, James Clark, Michael Collins, Suneal Gupta, Todd Herrmann, Drew Hykin, Mark Kimball, Brian Kujawa, Benjamin Lee, Yan Lui, Kajal Pancholi, Matthew Schnaubelt, Joseph Simons, Troy Sookdeo, Joseph Stecher

Advisors: Dr. David Akin, Dr. Mary Bowden

Abstract

In the hopes of paving the way for a permanently inhabited moon base, a six-mission program was designed, with missions being flown yearly from 2013 to 2018. Each mission will consist of a “habitat module” and an “ascent/descent module.” These modules will be launched on a Delta IV rocket and a Space Shuttle, and will then connect with booster stages in LEO before finally reaching the moon. Throughout each mission, four crew members will explore the lunar surface in detail, conducting various scientific experiments over their 90-day stay, with the goal of expanding knowledge of the lunar environment. Missions will explore both the near and far sides of the moon, with communication satellites providing a link to far side missions.

Introduction

In the early 1900s, Antarctica was a vast and virtually unexplored region of the world. Sir Ernest Shackleton decided that he would be the first person to cross the barren continent, and so in 1914, he set sail on the ship *Endurance*. During his voyage, however, his ship became trapped in ice and was destroyed. Shackleton and his crew miraculously survived the long winter night on Elephant Island and a perilous open boat crossing of the Antarctic Ocean. Though Shackleton did not succeed in his endeavor, his brave voyage paved the way for future explorations of the continent.

His story is the basis for Project Endurance. Just as Shackleton’s voyage opened the door for future Antarctic explorers, so did the Apollo program open the door for the detailed lunar exploration of Project Endurance. This series of six missions will pick up where the Apollo program left off, 40 years later, and hopefully lead the way for the first permanently inhabited moon base.

Site Selection

The six sites chosen were selected to provide the greatest scientific and exploratory return. Each site needed to have a 500-meter-wide portion of terrain, with slopes of less than 15 degrees, to allow for safe landing. Geological features, mineral concentration, the possibility of studying the formation of the moon, unique terrain, and possible ice deposits were some of the criteria considered in the site selection process. All sites also had to be within certain bounds in order to maintain constant communication with Earth. The sites chosen are as follows: Copernicus Crater (2013), Tycho Crater (2014), Korolev Crater (2015), Aitken Basin (2016), Apollo Crater (2017) and Mare Imbrium (2018).

Mission Architecture

Each mission will consist of a habitat module with seven boosters and an ascent/descent (A/D) module with four boosters. The A/D module will leave a trans-Earth injection (TEI) stage with a heat shield in low lunar orbit (LLO) when it descends to the Moon. Throughout the 90-day mission, the crew will live and work in the habitat module. They will use lunar rovers to travel and collect samples. At the end of the 90 days, the crew will ascend in the A/D vehicle to dock with the TEI in LLO, leaving the habitat module, lunar rovers, and descent stage on the lunar surface, and will then return to Earth.

Trajectories

The approximate ΔV 's for the mission are summarized in the following table:

Path	ΔV (m/s)
LEO to LS	6247
LS to ES	2890
LEO to LLO	3844
LLO to ES	837
LLO to LS	2706
LS to LLO	2334

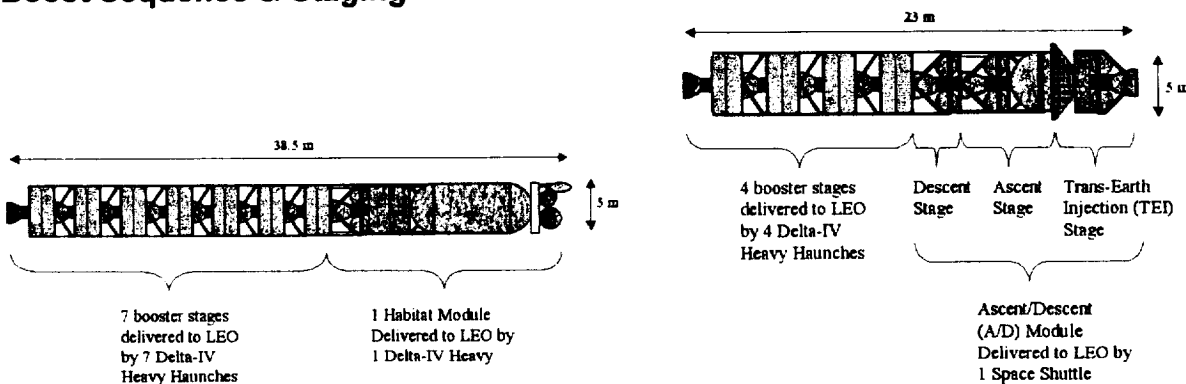
**LEO: Low Earth Orbit, LLO: Low Lunar Orbit,
LS: Lunar Surface, ES: Earth Surface**

The chosen transfer method from low earth orbit to lunar orbit is a one-tangent burn with a transfer time of approximately 3.46 days. This method was chosen because it provides a relatively short transfer time at a small ΔV cost.

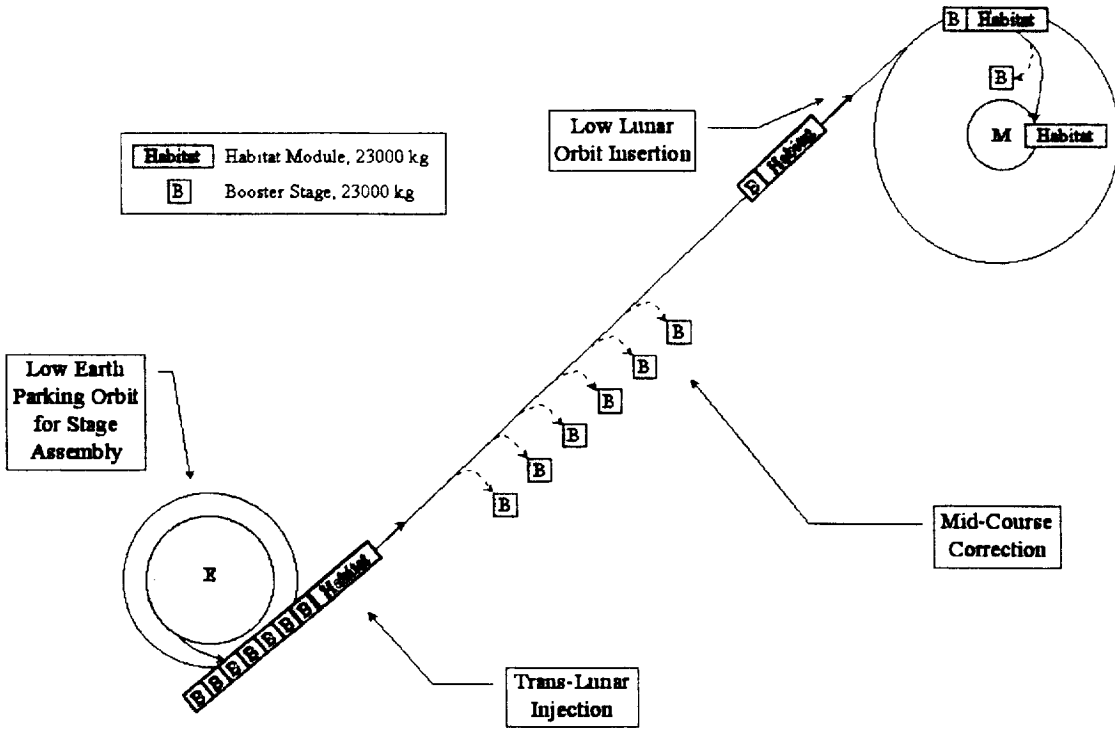
Attitude Control

The habitat module, ascent stage, and TEI stage each have 16 attitude control thrusters for all-axis rotational control. Each booster stage will also have at least 16 thrusters. The first 3 boosters launched into LEO, however, will contain 32 thrusters, in order to provide extra maneuvering ability to compensate for their prolonged exposure to atmospheric drag.

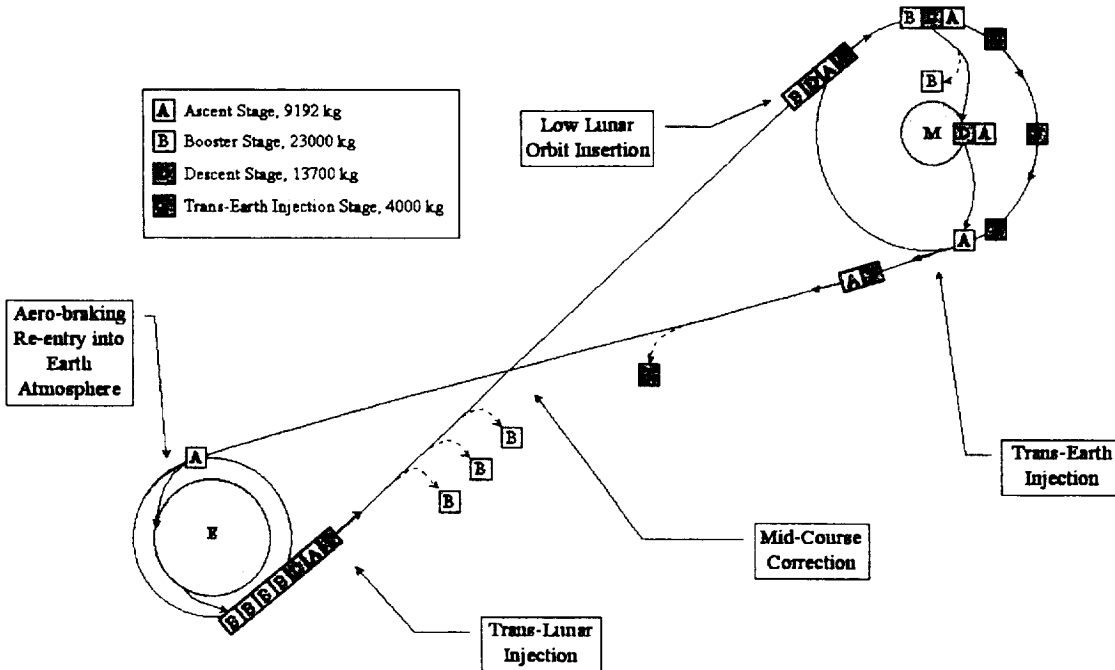
Boost Sequence & Staging



Habitat Module Trajectory



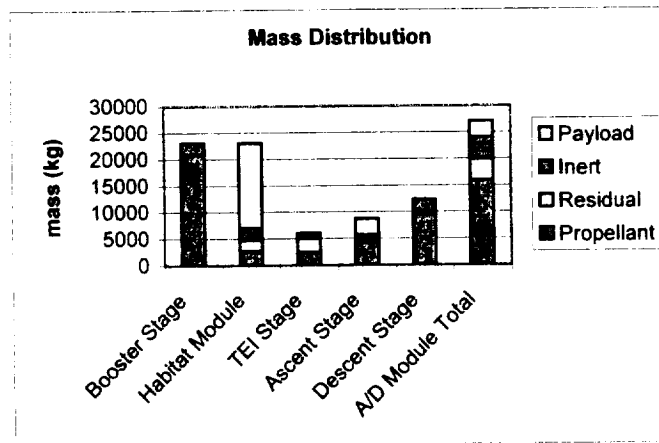
Ascent/Descent Module Trajectory



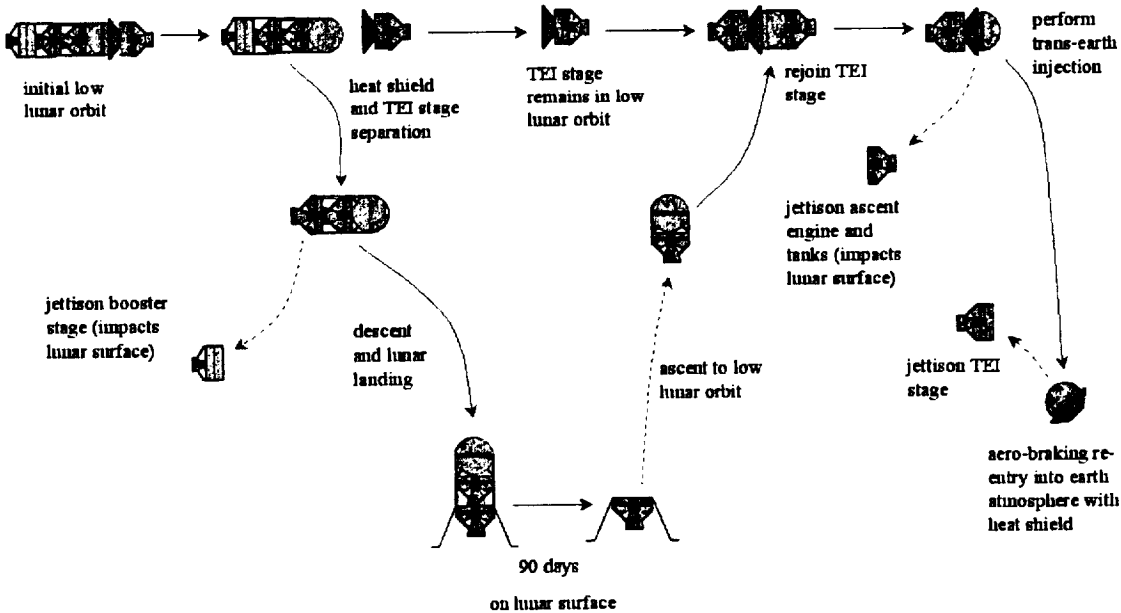
Payloads & Landed Masses

A breakdown of the total mass by vehicle component is shown in the following figures:
(all masses in kg)

	Payload	Inert	Propellant	Residual	Total
Booster Stage	-	2300	20700	0	23000
Habitat Module	16000	2300	2617	2083	23000
Ascent/Descent Module					
TEI Stage	-	1000	2386	2614	6000
Ascent Stage	3000	868	4168	648	8684
Descent Stage	-	2300	9305	710	12315
Total	3000	4168	15859	3972	26999



Return Scenario



Abort Scenarios

The TEI stage has been designed with a good deal of residual propellant, so that in the worst-case scenario, where its orbit has rotated 180° from the landing site, it can perform the needed inclination-changing burn. Once re-aligned with the landing site, the ascent module can rejoin it and return to earth.

Attitude Control

There are four main types of disturbance torques: gravity gradient, solar radiation, magnetic field, and aerodynamic. While each booster stage waits in orbit for docking with the other stages and the habitat or ascent/descent module, the relative weakness of solar radiation makes its presence almost negligible. As the spacecrafts leave low earth orbit, the solar radiation torque becomes more prominent since the other three are dependent upon orbital altitude (aerodynamic torque and magnetic torque disappear the quickest).

In order to maintain the proper attitude while in low earth orbit (it is important to avoid exposing a large cross-section to drag and losing too much altitude before rendezvous), extra attitude thrusters are required. This depends on how long each booster stage remains in orbit. The attitudes of some boosters may be intentionally changed to a non-optimal configuration in order to meet up with boosters that have a slightly lower orbit.

The habitat module will be landing first and requires a radar system to avoid any obstacles larger than one meter. This is a derived requirement from another: that the spacecraft be able to land on a 15 degree slope with a 1-meter obstacle. Since they are not designed to handle anything greater from a structural point of view, a collision avoidance system is necessary to ensure crew safety.

Once the ascent/descent module is within 15 miles of the habitat module, the states of both will have to be known very accurately by the ascent/descent module's onboard navigation system. In order to obtain the proper degree of accuracy, rendezvous radar measurements (range and range rate) will be taken from an altitude of 15 miles, until the crew can spot the habitat module. The attitude control engine chosen for all these applications is the DMT-600.

Docking Operations

The docking procedure will be fully automatic, and will closely resemble the current Kurs system. Automatic docking allows for greater flexibility in the launch windows of the boost stages, which is necessary as the period between Delta IV flights is restricted. The general operations for the docking procedure are outlined in the following table:

Time Before Docking (mins)	Operation
440	Radio rendezvous systems are activated on approaching vehicle
425	Transponder on target vehicle is activated
300	Distance closed to approx. 2.5 km
240	Distance closed to approx. 0.6 km
200	"Flyaround," the alignment process between the two docking ring antennas, begins
120	Flyaround complete, distance closed to 0.2 km
10	Probe deployed on approaching vehicle
0	Docking complete

Note that while this setup is similar to the Kurs system, it takes place over four times as long of a period. This is done to reduce the magnitudes of the relative velocities over final approach, which results in smaller docking loads than Kurs.

Landing Legs

The landing system is one of the most critical systems for each vehicle. In order to reduce the forces on the craft at landing, aluminum honeycomb shock absorbers will be used. The shock absorbers chosen are the Alcore Spiral-Grid with a crush strength of 9000 psi. Normally, the force on each leg at landing would be so high that the legs would have to be several hundred kilograms in order to avoid yielding. However, by placing a long section (~2 m) of Spiral-Grid in the load-bearing portion of the legs, the stress in that part is kept to only 9000 psi. The actual forces exerted on the legs, their corresponding accelerations, and several other values are summarized below.

Property	Habitat Module		Descent Module	
	Value	Units	Value	Units
Tread	7.0	m	7.0	m
Maximum Crush Length	1.469	m	1.304	m
Total honeycomb Length	2.099	m	1.863	m
Lower Leg Length	1.469	m	1.304	m
Spiral-Grid Crush Stress	62.1	Mpa	62.1	Mpa
Spiral-Grid Density	812.5	kg/m ³	812.5	kg/m ³
Spiral Grid Cross Section	0.001264	m ²	0.001086	m ²
Total Mass of One Leg	17.92	kg	14.69	kg
Mass of All Four Legs	71.68	kg	58.76	kg
Worst Case Force	313700	N	269700	N

Habitat Module Structure

The habitat module consists of a two-level pressurized living area, a power systems level, a cryogenic storage level, landing legs, and a 240-kN descent engine.

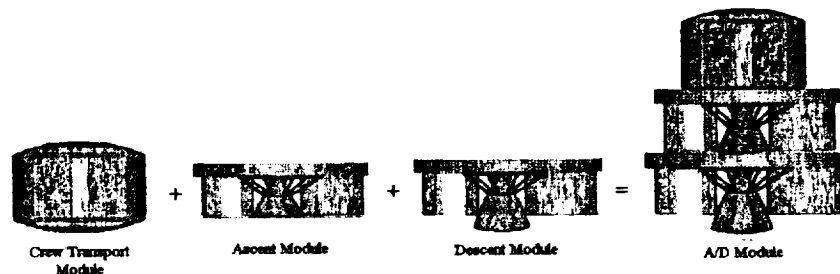
The habitat will experience launch accelerations of 4.5g vertically, with side loadings of 1.5g. Including dynamic loads such as vibration and staging shocks, the payload can experience combined loads of up to ± 3 g laterally, and from -2 to $+6$ g vertically. The pressure hull will only support its own mass during launch, so pressure loads cause the critical stress. The worst-case loading situation would occur if the hull failed to depressurize as it ascended through the atmosphere after liftoff.

To prevent the pressure hull from buckling, ribs and stringers will be used to support the forces caused by the launch accelerations. The worst-case loading that may occur would be the combined load of $+6$ g acceleration axially and $+2$ g acceleration laterally. The stringers have an I-beam cross-section, with overall dimensions of 8 cm by 8 cm, and web and flange thickness of 3.5 mm.

	Stress (kPa)	Load Condition	FOS	Margin
Pressure Hull - walls	126.3	Internal pressure	3.0	+0.10
- bulkhead	86.7	Internal pressure	3.0	+0.59
Stringers	79.3×10^3	Launch loads	2.0	+0.29

Ascent/Descent Module Structures

The ascent/descent module consists of three separate modules joined together; they are the crew transport module, the ascent module, and the descent module.



The specifications for the crew transport module are as follows: a 2-mm-thick, 2-meter-high cylindrical tube with a radius of 2 meters is attached to a 2-mm-thick hemispheric shell with a height of 0.5 meters and a curvature radius of 4.25 meters. Inside the pressure shell will be a structural cage that will support and distribute loads throughout the shell. The cage's structural members work by acting as stiffeners, and increasing the moment of inertia at different locations. The structural cage will also be used to attach life support and other vital equipment to the transport module. The descent module is the second structure of the A/D module. Its purpose is to land the A/D module after it enters lunar orbit.

To allow for a controlled landing, the descent engine must be able to throttle and rotate. This requires a thrust structure designed to hold and transfer its loads onto the ascent docking module and the transport module. The thrust structure must be designed not just to handle vertical loads, but also angular loads.

The ascent module is a structure whose purpose is to launch the crew back into orbit to meet with the orbiting TEI stage. It carries a smaller engine along with its fuel, and will separate via pyrotechnics. After separation, the ascent module's engine will ignite, sending the module back into lunar orbit. The ascent module's thrust structure is similar to the descent module's, but is smaller because it holds a smaller engine, and is only designed to transmit vertical loads.

Structures	Loads Source	Safety factor	Margin of Safety
Pressure Shell	Atmosphere	3.0	.3
Cage + Shell	Reentry/Landing	2.0	.1
Floors	Equipment/Crew/Landing	2.0	.16 and .2
Thrust structures	Launch	2.0	.2
Landing legs	Landing	2	1.08

Air Revitalization

Atmosphere must be generated or supplied on the lunar surface. This makes atmosphere generation and revitalization a necessity. Through water electrolysis, hydrogen and oxygen can be recovered through dissociation of water molecules. Point-eight-four kilograms of oxygen per person per day, along with stored nitrogen, can be vented into a pressure vessel, similar to filling a balloon. One kilogram of carbon dioxide per person per day can be removed from the atmosphere, before displacing vital oxygen, through regenerative carbon dioxide removal systems. An earth-like atmosphere can be maintained for maximum comfort.

Using the ideal gas equation, $PV=nRT$, one can calculate the critical elements inside the pressure vessel. By maintaining 57.6 kg O₂ at 32 kPa and 70.2 kg N₂ at 30 kPa, a stable, habitable, and ultimately viable atmosphere is achieved. This is agreeable for EVAs, fire containment, and overall mission fluidity.

Food

Nutritional standards will be met by using the foods available to Apollo astronauts, including: beverages, breakfast items, cubes and candy, desserts, salads and soups, sandwich spreads and bread, and meats. The crew will maintain a healthy and balanced diet that is pre-selected prior to mission launch.

Each crewmember receives up to 1.8 kg of dehydrated food per day. Rehydration is accomplished through a water dispenser that pierces the rubber septum on the food bag or, "spoonbowl," and inserts the desired amount of water for rehydration. Available are two meals per person per day with 24-hour access to nutritionally-selected snacks and candies. There is enough food to support 99 days of lunar exploration for a four-person crew, thus meeting the mission requirements.

Water Reclamation

The water reclamation subsystem consists of three main components: storage tanks, water use items, and a filtration subsystem. Water is used for drinking, food preparation and hygiene. The first table below summarizes water uses. The main components of the filtration subsystem are a vapor-phased catalytic ammonia removal (VPCAR) distiller and a multifiltration bed. The VPCAR system is redundant, and a reverse osmosis filter acts as a backup to the VPCAR system. Before the cleaned water flows into the potable water storage tank, a quality control station for contaminants checks the water. The second table below shows the entire system mass and power breakdown.

Input	kg
Water in food	0.23
Food Prep Water	1.68
Drink	1.62
Metabolized Water	0.35
Hand/Face wash water	4.09
Shower Water	2.73
Urinal Flush	0.50
Clothes Wash Water	4.18
Dish Wash Water	0.00
Water needed per person/day	15.30

System Summary

Water Savings Per Person	15	kg per person, per day
Total Water Use	498	kg per day
Equipment Mass	340	kg for entire mission
Power Use	1.3	kW Continuous
System Mass	837	kg total

Water Usage	Mass (kg)	Power (W)	Vol (m ³)
Toilet (2)	40	72	0.523
Sink (3)	48	0	0.432
Shower (1)	22	0	1.52
Hot Water Heater	20	522	0.05
Washer / Dryer	91	1400	0.33
Plumbing	100	0	0.005

A/D Crew Systems

The A/D module crew systems are 100% re-supplyable. The A/D module carries enough atmosphere and water for four astronauts to survive twelve days, three to the moon, three to earth, and six emergency. Its cabin is pressurized at 62 kPa with the exact same partial pressures as the crew habitat module. Carbon dioxide is scrubbed using non-regenerative four-bed molecular sieves. Water available constitutes water used in drinking, hygiene, and urine flushing.

There is no airlock, only a hatch. The atmosphere is completely vented during EVA from the A/D module, and must be resupplied. The module carries enough atmosphere to depressurize and re-pressurize three times (once upon landing and two emergency, in-flight depressurizations). The g-couches are stored on the ceiling and a safe distance from the radioactive DIPS power system onboard.

Radiation Remediation

For long-term interplanetary missions, the dangers of radiation exposure become a major limiting factor. Adequate amounts of shielding are needed to prevent harmful doses accumulated over the course of the mission and large short-term doses in the event of solar flares. For each mission, each astronaut will be subjected to a maximum radiation dose of 50 rem. To keep the dosage at this level, shielding must be present during all phases of the mission.

Shielding on the ascent/descent module provides protection while passing through the Van Allen radiation belts during transit to and from the moon. A total of 10 % of the entire mission radiation dose is accumulated during transit. Once on the surface of the moon, the astronauts spend their time in one of three places: crew habitat module, sleeping/storm shelter area, and on EVA. Combined, 30 % of the entire mission radiation dose is incurred during the lunar surface stay. The remaining 60 % is reserved in the event of two large solar flares in which each astronaut is exposed to a 15 rem short-term dose per flare in the polyethylene storm shelter.

Fire Protection

Fire detection and suppression systems are in place on both the ascent/descent module and habitat module. The systems are comprised of smoke detectors, visual and audible alarms, portable breathing apparatus, portable fire extinguishers, and suppression ports located throughout the modules. Each system has a 99.9 % probability of working in the event of a fire.

Medical Supplies

The habitat module is equipped with an extensive medical supply. The inventory consists of diagnostic and laboratory equipment as well as therapeutic and resuscitative medications and equipment. The two main kits in the medical supply are the Medications and Bandage Kit (MBK) and the Emergency Medical Kit (EMK). The MBK consists of oral medications, bandaging materials for minor abrasions, and topical medications. The EMK consists of intravenous medications, diagnostic items, and instruments to perform minor surgery. Medical supplies in the ascent/descent module are scaled-down versions of those aboard the habitat module and are designed to provide adequate treatment until reaching the habitat module or returning to earth.

Data Management

The computer systems in the habitat will be required to run many, if not all, of the habitat's life critical systems. These systems will include all equipment that is essential to keeping the crew of the mission intact and fully functioning. They will also include the systems that can help the crew to successfully leave the habitat and arrive back to Earth or any space station for rescue. These life-critical systems also pertain to all sensors inside and outside the habitat such as air, temperature, pressure, human biological, radiation, and communication sensors.

Along with the main computer system, each crew member will have a laptop for their individual use on research experiments they are conducting. These laptop systems can be connected to the main computer system through Ethernet connections, allowing the crew members to have access to data being acquired by the main computer system.

Sensor Systems

Sensor systems are located throughout the habitat and A/D module inside and out. Sensors are used for signifying the tolerable and intolerable levels of the system being monitored. Each system is being monitored to make sure that it is operating at a nominal, safe level, or a level that is suitable to the crewmembers. These systems monitor the critical systems for the mission and are composed of primary and secondary systems, which are key elements to crew safety and mission success. These systems include pressure, temperature, oxygen level, water reclamation, radiation, audio and video communication, controls, navigation, and guidance.

Thermal Control Systems

The two most important requirements of the thermal control system will be to minimize the heat flow out of the habitat module and to dissipate the excess heat generated by the humans and electronics onboard. This electronics include the computer, laptops, and the crew systems equipment. In minimizing this heat flow, this thermal control system must account for a number of external heat sources, including solar heat and the albedo effect and infrared heat from the Moon's surface. Also, this thermal control system will be designed to protect the habitat module from micrometeoroid debris.

Project Endurance will utilize multilayer insulation as its only form of a passive thermal control system. Multilayer insulation is a type of high-performance insulator, which uses multiple radiation heat transfer barriers to retard the flow of energy. After consideration of many different types of outer layers, a beta cloth was chosen to be draped around the outside of the entire structure of the habitat module. On the inside of the structure, next to the pressure vessels, will be placed 20 alternating layers of reflector and separator layers. The materials chosen for these layers are goldized Kapton and Dacron netting, respectively.

An active thermal control system (ATCS) is used in addition to a PTCS when the latter is inadequate, as is the case in manned missions. In addition to blocking out the damaging effects from the outside, a system is also needed to maintain a comfortable temperature level within the modules, in order for the crew and all of the electrical equipment to function properly. For Project Endurance, the inside cabin of the habitat module will be maintained at a temperature range of 16 – 24 °C (60 – 75 °F). The total amount of heat generated, by the astronauts, water

reclamation system, oxygen generation assembly, computer and laptops is 4060 watts. In order to dissipate all this heat that is generated, multiple components, which are outlined below, must be utilized.

Cooling plates will be mounted on the water reclamation system, the oxygen generation assembly and the computers. There will be a total of 12 cooling plates used around the habitat module, and will be placed as follows:

- 4 – 1 on each of the computers
- 3 on the water reclamation system
- 4 on the oxygen generation assembly
- 1 utilized for the air cooling system

In order to dissipate the rest of the heat, generated by the humans and the laptops a duct will be placed on the floor of the bottom level, and will contain a cooling plate. Air will be directed over this cooling plate, and will then be transferred to the top of the habitat module.

The types of pumped loop systems utilized by Project Endurance are water and ammonia coolant loops. The water loop uses cold water that is pumped through pipes located in the walls of the module. These loops will surround the crew cabin, and run through the cooling plates, including the one used for the air-cooling system. This loop will then transport the heat to an ammonia loop at a heat exchanger. Heat exchangers are used to transfer thermal energy between two or more fluids at different temperatures. Only one heat exchanger will be needed for the entire habitat module.

Radiators are heat-dissipating equipment that will be located on the outer surface of the habitat module. The size of the radiators will depend on both the heat loads that are to be expelled, and the temperature that is to be maintained inside the module. A thermal balance analysis was used to determine that the total surface area needed for the radiators is 7.95 m².

Should emergency cooling be required in the habitat module, the pumped-looped systems and the air-cooling system will simply operate at a faster rate. On the other hand, should emergency heating be required in the habitat module, the entire cooling system will be turned off.

The thermal system requirements for the Ascent / Descent Module are the same as those for the habitat module. Such a system should be capable of essentially maintaining the temperature within the module at a range where everything will function properly. Since the total surface area of this module is smaller, less multilayer insulation will be required. Also, since the total amount of heat generated is only 600 watts, the ascent / descent module will only require 2 cooling plates to fulfill the thermal requirements: 1 will be placed on the main computer, and 1 will be utilized for the air-cooling system. Due to this lowered amount of heat that needs to be dissipated, the radiators will only need to be 3.01 m². The emergency system will function the same as it does in the habitat module.

Communications

The communications requirement states that the surface spacecraft must be capable of continuously transmitting four channels of compressed high-definition television both to and from Earth. For four channels of HDTV, 180 Mbps of bandwidth will be needed. This large bandwidth drives the design of most of the communications system.

Communicating with missions on the near side of the moon is a relatively simple task. Since the moon is tidally locked to the Earth, a constant line of sight is always available. All communications with Earth will take place over NASA's Deep Space Network. A number of 34-m antennas located around the globe will provide constant communication with the two Endurance spacecraft. The table below gives the important parameters for various communication links with near side missions.

Link	Data Rate	Dish Diameter	Frequency Band
A/D Module to Earth	90 Mbps	0.5 m	Ku (14/12 GHz)
Habitat Module to Earth	180 Mbps	1.0 m	Ku (14/12 GHz)
Rover to Habitat Module	45 Mbps	0.5 m	S (4/2 GHz)
Rover to Earth	45 Mbps	0.5 m	S (4/2 GHz)
Suit to Habitat Module	80 kbps	0.05 m	UHF (470-890 MHz)

The missions to the far side of the moon present an interesting problem for communications. Since a direct line of sight to Earth is never available, the signals from the surface of the moon must be relayed somehow. It was

determined that the best solution to this problem is to place two satellites in a halo orbit about the Earth-Moon L2 point, a feat never before attempted.

These satellites would have two antennas, a large one pointing at Earth, and a smaller one pointing at the moon. Though they provide great access to the far side, the size of their orbit did constrain the location of certain landing sites. A mission to Mare Orientale was eliminated because the site was not in view of the satellites at all times. The table below gives the important parameters for links with the far side of the moon.

Link	Data Rate	Dish Diameter	Frequency Band
A/D Module to Earth	90 Mbps	0.5 m	Ku (14/12 GHz)
A/D Module to Satellite	90 Mbps	0.5 m	Ku (14/12 GHz)
Satellite to Earth	180 Mbps	1.0 m	Ku (14/12 GHz)
Habitat Module to Satellite	180 Mbps	1.0 m	Ku (14/12 GHz)
Rover to Habitat Module	45 Mbps	0.5 m	S (4/2 GHz)
Rover to Satellite	45 Mbps	0.5 m	S (4/2 GHz)
Suit to Habitat Module	80 kbps	0.05 m	UHF (470-890 MHz)

Power Systems

The Endurance missions' power system architecture involves multiple power systems for generation and storage. The primary energy source will supply the crew module with 20kW of power during the lunar day and 17kW of power during the lunar night. This power will provide for life support and daily activities once on the lunar surface. Separate mobile 2-2.5kW power systems will provide the astronauts with adequate power for lunar transportation and scientific exploration.

The mission will require multiple independently powered boosters, as well as a lunar habitat module and an ascent/descent module for crew transport. Each spacecraft will require a compact, long duration energy source for in-flight operations and systems monitoring and maintenance. To meet these requirements, photovoltaic array/rechargeable battery combination systems as well as the nuclear-based Dynamic Isotope Power Source will be utilized. The primary power source will be an independent system on the crew module functioning to provide for air revitalization, water reclamation, communications, science applications and various periodic loads once on the lunar surface. It will require subsystems for power generation and energy storage.

The power generation subsystem will operate during the day providing electricity via the Sun's radiant energy and storing energy for the lunar night. The energy will be stored in the form of hydrogen and oxygen chemical bonds. During the lunar night, hydrogen/oxygen regenerative fuel cells will supply all required power. During the day, the total power requirement will be provided by Gallium Arsenide (GaAs) photovoltaic arrays in the form of 27 individual sun tracking panels totaling 135m² cell arrays. Two electrically-powered rovers will provide lunar transportation. They will have small, compact chemical battery power systems that will provide a safe, reusable power source.

Experiments

The driving force behind the six lunar missions is the science that will be conducted there. The experiments to be conducted include mineralogy, very low frequency array observations, and physiological experiments. Mineralogy experiments conducted on the lunar surface will help scientists learn more about Earth's only natural satellite. By collecting geological samples, much can be learned about the development of the moon, including its age and composition. Samples from different geological formations such as mountain peaks, plateaus, craters and volcanic formations will be analyzed and compared. It will be important to notice trends in the moon's development, such as periods of intense volcanic activity and periods of frequent meteor strikes. Slices of rock and core samples will be taken to limit the mass of samples transported back to Earth. Also, as reported by the Lunar Prospector and Clementine, there is ice in the polar regions of the moon. Core samples will be taken from Aitken Basin to determine if this ice is evidence of water existing on the Moon or the remnants of a comet.

Due to absorption of radio waves by the Earth's ionosphere, there is very little known of the radio sky beyond 10 m wavelengths. If these observations were taken from the lunar surface, much more could be learned about radio wavelengths beyond 10 m. A very low frequency (VLF) radio astronomy observatory, consisting of a large array of wire antennas equipped with an amplifier and digitizer connected to a computer, could make observations of wavelengths from 10 ~ 100 m with high resolution and observations of wavelengths from 100 ~ 1000 m with low resolution. Another important scientific factor to consider is the effect of a 90-day mission, with frequent EVAs, on the human body. The following physiological observations will be carefully monitored for each

of the crewmembers: cardiovascular activity, bone and muscle loss, exercise and nutrition, immunology, and behavior and performance.

Airlock

The operational procedure for the airlock involves, first, suiting up outside the airlock. Next, the pair of astronauts would enter the airlock, close the inner hatch, and begin depressurization. Once the pressure inside the airlock has reached 5.75 torr by the vacuum pumps, the air release valves would be opened to finish the depressurization process. After the airlock has been fully depressurized, the outer hatch is opened and the astronauts climb down the ladder to perform their EVA. The airlock is left depressurized, and the outer hatch open, while the EVA is in progress, so as to minimize the chance of the astronauts being trapped outside the airlock. When the astronauts return from their EVA, the outer hatch is closed and the inner air release valves pressurize the airlock.

EVA

The suit chosen for lunar surface activities is ILC Dover's I-Suit. The I-Suit possesses several unique qualities such as: totally fabric construction for increased mobility, operability in a dusty environment, and a light weight due to the lack of massive solid pieces. The I-Suit is pressurized at 29 kPa 100% O₂. This is important when calculating the ratio between the suit pressure and the partial pressure of nitrogen in the cabin atmosphere. This value, represented as R, symbolizes the probability of side effects due to nitrogen bubbles formed during transit to the suit. In using the I-Suit, an R-value of 1.03 is maintained, requiring zero prebreathe before suit transit. This reduces the chances of dramatic side effects such as "the bends." In addition, it decreases the time necessary to transit between suit and cabin, and vice versa.

EVAs on the lunar terrain will require additional technology. This includes rovers and tools, which are stored externally, allowing easy access while on an EVA. They are placed directly in the bilge of crew habitat module, which helps to minimize dust contamination of the cabin. The suits, however, are stored internally on the first floor of the crew module in a storage bay. This allows quick access during emergencies and close proximity to the airlock.

To meet all mission requirements and to conduct experiments, the astronauts are required to make daily EVAs for almost the entire mission. EVAs in the beginning of the mission will be used to deploy the lunar rovers from the habitat module and to set up experiments such as the VLF array. Later EVAs will involve exploring the lunar landscape, taking samples, and conducting maintenance on the lunar rovers. The lunar rovers will be similar to those used on Apollo, and will run on two 36-volt rechargeable batteries. Two rovers will be taken on each mission, with one serving as a backup in case astronauts on EVA encounter an emergency situation. All EVAs will use the buddy system, meaning two astronauts will go on EVA, while two remain in the habitat, supporting the EVA and conducting their own experiments.

Reentry

Maximum entry accelerations are limited to 9 g's. A Matlab program was used to analyze lifting and nonlifting earth entries. The reentry corridor for the vehicle is approximately 0.5°. For a heat shield with a radius of 500 ft, stagnation point temperatures approach 3600°K and maximum total heating loads approach $1 \cdot 10^9$ J/m². A simple Chapman heating model is used with a blunt entry vehicle.

Testing Scenarios

Three precursor flights to the moon will take place from 2010 to 2012 prior to the annual missions from 2013 to 2018. The first flight test with an unmanned A/D Module is necessary to make sure that a fully functional system exists to safely ferry the crews to and from Earth. The second flight test sends a Habitat Module to the lunar surface one week prior to the astronauts' arrival on another A/D Module. The astronauts spend two weeks on the lunar surface in final checkout of the Habitat and Ascent/Descent Modules and then return to Earth.

Overall Timeline

First, research and development starts in 2002 and ends in 2006. Vehicle production starts in 2005 for the precursor missions; the final vehicle is completed in 2015. Next, testing and validation of flight hardware begins one year after production starts and finishes a year after all production ends. As indicated above, flight testing runs from 2010 to 2012. Finally, the six 90-day missions fly to the moon from 2013 to 2018.

Cost Analysis

Project Endurance, beginning in 2002 and ending in 2018, costs an estimated total of \$25.5 billion in Y2002 dollars. The price of research and development is approximately \$5.3 billion (Y2002). Production of all spacecraft for all missions will cost \$2.9 billion (Y2002). Launch costs for all missions sum up to over \$17.1 billion (Y2002). Operations throughout the life of the program will cost over \$304 million (Y2002).

Conclusion

Project Endurance will continue the efforts of the Apollo program. Through six lunar missions, beginning in 2013 and ending in 2018, humanity will vastly expand its knowledge of our closest neighbor. Advancements made during these missions will aid in future space exploration endeavors.

References

- "A Mission Radiation Calculation Program for Analysis of Lunar and Interplanetary Missions". NASA TP-3211, May 1992.
- Akin, David. "ENAE483 Course Notes", University of Maryland, 2001.
- Anderson, John D. "An Engineering Survey of Some Radiating Shock Layers". AIAA Journal Volume 7, Number 9 September 1969.
- Burke, Bernard. "Astronomical Interferometry on the Moon". Lunar Bases and Space Activities of the 21st Century. 1985.
- Chin, Derek, and Hermans, Mike. "A Flight to The Moon". <<http://webhome.idirect.com/~viking/themoon.html>>.
- Cintala, Mark and Paul Spudis and B. Ray Hawke. "Advanced Geologic Exploration Supported by a Lunar Base: A Traverse Across the Imbrium-Procellarum Region of the Moon". Lunar Bases and Space Activities of the 21st Century. 1985.
- Delta IV Payload Planners Guide, The Boeing Company, 1999.
- Douglas, James and Harlan Smith. "A Very Low Frequency Radio Astronomy Observatory on the Moon". Lunar Bases and Space Activities of the 21st Century. 1985.
- Finckenor, M. M. "Multilayer Insulation Material Guidelines." NASA/TP 1999-20923. April 1999.
- Greenberg, H. Stanley. Aerospace Structural Systems: Preliminary Design Techniques. Los Angeles: UCLA Department of Engineering, 1990.
- Hamilton Sundstrand. Electrochemical Energy Systems: Water Electrolysis and Natural Gas. March 10, 2002. United Technologies Company. <<http://www.hsssi.com/Applications/SpaceHabitat>>.
- Hibbler, R.C. Mechanics of Materials 3rd Ed. Upper Saddle River: Prentice Hall, 1997.
- Hoffman, David. "Station-keeping at the Collinear Equilibrium Points of the Earth-Moon System." NASA JSC-26189. January 1993.
- Horz, Friedrich. "Mass Extinctions and Cosmic Collisions: A Lunar Test". Lunar Bases and Space Activities of the 21st Century. 1985.
- Leondes, C.T., and Vance, R. W. 1964. Lunar Missions and Exploration. New York: John Wiley & Sons.
- Marcus, Martin. "The Efficiency of Computers and Optimizations in Performing Finite Element Computation". U.S. Naval Research Laboratory. May 17, 2001.
- "Monitoring Bone Loss in Astronauts", Space Daily. <<http://www.spacedaily.com/news/spacemedicine-01a.html>>.
- Shuttle Orbiter/Cargo Standard Interfaces (Core) ICD 2-19001, Revision-L, Boeing North American, Inc. 1998. <<http://www.unitedspacealliance.com/icd/core/contents.html>>.
- Sonntag, Richard and Claus Borgnakke. Fundamentals of Thermodynamics. John Wiley and Sons, New York, 1998.
- Sutton, George P. Biblarz, Oscar. 2001. Rocket Propulsion Elements Seventh Edition. New York: John Wiley & Sons, Inc.
- Taylor, Lawrence and Dong-Hwa Taylor. "Location of a Lunar Base: A Site Selection Strategy". Engineering, Construction and Operations in Space V: Proceedings of the Fifth International Conference on Space '96, 1996.
- The Lagrangian Points. March 5, 2002. Castle Point Astronomy Club. <<http://www.cpac.freereserve.co.uk/docs/lagrange.htm>>.
- Vallado, David A. 1997. Fundamentals of Astrodynamics and Applications. New York: McGraw Hill.

- Wade, Mark. Encyclopedia Astronautica. <<http://www.astronautix.com>>.
- Weiland, Paul O. Designing for Human Presence in Space: An Introduction to Environmental Control and Life Support Systems. NASA Reference Publication 1324 (1994).
- Wilhelms, Don. To a Rocky Moon: A Geologist's History of Lunar Exploration, The University of Arizona Press, 1993.
- Wydeven, Theodore; "A Survey Of Some Regenerative Physio-Chemical Life Support Technology". NASA Technical Memorandum 101004 (1988).
- Whitaker, Alana. "Overview of ISS US Fire Detection and Suppression System", June 25, 2001. <<http://spaceresearch.nasa.gov>>.
- Young, Warren, Roark's Formulas for Stress & Strain. 1989 McGraw-Hill.

Self-Sustained Closed Ecological Systems

University of Washington, Seattle, WA

Authors: David Barbee

Research Team: Emily Augustein, David Barbee, Zach Frazier, Mike Guerquin, Hillary Marshal, Yuichi "Eugene" Saito, Emily Thompson

Faculty Advisor: Dr. Frieda Taub, University of Washington, School of Aquatic and Fishery Sciences

Abstract

The focus of this project is the development of closed ecological systems (CES) to sustain a population of aquatic invertebrates for more than 30 days. Permanent habitation of space will require the development of CES capable of meeting the biological needs of human inhabitants. Such a system must provide water, oxygen, and food while removing waste products and recycling the mass of the system. Ideally, the ecological system will recycle wastes into requirements and function with minimal mass exchange. Current NASA research has been directed toward the optimization (in terms of volume, energy, mass) of the components of closed systems (i.e. crop production in space). This project explores the creation of small (75ml) aquatic CES testing different chemical media, temperature, light cycles, and physical conditions. Experimental CES consisted of freshwater algae and the grazer *Daphnia magna*. Computerized image analysis techniques were developed and implemented for abundance estimation and modeling population dynamics. Rotation of the containers, to vary the direction of gravity, did not alter survival or reproduction. Increased inorganic nutrients (Nitrate and Phosphate) were tested to determine if inorganic limitations prevented additional generations. Most CES conditions resulted in the survival of *D. magna* population including the F1 (offspring of original animals) generation. Ongoing work focuses on conditions that will permit an F2 generation (Grandchildren of original animals) and beyond.

Introduction

Problem statement: Create an ecological community including all of the chemical requirements for photosynthetic organisms to produce food and oxygen and animals to use the food and oxygen and supply carbon dioxide and ammonia as nutrients for the photosynthetic organisms. The goal is to sustain the animal population for at least 30 days.

Establishing a balanced ecosystem appears to be difficult initially, but biological systems tend to self-organize. For example, as animals in an aquatic ecosystem feed, they reduce the abundance of the algae and the food shortage causes reduced animal reproduction and survival. As animal feeding is reduced, the algal population can increase. Evidence of this relationship can be seen in any nearby lake if one were to look closely. If the system was closed and the animals ate all of the algae, they would also eliminate their oxygen source, however this has not been observed to occur. Creating a biological community is painfully simple; every time one closes a bottle, a living ecosystem is created. Historically, space programs have neglected the effects of complex assemblages of organisms on space travel. We must deal with the fact that every human is a community of organisms. The evidence of this neglected viewpoint can be seen inside any space station. The effects of biology have not been addressed during design; MIR suffered repeated equipment failures from the acids produced by fungi. The offending fungi thrive on the sloughed tissues, lipid, and sweat from industrious astronauts. The glorious achievements of the 60's space race and the current ventures into space have been the biological equivalent of a fish jumping out of the water. A permanent human presence in space requires that we understand and can create a biological community to process our wastes into requirements for life in space.

The planet earth can be considered a giant space vessel with a functional ecosystem where processes occur on a vast scale in volume, time, and complexity to sustain its various astronauts (all life). Earth is essentially closed to mass exchange with its surroundings. Energy is input to the earth as sunlight, which drives physical and biological processes that power nutrient cycling. Life continues by the recycling of carbon, nitrogen, oxygen and other elements through the ecosystem in a self-sustaining manner that passes energy on until it is lost as heat. To create our own functional support systems for space exploration, testable hypotheses must be tried on an ecosystem-wide scale. The volumetric and time considerations of influencing the variables of our planet-scale ecosystem preclude any such experimentation or replication of experiments. Extreme variation can occur on a planet-wide scale that may obscure the true cause of some relationships. Thus, smaller self-sustaining ecosystems have been setup with light as the only quantifiable input, with the aim of studying the behavior of an ecosystem over time and to enable the trial of testable hypotheses. These systems would receive light energy from outside but would recycle everything needed for species survival without any external input (Beyers and Odum 1993). Small closed ecological systems allow perturbations to an ecosystem to be studied at a scale that humans can effectively observe. Using CES to study patterns and effects of elements within an ecosystem allows one to not only observe specific interactions, but also to replicate and reproduce experiments and results [Taub 1980]. Scientists can make the system as complex or as simple as needed in order to study as few or as many aspects of the ecosystem as desired [Odum 1989]. Eventually, a self-sustaining system for the support of humans can be engineered from the data gleaned from the study of closed ecological systems (referred to as CES, or microcosms).

Experimental approach: Background

A common theme in the scientific pursuit of knowledge is that one question asked usually results in many subsequent questions. In the creation of a self-sustaining CES, we addressed several resultant issues that were facets of the overall design goal. To set up a CES, we must construct a food web that cycles nutrients to sustain itself.

An aquatic ecosystem was selected as the base for study of CES dynamics. Aquatic environments facilitate matter transport in a time-scale conducive to lab study. Nutrients are transported by mixing, diffusion, and transport as a result of zooplankton movement. The celerity of matter transport in aquatic systems approximates facilitated transport that would occur in an anthropogenic system with pumps, etc. The physical characteristics of aquatic ecosystems need to be considered when constructing a self-sustaining CES. Natural aquatic systems are in constant motion, with wave action and temperature differentials driving mixing and facilitating nutrient transport over vast distances. Spacecraft are subject to non-uniform orientation of gravity. During maneuvers, the orientation of gravity may change substantially for long periods of time. Volumetric scales available in a lab scenario are limited by logistics, but what

scale is appropriate for CES study? Taking samples during experimentation is a necessity. However, small-volume (<100ml) systems can experience large variations in volume if samples of only a few milliliters are taken and replaced. To avoid taking samples from small ecosystems, we used visual observation. Animals require oxygen; their persistence indicates the presence of oxygen. The intensity of greenness in CES was used to estimate algal density. The number and size of animals is indicative of reproduction and growth. Our team conducted several studies to evaluate the physical and chemical variables of aquatic ecosystems for CES study.

A liquid's chemical composition defines the aquatic ecosystem. The media used for traditional open ecosystem studies may be inadequate to sustain a closed ecosystem. Liquid media must contain the correct balance of pH, nutrients, and salts to support a food web consisting of algae and an invertebrate grazer. T82-LoSi (Low silicate) medium is chemically defined mixture (22 elements) designed for the growth of algae. It does not contain an inorganic carbon source because most algae are grown in open containers where the atmosphere supplies carbon dioxide. The limiting nutrient for algal growth in T82-LoSi is 0.5 mM nitrate and all other elements except carbon are in excess. Therefore, in closed systems an inorganic carbon source is necessary. Kent media is a commercial mixture of salts that supplies inorganic carbon as sodium bicarbonate; it does not supply nitrate or phosphate. Thus, T82-LoSi and Kent media together could provide an adequate collection of elements to support a CES. We conducted two studies to explore the characteristics of different media in CES conditions.

The grazing invertebrate *Daphnia magna* was selected as the research animal due to availability and in-depth background knowledge of biology. *Daphnia magna* are easy to see with the unaided eye, are hardy, and reproduce quickly. *Daphnia* are used commonly in studies of toxicology and freshwater ecology. We have a large knowledge base accumulated on varied aspects of *Daphnia* ecology. *Daphnia* will graze algae and use oxygen during respiration, and excrete ammonia and carbon dioxide as byproducts. Algae in the CES occupy the role of primary producer, and will fix inorganic nutrients into lipid, protein, and carbohydrate that feed *Daphnia*.

The population of *Daphnia magna* was used for hypothesis testing to determine the significance of a treatment. *Daphnia magna* are the largest *Daphnia* species available for study, but their biology poses another problem for hypothesis testing. Counting by eye is limited by detection and availability biases to very small populations (< 20 individuals) that are frequently reached in the smallest volumes. Detection bias is introduced when large populations occur and individual *Daphnia* become difficult to track. Availability bias is introduced when clumps of algae and crowding from other individuals obstructs *Daphnia* enumeration. Since *Daphnia* population is the variable that we observe to determine significance, we developed new computer-aided methods for population enumeration to improve the resolution of our data. Computerized methods enable large populations and volumes to be accurately evaluated; where in the past populations would be measured in "dozens" now exact counts are feasible. Additionally, data gathered with a computer can be archived for future study.

Freshwater CES were housed in tissue culture flasks of various dimensions. Tissue culture flasks are useful for CES study due to their universal availability, impermeability, low procurement cost, and optical characteristics. Tissue culture flasks are optically flat and transparent, allowing systems to be visually sampled without introducing distortion from rounded surfaces. Figure 1. shows an example of CES in three different sizes of tissue culture flasks.

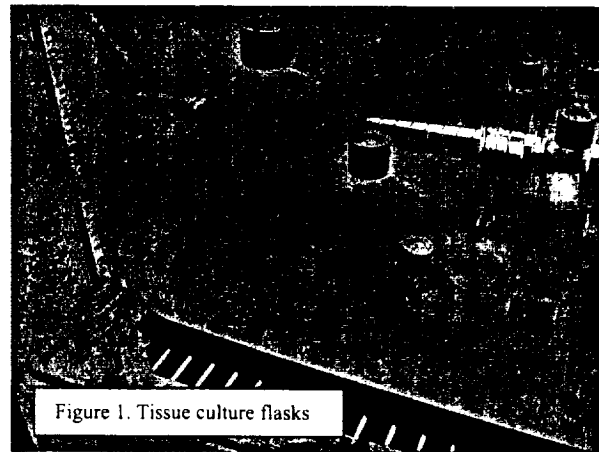


Figure 1. Tissue culture flasks

Experimental approach: methods

Techniques common among studies were culture setup and population enumeration. Typically, a culture flask was filled with media and two types of algae—*Ankistrodesmus* and *Scenedesmus* were introduced. The flask was allowed to sit open for a five-day setup period, letting unknown organics oxidize and to let algal growth begin. After the setup period, six *Daphnia* were introduced to the flasks and then the systems were sealed. CES replicates were then placed into an incubator where temperature and light cycle were controlled. Observation commenced for thirty days at intervals of at most every three days. In CES with large populations, computer-aided enumeration was utilized. Freshwater closed ecological systems for various studies followed the same initial set-up and composition: Kent water and T82-LoSi served as the liquid environment and initial source of nutrients for the algae. A small amount of media (<2ml) was added with zooplankton introduction. Figure 2. shows a typical experimental setup in an incubator. Computer enumeration techniques allowed large populations to be accurately evaluated, enabling the volume studies performed by our team. In all cases, care was taken to devise a technique that samples the entirety of a CES simultaneously with our sub-sampling. Sub-sampling would introduce a large availability bias to abundance assessment because zooplankton exhibit mild flocking behavior. Several complimentary sampling methods were used.

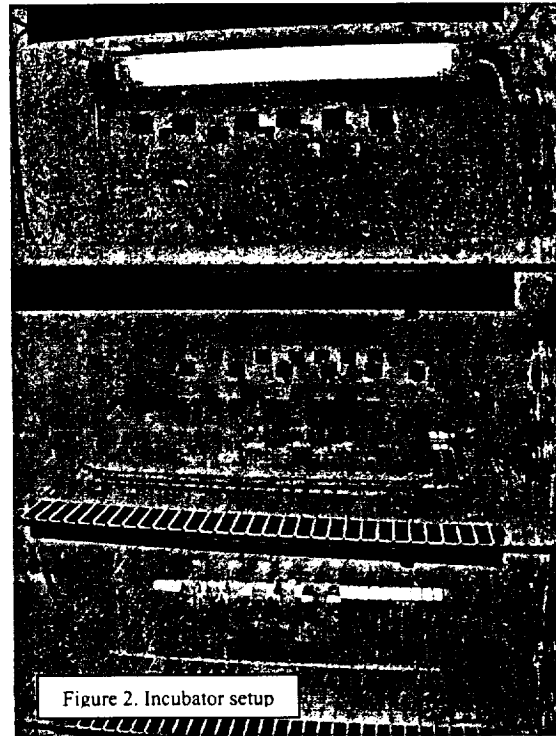


Figure 2. Incubator setup

A digital camcorder was used to observe CES replicates. Video of CES replicates was re-played to manually enumerate *Daphnia* from recorded movement.

A program to track groups of pixels was implemented in MATLAB using the image processing toolbox. The program inputs series of pre-formatted TIFF files and outputs track length, object size and velocities.

Adobe Photoshop 6.0 was used to enumerate *Daphnia* from high-resolution (3.2Mpixel CCD, image size 2048X1536 pixels) digital still images. A custom script was implemented to improve contrast between *Daphnia* and the surrounding media, so that manual enumeration could result. Figure 3. shows the input and output of the contrast enhancement script. Observers were instructed to recognize *Daphnia* by the crooked gut, defined carapace, and eyes. Aspect differences prevent automated image recognition of *Daphnia*, but Photoshop enabled large populations to be enumerated.

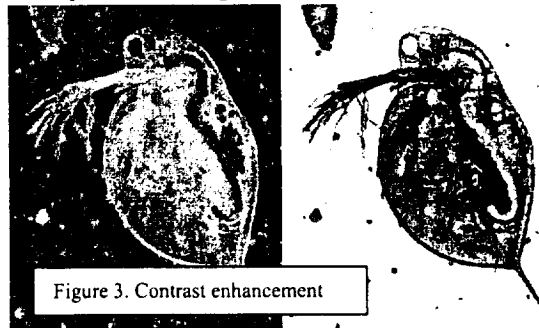
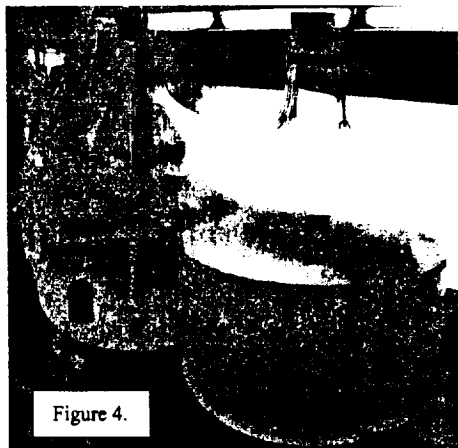


Figure 3. Contrast enhancement

Physical CES studies

Natural systems have wave action to aid in nutrient cycling. To determine if motion affects the sustainability of CES, six replicates of CES were attached to a Cell culture roller drum (New Brunswick Scientific Inc.) that completed one full revolution every five minutes. As a control, six replicates of CES and six replicates of open ecosystems were left stationary under similar light conditions.



Difficulty of counting large zooplankton population has restricted our previous research to using small-volume ecosystems. The small (75-ml) ecosystems that we have been using for CES study may not be the optimal scale for our work. Taking a 1-ml sample for chemical analysis represents a large mass exchange for small systems. Computer-aided enumeration has enabled large volume CES to be accurately assessed. Two studies were conducted on a range of flask sizes. One study used three (75, 250, 750-ml) volumes of tissue culture flasks with the same media to explore the relationship between volume scaling and *Daphnia* abundance. Another study setup a 33-Liter salt-water CES in a 60-Liter carboy and measured carbon dioxide and zooplankton density to determine the dynamics of a large CES. Figure 4. to the left shows two 60-Liter sized CES.

Chemical CES studies

Two studies were conducted to explore the viability of the chemically defined media that we use in CES work. A mixture of T82-LoSi and Kent water was used as the chemically defined media. The first study evaluated the sustainability of chemically defined freshwater media versus natural media. In long-term culture, *Daphnia* populations often grow better if lake water is occasionally used, suggesting that some trace elements may be lacking (Taub, 2002, personal communication). It is conceivable that synthetic media are not supplying the necessary nutrients to algae for long-term survival and reproduction of *Daphnia*. The defined media was compared to a natural media, in this case autoclaved water from Lake Washington. Open and closed ecological systems with both types of media were also compared. The second study augmented the nitrate (N) and phosphate (P) loading of defined media to explore the effects of nutrient enrichment on *Daphnia* population dynamics.

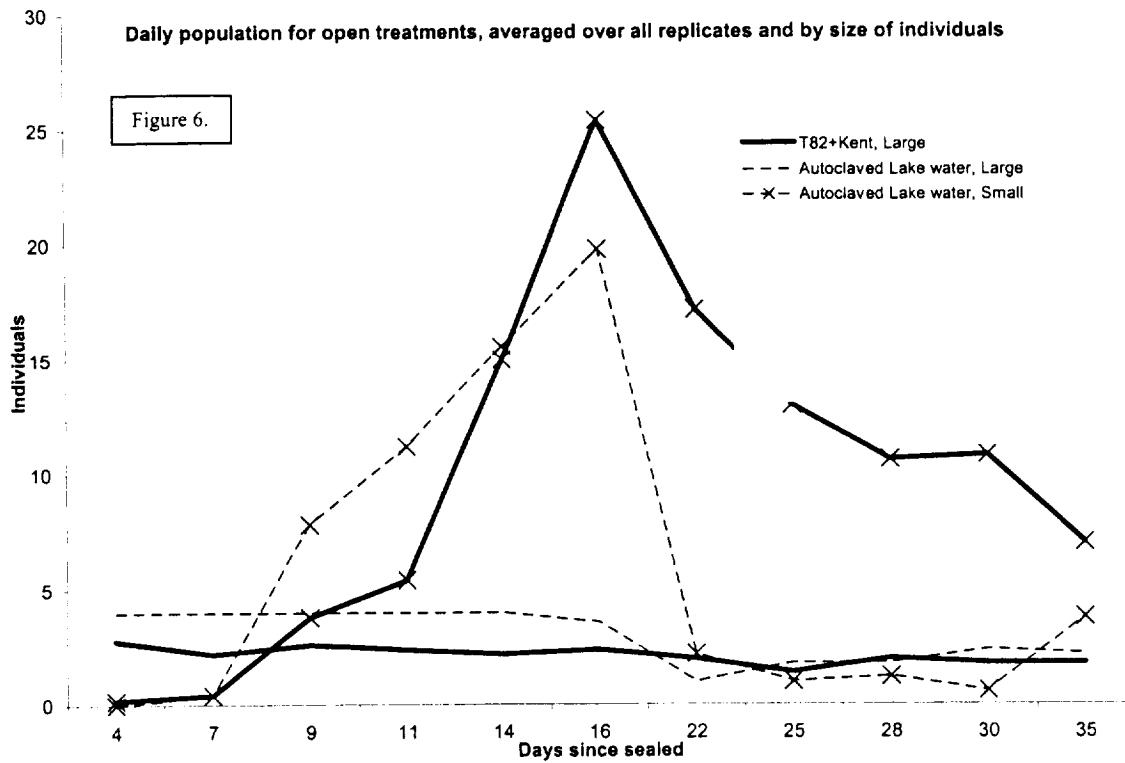
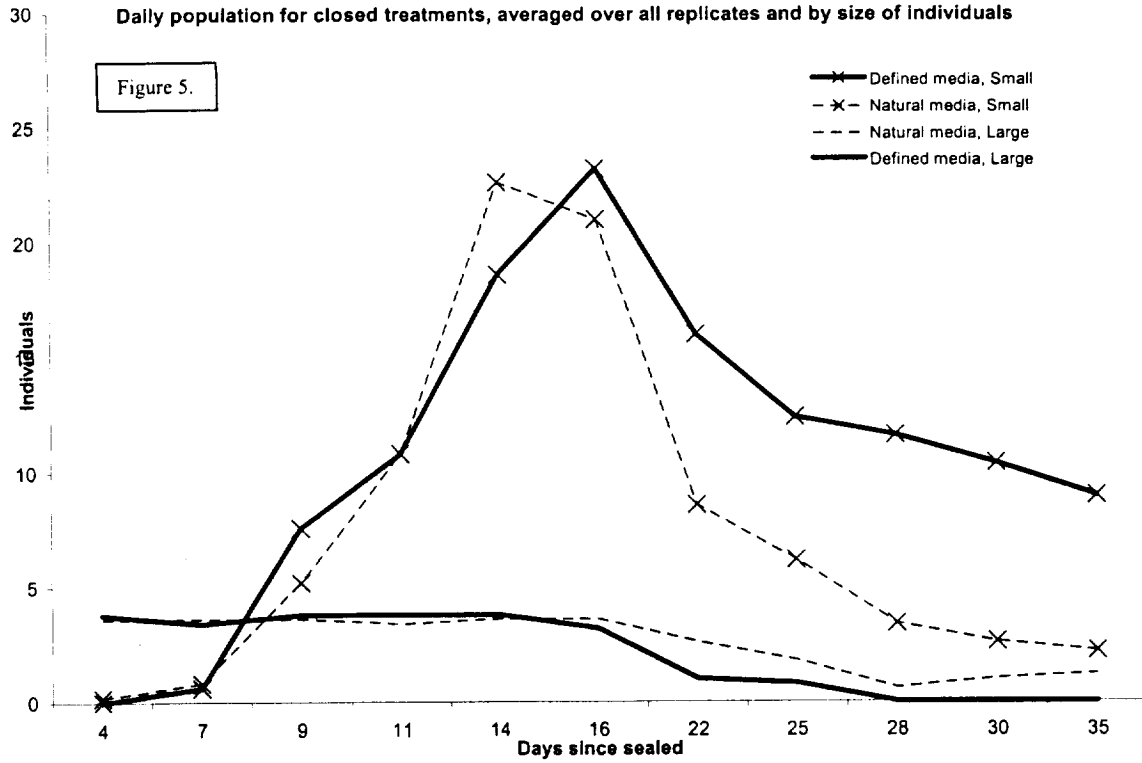
Results: Physical CES studies

Daphnia density was inversely related to microcosm volume, while smaller volume microcosms (75-ml) experience higher extinction rates. More animals were found in larger volumes, but their density was not as high as that of smaller systems. Computer-aided enumeration allowed accurate counts of *Daphnia* population. Populations of up to 200 individuals were observed only in flask sizes of only 750-ml. Orientation was not observed to affect *Daphnia* populations.

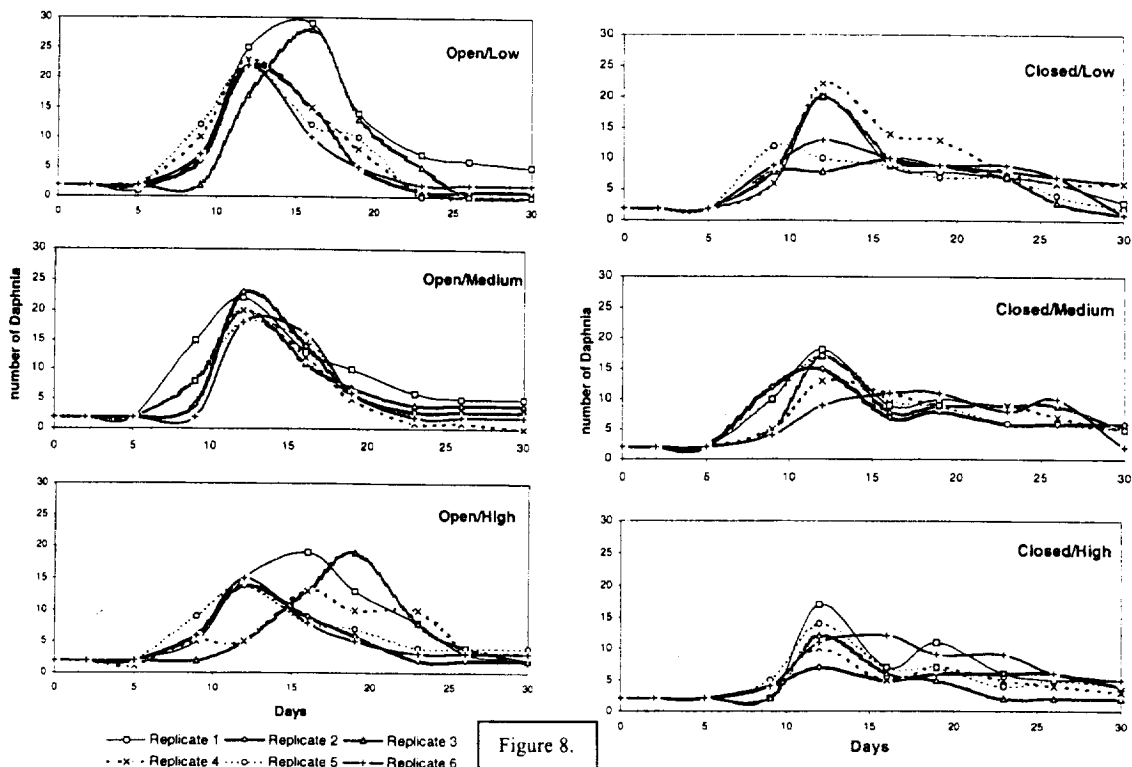
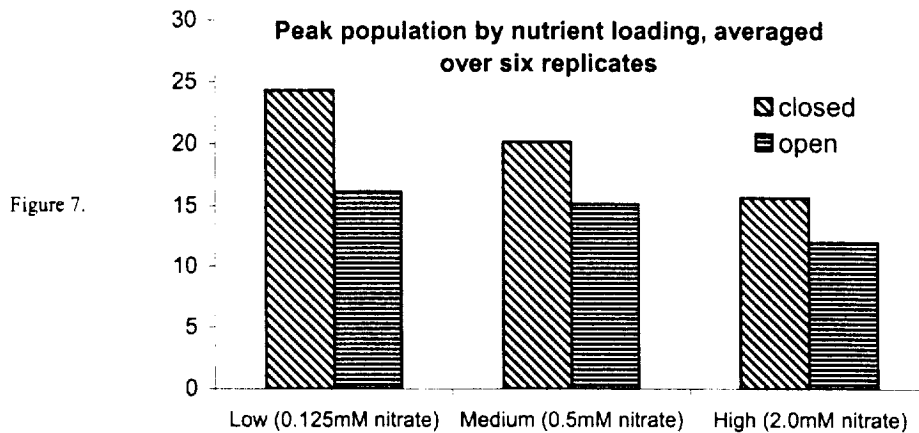
60-liter CES studies are feasible for long-term study and allow sampling with a low percentage of total mass to be exchanged. Atmospheric carbon dioxide was observed to decline precipitously within the first week of observation. The copepod *Tigriopus californicus* (Monk, 1941) became dominant in the salt-water CES.

Results: Chemical CES studies

T82-LoSi+Kent media supported higher *Daphnia* populations than autoclaved lake water, suggesting that it does supply necessary elements for survival. Figures 5 and 6 show population dynamics for closed and open systems of natural and defined media, averaged over six replicates and categorized by size of individual *Daphnia*. The small animals are the offspring of the initially introduced animals. It was noted that small animals peaked around day fifteen and then declined without maturing and reproducing.



T82 has been used as an algal culture media and nitrogen and phosphorous than natural media. Natural media would be expected to have less algal carrying capacity compared to T82 and would support less *Daphnia*. It was observed that the large animals declined in all replicates in all treatments. Offspring (F_1 generation) of the animals introduced initially were not observed to grow to maturity and reproduce. It may be that T82-LoSi+Kent media, while more suited for CES study than natural media, still lacks necessary ingredients for the maturation of *Daphnia magna*. Open systems did not support significantly different *Daphnia* populations, suggesting that both carbon dioxide and oxygen are not limiting. Nutrient loading (N, P) increase has an inverse effect on peak *Daphnia* population, possibly due to toxic effects of nitrate at high concentrations, also indicates that N, P are not limiting in CES studies. Figure 7. shows the peak population of *Daphnia* at each nutrient loading, averaged over six replicates per treatment. Figure 8. illustrates the variability of replicates in each treatment, and show dynamics of *Daphnia* population at different nutrient loading.



Lessons Learned, Future studies

It has been demonstrated that freshwater closed ecological systems are a viable basis for support of an algae-grazer food chain for at least 30 days. Chemical evaluations suggest that the defined media (T82-LoSi and Kent) does supply enough nutrients for algal growth and *Daphnia* sustainability; however no F₂ generation has been observed (grandchildren of original animals). Algae may be the limiting component to our current model. The ecology of *Daphnia magna* introduces problems for long term stability. In natural environments, *Daphnia* species are heavily predated by a large number of organisms. *Daphnia* have evolved with this pressure on their population and reproduce rapidly until all resources are used, compensating for predation pressure with a high birth rate. There is no such predation pressure in the CES that we have constructed, so *Daphnia* are free to over-graze the algal population. *Daphnia magna* populations in CES have exhibited dynamics similar to the classic predator-prey model with unrestricted birth. *Daphnia* graze the available standing crop of algae and reproduce until algae are depleted. The algae do not reproduce rapidly enough to sustain *Daphnia* growth, and the population slowly declines because each animal is getting enough food to survive, yet not enough to reproduce. *Daphnia* must shed their exoskeletons (molt) to grow. Many molts have been observed to accumulate in CES flasks. Molts are composed of Chitin, a structural polysaccharide that contains non-trivial amounts of carbon and nitrogen. Chitin is broken down by the action of bacteria, but the process is very slow. It is possible that the molts of *Daphnia* act as a sink for nutrients that the algae need to grow, causing the system to "run-down" as nutrients are deposited faster than bacteria can liberate them. A way to increase the rate of nutrient cycling from molts should be explored. Increasing the rate of a chemical reaction usually means increasing the temperature at which the reaction occurs, increasing the surface area, or the addition of a catalyst. Of these methods, increasing the surface area available for bacteria may prove the most beneficial. A substrate such as sand would provide large surface area for bacteria and may provide algae with a refuge from grazing by zooplankton. Some chitin should also be added to the substrate to account for the rate at which *Daphnia* molts accumulate, allowing a standing crop of bacteria to develop to continuously cycle nutrients from molts.

Daphnia magna may not be the ideal CES organism, but we have been constrained by visual sampling techniques (naked eye) to using them as our study organism. Computer-aided enumeration techniques that were developed during this study will enable greater populations of smaller organisms to be enumerated, increasing our selection of research organisms. In future studies, we should consider an organism that has population dynamics that do not tend to bloom and crash so that we can more closely approximate a crew of human astronauts.

An ideal volume for CES study has yet to be found. Large volume systems (many liters) allow for sampling without a high percentage of system mass to be exchanged, but are logistically intensive. Small volume CES allow for greater replication. In future studies, a small volume CES with a smaller organism and substrate with chitin may provide greater sustainability.

Future work will focus on discerning the mechanisms associated with self-organization of CES and of obtaining a reproducing population of *Daphnia* with an F₂ generation and beyond. Improving the computer-aided enumeration techniques will enable very large populations to be automatically, remotely, and continuously assessed. Many improvements can be made to the student-developed tracking software. MATLAB requires a high level of aptitude to use, and is expensive. Implementation in C++ and the addition of an intuitive interface would allow greater transparency of the enumeration process. A future goal of enumeration methods is to reduce the number of steps that need to be taken for counting of zooplankton populations and implement more motion analysis software.

Once an indefinitely sustainable model has been determined, we can use it as a research tool to plan the ecosystems that will some day support a human population in space. The brief leaps of a fish out of water will someday give way to the ability to swim in the sea of stars.

References

- Adey and Loveland, 1998. *Dynamic Aquaria*. Academic Press.
- Byers, R. J. and H. T. Odum. 1993. *Ecological Microcosms*. Springer-Verlag.
- McLachlan, J. 1973. p. 42-45 in Stein, J.R. (ed.) *Handbook of Phycological Methods: Culture Methods and Growth Measurements*. Cambridge University Press.
- Monk, C. R. 1941. Marine Harpacticoid Copepods from California. *Trans Am Microscopic Soc.* Vol. 60, 75-99.
- NASA 1982. *Workshop on Closed System Ecology*. Jet Propulsion Laboratory. 82-64. July 15 th , 1982.
- Straight, C. L., Bubenheim, D. L., Bates, M. E. and Flynn, M. T. 1994. The CELSS Antarctic Project: An Advanced Life Support Testbed at the Amundsen – Scott South Pole Station, Antarctica. *Life Support and Biosphere Science*. Vol. 1, 52-60.
- Taub, F. B. and Michael E. Crow. 1980. *Synthesizing Aquatic Microcosms*. Microcosms in Ecological Research. Symposium in Augusta Georgia, November 8-10 th , 1978.
- 1993. Standardizing an aquatic microcosm test. p. 150-188 in Soares, A. and P. Calow. (eds.) *Progress in Standardization of Aquatic Toxicity Tests*. Pergamon Press.

LIST OF PARTICIPANTS

Michael R. Aherne
Embry-Riddle Aeronautical University

Kristina Alemany
Princeton University

David H. Barbee
University of Washington

Kristen Bethke
Princeton University

Mary Bowden
University of Maryland

Nichols F. Brown
Georgia Institute of Technology

William A. Burnett
Colorado School of Mines

Jonathan D. Bush
Colorado School of Mines

Jeff Cardenas*
Universities Space Research Association

Huitung Chu
University of California, Berkeley

George Cooper
University of California, Berkeley

Philip A. Davis
Embry-Riddle Aeronautical University

Mike Duke*
Lunar and Planetary Institute

Kristen Durance
University of Washington

Matthew T. England
Embry-Riddle Aeronautical University

Wallace Fowler*
University Texas at Austin

David Gan
University of California, Berkeley

Jake E. Gustavsson
Embry-Riddle Aeronautical University

Ben Hauser
Lunar and Planetary Institute

Todd Herrmann
University of Maryland

Attrice L. Hunt-Malone*
Lunar and Planetary Institute

Alan J. Jones
Colorado School of Mines

Joyce M. Kaneta
Colorado School of Mines

Josip Loncaric*
ICASE, NASA Langley Research Center

John J. Maatsch
Georgia Institute of Technology

Mara McFadden
University of California, Berkeley

Mike McGee*
Lockheed Martin

Steve McGuire
Pennsylvania State University

Barbara J. McKinney
Colorado School of Mines

Daniel M. Nosenchuck
Princeton University

Seigo Ohi
Howard University and Hospital

John R. Olds*
Georgia Institute of Technology

Steven M. Pankow
Embry-Riddle Aeronautical University

Michael C. Quayle
University of California, Berkeley

* RASC-AL Steering Committee Member

Mahmut Reyhanoglu
Embry-Riddle Aeronautical University

Joel D. Richter
Pennsylvania State University

Allana N. Roach
Howard University and Hospital

Reuben R. Rohrschneider
Georgia Institute of Technology

Chere M. Sampaio
Embry-Riddle Aeronautical University

Philip A. Savella
Embry-Riddle Aeronautical University

William Sheng
University of California, Berkeley

William Siegfried*
Boeing

Joseph Simons
University of Maryland

Kevin F. Sloan
Pennsylvania State University

Frieda B. Taub
University of Washington

Pat Troutman
NASA Langley Research Center

Serdar Uckun
RIACS, NASA Ames Research Center

David A. Young
Georgia Institute of Technology

Kris A. Zacny
University of California, Berkeley

* *RASC-AL Steering Committee Member*